The evolution of the cervid skull

Dissertation zur Erlangung des Doktorgrades
an der Fakultät für Geowissenschaften
der Ludwig-Maximilians-Universität München

vorgelegt von
Ann-Marie Schilling

München, 07.09.2021

Erstgutachterin: PD Dr. Gertrud E. Rössner
Zweitgutachter: Prof. Dr. Oliver Rauhut
Tag der mündlichen Prüfung: 08.12.2021

Table of contents

Statutory declaration and statement

I hereby confirm that my thesis entitled *"The evolution of the cervid skull"* is the result of my own original work. Furthermore, I certify that this work contains no material which has been accepted for the award of any other degree or diploma in my name, in any university and, to the best of my knowledge and belief, contains no material previously published or written by another person, except where due reference has been made in the text. In addition, I certify that no part of this work will, in the future, be used in a submission in my name, for any other degree or diploma in any university or other tertiary institution without the prior approval of the Ludwig-Maximilians-University Munich.

Landshut, 20.05.2022 Ann-Marie Schilling

Summary

Cervidae (deer) forms a large family of cud-chewing, even-toed mammals (Artiodactyla: Ruminantia). It is closely related to Moschidae (musk deer), Bovidae (cattle, goats, sheep and antelopes), Giraffidae (giraffes), and Antilocapridae (American pronghorns); Tragulidae (mouse-deer and chevrotains) comprises somewhat more distant relatives. Cervids originated in the Early Miocene (~ 20 mya) in Europe.

Cervids form a highly diversified group and occupy a wide range of ecological niches, from tropical forests to Arctic tundra. They may be found in Europe and Asia, and the Americas. In Africa, cervids are native only to a narrow range along the Mediterranean. No native cervids are known from Australia and Antarctica. This wide geographic and ecological distribution goes along with extensive adaptations. Extant cervids range in size from the small South American pudus, weighing about 6 kg to the large moose, weighing up to 600 kg. They also differ in their social behaviour, living either solitary or in male-dominated groups. However varied cervids may be, their best-known and diagnostic commonality is that males develop antlers which are shed and regularly regrown. The one exception is the water deer which lacks antlers but shows enlarged upper canines.

A central theme of the present thesis is whether and how the development of antlers and the ecological diversification affected the structure of the skull. Specifically, we wanted to clarify how the size and shape of the facial facet of the lacrimal bone vary in extant cervids and two iconic extinct cervids from the last glacial. The lacrimal facial facet holds a central position between the frontal bone, where antlers arise, and the maxilla.

We compared the size and shape of the lacrimal facial facet of ten extant cervid species using *Moschus* and *Tragulus* as outgroups. Neither size nor shape of this central bone of the facial skeleton could be related to a specific ecology or behaviour of the species analyzed. However, both measures were found to correlate with skull length. Size scales positively with skull length, as does the lacrimojugal length. In contrast, lacrimomaxillar length shows negative allometric scaling. We propose that during cervid evolution the lacrimal facial facet was exapted to dampen the transfer of stress originating from antlers to the maxilla. In the extinct “Irish Elk”, the giant deer *Megaloceros*, and the dwarf cervid from Crete, *Candiacervus* we observed quite small lacrimal facial facets relative to their skull length. Further, the shapes of the lacrimal facial facets are similar in the two fossil cervids but differ from those observed in extant cervids. We argue that these morphological differences in the lacrimal facial facet may suggest that *Megaloceros* and *Candiacervus* used their exceedingly large antlers as ornaments, and not also as weapons.

In order to better interpret the quantitative data of the lacrimal facial facet in Pleistocene cervids, we re-assessed the cranial morphology of *Candiacervus*, taking advantage of eight skulls, hitherto undescribed and housed at the SNSB-Bayerische Staatssammlung für Paläontologie und Geologie. Five of these skulls could be assigned to the large-antlered *C. ropalophorus*. An unexpected observation was that the dentition pattern of *Candiacervus* as suggested by the present sample differed from that typical for cervids. This may be tentatively interpreted as an adaptation to their specific insular environment.

In all analyses of the cervid skull, the water deer, *Hydropotes inermis*, commands special attention because it is the only deer that has no antlers. An early challenge of the current research project was to collect and integrate data available for this peculiar but still poorly understood cervid. To this end, we conducted an extensive search of literature covering its biogeography, its physical appearance and morphology, ecology and behaviour, aspects of genetics and phylogenetics and the fossil record. The critical review and integration of these data not only constitute a solid basis for our comparison of the skull of *H. inermis* with those of antlered cervids, but it also provides a compact and compassing guide for anyone interested in cervid biology. As detailed in the final chapter and concluding discussion of this dissertation, a comprehensive assessment of the biology of *H. inermis* puts into question the recently proposed genetic mechanism underlying the antler-less status of this species.

Arguably, unravelling the genetic basis of antler ontogenetic induction and phylogenetic origin, and its relation to the phylogenetic regression of upper canines should be a key to understanding the specifics and evolutionary diversification of the cervid skull.

Acknowledgements

I would like to thank my supervisor Gertrud Rössner for her scientific support, patience and compassionate and understanding guidance. She introduced me to a fascinating research topic and gave me the possibility to get in touch with and study cervids, which I discovered to be an amazing group of ungulates. She continuously made sure that I had access to the material I needed. I would like to thank Gertrud for her attentive supervision, numerous discussions, and for introducing me to colleagues and collaborators.

I am grateful to Prof. Wörheide and PD Mike Reich that I could pursue my studies at the SNSB-Bayerische Staatssammlung für Paläontologie und Geologie. Here, I could get insights into the different types of occupations in its paleontological collections and, yes, find the one or other job that helped me to finance my studies. Martin Nose introduced me to the public relations work of the museum and experience that I very much appreciate. Thank you, Martin!

I would like to thank all the people with whom I had the opportunity to discuss the most diverse topics regarding my Ph.D., during conferences, coffee breaks, and travelling. They gave me inspiration, ideas, and moral support. Especially, I would like to thank PD Mike Reich, Prof. Alexander Nützel, Ella Schönhofer, Herr Gregor, Bastien Mennecart, Nicola Heckeberg, Jonathan Gùzman, Angelo Poliseno, Warren Francis, and Ulla Lächele. I am also indebted to Prof. Ruijin Huang (Bonn) for his help with translating and explaining papers written in Chinese.

I am grateful to the collection managers and curators, who helped and provided me access to the collections. Without their help, this dissertation would not have been possible: Dr. Anneke van Heteren and Michael Hiermeier (Zoologische Staatssammlung München), Dr. Henriette Obermaier and Britta Möllenkamp (Staatssammlung für Anthropologie und Paläoanatomie München), PD Frank Zachos and Alexander Bibl (Naturhistorisches Museum Wien, Austria), Reinhard Ziegler (Staatliches Museum für Naturkunde Stuttgart), Christiane Funk and Steffen Bock (Museum für Naturkunde, Berlin).

I would like to acknowledge the support received by the Ludwig-Maximilians-Universität München (LMU). I was awarded an LMU TravelGrant twice. I very much appreciated the opportunity to integrate my research work with my maternal duties and pleasures.

Finally, I would like to thank my beloved ones: my family, my parents, my closest friends and all those who had open ears about deer and the ups and downs during the time I worked on this thesis.

Chapter 1

General introduction

This thesis aims to contribute to a better understanding of the skeletal biology of extant and extinct cervids. Of all parts of the skeleton, the skull arguably best informs us about the morphology, ecology, and possible behaviour of an individual, since it is involved in different functional systems.

In all jawed vertebrates (Gnathostomata), the skull houses and protects the brain as well as the large, specialized sensory organs, i.e. the eyes, the nose, the ears, and the taste buds on the tongue. Furthermore, it forms the entrance to the digestive and respiratory systems (Lieberman, 2011; Liem, Bemis, & Grande, 2011). These sensory organs and structures are crucial for interacting with the environment. The head as a whole participates in vision, smell, taste, hearing, and equilibrium as well as chewing, swallowing, and respiration. Accordingly, changes in sensory requirements, food processing, or respiration affect the respective organs and structures. Thus, adaptations to new environments will also be reflected in supporting hard tissues (Hildebrand & Goslow, 2004). A classic example is the evolution of the mammalian middle ear (e.g., Ji et al., 2009; Rich et al., 2005). Here, bones of the lower jaw were transformed and repurposed to an impedance-adapting and amplifying device.

The mammalian skull covers a wide range of sizes and shapes across species to accomplish its functions in the most different environments and lifestyles. This is particularly well documented for different diets and the concomitant changes in the masticatory apparatus (Van Valkenburgh, 1989; Schwenk, 2000; Harris & Cerling, 2002; Ungar, 2015). Other examples include the modifications of the nasal skeleton to support a trunk; the position and the orientation of the orbits, which affect the visual field and stereoscopy, or the specialized structures to support echolocation in bats and whales (Cox, 2008; Churchill et al., 2016; Orr et al., 2016). Finally, the braincase mirrors the size and the gross structure of the brain (e.g., Palombo *et al.*, 2008; Zollikofer & De León, 2013).

Consequently, for the study of extinct mammals, fossil skulls or parts thereof are particularly valuable, as they allow inferring the ecology and even conjecturing behavioural traits (Hildebrand & Goslow, 2004). Skulls, their appendices, and teeth are arguably also the most informative part of the skeleton when it comes to species characterization and identification. They have also been used to infer phylogenetic relationships (Gingerich & Schoeninger, 1977; Caumul & Polly, 2005; Cardini & Elton, 2008; Vislobokova, 2013). Thus, the investigation of skulls offers a unique view of evolution and adaptation.

1.1 The morphology of the mammalian skull

From an anatomical point of view, the skeleton of the head may be divided into two parts: the neurocranium and the viscerocranium (Starck, 1979; Nickel, Schummer, & Seiferle, 1992). The bones that form the adult skull (*osteocranium*) may be classified by their mode of ossification, i.e. whether they replace chondral anlagen (*chondrocranium*) or whether they form directly by intramembranous ossification of mesenchymal cells. They may also be classified based on their developmental origin from the mesoderm or the neural crest (for overviews, see Gross & Hanken, 2008; Kardong, 2012; Hirasawa & Kuratani, 2015). Almost all of the viscerocranium originates from the neural crest. In contrast, most bones of the neurocranium, which houses the brain, are derived from the mesoderm. Exceptions are the frontal bone, the alisphenoid, and parts of the interparietal bone, which are also derived from the neural crest (for a review, see Chai & Maxson, 2006).

From a functional point of view, the skeleton of the head of a typical mammal may be subdivided into the braincase and the facial skeleton. The former comprises the occipital, the sphenoid, the frontal, the ethmoid, the temporal, and the parietal bones. The facial skeleton is formed by the bones of the nose, the palatine, the maxillary, the vomer, the premaxillary, the mandibular, the zygomatic, and the lacrimal bones. Except for the bones forming the base of the skull (the chondrocranium) and the vomer, most of these bones occur in pairs, all of them in a bilaterally symmetric fashion.

At this point, it seems appropriate to briefly mention how the term “skull” is used in this thesis. In a strict sense, the term "skull" is used to describe all skeletal elements of the head, including the mandibula, the hyoid, and the chondral elements of the splanchnocranium (e.g., Kardong, 2012). However, the term "skull" is used variably in the literature, often meaning only the "bony skull", either including or excluding the mandibula and/or the hyoid bone. In his influential textbook, Hildebrand suggests using the term "skull" to describe "the single unit that forms the braincase and upper jaw and houses the nose and ear" (Hildebrand, 1974, p. 128) noting that the term is inexact but useful. It is in this latter sense that the term "skull" is used in this thesis.

Beyond the subdivision into braincase and facial skeleton, the skull is often partitioned into modules. These modules are typically centred about a cranial area characterized by a specific function and/or developmental origin. They are defined as a set of measures that statistically covary with each other more strongly than with other measures of the skull (Weiss, 2017). Thus, it has been proposed that the skull may be viewed as a composition of oral, nasal, vault, orbit, zygomatic, and base modules (Marroig & Cheverud, 2001; Porto et al., 2009; Haber, 2014); alternatively, a subdivision in oral-nasal, molar, orbit, zygomatic-pterygoid, cranial vault, and cranial base modules has been suggested

(Goswami, 2007; Bärmann & Sánchez-Villagra, 2012). Thus, different authors not only suggest that the skull is composed of different numbers of modules; they also suggest that these are formed by variable sets of bones and/or measures. These differences in the numbers and compositions of modules may essentially be traced to distinct views of which covariations may be considered statistically significant. Importantly, while morphological modules are defined and distinguished by statistical cut-off criteria, they are also integrated with each other (e.g., Percival & Richtsmeier, 2017, pp. 19, 53).

Recently, the evolution of these modules, their interactions, and the quantification of integration, i.e. the way modules are combined into a unit (Lieberman, 2011) have been of great scientific interest (see Klingenberg, 2008, 2014, and references therein; Porto *et al.*, 2013). According to Lieberman (2011), it is modularity and morphological integration that allow the skull to fulfil its multiple functions properly. It is also considered to be central to the evolvability of the complex structure of the skull (Goswami & Polly, 2010; Parsons *et al.*, 2018; for a review, see Klingenberg, 2008).

Arguably, the extensive interest in modules relates to their association with (macroscopic) functions. How the components of individual modules correlate with each other and how modules are integrated into a functional skull is considered to reflect evolutionary-shaped developmental processes. These should ultimately be traceable to differences in the patterns, strength, and timing of gene expression (e.g., Pavličev & Cheverud, 2015; Melo et al., 2016; Percival & Richtsmeier, 2017, p. 53).

1.2 The cervid skull

Besides the skull functions common to all mammals as described above, in some mammalian groups, the skull fulfils additional and very specific functions. Thus, the skull had to adapt to the sometime extreme modification of teeth and the development of cranial appendages like horns and antlers. For instance, teeth have become tusks in narwhales, elephants, and the mammoth. In babirusas (deer pigs), both the upper and lower canines grow upwards and curve backward. Another example is the horns of rhinos. Arguably, the most remarkable and most extensively studied cranial appendages with specific functions are the horns of bovids and cervid antlers.

Males of all but one extant cervid species bear antlers. The one exception is the water deer, *Hydropotes inermis*. In reindeer (*Rangifer*), females are also antlered. Antlers are bony outgrowths of the frontal bone which are shed and regenerated regularly. Between species, antlers differ widely in size and shape. Within species, variation in size and shape has been directly related to their function as sexual ornaments and weapons (Clutton-Brock, 1982; Kruuk *et al.*, 2002). Further functions of ant-

lers include the defence from predators (Metz *et al.*, 2018) and the establishment of social rank and, hence, access to scarce food. The latter has been well-documented for *Rangifer*, where females are known to use their antlers to compete for food for themselves and their offspring (Espmark, 1964; Loe *et al.*, 2019).

Whatever function of antlers we consider, it is clear that their weight alone loads on the skull and so do forces generated during intraspecific competition and defence against predators. While antlers *per se* have been extensively studied (e.g., Bubenik & Bubenik, 1990; Lincoln, 1992; Price *et al.*, 2005; Kierdorf & Kierdorf, 2010; Pita-Thomas *et al.*, 2017; Wang *et al.*, 2019), how their functions are integrated with the basic functions of the skull mentioned above, is still poorly understood. In particular, how mechanical strains originating from antlers and those from mastication are balanced with, or isolated from each other in the skull has not been studied.

Generally, the cervid skull shows a series of characteristics. These include the presence of a fissure between the nasal, frontal, lacrimal, and maxillary bones, the so-called "ethmoidal gap" (**Fig. 1.1**), that may, however, also be found in some other ruminants. Another characteristic is a bony depression located on the lacrimal bone housing the preorbital gland, an organ used for intraspecific communication. Cervids have also a quite large lacrimal facial facet and double lacrimal orifices. The size and the shape of the latter bone have since long attracted scientific attention, and have been used repeatedly for diagnostic purposes (Rütimeyer, 1881; Knottnerus-Meyer, 1907; Gregory, 1920). However, despite this longstanding interest, a quantitative morphometric study of this central bone of the facial skull has not been done so far.

Finally, the dentition, functionally tightly integrated with the skull is of interest, in particular the upper canine. In most cervids, upper canines are lacking or cryptic (Valli, 2010); in some species, e.g., reindeer or red deer, these teeth are rudimentary; yet in a few, these teeth are well-developed tusks. The presence, or absence, of tusks, is just one example for which cervid species differ remarkably.

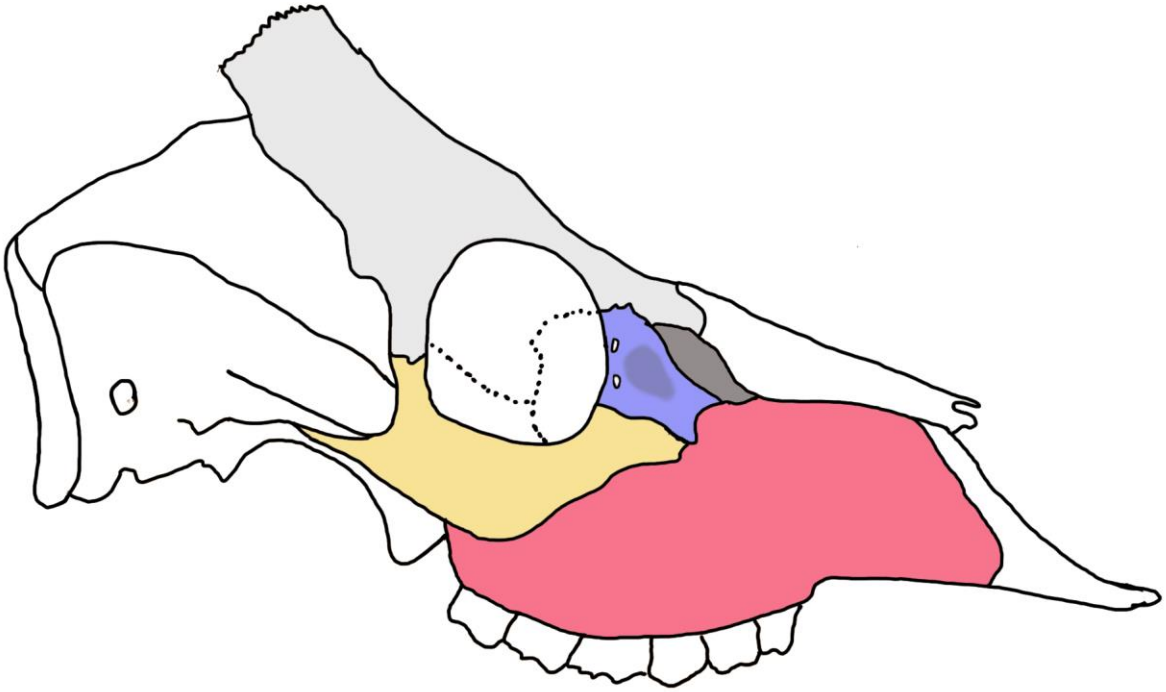

Figure 1.1 Schematic lateral view of a typical cervid skull, sketched after that of a male roe deer (*Capreolus capreolus*). Bones and structures central to the present thesis are coloured as follows: the ethmoidal gap is marked in dark grey. The facial facet of the lacrimal bone is labelled blue, while the preorbital depression is indicated by a darker hue. The maxilla is labelled red, the jugal (also known as the zygomatic bone) in ochre, and the frontal, including the pedicles of the antlers, in light grey. Overall skull length in *C. capreolus* is in the range of about 18 – 22 cm.

1.3 Some notes on the systematics, evolution, and ecology of cervids

Before I come back to those cervids which seem particularly interesting and paradigmatic considering their skull morphology, and which, therefore, I will present and discuss in this thesis in more detail, I briefly sketch out a framework on the distribution of cervids, their relationships, and the evolution of this group.

Cervids are ruminant artiodactyls, that comprise some 54 extant species (Mattioli, 2011; Heckeberg *et al.*, 2016), found in all climatic zones and diverse habitats, including the harsh conditions of the Arctic tundra (Ker & Yang, 2019). They are found on all continents but Australia and Antarctica (Mattioli, 2011). In Africa, native deer are only found along the Mediterranean: the Barbary stag (*Cervus elaphus barbarus*) and the giant deer (*Megaceros algericus*) are thought to have invaded this continent during the Plio- and Pleistocene (Goss, 1983, p. 92; Kingdon, 2013). From this region, a number of paleontological finds of *M. algericus* have been reported (e.g., Croitor, 2016). Other spe-

cies, including species of the sambar deer (*Rusa unicolor*) and the chital deer (*Axis axis)*, have likely been introduced to Africa (Leslie, 2011; Kingdon, 2013; Mattioli & Ferretti, 2014).

Cervids are closely related to Bovidae (bovids), Moschidae (musk deer), Giraffidae (giraffes), and Antilocapridae (American pronghorns), while Tragulidae (chevrotains and mouse-deer) comprises more distant relatives. With all these artiodactyl groups, cervids share a multi-chambered stomach specialized for digesting tough plant fibres through microbial-aided fermentation. This may have contributed to their evolutionary success and wide distribution (Mattioli, 2011). Suidae (pigs and peccaries), Tylopoda (camels) and Cetancodonta (whales and hippos) are even more distant relatives (**Fig. 1.2**).

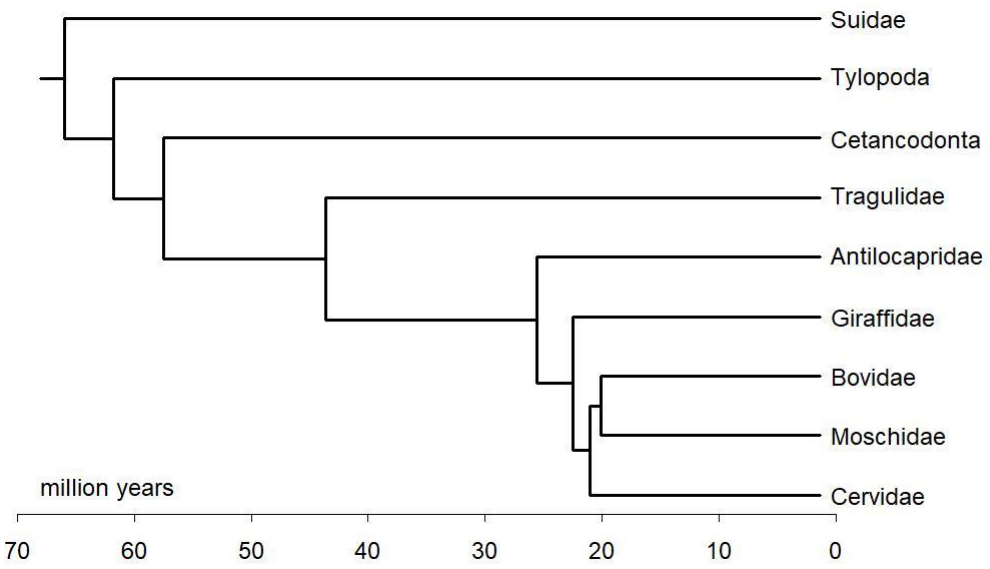

Figure 1.2 A general phylogenetic tree of artiodactyls based on molecular data of recent species. Data from Zurano *et al.* (2019).

The phylogenetic relationships among these groups as well as within cervids have been repeatedly studied, based on morphological and molecular data (e.g., Kraus & Miyamoto, 1991; Randi *et al.*, 1998; Hassanin & Douzery, 2003; Heckeberg *et al.*, 2016; Zurano *et al.*, 2019; Heckeberg, 2020). Such a combined approach is justified and indeed needed for several reasons. First, modern, DNA-based approaches are feasible only for extant species and those extinct animals, for which DNA is still available. Second, fossils may reveal morphological variation beyond that of extant animals, and hence, they may highlight gradual morphological changes that may help to interpret DNA diversity. Importantly, fossils allow the observation and dating of evolutionary changes in deep-time, and calibration of DNA-based phylogenetic trees (Bibi, 2013; Koch & Parry, 2020).

An important goal of evolutionary biology is to link DNA-based and morphology-based phylogenetic trees to understand how morphological variation reflects changes in the genome (e.g., Parker, Shearin, & Ostrander, 2010; Feiner, 2016). This challenge is not only fraught with the inevitable "gaps" in molecular and morphological datasets; it is also aggravated by the fact that palaeontologists and molecular biologists define clades differently, in basing their nomenclatures on shared anatomical characteristics or genetic similarity, respectively. This issue was addressed recently by Bibi (2014), and in the following, we use the standardized nomenclature for the ruminant clades he proposed.

According to the current view (Mennecart *et al.*, 2017; Chen *et al.*, 2019; Heckeberg, 2020), Cervidae originated in the Early Miocene (≈ 20 mya), during the radiation of Pecora. It may be divided into two subfamilies, the Cervinae and the Capreolinae (Hassanin *et al.*, 2012; Heckeberg *et al.*, 2016, fig. 1 therein; Heckeberg, 2020). The distinction between these two groups is classically based on the anatomy of the second and fifth metacarpal: in Cervinae, only the proximal parts of these metacarpals are retained, while in Capreolinae, the distal parts of these bones are retained (Brooke, 1878). These clades are also strongly supported by molecular data (e.g., Gilbert, Ropiquet, & Hassanin, 2006). Furthermore, most members of Capreolinae may be distinguished from Cervinae by a vomerine septum, that extends posteriorly and that divides the nasal cavities completely (Bouvrain, Geraads, & Jehenne, 1989). However, in *Alces* (the moose), *Capreolus* (the roe deer), and *Hydropotes* (the water deer), the nasal cavities are not completely separated by the vomer (Brooke, 1878; Allen, 1940; Croitor, 2018).

Figure 1.3 builds on the recent classification provided by Heckeberg (2020) and presents a simplified excerpt of her classification, as relevant for the present work. In this context, two aspects should be mentioned: Within the Pan-Ruminantia, Cervidae belongs to the Pan-Pecora *sensu* Bibi (2014) and so do Moschidae, Bovidae, Giraffidae, Antilocapridae, and some extinct groups. All living pecorans but *Moschus* (the musk deer) and *Hydropotes* bear group-specific cranial appendages, namely, antlers, horns, ossicones, or pronghorns. Traditionally, evidence from developmental biology and histology has been interpreted as indicating that these different cranial appendages were convergent organs (Janis & Scott 1987, Davis et al. 2011). Recent data suggest a single origin in the pan-pecoran ancestor which then diversified into the four types of headgear. Based on these data, it has also been proposed that *Hydropotes* and *Moschus* secondarily lost their headgear due to pseudogenization of the gene, *Rxfp2* (Chen *et al.*, 2019; Wang *et al.*, 2019).

As exemplified by *Hydropotes* and *Moschus*, Pecora also comprise members that lack cranial appendages and that bear large, sabretooth-like upper canines. This character combination is also known from stem Pecora and fossil ruminants predating the origin of Pan-Pecora, members of their

sister-group Pan-Tragulina, as well as their living descendants, members of the Tragulidae. Therefore, the combination of cranial appendages and large upper canines is considered plesiomorphic. The fossil record of cervids also documents the successive reduction of upper canines up to the complete loss thereof. This was correlated with the appearance and size increase of antlers (e.g., Scott & Janis, 1987; Gentry, 1994; Janis, 2007; Emlen, 2008; DeMiguel, Azanza, & Morales, 2014). As mentioned above, only a few species retained small upper canines and even fewer show tusk-like upper canines. The latter are the muntjacs (*Muntiacus*), the tufted deer (*Elaphodus*), and the water deer (*Hydropotes*) (**Fig. 1.3**).

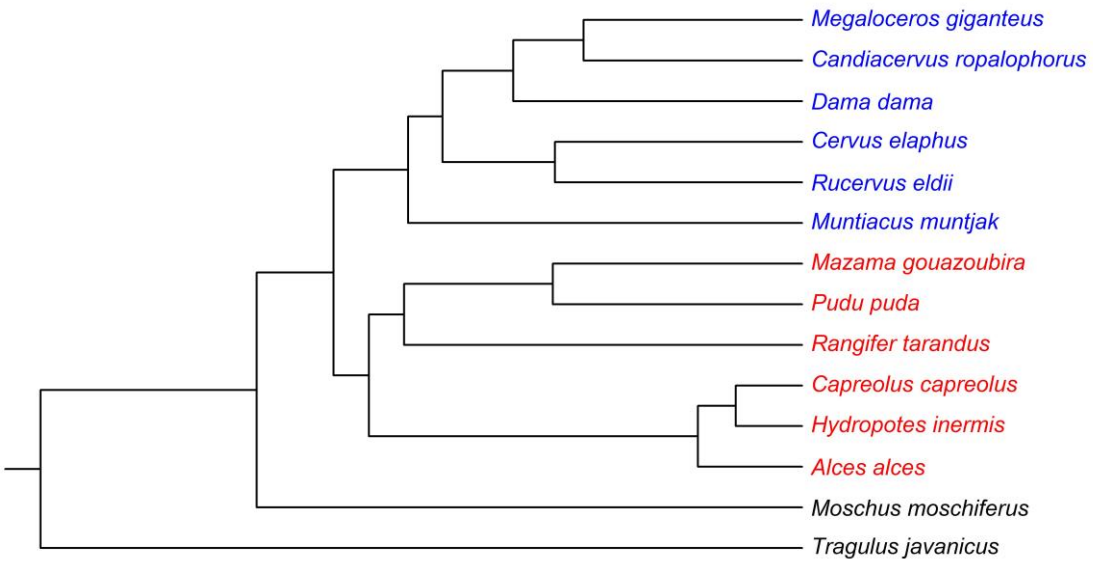

Figure 1.3 Phylogenetic relationships between the cervid species studied in this thesis. Cervinae is shown in blue, and Capreolinae in red. The topology is in agreement with those presented in Bärmann & Sánchez-Villagra, 2012; Mennecart *et al.*, 2017; Heckeberg, 2020, fig. 14C). *Megaloceros* was placed following Lister *et al.*, 2005; Hughes *et al.*, 2006; and Immel *et al.*, 2015. Whether *Candiacervus* is closer to *Megaloceros* (as shown here; de Vos, 1979) or closer to *Dama* (see e.g., van der Geer, 2018) is still debated (see also **Chapter 4** for additional references). The branch length is not scaled.

Beyond the development, diversification, and loss of antlers and canines, cervids have also undergone (extreme) changes in body size during evolution. Their body weights range from that of first cervids from the Miocene, e.g., *Procervulus praelucidus (*18 kg; Kolb *et al.*, 2015) and *Heteroprox eggeri (*ca. 24 kg; Rössner, 2010), which were comparable in size with extant "small solitary forest deer" (Barrette, 1987, p. 202), to that of the Pleistocene giant deer, *Megaloceros giganteus* (ca. 600 kg; Geist, 1998) and *Cervalces latifrons* (ca. 1000 kg; Saarinen *et al.*, 2016). The evolutionary history of cervids seems to document a general trend toward increased body size, although for some species, notably the Jersey deer (Lister, 1989), and the South American pudus (*Pudu*) and brocket deer (*Mazama*) (Eisenberg, 2000) dwarfing has been described, or discussed.

Changes in skull size are typically proportional to changes in body size (Costeur *et al.*, 2019; for a more general perspective and discussion, see e. g., Gould, 1975; Cardini & Polly, 2013; Cardini et al., 2015) and reflect metabolic needs to build and maintain a larger body. However, they also went along with changes in antler size and branching pattern. Antler size shows strong positive allometry with both body size and skull size (Gould, 1973, 1974; Clutton-Brock, Albon, & Harvey, 1980; Hayden, Lynch, & O'Corry-Crowe, 1994; Melnycky *et al.*, 2013). As scaling of the masticatory apparatus, crucial to supporting metabolic needs, and that of antlers differ, changes in body size are predicted to affect the way the skull is integrated. Two notorious examples of size divergence from the fossil record are the giant deer, e.g. *Megaloceros*, which had the absolute largest antlers ever known, and some species of *Candiacervus*, the Cretan deer. The latter, closely related to giant deer, are of particular interest, as they attained their stature by dwarfing. Intriguingly, the smallest of these dwarfs also maintained apparently extremely long antlers relative to their body size.

1.4 Questions and topics addressed

This evolutionary diversification of skull and antler size and structure brings up the question of how the contrasting mechanical functions that the skull supports are integrated throughout the cervid clade. Of note, forces acting through antlers and those mediated through the masticatory apparatus may be presumed to require tight integration between the braincase and the facial skeleton. For a general background on the mechanical integration of the neuro- and viscerocranium, the reader may be referred to Ross & Metzger (2004) and Franks *et al.* (2016).

As mentioned above, cervids show a quite prominent facial facet of the lacrimal bone, which is located between the facial skeleton and the braincase. Therefore, we first sought to provide a systematic, quantitative analysis of the size, shape, and variability of this bone in a selected set of extant cervids and relate its variability to the ecology and phylogeny of cervids (Schilling, Calderón-Capote, & Rössner, 2019; **Chapter 2**). Next, we asked how the morphology of the lacrimal bone of two extreme fossil cervids, the giant deer, *Megaloceros*, and the dwarf deer, *Candiacervus* compares to that of living cervids (**Chapter 3**).

Third, we analysed the specific structure of the skull of the dwarfed deer from Crete, *Candiacervus*. This required the description and taxonomic classification of hitherto undescribed material housed at the SNSB-Bayerische Staatssammlung für Paläontologie und Geologie, Munich, Germany (Schilling & Rössner, 2021; **Chapter 4**). The goal of this study was to set a framework that would allow to put the

lacrimal facial facet of *Candiacervus* into an anatomical context and to relate it to the ecological conditions to which this cervid had adapted.

The skull of the only deer without antlers, *Hydropotes inermis*, the males of which carry, however, impressive upper canines, certainly deserves special attention in any attempt to analyse the cervid skull. Yet the interpretation of its specific structure is hindered by the fact that description of this species, its behaviour, and its ecology are scattered widely in the literature. One of the goals of the present thesis, therefore, was to compile and critically review what we know about this still enigmatic animal. This is presented in **Chapter 5** (Schilling & Rössner, 2017).

The results of these questions and their discussion are presented in the next four chapters of this thesis. Each of these chapters was conceived as an independent scientific article, and three of them (**Chapters 2**, **4**, and **5**) have been published recently. Finally, in **Chapter 6**, I connect these four studies and discuss the results in a wider evolutionary context, that should give hints for future studies in this research field.

1.5 Overview of the studies presented in Chapters 2 through 5

In **Chapter 2**, we summarize results from a detailed investigation of the morphology of the lacrimal bone of living cervids. As mentioned above in sections 1.2 and 1.3, cervids are known for their relatively conspicuous lacrimal bone with a particularly large facial facet. A number of studies mostly performed in the late 19th and early 20th centuries have reported detailed morphological descriptions of qualitative characters of the lacrimal bone in multiple species, including cervids (Kober, 1880; Knottnerus-Meyer, 1907; Gregory, 1920), and these have also been used to discriminate cervid species. However, quantitative analysis and notably any attempt to explain this morphological variability within the context of cervid evolution and ecology were so far missing.

At first glance, the main functions of the lacrimal bone arguably consist in supporting the facial skeleton. Significantly, the lacrimal facial facet holds a central position linking the antler-bearing frontal bone of the neurocranium with the facial skeleton, and in particular the maxilla. It directly abuts the frontal bone anteriorly to the orbita. Further, it is connected indirectly to the frontal bone by way of the jugal, which shares a rather long suture with the lacrimal bone (Schilling *et al.*, 2019, fig. 2). On the one hand, the part of the jugal bone intercalated between the lacrimal and the maxilla connects these two bones. On the other hand, the lacrimojugal suture may add to the dissipation of stress originating from the frontal and hence, may help to insulate the maxilla. Moreover, the lacrimal facial facet also houses the preorbital gland, that is located in a conspicuous bony depression. One open

question is how the size of the lacrimal facial facet relates to the size of the depression and whether such a relationship could be interpreted in terms of cervid ecology.

Thus, a better knowledge of the size, shape and (functional) integration of the lacrimal facial facet should add to our understanding of the specifics of the skull of cervids. Further, a functional signal in the lacrimal bone of living cervids might be useful to infer ecology and behaviour in fossil cervids.

To approach this issue, we morphometrically analysed the lacrimal facial facet in ten genera of cervids, from the small, antler-less water deer (*Hydropotes inermis*) to the largest extant cervid, the moose (*Alces alces*). Specimens from *Moschus moschiferus* and *Tragulus spp.* were used as ruminant outgroups. In the resultant publication, we provide a detailed quantitative description of the morphology of the facial facet of the lacrimal and a concise database of linear measurements. We address the relationships between the size of the lacrimal facial facet and that of the preorbital depression and the inference that can be made concerning the gland. The quantitative results obtained allowed us to relate the size and shape of the lacrimal facial facet to antler size, and we discuss them within the context of whether and how the lacrimal may contribute to dissipating stress resulting from antlers and their usage. We conclude that the lacrimal bone in cervids has probably exapted to better support large antlers. These quantitative data also provide a background for the analysis and interpretation of the lacrimal facial facet in extinct cervids.

In **Chapter 3**, then, we present the analysis of the lacrimal facial facet of two emblematic, well-known extinct cervids from the Pleistocene, *Megaloceros* and *Candiacervus*. The giant deer and its dwarfed relative show morphological characteristics that are not found in any living cervid. As far as technically possible, we applied the methods described in **Chapter 2**. The results obtained document that both fossil cervids have relatively small lacrimal facial facets. Its shape is similar in *Megaloceros* and *Candiacervus,* but clearly distinct from that observed in living cervids. We discuss these findings with a focus on the peculiar antler structure of these fossil cervids and their potential use.

In **Chapter 4,** we describe the skulls of the *Candiacervus* specimens used in the previous chapter in detail. *Candiacervus* is an extinct deer that lived in Crete during the Pleistocene in a predator-free environment. Its phylogeny and affinity with other deer are still controversial. It is often considered to be a descendant of large mainland deer, possibly *Megaloceros*, and to have undergone secondary size reduction, as is often found in isolated island populations (e.g., Foster, 1964; Lomolino, 2005). Another contested question is how many different species of *Candiacervus* actually existed, and how they may be related (de Vos, 1984; for a recent review and further references see also van der Geer, 2018).

The material analysed here was collected nearly 50 years ago from a little-known fossil site located close to the village Gerani, Rethymnon, Crete, and it was recently "rediscovered" in the drawers of the Munich collection. This new material, partially outstandingly well-preserved, offered the unique opportunity to broaden our knowledge about this cervid, giving insights into its presumable biology and adaptation.

I had the opportunity to talk to Dr H.-J. Gregor, who had excavated these specimens and, hence, I was able to reconstruct at least some details about the location and circumstances where this material was found. The qualitative description and the quantitative morphometric analysis of this new material presented here revealed that *Candiacervus* had a dental eruption sequence atypical for cervids, that may be interpreted as an adaption to its particular environment, to mention just one key finding. Finally, yet importantly, we present an in-depth comparison of an extensive set of qualitative and quantitative character traits of the present specimens with those of Megaloceros and other giant deer.

In **Chapter 5**, we present an extensive review and critical assessment of the biology and phylogeny of the water deer, *Hydropotes inermis*. As mentioned in Sections 1.2 and 1.3, *H. inermis* is arguably the cervid with the most particular cranial phenotype. The lack of antlers and the presence of sabre-tooth-like upper canines in males constitute a unique combination of traits among extant cervids. This phenotype largely dominated the scientific interest in this species, both from a behavioural (e.g., Barrette, 1987; Cap, Aulagnier, & Deleporte, 2002; Cap *et al.*, 2008) and a phylogenetic perspective. Phylogenetically, this character combination resembles the situation seen in living Moschidae and Tragulidae, and also often in fossil ruminants (Janis & Scott, 1987, table 3), including those that either had a common ancestor with cervids, or that may even have been on the lineage towards cervids (e.g., *Dremotherium*; Heckeberg, 2020 and references therein). Consequently, this character combination has been considered a plesiomorphic condition for cervids, and *Hydropotes inermis* was labelled as representative of an archaic lineage constituting a sister group to all other living cervids (Lister, 1984; Groves & Grubb, 1987; Janis & Scott, 1987; Hernández Fernández & Vrba, 2005). In contrast, others have classified *H. inermis* as a close relative of roe deer (*Capreolus capreolus*), based on genetic, mostly mitochondrial evidence, as well as on morphological characters (Bouvrain *et al.*, 1989; Douzery & Randi, 1997; Randi *et al.*, 1998; Meyer *et al.*, 2001; Hassanin & Douzery, 2003; S. A. Price, Bininda-Emonds, & Gittleman, 2005; Gilbert *et al.*, 2006; Hassanin *et al.*, 2012). This implicates that the cranial phenotype of *H. inermis* reflects a reversion to an ancestral status. Such a secondary loss of antlers seems to be supported by recent analyses based on whole-genome sequencing of cervids (Chen *et al.*, 2019; Wang *et al.*, 2019). This latter study highlights the important role of *H. inermis* as a potential model organism to understand cervid evolution and ecol-

ogy. This is certainly true for the quest to unveil the genetic basis of antler formation. It also provides additional motivation to study the relationship between antlers and the structure of the facial skull.

When work on the present project started, it was agreed upon that *Hydropotes inermis* was particular among cervids, but its specific phylogenetic affinities were still debated, as were several aspects of its biology. One issue here was that information about this species was widely scattered throughout the literature. Following the species' discovery by the end of the 19th century, Allen, in 1940, provided a major summary of what was known by then. Cooke & Farrell (1998) presented another detailed description of *Hydropotes*, with a strong focus on the ecology and conservation of this species, drawing mainly on data obtained from British populations. Apart from these two references, information on the biology of *H. inermis* is typically found "between the lines" of publications primarily focussing on other artiodactyls or ruminants. Indeed, in most of these studies, it is the phylogenetic position of *H. inermis* that is the primary interest, rather than the biology of this species. Studies dedicated to the biology, behaviour, and ecology of this species are rather rare, and often hard to access due to their age or the fact that they are published in languages other than English.

In the review presented in **Chapter 5**, therefore, we summarize data about *Hydropotes inermis* drawn from the literature published in English, French, Italian, German, and also in Chinese. Relevant publications were identified by an extensive and multi-pronged search of several databases, including, among others, PubMed, Google Scholar, and Biodiversity Heritage Library, and covering the period from 1870, when *H. inermis* was first described up to when our review was submitted. This allowed us to combine and synthesize data that had been widely dispersed, and thus obtain an integrative view of the biogeography and conservation, the morphology, the ecology and behaviour, and the systematics, evolutionary history, and phylogeny of *H. inermis.*

Together, this critical survey provides a concise basis to compare *Hydropotes inermis* with its cervid relatives, and for probing the basis of any differences. It should also be helpful to understand the functional consequences of the genetic differences between *H. inermis* and other cervids, that have recently become accessible for analysis with the establishment of the ruminant genome database (RGD; see: http://animal.nwsuaf.edu.cn/code/index.php/Ruminantia; Chen *et al.*, 2019; Ker & Yang, 2019; Wang *et al.*, 2019).

1.6 References

ALLEN, G.M. (1940) The mammals of China and Mongolia. Part 2. *Natural History of Central Asia Series.* **XI**, 621–1350. American Museum of Natural History, New York.

BÄRMANN, E. V. & SÁNCHEZ-VILLAGRA, M.R. (2012) A Phylogenetic Study of Late Growth Events in a Mammalian Evolutionary Radiation-The Cranial Sutures of Terrestrial Artiodactyl Mammals. *Journal of Mammalian Evolution* **19**, 43–56.

BARRETTE, C. (1987) The comparative behavior and ecology of chevrotains, musk deer and morphologically conservative deer. In *Biology and management of the Cervidae* (ed C.M. WEMMER), pp. 200–213. Smithsonian Institution Press, Washington.

BIBI, F. (2013) A multi-calibrated mitochondrial phylogeny of extant Bovidae (Artiodactyla, Ruminantia) and the importance of the fossil record to systematics. *BMC Evolutionary Biology* **13**, 1–15.

BIBI, F. (2014) Assembling the ruminant tree: Combining morphology, molecules, extant taxa, and fossils. *Zitteliana B*, 197–211.

BOUVRAIN, G., GERAADS, D. & JEHENNE, Y. (1989) Nouvelles données relatives à la classification des Cervidae (Artiodactyla, Mammalia). *Zoologischer Anzeiger* **223**, 82–90.

BROOKE, V. (1878) On the Classification of the Cervidae, with a Synopsis of the existing Species. *Proceedings of the Zoological Society of London* **46**, 883–928.

BUBENIK, G.A. & BUBENIK, A.B. (1990) *Horns, Pronghorns, and Antlers: Evolution, Morphology, Physiology, and Social Significance*, 1st edition. Springer, New York.

CAP, H., AULAGNIER, S. & DELEPORTE, P. (2002) The phylogeny and behaviour of Cervidae (Ruminantia Pecora). *Ethology Ecology and Evolution* **14**, 199–216.

CAP, H., DELEPORTE, P., JOACHIM, J. & REBY, D. (2008) Male vocal behavior and phylogeny in deer. *Cladistics* **24**, 917–931.

CARDINI, A. & ELTON, S. (2008) Does the skull carry a phylogenetic signal? Evolution and modularity in the guenons. *Biological Journal of the Linnean Society* **93**, 813–834.

CARDINI, A., POLLY, D., DAWSON, R. & MILNE, N. (2015) Why the Long Face? Kangaroos and Wallabies Follow the Same 'Rule' of Cranial Evolutionary Allometry (CREA) as Placentals. *Evolutionary Biology* **42**, 169–176.

CARDINI, A. & POLLY, P.D. (2013) Larger mammals have longer faces because of size-related constraints on skull form. *Nature Communications* **4**, 2458.

CAUMUL, R. & POLLY, P.D. (2005) Phylogenetic and environmental components of morphological variation: Skull, mandible, and molar shape in marmots (Marmota, Rodentia). *Evolution* **59**, 2460–2472.

CHAI, Y. & MAXSON, R.E. (2006) Recent advances in craniofacial morphogenesis. *Developmental Dynamics* **235**, 2353–2375.

CHEN, L., QIU, Q., JIANG, Y., WANG, K., LIN, Z., LI, Z., ET AL. (2019) Large-scale ruminant genome sequencing provides insights into their evolution and distinct traits. *Science* **364**, eaav6202.

CHURCHILL, M., MARTINEZ-CACERES, M., DE MUIZON, C., MNIECKOWSKI, J. & GEISLER, J.H. (2016) The Origin of High-Frequency Hearing in Whales. *Current Biology* **26**, 2144–2149.

CLUTTON-BROCK, T.H. (1982) The Functions of Antlers. *Behaviour* **79**, 108–124.

CLUTTON-BROCK, T.H., ALBON, S.D. & HARVEY, P.H. (1980) Antlers, body size and breeding group size in the Cervidae. *Nature* **285**, 565–567.

COOKE, A. & FARRELL, L. (1998) *Chinese Water Deer*. The Mammal Society, London and The British Deer Society, London, Hampshire.

COSTEUR, L., MENNECART, B., MÜLLER, B. & SCHULZ, G. (2019) Observations on the scaling relationship between bony labyrinth, skull size and body mass in ruminants. In *Proceedings of SPIE* pp. 1–10. International Society for Optics and Photonics, San Diego.

COX, P.G. (2008) A quantitative analysis of the Eutherian orbit: correlations with masticatory apparatus. *Biological Reviews* **83**, 35–69.

CROITOR, R. (2016) Systematical position and paleoecology of the endemic deer *Megaceroides algericus* Lydekker, 1890 (Cervidae, Mammalia) from the late Pleistocene-early Holocene of North Africa. *Geobios* **49**, 265–283.

CROITOR, R. (2018) *Plio-Pleistocene Deer Of Western Palearctic: Taxonomy, Systematics, Phylogeny*. Institute of Zoology of the Academy of Sciences of Moldova, Chișinău.

DEMIGUEL, D., AZANZA, B. & MORALES, J. (2014) Key innovations in ruminant evolution: A paleontological perspective. *Integrative Zoology* **9**, 412–433.

DOUZERY, E. & RANDI, E. (1997) The Mitochondrial Control Region of Cervidae: Evolutionary Patterns and Phylogenetic Content. *Molecular Biology and Evolution* **14**, 1154–1166.

EISENBERG, J.F. (2000) The contemporary Cervidae of Central and South America. In *Antelopes, deer, and relatives: fossil record, behavioral ecology, systematics, and conservation* (eds E.S. VRBA & G.B. SCHALLER), pp. 189–202. Yale University Press, New Haven.

EMLEN, D.J. (2008) The Evolution of Animal Weapons. *Annual Review of Ecology, Evolution, and Systematics* **39**, 387–413.

ESPMARK, Y. (1964) Studies in dominance-subordination relationship in a group of semi-domestic reindeer (*Rangifer tarandus* L.). *Animal Behaviour* **12**, 420–426.

FEINER, N. (2016) Accumulation of transposable elements in *Hox* gene clusters during adaptive radiation of *Anolis* lizards. *Proceedings of the Royal Society B* **283**, 20161555.

FOSTER, J.B. (1964) Evolution of mammals on Islands. *Nature* **202**, 234–235.

FRANKS, E.M., HOLTON, N.E., SCOTT, J.E., MCABEE, K.R., RINK, J.T., PAX, K.C., PASQUINELLY, A.C., SCOLLAN, J.P., EASTMAN, M.M. & RAVOSA, M.J. (2016) Betwixt and Between: Intracranial Perspective on Zygomatic Arch Plasticity and Function in Mammals. *Anatomical Record* **299**, 1646–1660.

VAN DER GEER, A. (2018) Uniformity in variety: Antler morphology and evolution in a predator-free environment. *Palaeontologia Electronica* **21**, 1–31.

GEIST, V. (1998) *Deer of the World: Their Evolution, Behaviour, and Ecology*, 1st edition. Swan Hill Press, Shrewsbury.

GENTRY, A.W. (1994) The Miocene Differentiation of Old World Pecora (Mammalia). *Historical Biology* **7**, 115–158.

GILBERT, C., ROPIQUET, A. & HASSANIN, A. (2006) Mitochondrial and nuclear phylogenies of Cervidae (Mammalia, Ruminantia): Systematics, morphology, and biogeography. *Molecular Phylogenetics and Evolution* **40**, 101–117.

GINGERICH, P.D. & SCHOENINGER, M. (1977) The fossil record and primate phylogeny. *Journal of Human Evolution* **6**, 483–505.

GOSS, R.J. (1983) *Deer Antlers - Regeneration, Function and Evolution*. Academic Press, London.

GOSWAMI, A. (2007) Cranial modularity and sequence heterochrony in mammals. *Evolution and Development* **9**, 290–298.

GOSWAMI, A. & POLLY, P.D. (2010) The influence of modularity on cranial morphological disparity in Carnivora and Primates (Mammalia). *PLoS ONE* **5**, e9517.

GOULD, S.J. (1973) Positive allometry of antlers in the "Irish Elk", *Megaloceros giganteus*. *Nature* **244**, 375–376.

GOULD, S.J. (1974) The Origin and Function of "Bizarre" Structures: Antler Size and Skull Size in the "Irish Elk," *Megaloceros giganteus*. *Evolution* **28**, 191.

GOULD, S.J. (1975) On the scaling of tooth size in mammals. *Integrative and Comparative Biology* **15**, 353–362.

GREGORY, W.K. (1920) Article II. - Studies in Comparative Myology and Osteology: No. IV. - A Review of the Evolution of the Lacrymal Bone of Vertebrates with Special Reference to That of Mammals. *Bulletin of the American Museum of Natural History* **XLII**, 95–263.

GROSS, J.B. & HANKEN, J. (2008) Review of fate-mapping studies of osteogenic cranial neural crest in vertebrates. *Developmental Biology* **317**, 389–400.

GROVES, C.P. & GRUBB, P. (1987) Relationships of Living Deer. In *Biology and Management of the Cervidae* (ed C.M. WEMMER), pp. 20–59. Smithsonian Institution Press, Washington.

HABER, A. (2014) The Evolution of Morphological Integration in the Ruminant Skull. *Evolutionary Biology* **42**, 99–114.

HARRIS, J.M. & CERLING, T.E. (2002) Dietary adaptations of extant and Neogene African suids. *Journal of*

Zoology **256**, 45–54.

HASSANIN, A., DELSUC, F., ROPIQUET, A., HAMMER, C., JANSEN VAN VUUREN, B., MATTHEE, C., RUIZ-GARCIA, M., CATZEFLIS, F., ARESKOUG, V., NGUYEN, T.T. & COULOUX, A. (2012) Pattern and timing of diversification of Cetartiodactyla (Mammalia, Laurasiatheria), as revealed by a comprehensive analysis of mitochondrial genomes. *Comptes Rendus Biologies* **335**, 32–50.

HASSANIN, A. & DOUZERY, E.J.P. (2003) Molecular and morphological phylogenies of Ruminantia and the alternative position of the Moschidae. *Systematic Biology* **52**, 206–228.

HAYDEN, T.J., LYNCH, J.M. & O'CORRY-CROWE, G. (1994) Antler growth and morphology in a feral sika deer *Cervus nippon* population in Killarney, Ireland. *Journal of Zoology* **232**, 21–35.

HECKEBERG, N.S. (2020) The systematics of the Cervidae: A total evidence approach. *PeerJ* **8**, e8114.

HECKEBERG, N.S., ERPENBECK, D., WÖRHEIDE, G. & RÖSSNER, G.E. (2016) Systematic relationships of five newly sequenced cervid species. *PeerJ* **4**, e2307.

HERNÁNDEZ FERNÁNDEZ, M. & VRBA, E.S. (2005) A complete estimate of the phylogenetic relationships in Ruminantia: A dated species-level supertree of the extant ruminants. *Biological Reviews of the Cambridge Philosophical Society* **80**, 269–302.

HILDEBRAND, M. (1974) *Analysis of the Vertebrate Structure*. John Wiley & Sons, New York.

HILDEBRAND, M. & GOSLOW, G. (2004) *Vergleichende und funktionelle Anatomie der Wirbeltiere*, 1st edition. Springer, Berlin.

HIRASAWA, T. & KURATANI, S. (2015) Evolution of the vertebrate skeleton: morphology, embryology, and development. *Zoological Letters* **1**, 1–17.

HUGHES, S., HAYDEN, T.J., DOUADY, C.J., TOUGARD, C., GERMONPRÉ, M., STUART, A., LBOVA, L., CARDEN, R.F., HÄNNI, C. & SAY, L. (2006) Molecular phylogeny of the extinct giant deer, *Megaloceros giganteus*. *Molecular Phylogenetics and Evolution* **40**, 285–291.

IMMEL, A., DRUCKER, D.G., BONAZZI, M., JAHNKE, T.K., MÜNZEL, S.C., SCHUENEMANN, V.J., HERBIG, A., KIND, C.J. & KRAUSE, J. (2015) Mitochondrial genomes of giant deers suggest their late survival in central Europe. *Scientific Reports* **5**, 10853.

JANIS, C.M. (2007) Evolutionary patterns and paleobiology. In *The Evolution of Artiodactyls* (eds D.R. PROTHERO & S.E. FOSS), pp. 292–302. John Hopkins University Press, Baltimore.

JANIS, C.M. & SCOTT, K.M. (1987) The Interrelationships of Higher Ruminant Families with Special Emphasis on the Members of the Cervoidea. *American Museum Novitates* **2893**, 1–85.

JI, Q., LUO, Z.X., ZHANG, X., YUAN, C.X. & XU, L. (2009) Evolutionary development of the middle ear in mesozoic therian mammals. *Science* **326**, 278–281.

KARDONG, K. V (2012) *Vertebrates: comparative anatomy, function, evolution*, 6th edition. McGraw-Hill, New York.

KER, D.F.E. & YANG, Y.P. (2019) Ruminants: Evolutionary past and future impact. *Science* **364**, 1130–

1131.

KIERDORF, U. & KIERDORF, H. (2010) Deer antlers - A model of mammalian appendage regeneration: An extensive review. *Gerontology* **57**, 53–65.

KINGDON, J (2013) Superfamily Cervoidea. In *Mammals of Africa: Volume VI: Pigs, Hippopotamuses, Chevrotain, Giraffes, Deer and Bovids* (eds JONATHAN KINGDON & M. HOFFMANN), pp. 116–119. Bloomsbury Publishing, London.

KLINGENBERG, C.P. (2008) Morphological integration and developmental modularity. *Annual Review of Ecology, Evolution, and Systematics* **39**, 115–132.

KLINGENBERG, C.P. (2014) Studying morphological integration and modularity at multiple levels: Concepts and analysis. *Philosophical Transactions of the Royal Society B* **369**, 20130249.

KNOTTNERUS-MEYER, T.C.B. (1907) Über das Tränenbein der Huftiere: Vergleichend -anatomischer Beitrag zur Systematik der rezenten Ungulata. *Archiv für Naturgeschichte* **73**, 1–152.

KOBER, J. (1880) Vergleichend-anatomische Beiträge zur Geschichte des Thränenbeins. *Jahreshefte des Vereins für Vaterländische Naturkunde in Württemberg* **36**, 118–154.

KOCH, N.M. & PARRY, L.A. (2020) Death is on our side: Paleontological data drastically modify phylogenetic hypotheses. *Systematic Biology* **69**, 1052–1067.

KOLB, C., SCHEYER, T.M., LISTER, A.M., AZORIT, C., DE VOS, J., SCHLINGEMANN, M.A.J., RÖSSNER, G.E., MONAGHAN, N.T. & SÁNCHEZ-VILLAGRA, M.R. (2015) Growth in fossil and extant deer and implications for body size and life history evolution. *BMC Evolutionary Biology* **15**, 19.

KRAUS, F. & MIYAMOTO, M.M. (1991) Rapid Cladogenesis Among the Pecoran Ruminants: Evidence from Mitochondrial DNA Sequences. *Systematic Zoology* **40**, 117–130.

KRUUK, L.E.B., SLATE, J., PEMBERTON, J.M., BROTHERSTONE, S., GUINNESS, F. & CLUTTON-BROCK, T. (2002) Antler size in red deer: Heritability and selection but no evolution. *Evolution* **56**, 1683–1695.

LESLIE, D.M. (2011) *Rusa unicolor* (Artiodactyla: Cervidae). *Mammalian Species* **43**, 1–30.

LIEBERMAN, D.E. (2011) *The Evolution of the Human Head*. Harvard University Press, Cambridge.

LIEM, K.F., BEMIS, W.E. & GRANDE, L. (2011) *Anatomia comparata dei vertebrati: una visione funzionale ed evolutiva*, 3rd edition. Edises, Napoli.

LINCOLN, G.A. (1992) Biology of antlers. *Journal of Zoology* **226**, 517–528.

LISTER, A.M. (1984) Evolutionary and ecological origins of British deer. *Proceedings of the Royal Society of Edinburgh* **82**, 205–229.

LISTER, A.M. (1989) Rapid dwarfing of red deer on Jersey in the Last Interglacial. *Nature* **342**, 539–542.

LISTER, A.M., EDWARDS, C.J., NOCK, D.A.W., BUNCE, M., VAN PIJLEN, I.A., BRADLEY, D.G., THOMAS, M.G. & BARNES, I. (2005) The phylogenetic position of the "giant deer" *Megaloceros giganteus*. *Nature* **438**, 850–853.

LOE, L.E., PIGEON, G., ALBON, S.D., GISKE, P.E., IRVINE, R.J., ROPSTAD, E., STIEN, A., VEIBERG, V. & MYSTERUD,

A. (2019) Antler growth as a cost of reproduction in female reindeer. *Oecologia* **189**, 601–609.

LOMOLINO, M. V. (2005) Body size evolution in insular vertebrates: Generality of the island rule. *Journal of Biogeography* **32**, 1683–1699.

MARROIG, G. & CHEVERUD, J.M. (2001) A comparison of phenotypic variation and covariation patterns and the role of phylogeny, ecology, and ontogeny during cranial evolution of New World Monkeys. *Evolution* **55**, 2576–2600.

MATTIOLI, S. (2011) Family Cervidae (Deer). In *Handbook of the Mammals of the World - Volume 2* (eds D.E. WILSON & R.A. MITTERMEIER), pp. 350–443, 1st edition. Lynx Ediciones, Barcelona.

MATTIOLI, S. & FERRETTI, F. (2014) Morphometric characterization of Mesola red deer *Cervus elaphus italicus* (Mammalia: Cervidae). *Italian Journal of Zoology* **81**, 144–154.

MELNYCKY, N.A., WELADJI, R.B., HOLAND, Ø. & NIEMINEN, M. (2013) Scaling of antler size in reindeer (*Rangifer tarandus*): Sexual dimorphism and variability in resource allocation. *Journal of Mammalogy* **94**, 1371–1379.

MELO, D., PORTO, A., CHEVERUD, J.M. & MARROIG, G. (2016) Modularity: Genes, Development, and Evolution. *Annual Review of Ecology, Evolution, and Systematics* **47**, 463–486.

MENNECART, B., DEMIGUEL, D., BIBI, F., RÖSSNER, G.E., MÉTAIS, G., NEENAN, J.M., WANG, S., SCHULZ, G., MÜLLER, B. & COSTEUR, L. (2017) Bony labyrinth morphology clarifies the origin and evolution of deer. *Scientific Reports* **7**, 13176.

METZ, M.C., EMLEN, D.J., STAHLER, D.R., MACNULTY, D.R., SMITH, D.W. & HEBBLEWHITE, M. (2018) Predation shapes the evolutionary traits of cervid weapons. *Nature Ecology and Evolution* **2**, 1619–1625.

MEYER, W., POHLMEYER, K., SCHNAPPER, A. & HÜLMANN, G. (2001) Subgroup differentiation in the Cervidae by hair cuticle analysis. *Zeitschrift für Jagdwissenschaft* **47**, 253–258.

NICKEL, R., SCHUMMER, A. & SEIFERLE, E. (1992) *Lehrbuch der Anatomie der Haustiere. Band I: Bewegungsapparat*, 6th edition. Parey, Berlin, Hamburg.

ORR, D.J.A., TEELING, E.C., PUECHMAILLE, S.J. & FINARELLI, J.A. (2016) Patterns of orofacial clefting in the facial morphology of bats: a possible naturally occurring model of cleft palate. *Journal of Anatomy* **229**, 657–672.

PALOMBO, M.R., KOHLER, M., MOYA SOLA, S. & GIOVINAZZO, C. (2008) Brain versus body mass in endemic ruminant artiodactyls: A case studied of *Myotragus balearicus* and smallest *Candiacervus* species from Mediterranean Islands. *Quaternary International* **182**, 160–183.

PARKER, H.G., SHEARIN, A.L. & OSTRANDER, E.A. (2010) Man's best friend becomes biology's best in show: Genome analyses in the domestic dog. *Annual Review of Genetics* **44**, 309–336.

PARSONS, K.J., SON, Y.H., CRESPEL, A., THAMBITHURAI, D., KILLEN, S., HARRIS, M.P. & ALBERTSON, R.C. (2018) Conserved but flexible modularity in the zebrafish skull: Implications for craniofacial

evolvability. *Proceedings of the Royal Society B* **285**, 20172671.

PAVLIČEV, M. & CHEVERUD, J.M. (2015) Constraints Evolve: Context Dependency of Gene Effects Allows Evolution of Pleiotropy. *Annual Review of Ecology, Evolution, and Systematics* **46**, 413–434.

PERCIVAL, C.J. & RICHTSMEIER, J.T. (2017) *Building bones: Bone formation and development in anthropology*. In *Building Bones: Bone Formation and Development in Anthropology* p. , 1st edition. Cambridge University Press, Cambridge.

PITA-THOMAS, W., BARROSO-GARCÍA, G., MORAL, V., HACKETT, A.R., CAVALLI, V. & NIETO-DIAZ, M. (2017) Identification of axon growth promoters in the secretome of the deer antler velvet. *Neuroscience* **340**, 333–344.

PORTO, A., DE OLIVEIRA, F.B., SHIRAI, L.T., DE CONTO, V. & MARROIG, G. (2009) The evolution of modularity in the mammalian skull I: Morphological integration patterns and magnitudes. *Evolutionary Biology* **36**, 118–135.

PORTO, A., SHIRAI, L.T., DE OLIVEIRA, F.B. & MARROIG, G. (2013) Size variation, growth strategies, and the evolution of modularity in the mammalian skull. *Evolution* **67**, 3305–3322.

PRICE, J.S., ALLEN, S., FAUCHEUX, C., ALTHNAIAN, T. & MOUNT, J.G. (2005) Deer antlers: A zoological curiosity or the key to understanding organ regeneration in mammals? *Journal of Anatomy* **207**, 603–618.

PRICE, S.A., BININDA-EMONDS, O.R.P. & GITTLEMAN, J.L. (2005) A complete phylogeny of the whales, dolphins and even-toed hoofed mammals (Cetartiodactyla). *Biological Reviews of the Cambridge Philosophical Society* **80**, 445–473.

RANDI, E., MUCCI, N., PIERPAOLI, M. & DOUZERY, E. (1998) New phylogenetic perspectives on the Cervidae (Artiodactyla) are provided by the mitochondrial cytochrome b gene. *Proceedings of the Royal Society B* **265**, 793–801.

RICH, T.H., HOPSON, J.A., MUSSER, A.M., FLANNERY, T.F. & VICKERS-RICH, P. (2005) Independent origins of middle ear bones in monotremes and therians. *Science* **307**, 910–914.

ROSS, C.F. & METZGER, K.A. (2004) Bone strain gradients and optimization in vertebrate skulls. *Annals of Anatomy* **186**, 387–396.

RÖSSNER, G.E. (2010) Systematics and palaeoecology of Ruminantia (Artiodactyla, Mammalia) from the Miocene of Sandelzhausen (southern Germany, Northern Alpine Foreland Basin). *Palaontologische Zeitschrift* **84**, 123–162.

RÜTIMEYER, L. (1881) Beiträge zu einer natürlichen Geschichte der Hirsche. *Abhandlungen der Schweizerischen Paläontologischen Gesellschaft* **VIII**, 1–268. Zürcher und Furrer, Zürich.

SAARINEN, J.J., ERONEN, J.T., FORTELIUS, M., SEPPA, H. & LISTER, A. (2016) Patterns of body mass and diet of large ungulates from Middle and Late Pleistocene of Western Europe and their connections with vegetation openness. *Paleontologia Electronica* **19**, 1–58.

SCHILLING, A.-M., CALDERÓN-CAPOTE, M.C. & RÖSSNER, G.E. (2019) Variability, morphometrics, and co-variation of the *os lacrimale* in Cervidae. *Journal of Morphology* **280**, 1071–1090.

SCHILLING, A.-M. & RÖSSNER, G.E. (2017) The (Sleeping) Beauty in the Beast – A review on the water deer, *Hydropotes inermis*. *Hystrix* **28**, 121–133.

SCHILLING, A.-M. & RÖSSNER, G.E. (2021) New skull material of Pleistocene dwarf deer from Crete (Greece). *Comptes Rendus Palevol* **20**, 141–164.

SCHWENK, K. (2000) *Feeding: Form, function, and evolution in tetrapod vertebrates*. Academic Press, London.

SCOTT, K.M. & JANIS, C.M. (1987) Phylogenetic relationships of the Cervidae, and the case for a superfamily' Cervoidea'. In *Biology and management of the Cervidae* pp. 3–20. Smithsonian Institution Press, Washington.

STARCK, D. (1979) *Vergleichende Anatomie der Wirbeltiere auf evolutionsbiologischer Grundlage: Band 2: Das Skelettsystem*, 1st edition. Springer, Berlin.

UNGAR, P.S. (2015) Mammalian dental function and wear: A review. *Biosurface and Biotribology* **1**, 25–41.

VAN VALKENBURGH, B. (1989) Carnivore Dental Adaptations and Diet: A Study of Trophic Diversity within Guilds. In *Carnivore Behavior, Ecology, and Evolution* (ed J.L. GITTLEMAN), pp. 410–436. Springer, Ithaca.

VALLI, A.M.F. (2010) Dispersion of the genus *Procapreolus* and the relationships between *Procapreolus cusanus* and the roe deer (*Capreolus*). *Quaternary International* **212**, 80–85.

VISLOBOKOVA, I.A. (2013) Morphology, taxonomy, and phylogeny of megacerines (Megacerini, Cervidae, Artiodactyla). *Paleontological Journal* **47**, 833–950.

DE VOS, J. (1979) The endemic Pleistocene deer of Crete. I. *Proceedings of the Koninklijke Nederlandse Akademie van Wetenschappen, Series B* **82**, 59–90.

WANG, Y., ZHANG, C., WANG, N., LI, Z., HELLER, R., LIU, R., ET AL. (2019) Genetic basis of ruminant headgear and rapid antler regeneration. *Science* **364**, eaav6335.

WEISS, K. (2017) What is a biological 'trait'? In *Building Bones: Bone Formation and Development in Anthropology* (eds C.J. PERVICAL & J.T. RICHTSMEIER), pp. 13–25. Cambridge University Press, Cambridge.

ZOLLIKOFER, C.P.E. & DE LEÓN, M.S.P. (2013) Pandora's growing box: Inferring the evolution and development of hominin brains from endocasts. *Evolutionary Anthropology* **22**, 20–33.

ZURANO, J.P., MAGALHÃES, F.M., ASATO, A.E., SILVA, G., BIDAU, C.J., MESQUITA, D.O. & COSTA, G.C. (2019) Cetartiodactyla: Updating a time-calibrated molecular phylogeny. *Molecular Phylogenetics and Evolution* **133**, 256–262.

Chapter 2

Variability, morphometrics, and co-variation of the *os lacrimale* in Cervidae

Research article published in *Journal of Morphology 280: 1071-1090, 2019*

© 2019 Wiley Periodicals Inc. All rights reserved. No part of this publication may be reproduced, stored or transmitted in any form or by any means without the prior permission in writing from the copyright holder.

Author contributions:

Ann-Marie Schilling collected data, designed and performed statistical analyses, wrote and revised the paper.
Gertrud E. Rössner supervised study design and performance and reviewed drafts of the paper.
María C. Calderón-Capote collected data

Received: 28 July 2018 | Revised: 15 April 2019 | Accepted: 24 April 2019

DOI: 10.1002/jmor.21002

Check for updates

RESEARCH ARTICLE

Journal of morphology WILEY

Variability, morphometrics, and co-variation of the *os lacrimale* in Cervidae

Ann-Marie Schilling[1,2] | María C. Calderón-Capote[3] | Gertrud E. Rössner[1,2]

[1]SNSB-Bayerische Staatssammlung für Paläontologie und Geologie, Munich, Germany

[2]Department of Earth and Environmental Sciences, Palaeontology & Geobiology, Ludwig-Maximilians-Universität München, Munich, Germany

[3]Department Biology II, Ludwig-Maximilians-Universität München, Martinsried

Correspondence
Ann-Marie Schilling, SNSB-Bayerische Staatssammlung für Paläontologie und Geologie, Munich, Germany.
Email: schilling@snsb.de

Funding information
Ludwig-Maximilians-Universität München, Grant/Award Number: LMU Travel Grant 2015

Abstract

In Ruminantia, the lacrimal bone forms a considerable part of the facial skeleton, and the morphology of its facial facet is highly variable when compared to other mammals. In this study, we quantify the species-specific variability in size and shape of the lacrimal facial facet in species of Cervidae (deer) and relate it to systematics and various aspects of their ecology and behavior. We sampled 143 skull specimens from 10 genera; 12 *Moschus* and 3 *Tragulus* specimens were used as outgroups. We find that size and shape of the lacrimal facial facet allow differentiating most species analyzed here, except for *Mazama gouazoubira* and *Capreolus capreolus*. Size and shape of the lacrimal facial facet vary widely across Cervidae regardless of their systematic relationships, ecology or behavior. Thus, we could not detect a unique signature of adaptational criteria in lacrimal morphology. Our data indicate that the lacrimal facial facet scales allometrically with skull size, in particular, the lacrimojugal length scales positively and the lacrimomaxillar length scales negatively. However, correlation analyses did not reveal any differences in the integration of the lacrimal bone with any specific skull module in any of the species compared. Lastly, we could not ascertain any correlation between the size and position of the preorbital depression with the size and shape of the lacrimal facial facet. We conclude that the lacrimal facial facet is highly flexible and may rapidly adjust to its surrounding bones. Its allometric growth appears to be an example of exaptation: changes in size and shape in the context of the increase of the skull length provide lacrimal contacts, in particular, a lacrimojugal one, which may serve to reduce mechanical loads resulting from increasingly larger antlers in large cervids.

KEYWORDS
allometry, antlers, exaptation, lacrimal facial facet

1 | INTRODUCTION

The lacrimal bone, *os lacrimale*, is a central structure of the facial skull of most mammals. Generally, it is a comparatively small bone, composed of an orbital and a facial facet. The facets can differ in proportions, and in some mammals, one or the other facet can hardly be identified (e.g., Carnivora, Rodentia, Lipotyphla, Primates, Chiroptera). The orbital facet contributes to the orbita; the lacrimal facet belongs to the lateral aspect of the facial skeleton, being located between the *os frontale* and the *os maxillare*. It is often also connected to the *os jugale* (i.e., *os zygomaticum* in the veterinary anatomical nomenclature) and encases the caudal origin of the nasolacrimal duct. The junction between the orbital and facial lacrimal facet forms part of the rostral orbital rim.

The external appearance of the lacrimal bone is tightly linked to taxon-specific changes of the shape and relative size of its surrounding

 © 2019 Wiley Periodicals, Inc.

bones. In the past, several studies suggested that the appearance of the lacrimal bone might be used to differentiate mammalian taxa (Gregory, 1920; Knottnerus-Meyer, 1907; Rütimeyer, 1881) and to reconstruct mammalian evolution and phylogenetic relationships (Gregory, 1920). Recently, the relative timing of the closure of lacrimal sutures was identified as yet another useful parameter to unravel ruminant phylogeny (Bärmann & Sánchez-Villagra, 2012; Oh, Kim, Yasuda, Koyabu, & Kimura, 2017; Sánchez-Villagra, 2010).

In his extensive review of the lacrimal bone in vertebrates, and in particular mammals, Gregory (1920) drew attention to the fact, that changes in the facial skull co-varied with changes in the lacrimal bone appearance: he hypothesized that "specialization in food habits, etc., has affected the lacrymal region of mammals in several ways" (p. 215). For instance, he reported that an anteroposterior displacement of the orbit and a change in size and orientation of the orbit might have influenced the size of the lacrimal bone. Similarly, so may have done changes in the olfactory region, the evolution of hard or soft-tissue appendages, or dietary specialization to grass. For instance, Gregory (1920) stated that the evolution of proboscides in elephants (Proboscidea) and tapirs (Perissodactyla) went along with a reduction and posterior displacement of the nasal bone. Consequently, their lacrimal facial facets shrunk and lost the lacrimonasal contact. Gregory (1920) saw a relationship between the presence of horns in African Rhinos, the anterior displacement of the nasal bone and the consequent loss of the nasolacrimal contact. For horses (Perissodactyla), Gregory (1920) noted a size increase of the lacrimal facial facet with skull length increase. He compared horses with Artiodactyla and found the lacrimal facial facet to be more or less square in the former and rectangular in larger species of the latter. In addition, Gregory (1920) connected the extremely large size of the lacrimal facial facets in bovid artiodactyls with a strengthening function of the face below the horns.

All these observations indicate that the variability of the lacrimal bone in general and its facial facet, in particular, may reflect adaptation, as suggested before (Cobb, 1943; Cox, 2008; Gregory, 1920). Yet, the potential significance of this (part of the) bone remains elusive. Cobb (1943) pointed out the potentially important functional role of the lacrimal bone as part of the stress-bearing region of the facial skeleton. In particular, in artiodactyls, the large lacrimal facial facet is stretched between the maxilla and the frontal bones and thus susceptible to mechanical loads transmitted from these bones. This seems to be supported by more recent finite-element modeling studies that assessed stress-transfer across the facial skeleton during feeding in suids and diprotodont marsupials (Bright, 2012; Sharp, 2015).

Along this line of research, we investigated the lacrimal facial facet of Cervidae (deer, moose, elk, and kin; Groves & Grubb, 2011) in order to substantiate the possible relationships between the morphology of the lacrimal facial facet and either the systematics or adaptation. Cervids provide a unique paradigm to address this issue: First, Cervidae form one of the most diverse groups of large mammals with more than 50 accepted species (Groves, 2007; Groves & Grubb, 2011; Wilson & Mittermeier, 2011). Their lacrimal bones, and in particular, their lacrimal facial facets, are relatively large (Figure 1). The lacrimal facial facet contacts the jugal bone and maxilla ventrally and the frontal bone dorsally. It does not contact the nasal bone, leaving the so-called ethmoidal gap. The lacrimal facial facet is characterized by the preorbital depression (Langguth & Jackson, 1980; Ungerfeld et al., 2008), also known as preorbital fossa (Emery, 2016), lacrimal pit (Hou, 2015; Wang & Hoffmann, 1987), or lacrimal fossa (McDonald & Ray, 1989; Mennecart & Métais, 2015; Scott & Janis, 1987). This depression hosts the preorbital gland, an organ used for chemical and for visual communication (Geist & Bayer, 1988; Mattioli, 2011; and also Rehorek, Hillenius, Kennaugh, & Chapman, 2005), in a species-related and maybe habitat-related manner. Similar to the form, that is, size and shape (Mitteroecker, Gunz, Windhager, & Schaefer, 2013), of the lacrimal facial facet itself, the form of the depression varies species-specifically. Both have been used to establish alpha taxonomy (Knottnerus-Meyer, 1907; Kober, 1880; Rütimeyer, 1881).

Second, cervids are adapted to a wide variety of ecological niches and show a range of behaviors. They are found from the cold polar zone, for example, *Rangifer* and *Alces*, to the tropic zone, for example, *Muntiacus* and *Rucervus*; from the coast to high mountains. While most cervids prefer to dwell in forests or ecotones, others are prone to live in open-space habitats, for example, *Rucervus* and *Rangifer* (Mattioli, 2011). Some species are solitary, while others stay in groups (Geist, 1998; Mattioli, 2011). In all but one cervid species males bear and fight with antlers. *Muntiacus* and *Elaphodus*, carry also enlarged upper canines in addition to the antler, and fight with both head structures. *Hydropotes*, the water deer, lacks antlers altogether but has large upper canines, which are used during intraspecific combat (for a recent review on *Hydropotes* see Schilling & Rössner, 2017). This lack of headgear and the presence of large upper canines is reminiscent of what is seen in closely related ruminant artiodactyls, that is, *Tragulus*, *Moschiola*, and *Hyemoschus* (Tragulidae) as well as *Moschus* (Moschidae). Finally, yet important, cervids cover a wide range of body size. The smallest, *Pudu spp.*, weigh about 6 kg and the largest, *Alces alces*, weighs up to 770 kg (Mattioli, 2011).

In contrast to the previously mentioned qualitative studies, quantitative studies of lacrimal bone size and shape within cervids and its phylogenetic or adaptive relationships are missing. In the present study, we complement existing qualitative data by presenting a detailed morphometric analysis of the lacrimal facial facet of a sample of cervid species. We test whether the variability of the lacrimal facial facet mirrors cervid systematics or adaptation to ecology and behavior. To do so, we aim at (a) quantifying morphometric variability of the lacrimal facial facet; (b) finding and quantifying relationships between the lacrimal facial facet and other cranial regions; (c) assessing relationships between the morphology of the lacrimal facial facet and cervid systematics, ecology, behavior as well as size and position of the preorbital depression.

2 | MATERIALS AND METHODS

2.1 | Materials

We analyzed skull specimens of 158 adult males from 3 ruminant families and 13 species (Table 1; for detailed list of specimens see supplementary online material, Table S1). The cervid species we selected

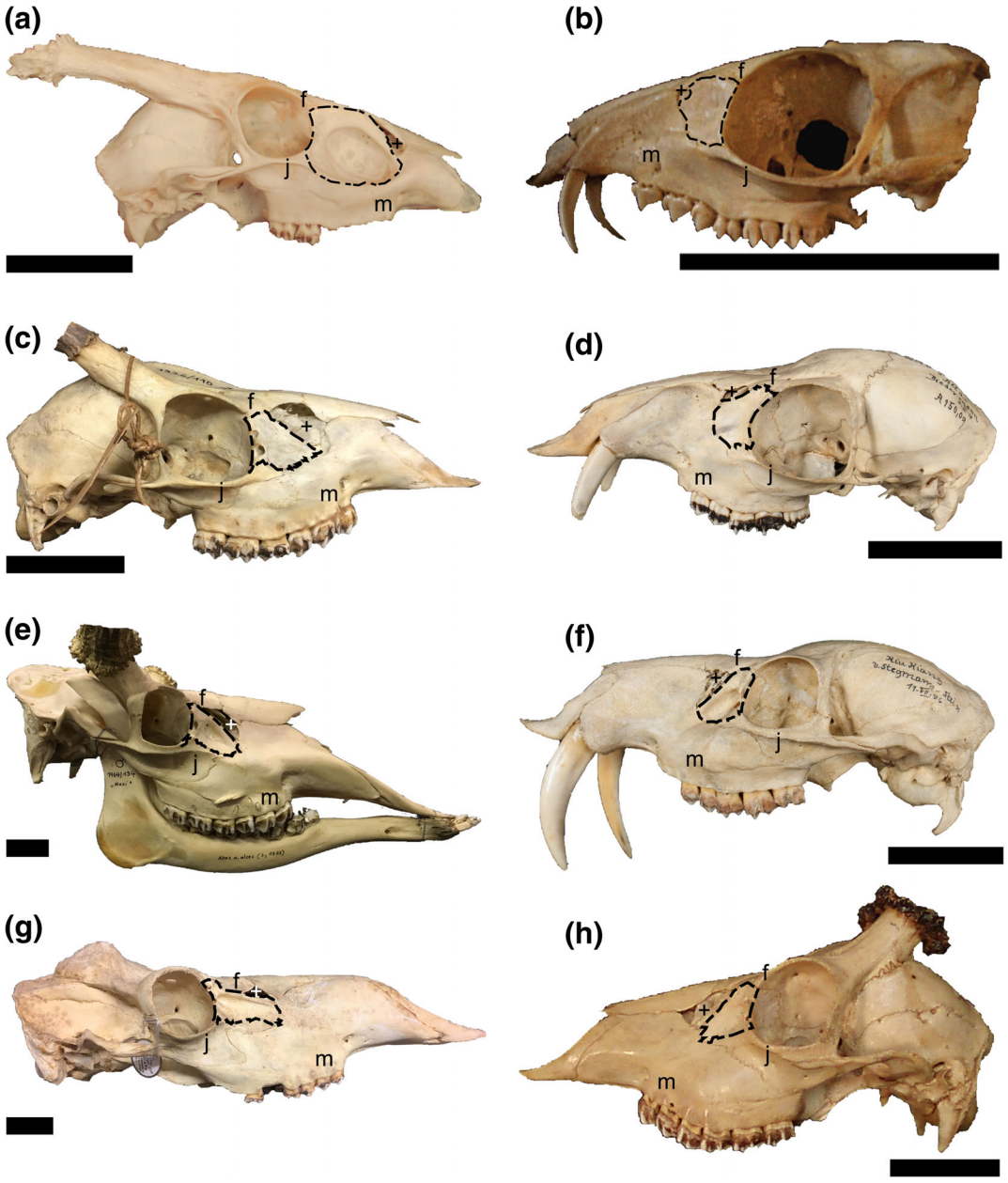

FIGURE 1 Sample of male ruminant skulls representing the diversity in size and shape of the lacrimal facial facet (outlined by the dashed line). a, *Muntiacus muntjak* (SAPM #9); b, *Tragulus javanicus* (NHMW 7595/St476); c, *Mazama gouazoubira* (ZSM 1926/110); d, *Moschus moschiferus* (ZMB_Mam_70941); e, *Alces alces* (ZSM 1964/134); f, *Hydropotes inermis* (ZMB_Mam_70999); g, *Rangifer tarandus* (ZSM 1968/694); h, *Capreolus capreolus* (ZSM 1939/77); i, *Cervus elaphus* (ZSM 1953/176); j, *Dama dama* ("Heidemann", no specimen label, ZSM); k, *Rucervus eldii* (ZSM 1905/14); l, *Pudu puda* (ZSM 1954/453). Bones are labelled as follows: f, frontal bone; j, jugal bone; m, maxillary; +, ethmoidal gap. *Tragulus javanicus* has a bony plate instead of an ethmoidal gap. Scale bars = 5 cm [Color figure can be viewed at wileyonlinelibrary.com]

(a) represent all higher hierarchical systematic units, (b) span a wide range of the above-mentioned ecological and behavioral variability, and (c) cover the range of body size of extant cervids. In Table 1, we also indicated the respective cervid subfamily, head weapons, preferred habitat, and social behavior of the species analyzed. The two tragulid species analyzed were considered as one outgroup, and we refer to them as "*Tragulus*" below. Only skulls of adult individuals in which third molars had erupted were included in our sample. Specimens are housed in the following collections and institutions: Naturhistorisches Museum Wien (NHMW), Museum für Naturkunde Berlin (ZMB), Zoologische Staatssammlung München (ZSM), and Sammlung für Anthropologie und Paläoanatomie München (SAPM).

2.2 | Measurements of the lacrimal facial facet

We identified five landmarks on the lacrimal facial facet based on homologous points. These points were located where sutures of the lacrimal facial facet meet with sutures of neighboring bones, or with the orbital rim, or with the ethmoidal gap. By connecting these points, we obtained straight-line approximations of the lacrimal facet outline. We

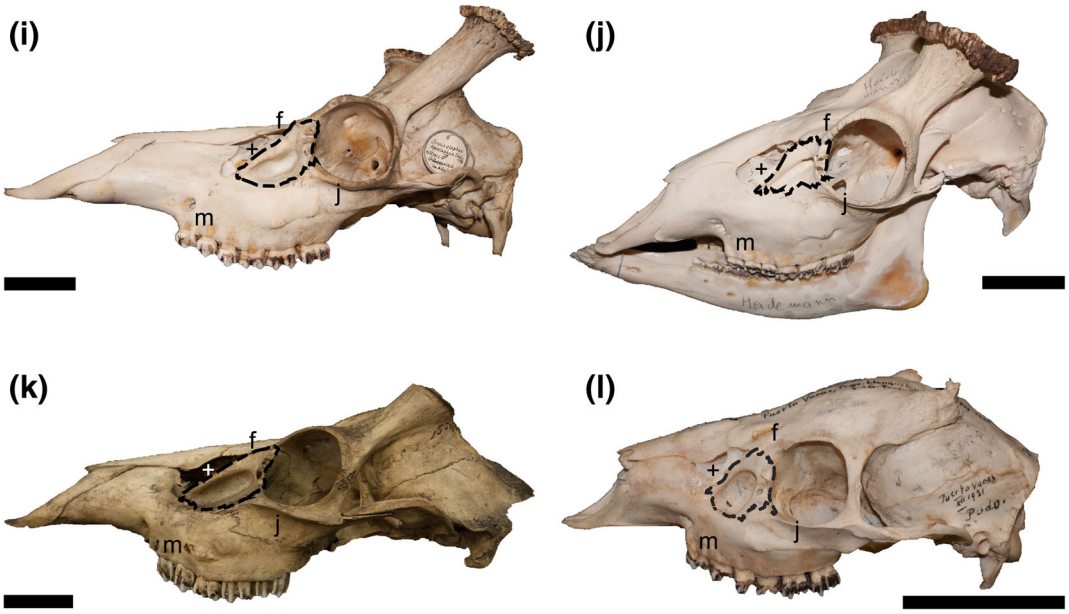

FIGURE 1 (Continued) [Color figure can be viewed at wileyonlinelibrary.com]

TABLE 1 Materials used in this study. The ecological classification is based on Mattioli (2011) and Meijaard (2011)

Family	Subfamily	Common name	Scientific name	n	Preorbital depression		Head weapons	Preferred habitat	Social behavior
					Size	Position			
Cervidae	Capreolinae	Moose	*Alces alces* (Linnaeus, 1785)	11	M	C	A	TB; closed	SOL
		Roe deer	*Capreolus capreolus* (Linnaeus, 1785)	33	L	V	A	TE; closed	SOL
		Water deer	*Hydropotes inermis* Swinhoe, 1870	9	M	V	CA	ST; open	SOL
		Gray brocket	*Mazama gouazoubira* (Fischer, 1814)	34	S	V	A	TR; closed	SOL
		Southern pudu	*Pudu puda* (Molina, 1782)	7	L	C	A	TE; closed	SOL
		Reindeer	*Rangifer tarandus* (Linnaeus, 1758)	12	L	D	A	PB; mixed	GR
	Cervinae	Common red deer	*Cervus elaphus hippelaphus* Linnaeus, 1785	10	L	C	A	TE; closed	GR
		Fallow deer	*Dama dama* (Linnaeus, 1785)	7	L	C	A	TE; closed	SGR
		Indian muntjak	*Muntiacus muntjak* (Zimmermann, 1780)	10	L	V	A[a]	TR; closed	SOL
		Eld's deer	*Rucervus eldii siamensis* (M'Clelland, 1842)	10	L	C	A	TR; open	SOL
Moschidae	-	Musk deer	*Moschus moschiferus* Linnaeus, 1758	12	W	W	CA	TE; closed	SOL
Tragulidae	-	Java mouse deer	*Tragulus javanicus* (Osbeck, 1765)	2	W	W	CA	TR; closed	SOL
		Lesser oriental chevrotain	*Tragulus kanchil* (Raffles, 1821)	1	W	W	CA	TR; closed	SOL

Abbreviations: Preorbital depression size and position: C, central; V, ventral; D, dorsal; W, depression wanting; S, small; M, medium; L, large; head weapons: A, antlers; CA, canines; habitat: PB, polar/boreal; ST, subtropical; TB, temperate/boreal; TE, temperate; TR, tropical; closed, forests; open, grasslands or meadows with shrubs; mixed, open and closed habitat; sociality: SOL, solitary; GR, groups; SGR, solitary or groups.
[a]*Muntiacus* has both antlers and canines, though antlers are the weapon of choice (Barrette, 1977).

also measured the maximal lacrimal length and thus obtained six linear measurements (referred to below as "variables") describing the lacrimal facial facet (Table 2, Figure 2). We measured the maximal skull length as the distance between the prosthion and the akrokranion (for a definition of landmarks see Appendix 1 and von den Driesch, 1976). For six of the 13 species analyzed (*Tragulus javanicus*, *Tragulus kanchil*, *Moschus*

TABLE 2 Measured inter-landmark distances at the lacrimal bone

Distance	Landmarks from Figure 2	Junction points between sutures and/or skull openings (from; to)
Lacrimal height	FLO—JLO	Frontal-lacrimal-orbital rim; jugal-lacrimal-orbital rim
Lacrimojugal length	JLO—MLJ	Jugal-lacrimal-orbital rim; maxilla-lacrimal-jugal
Lacrimomaxillar length	MLJ—MLE	Maxilla-lacrimal-jugal; maxilla-lacrimal-ethmoidal gap
Lacrimoethmoid length	MLE—FLE	Maxilla-lacrimal-ethmoidal gap; frontal-lacrimal ethmoidal-gap
Lacrimofrontal length	FLE—FLO	Frontal-lacrimal-ethmoidal gap; frontal-lacrimal-orbital rim
Maximal lacrimal length	FLO—MLE	Frontal-lacrimal-orbital rim; maxilla-lacrimal-ethmoidal gap

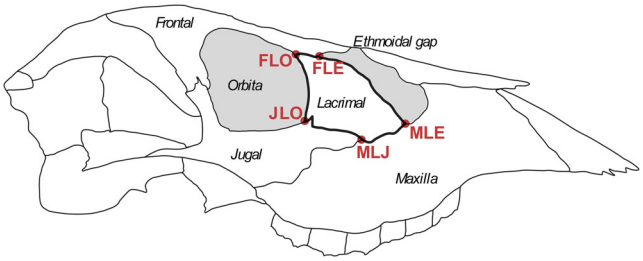

FIGURE 2 Schematic representation of the lacrimal facial facet. The facial facet contacts the frontal, jugal, and maxillary bone. It also forms part of the orbit and the rim of the ethmoidal gap. FLO, Frontal-lacrimal-orbital rim; JLO, Jugal-lacrimal-orbital rim; MLJ, maxilla-lacrimal-jugal; MLE, maxilla-lacrimal-ethmoidal gap; FLE, frontal-lacrimal-ethmoidal gap. Distances are defined in Table 2 [Color figure can be viewed at wileyonlinelibrary.com]

moschiferus, *Muntiacus muntjak*, *Hydropotes inermis*, and *C capreolus)*, we obtained an additional 56 inter-landmark distances (Appendix 1). As far as possible, these were assigned to previously defined modules (Haber, 2014; Marroig & Cheverud, 2001; Porto, de Oliveira, Shirai, de Conto, & Marroig, 2009). Module assignment of individual distances is given in Appendix 1. Measurements that span more than one module (e.g., maximal skull length) were not assigned to any module ("none" in Appendix 1). Raw data of these measurements and species-specific summary statistics are provided as supplemental material (Tables S1-S3), and Figure S1 shows the skull landmarks.

We took measurements up to 150 mm using digital calipers and measurements in the range of 150 to 300 mm using mechanical calipers. We recorded these measurements to the nearest 0.1 mm. Measurements larger than 300 mm were taken with a yardstick and rounded to the nearest 1.0 mm.

2.3 | Traits of the preorbital depression

To assess the size and position of the preorbital depression, we used a semi-quantitative, categorical approach, inspired by Knottnerus-Meyer (1907). We designated a preorbital depression as "large" when it occupied more than 75% of the area of the lacrimal facet. We designated it as "intermediate" when it occupied between 50% and 75% of the area of the lacrimal facet. We designated as "small", when it occupied less than 50% of the area of the lacrimal facial facet. Furthermore, we classified a preorbital depression as "dorsal," when its distance from the lacrimofrontal suture or lacrimoethmoid edge was smaller than that from the lacrimojugal or lacrimomaxillar sutures. We classified it as "ventral" when its distance from the lacrimojugal or lacrimomaxillar sutures was smaller than that from the lacrimofrontal suture or lacrimoethmoid edge; we classified it as "central" when the depression was located right in the middle of the facial facet of the lacrimal bone.

2.4 | Quantification of size, shape, and variability of the facial facet of the lacrimal facial facet

All statistical procedures described below were performed in R software (version 3.5.1; R Core Team, 2018). Prior to statistical analyses, original measurements were $\log_{10}$-transformed. For analyses based on size-normalized data, normalization was obtained by subtracting, from individual $\log_{10}$-transformed measurements, the $\log_{10}$ of the geometric mean of all measurements of a given specimen (Darroch & Mosimann, 1985; Falsetti, Jungers, & Cole, 1993). As a proxy for skull size, we used the maximal skull length. This single variable is a dependable and practical measure for skull size estimation (Klingenberg, 2016; Mosimann, 1970).

To test for interspecific allometric scaling of the lacrimal facial facet, we used major axis regression as described by Warton, Wright, Falster, & Westoby (2006); (see also Klingenberg, 2016) and implemented in the R package "smatr" (version 3.4–8.; Warton, Duursma, Falster, & Taskinen, 2012).

We used principal component analysis (PCA) to summarize the morphological variability of the lacrimal facial facet across species. Furthermore, PCA allows separating size from the shape and therefore allowed probing how differences in size and those in shape of the lacrimal facial facet might relate to cervid systematics or the ecology and behavior of the species analyzed. Two PCA-based approaches are commonly used to distinguish the effects of size from effects of shape: one approach may be traced to the work of Jolicoeur (1963), the other one to the work of Mosimann (1970). However, the effectiveness of these approaches may vary depending on the structure of the data analyzed (see e.g., Darroch & Mosimann, 1985; Falsetti et al., 1993) and, therefore, we tested which of the two approaches was more effective for the present dataset.

We used a robust variant that uses an MM-estimator of the covariance matrix (Salibián-Barrera, Van Aelst, & Willems, 2006); implemented in the R-package "rrcov" (version 1.4–3; Todorov & Filzmoser, 2009). Confidence intervals for the loadings obtained were established by bootstrapping (with 999 samples) using the R-package "FRB" (version 1.8; van Aelst & Willems, 2013).

2.5 | Relationships between the lacrimal facial facet and other skull variables

To test how lacrimal variables may relate with other skull regions, we performed a correlation analysis of lacrimal variables with other skull variables. To do so, we handled missing data using a two-step approach. First, we considered only measurements that were available for at least 50% of all individuals per species. Second, we imputed the few missing data points in this reduced set using a Bayesian PCA approach (Oba et al., 2003), implemented in the bpca function of the R package "pcaMethods" (version 1.66.0; Stacklies, Redestig, Scholz, Walther, & Selbig, 2007). We then normalized the data by subtracting their geometric mean and analyzed them using Spearman's rank correlation.

This allowed calculating 246 correlations per species. To test whether any one of the lacrimal variables correlated preferentially with any other skull variable, we focused on the 26 (~ 10%) the strongest correlations of each species, regardless of their direction. Under the null hypothesis, correlations between lacrimal and skull variables would not be formed preferentially with skull variables of a given module. That is, if the null hypothesis holds, we expect that (a) for each of the modules, the number of strong correlations should be proportional to the number of possible correlations and that (b) all non-lacrimal variables should be involved in these strong correlations with lacrimal variables with about equal frequency. We tested these predictions using Fisher's exact test (Mangiafico, 2017). We adjusted *p*-values for multiple comparisons using the Benjamini–Hochberg false discovery rate (FDR) to reduce the number of false positive P-values. This test is implemented in the R package "rcompanion" (version 2.0.0; Mangiafico, 2017).

2.6 | Relationships between the size of the lacrimal facial facet and the morphology of the preorbital depression

To test how the size and position of the preorbital depression relate to the size of the lacrimal facial facet we used the Kruskal-Wallis rank sum test (Logan, 2011; Whitlock & Schluter, 2015). This nonparametric alternative to ANOVA was chosen since the size distribution of the lacrimal facial facets investigated did not meet the requirements for standard parametric tests ($p < .05$ for Shapiro-Test and Levene-Test). For those cases where the Kruskal-Wallis tests were significant ($p < .05$), we applied Mood's Median test, implemented in the R package "RVAideMemoire" (version 0.9–69; Hervé, 2015), for pairwise post-hoc comparisons.

3 | RESULTS

3.1 | Allometric scaling of the lacrimal facial facet and separating its size from its shape

As a first step toward understanding how the lacrimal facial facet changes in size and shape across cervid species, we performed interspecific allometric analyses (Klingenberg, 2016). We related the skull length to the size of the lacrimal facial facet, defined as the geometric mean of its describing measures. The slope of this fit is 1.12 (95% *CI*: 1.04–1.20; R^2 = 0.87; Figure 3). This is slightly but significantly ($p < .001$) different from isometry, for which a slope of 1.0 would be expected (Figure 3, dashed line).

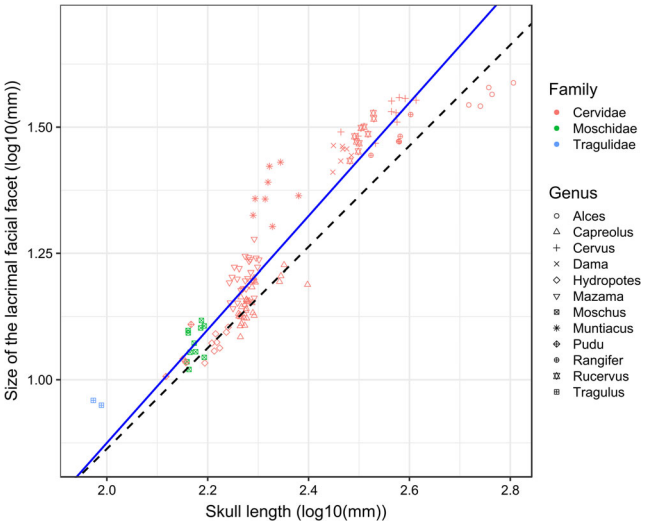

FIGURE 3 Relationships between skull length and size (geometric mean) of the lacrimal facial facet. Lacrimal size shows positive interspecific allometry (solid line; slope = 1.12; 95% *CI* = 1.04–1.20; R^2 = 0.87). Isometry (slope = 1) is represented by the dashed line [Color figure can be viewed at wileyonlinelibrary.com]

Next, we aimed to separate allometric changes of the lacrimal facial facet from size-independent variability of shape. To do so, we investigate how size, and in particular, how size-independent shape correlate with cervid systematics, ecology, and behavior. A critical first step of this analysis was to verify whether consideration of the first principal component (PC1) or of the geometric mean of the lacrimal variables results in more efficient separation of size and shape *with our data*. This verification may be achieved by comparing PC2 and PC3 of the original measurements, which may be interpreted as reflecting shape differences (sensu Jolicoeur, 1963; see e.g., Klingenberg, 2016; Figure 4a), with PC1 and PC2 of geometric mean-corrected data, which may be interpreted as shape data sensu Mosimann (1970) (Figure 4b).

Conversion of the original measurements to shape data sensu Mosimann (1970) reduces the total variance from 0.267 to 0.072, that is, by 73%. Conversely, PC1 of the original data accounts for 81.6% of the total variability; consequently, only 18.4% of the total variability, partitioned between PC2 and PC3 of the original data, are associated with shape sensu Jolicoeur (1963) (Figure 4 and Table 3). This difference suggested either that the shape data sensu Mosimann (1970) still contain some size information, or that PC1 of the original data not only accounts for size, but also for some part of shape differences. To decide between these possibilities we correlated the variation along each PC axis with the size, that is, the geometric mean, of the lacrimal facial facet (Table 4). To clarify the biological significance of this difference, we compared eigenvalues and the partitioning of the total variances obtained with the PCAs of the original or the size-corrected data (Table 3).

The first principal component obtained with original measurements strongly correlates with size. Conversely, PC2 is no longer

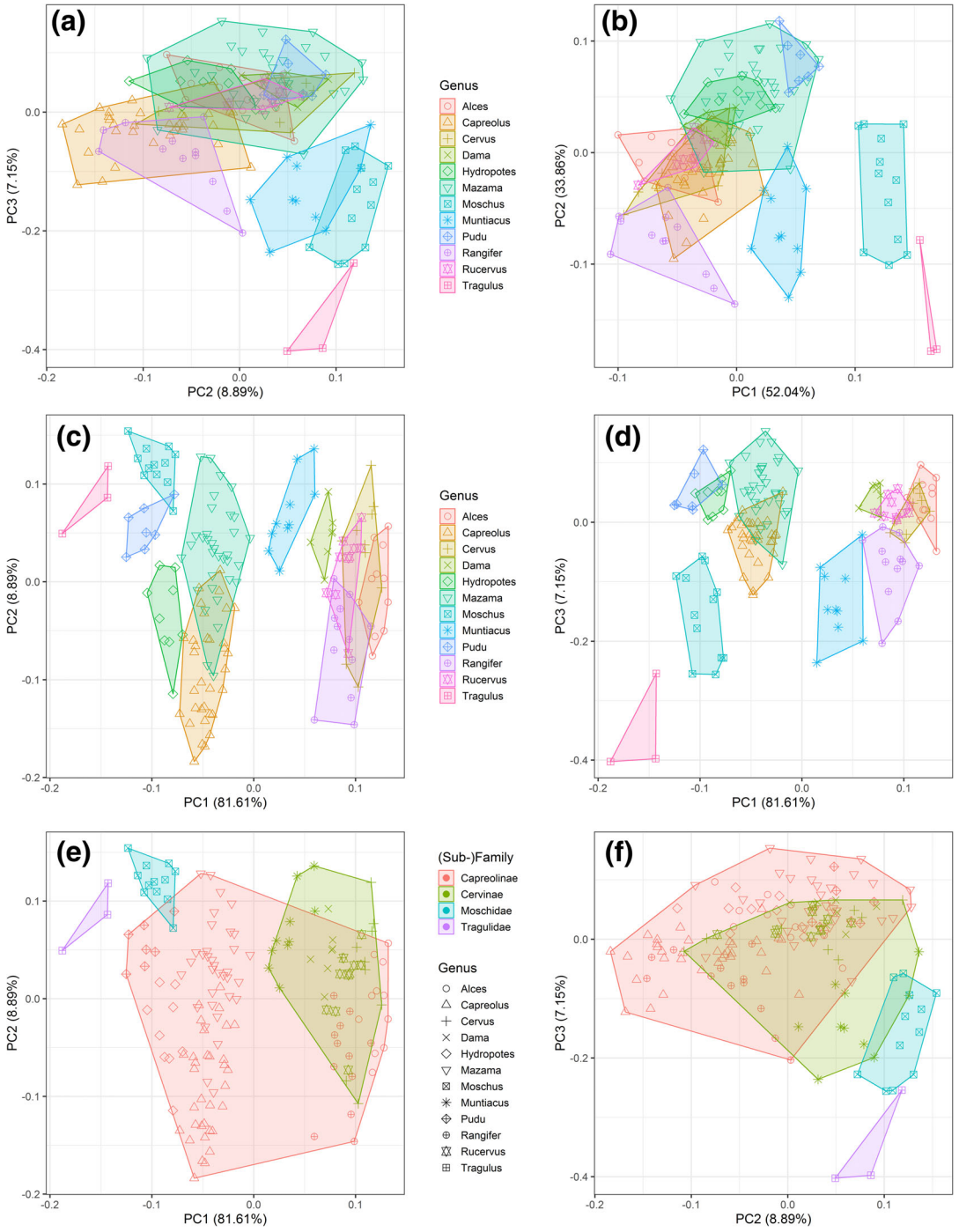

FIGURE 4 Principal component analyses of variables describing the lacrimal facial facet. (a, b) Separation on the genus level by shape sensu Jolicoeur (1963; panel a) and sensu Mosimann (1970, panel b). Shape data sensu Mosimann (1970) still contain a size signal (see main text), which results in an apparently better resolution. Shape data sensu Jolicoeur (1963; panel a) allows to separate all cervids from the *Tragulus* outgroup and, except *Muntiacus*, also from the *Moschus* outgroup. Cervids, except *Muntiacus*, occupy a continuous shape space and show extensive overlap. (c, d) Separation of cervid species. The combination of size (PC1) and shape (PC2, panel c; or PC3, panel d) allows for effective differentiation of cervid species except for *Capreolus capreolus* and *Mazama gouazoubira*. (e, f) Separation of (sub-)family. Separation by shape is more pronounced than size alone. The combination of the shape axes (PC2 and PC3, panel f) allows the effective separation of Capreolinae and Moschidae, when the size axis and shape axis are considered independently, these groups overlap completely. Capreolinae and Cervinae overlap regardless of size or shape, while the *Tragulus* outgroup may be separated from all other groups by shape or size alone. (g, h) Separation by head weapons. Along the size axis, antlered and enlarged canine-bearing animals show extensive overlap. The one species carrying antlers and enlarged canines, *Muntiacus muntjak*, groups with antlered species based on size; it takes a position at the border of antlered and closer to canine-bearing species, based on shape. Enlarged canine-bearing *Hydropotes inermis* is within the size and shape space of antlered deer. (i, j) Separation by habitat and separation by social behavior (k, l). Neither size nor shape can distinguish any of the groups within either category. PB, polar/boreal; TB, temperate/boreal; STR, subtropical; TE, temperate; TR, tropical; closed-forests, open-grasslands or meadows with shrubs, mixed-open and closed habitat [Color figure can be viewed at wileyonlinelibrary.com]

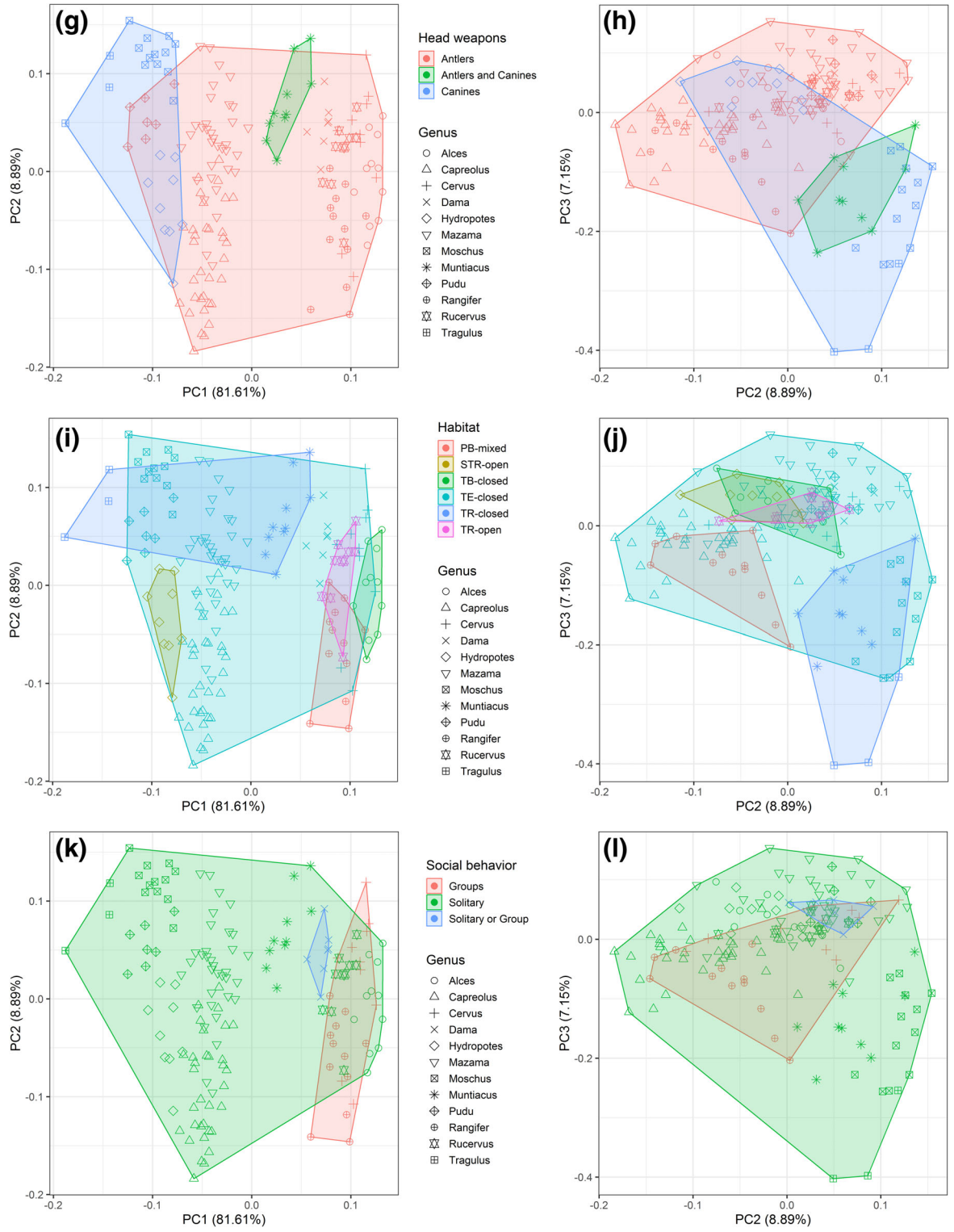

FIGURE 4 (Continued) [Color figure can be viewed at wileyonlinelibrary.com]

correlated with size and PC3 is only weakly correlated with it, accounting for some 3.6% (R^2 = 0.0361) of size-associated variation. For size-corrected data, that is, shape data sensu Mosimann, 1970, which should no longer be correlated with size, PC1 still correlated considerably with size and accounted for about 32% (R^2 = 0.325) of size-associated variation. PC2 of size-corrected data is again only weakly correlated with size and explains some 3.2% of its variation (R^2 = 0.0324). Thus, for our sample, the approach outlined by Jolicoeur (1963) provides the more efficient way to separate size from shape of the lacrimal facial facet, with size-related changes reflected by PC1 and size-independent shape reflected by PC2 and PC3. Therefore, we used this approach to probe how size and shape differences of the lacrimal facial facet relate to cervid systematics, ecology, and behavior.

TABLE 3 Loadings, eigenvalues, and proportion of variance explained from robust principal components (PC1-PC3) of raw size-and shape and size-corrected variables *sensu* Mosimann, 1970

	Size-and-shape data				Size-corrected data		
	PC1	PC1 95% *CI*	PC2	PC3	PC1	PC2	PC3
Lacrimal height	0.27	0.24–0.30	0.09	−0.04	−0.23	0.01	**−0.86**
Lacrimojugal length	**0.57**	0.55–0.61	−0.46	−0.20	**0.50**	−0.45	0.01
Lacrimomaxillar length	0.25	0.19–0.31	**−0.87**	−0.09	**−0.65**	0.30	0.32
Lacrimoethmoid length	0.41	0.36–0.47	0.09	**0.72**	0.45	**0.64**	0.17
Lacrimofrontal length	0.42	0.38–0.47	0.15	**−0.63**	−0.23	**−0.54**	0.35
Maximal lacrimal length	0.43	0.42–0.44	−0.01	0.18	0.16	0.04	0.02
Eigenvalue	0.21	–	0.03	0.02	0.04	0.02	0.01
Total variance	0.26				0.07		
Proportion of variance explained (%)	81.61	–	8.89	7.15	52.04	33.86	7.53
Cumulative variance explained (%)	97.65				93.43		

Note: Highest loadings that contribute to most of the variation along the respective axis are in bold. Data have been $\log_{10}$-transformed prior to analyses. 95% confidence interval (CI) determined by bootstrapping.

TABLE 4 Correlations of the principal components with the size of the lacrimal facial facet, defined as the geometric mean of the six describing variables

	r	95% CI	*p*
Original data			
PC1	0.997	0.996–0.998	<.001
PC2	−0.01	0.146–0.166	.9
PC3	0.19	0.037–0.338	.02
Size-corrected data			
PC1	0.57	0.454–0.667	<.001
PC2	−0.18	−0.33– −0.027	.02

3.1.1 | The lacrimal facial facet and systematics

Given the size differences between Tragulidae and both Moschidae and Cervidae (Figure 3), it came as no surprise that the size axis (PC1) allows distinguishing small Tragulidae from both Moschidae and Cervidae (Figure 4e). Both outgroups can be separated from Cervinae. The latter overlaps extensively, along PC1 with the larger Capreolinae. The smaller Capreolinae overlap fully with Moschidae (Figure 4e).

Shape alone also allows separating Tragulidae from both Moschidae and Cervidae. Moschidae overlap with Cervidae, when PC2 and PC3 are considered separately. However, when shape information on these axes is combined, *Moschus* may be separated from all cervids except *Muntiacus*. The two cervid subfamilies overlap extensively in shape as well (Figure 4f). The capreolines *Capreolus capreolus* and *Mazama gouazoubira* overlap with both all other Capreolinae and the Cervinae, and essentially define the shape space occupied by all cervids except *M muntjak*.

Differences in shape of the lacrimal facial facet distinguish some species for which the size of this bone overlaps. In Figure 4c,d, PC2 and PC3 are shown separately, since the extensive overlap seen when plotting them together (see Figure 4a) makes it difficult to judge their separating power. PC2 allows complete separation of capreoline *Pudu puda* and *H inermis*, as well as cervine *Dama dama* and capreoline *Rangifer tarandus* (Figure 4c). However, both of these two couples extensively overlap on the size axis. PC2 also allows for some separation between the same-sized capreoline *M gouazoubira* and *C capreolus*, though the overlap along this shape-axis is still quite large. PC2 allows distinguishing the capreoline *P puda* from both capreolines *R tarandus* and *C capreolus* regardless of the size-differences of the lacrimal facial facet in these species. The same holds for the cervine *M muntjak* and the capreoline *H inermis*, and *M muntjak* and *C capreolus*. PC3 allows clearly separating *R tarandus* from cervines *Rucervus eldii* and *D dama*, which largely overlap along PC1 (Figure 4d). It further allows separating, regardless of size, *R tarandus* from *H inermis* and *P puda*, and *M muntjak* from *R eldii*, *D dama*, *H inermis*, and *P puda*. In summary, differences in shape or size of the lacrimal facial facet, or their combination, distinguish most species analyzed. However, we cannot discern a clear pattern linking the morphology of the lacrimal facial facet with cervid systematics.

3.1.2 | The lacrimal facial facet and ecology and behavior

When specimens were grouped based on head weapons, their distribution along PC1 concurred with the observation that enlarged canines are found only in smaller-sized species (Figure 4g). When shape is considered (Figure 4h), *M muntjak* is at the border of antlered deer, in a region between the latter and the two cervid outgroups, both of which bear enlarged upper canines. It may be worthwhile to recall here that *M muntjak* has small antlers and enlarged upper canines. *H inermis*, also characterized by enlarged upper canines, but have no antlers, cannot be discerned from other, antlered cervids. Thus, no general pattern indicating a relation between the morphology of the lacrimal facial facet and the type of head weapons is apparent.

When species were grouped by their habitat, essentially the complete size range (PC1, Figure 4i), and also most of the shape space (PC2 and PC3, Figure 4j) was occupied by species living in temperate, closed environments. Unfortunately, the remaining habitats are represented by only one cervid species each. Hence, we cannot decide whether the separation due to size and/or shape between them is related to species or habitat.

The situation is analogous when species were grouped by their social behavior. The lacrimal facial facets of solitary species were spread out over the complete size range (PC1, Figure 4k), and shape space (PC2 and PC3, Figure 4l). The size range and shape space of species living in groups or said to live in groups and/or solitarily appear much smaller. However, we must realize that these latter categories are represented by two or even a single species, respectively.

3.2 | Allometric scaling of single lacrimal variables

As neither size nor size-independent shape revealed any clear relationship with cervid systematics, ecology, or behavior, we asked whether size-related *changes* in shape might be more informative. To understand how differences in shape relate to the allometric scaling of the lacrimal facial facet (Figure 3), we analyze the loadings of principal components. In particular, a comparison of the loadings of PC1 allows for a comparison of the growth of the individual variables characterizing the lacrimal facial facet (see Jolicoeur, 1963, for a rationale). If all variables subjected to PCA scaled isometrically, the loadings of PC1 would all be equal to 0.408 (Jolicoeur, 1963). Some of the estimated loadings significantly deviate from this value (Table 3). Specifically, the upper 95% bootstrap boundary is smaller than the value of isometry for the loadings of the lacrimal height and of the lacrimomaxillar length. This suggests that the two variables are negatively allometric with respect to PC1. In contrast, the lower 95% bootstrap boundary of both the loadings of the lacrimojugal length and of the maximal lacrimal length are larger than expected for isometry, which means that these measures show positive allometry. Lastly, the loadings of the lacrimoethmoidal gap and the lacrimofrontal length are within the bootstrap confidence interval; hence, these measures appear to grow isometrically with respect to PC1.

These findings suggest that single variables of the lacrimal facial facet contribute differently to its allometric growth with skull size (Figure 3). In order to test this, we used major axis regression and related individual measures defining the lacrimal facial facet to skull length. The results obtained are summarized in Table 5. Lacrimal height scales negatively with skull length, that is, its slope is smaller than 1.0. The scaling of the lacrimomaxillar length cannot be distinguished from isometry, as its confidence interval encompasses the value of 1.0. All other variables show positive allometric growth, which is particularly strong for the lacrimojugal length.

The differential allometric scaling entails that the relative length of individual sutures of the lacrimal facial facet varies across the species analyzed here. Figure 5 shows parallel coordinates plots (Heintz, 1970; Simonelli, 1908), where lacrimal variables are depicted in their anatomical order, proceeding clockwise for the left lacrimal facial facet and counter-clockwise for the right one. Variables are size-corrected, and the relative length of any individual lacrimal suture can thus be compared across specimens and species.

TABLE 5 Slopes, their 95% confidence intervals, and variance explained (R^2) by regression of lacrimal measures on skull length using major axis regression

	Scaling with skull length		
Distance	Slope	95% CI	R^2
Lacrimal height	0.75	0.67–0.83	0.75
Lacrimomaxillar length	1.30	0.98–1.75	0.28
Lacrimojugal length	1.72	1.60–1.85	0.85
Lacrimoethmoid length	1.47	1.33–1.62	0.72
Lacrimofrontal length	1.34	1.16–1.56	0.58
Maximal lacrimal length	1.28	1.19–1.38	0.85

Note: Slopes larger than unity indicate positive, those smaller than unity negative allometric scaling. Slopes that cannot be distinguished from unity signify isometric scaling.

The least differentiated pattern can be seen in *M muntjak*, in which all lacrimal measures but the maximal lacrimal lengths are of about the same length. This distinguishes *M muntjak* from all other cervid species and also from the two outgroups. In the remaining cervids, the lacrimomaxillar length and the lacrimofrontal length are shorter than the lacrimoethmoid length. In the outgroups, this pattern is opposite, with lacrimomaxillar and lacrimofrontal lengths longer than the lacrimoethmoid length. Except for *M muntjak*, cervid species can be distinguished based on the relative length of the lacrimal height, the lacrimojugal length, and the lacrimomaxillar length. The lacrimojugal length may be longer than the lacrimomaxillar length and also longer, or at least as long as the lacrimal height. This pattern is seen in *Alces*, *Rangifer*, *Cervus*, *Rucervus*, *Dama*, and also *Capreolus*. Alternatively, the lacrimojugal length may be shorter than the lacrimomaxillar length, and also shorter than the lacrimal height. This pattern is seen in *Pudu* and *Mazama*, and *Hydropotes* as well as the outgroups, *Moschus* and *Tragulus*.

The relative length of these three sutures does not mirror cervid systematics, that is, their proportions do not allow discriminating Cervinae from Capreolinae (e.g., capreoline *Alces*, *Rangifer*, *Capreolus* are similar *to cervine Cervus*, *Rucervus*, and *Dama).* The cervine *Muntiacus* shows a pattern distinct from those observed in both subfamilies. Furthermore, the relative length of these three sutures does not allow distinguishing the two outgroups from the cervids *Pudu* and *Mazama*.

The relative suture lengths do not reflect habitat preferences. Thus, *Alces*, *Rangifer*, *Cervus*, and *Rucervus*, which live in quite distinct habitats (see Figure 4i,j) all share the same basic pattern of suture lengths. As *Rangifer* and *Cervus* are living in groups, whereas *Alces* and *Rucervus* prefer to be solitary, this also indicates that the pattern of suture length cannot be related to social behavior. However, we note that species in which the lacrimojugal length is longer than the lacrimomaxillar length tend to have large, complex antlers, whereas species in which the lacrimojugal length is shorter than the lacrimomaxillar length have small, simple antlers or none at all.

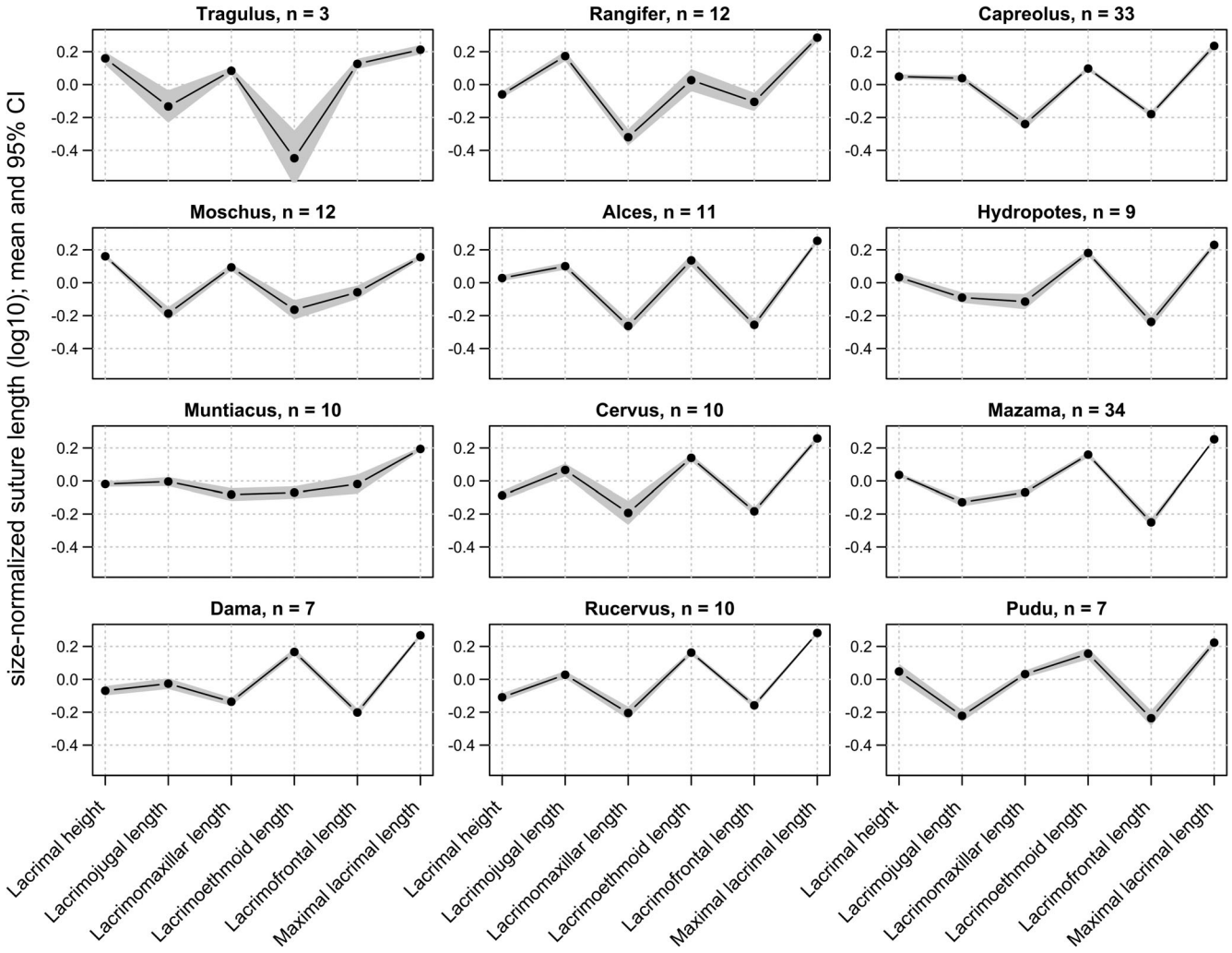

FIGURE 5 Interspecific differences of the size-normalized variables describing the lacrimal facial facet. Variables are ordered following their anatomical order, with the maximal lacrimal length in the last position. Variables are shown on a $\log_{10}$ scale, and consequently, positive values indicate that a variable is larger than the geometric mean of the specimen, negative values that it is smaller. Mean data points are connected by a line, the 95% CI is shaded in grey. *Muntiacus* can be grouped neither with cervids nor with any of the two outgroups (*Moschus* and *Tragulus*), having sutures of approximately equal length. All other cervids have a longer lacrimoethmoid length than the lacrimofrontal length, which discriminates them from the outgroups

3.3 | Relationships between the shape of the lacrimal facial facet and other skull regions

In order to test for relationships between the six variables describing the lacrimal facial facet and other variables describing overall skull structure, notably of bones not *directly* contacting the lacrimal facial facet, we performed correlation analyses. The goal was to find out if lacrimal variables correlated preferentially with variables assigned to one skull module.

We calculated these correlations separately for four similarly sized species, three cervids (*C capreolus*, *H inermis*, and *M muntjak*) and *Moschus moschiferus* as outgroup. Of the full set of 57 skull measurements, 16 were not used because they were available for only less than 50% of all specimens (see Appendix 1). The remaining set of six lacrimal and 41 non-lacrimal skull variables still contained a few missing values for each species (*C capreolus*: 0.83%, *H inermis*: 4%, *M muntjak*: 9.4%, *M moschiferus*: 3.4%). These were imputed using Bayesian PCA (see Materials and Methods), an approach that seems justified and appropriate for our data given the low numbers of missing data (see Brown, Arbour, & Jackson, 2012; Mallon, 2017). With these data, 246 correlations could be calculated for each species. Figure 6 shows the correlation patterns of measures of the lacrimal facial facet with skull measures assigned to the nasal module. This plot gives a first impression of the variability of the correlations within this module and across species. Analogous plots for the modules *base*, *vault*, *oral*, *jugal*, and *none* look similar (data not shown).

Asking how these correlations vary across species and whether this variability can be related to functional morphology, we focused on the 26 (~ 10%) the strongest correlations of each species. These were all larger than 0.53 or smaller than –0.53 for *H inermis*, *M muntjak*, and *M moschiferus*, and larger than 0.38 or smaller than –0.38 for *C. capreolus*. We expected that, if the lacrimal facial facet

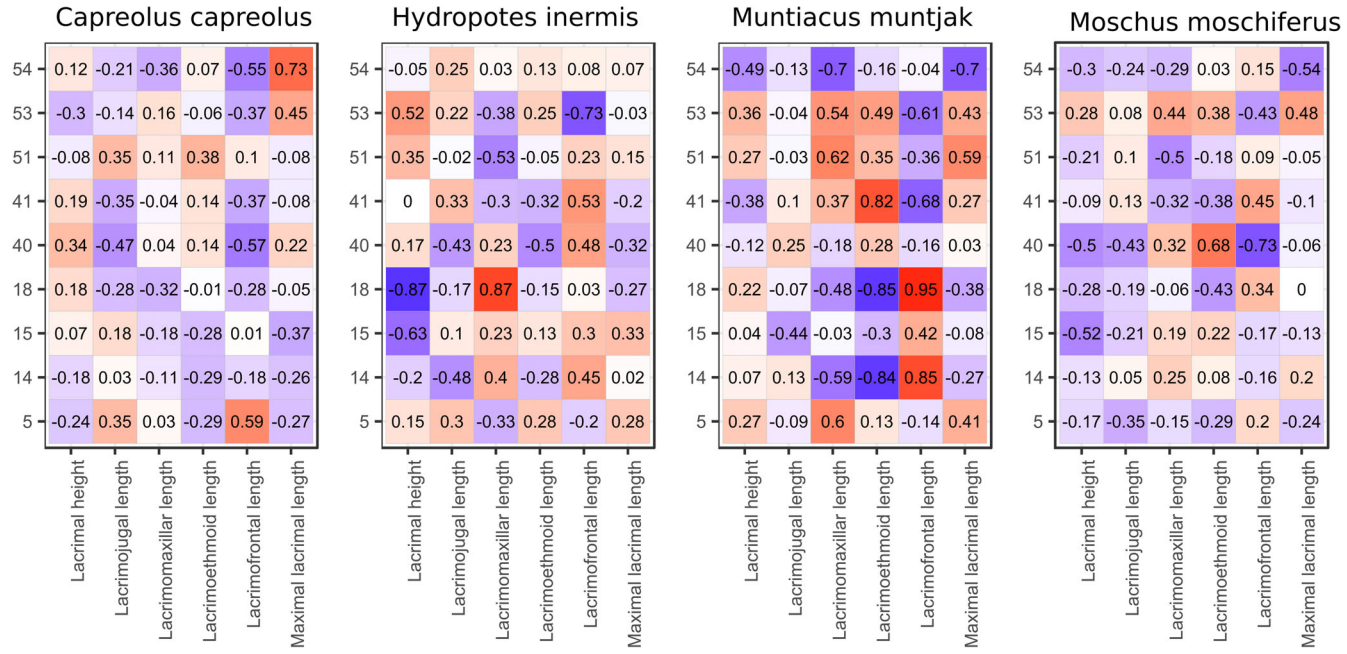

FIGURE 6 Spearman-rank correlations between the six size-normalized measures defining the lacrimal facial facet and measures assigned to the nasal module observed in three cervid species and *Moschus moschiferus* as outgroup. The strength of correlations is color-coded with positive correlations (i.e., both measures increase) coded in hues of red, and negative correlations (i.e., the lacrimal measure increases and the measures in the nasal module decreases) in hues of blue. White indicates that no correlation was detectable. Row numbers indicate the following measures of the nasal module: 5—Dorsal length of the nasal bone; 14—Nasal width at nasopremaxillar suture; 15—Nasal width at nasomaxillar suture; 18—Maximal distance between the foramina infraorbitalia; 40—Anteriour snout length; 41—Anteriour snout height; 51—Length of nasomaxillar rim; 53—Anteriour height of ethmoidal gap; 54—Ventral length of the ethmoidal gap [Color figure can be viewed at wileyonlinelibrary.com]

TABLE 6 Pairwise species comparison of strong correlations using Fisher's exact test

Species comparison	*p*-values for modules	*p*-value for lacrimal measures
Capreolus capreolus vs. *Hydropotes inermis*	.98	.08
C capreolus vs. *Muntiacus muntjak*	.75	.08
C capreolus vs. *Moschus moschiferus*	.54	.15
H inermis vs. *M muntjak*	.75	.22
H inermis vs. *M moschiferus*	.54	.60
M muntjak vs. *M moschiferus*	.75	.08

Note: *p*-values were adjusted using the Benjamini–Hochberg false discovery rate. Species do not differ based on the distribution of the number of strong correlations across modules or lacrimal measures.

were functionally or developmentally integrated with any module, strong correlations should occur preferentially within that module.

We found that in each of the four species, the correlations observed are distributed randomly across modules (p = .8, p = 1.0, p = .6, p = .5 for *C capreolus*, *H inermis*, *M muntjak*, and *M moschiferus*, respectively). In other words, the measures defining the lacrimal facial facet do not preferentially correlate with measures from any one module. Similarly, comparison across species showed that species could not be distinguished from each other based on this criterion (Table 6). Furthermore, we found that in each of the four species, the correlations observed are distributed randomly across lacrimal variables (p = .2, p = 1.0, p = .3, p = .7 for *C capreolus*, *H inermis*, *M muntjak*, *and M moschiferus*, respectively). Thus, there is no one variable of the lacrimal facial facet for which strong correlations with other skull variables occur more frequently than for any other lacrimal variable.

Finally, there was only little overlap between the top 26 correlations identified in the four species. Specifically, in *C capreolus* and *H inermis*, only two correlations involved the same variables. The same was true for *C capreolus* and *M muntjak*. *C capreolus* and *M moschiferus* shared five correlations: these were the correlations between the lacrimojugal length and the skull length 1 (no. 1); the lacrimojugal length and the skull length 2 (no. 2), the lacrimofrontal length and the skull length 2 (no. 3); the lacrimofrontal length and the nasal length (no. 4); and finally the lacrimal height and the greatest breadth of occipital condyles (no. 5). *H inermis* and *M muntjak* shared correlations, that is, that of the maximal lacrimal length with the skull length; that between the maximal lacrimal length and the length of the palatine; that of the lacrimal height and the braincase height; and that between the lacrimomaxillar length and the length of the nasomaxillar rim. For *H inermis* and *M moschiferus*, two overlapping correlations were found. Finally, *M moschiferus* and *M muntjak* overlapped for one correlation, that is, that between the maximal lacrimal length and the facial length (prosthion-M^3).

Generally, these values may be compared to the expected occurrence of such overlaps based on two random draws of 26 from 246, which is 2.74. The overlaps found for *C capreolus* and *M*

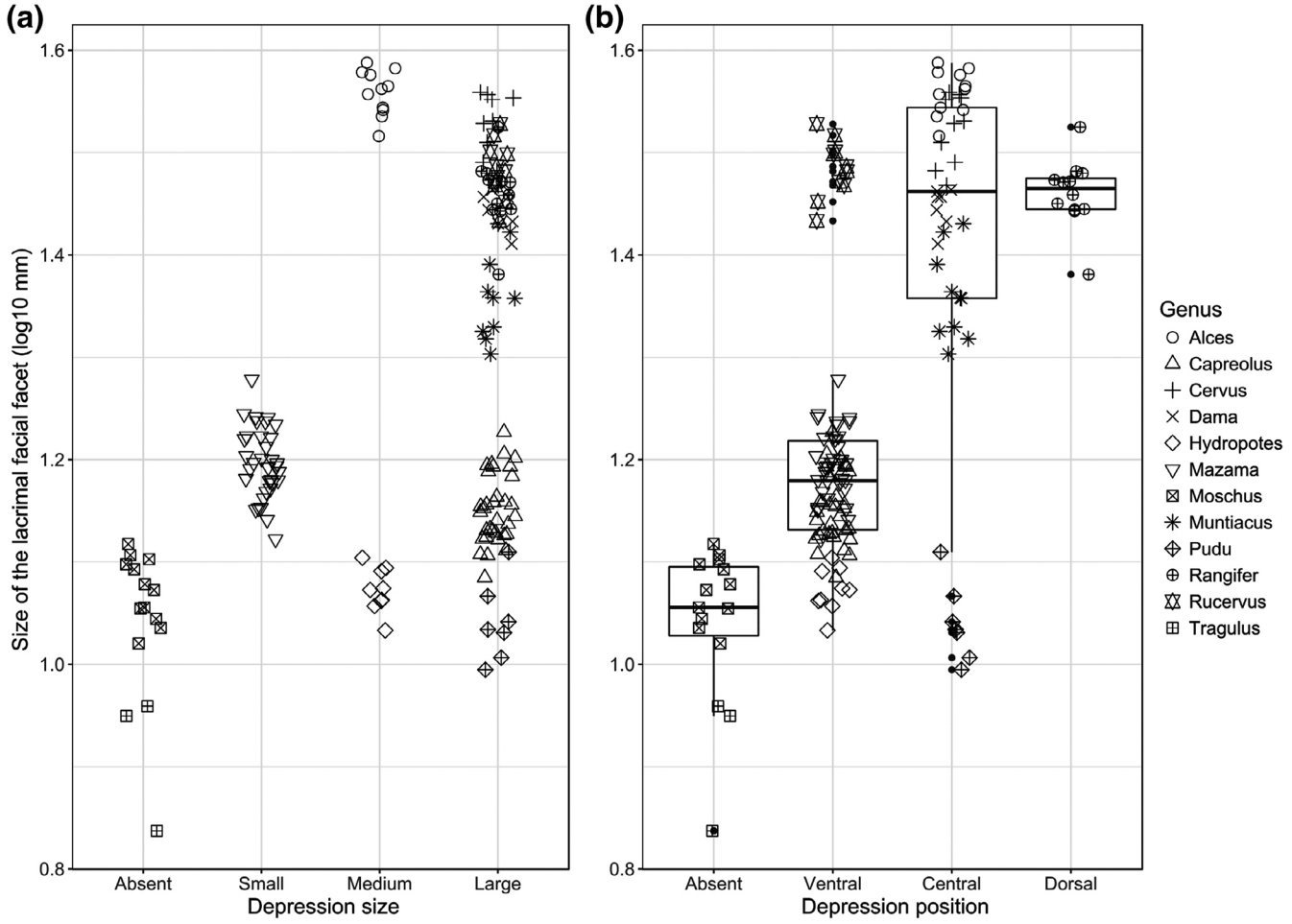

FIGURE 7 Relationships between the size of the lacrimal facial facet and preorbital depression size (a) and position (b). The (relative) size of the depression (a) is not systematically related to the size of the lacrimal facial facet. Thus, large depressions may be found in species that differ in bone size by a factor of at least 1.5, and *Hydropotes*, and *Pudu*, which have about the same bone size, have medium and large sized depressions, respectively. Note also that *Moschus*, which has no depression, has a lacrimal facial facet in the same size range as *Hydropotes* and *Pudu*. The position of the preorbital depression (b) shows no concordance with the size of the lacrimal facial facet, nor with the size of the depression (compare panels a and b)

moschiferus and H inermis and *M muntjak*, though higher than the random number, again could not be assigned to a specific module or lacrimal variable.

3.4 | Size of the lacrimal facial facet and the morphology of the preorbital depression

The size and topographic position of the preorbital depression varied widely across species (Figure 1). A summary overview of the morphology of the preorbital depression as observed in our specimens is given in Table 1. Large depressions are found in both animals with large and in animals with small lacrimal facial facets. In all large facial facets, the depressions consistently occupy a substantial fraction of the area of the facial facet, that is, are never "small." Moreover, on large lacrimal facial facets, the depressions tend to be located centrally or dorsally. On smaller lacrimal facial facets, the depression is typically located ventrally and never dorsally (Figure 7b). Yet, this again seems not to be a fixed rule, as *R eldii* and *M muntjak*, which have large facial facets, have ventrally located depressions and *P puda*, which has a small facial facet, has a central depression.

Pairwise comparisons using Mood's median tests confirmed the above conjecture that neither the size nor the position of the preorbital depression correlates with the size of the lacrimal facial facet ($p > .05$ for the combinations between small/medium/large depressions; Figure 7a,b). Thus, the relative size of the preorbital depression in cervids does not follow facet size and thus, skull length (Figure 3).

4 | DISCUSSION

Our quantitative data document a high variability of the morphology of the lacrimal facial facet in cervids, as has been previously conjectured based on qualitative data (Gregory, 1920; Knottnerus-Meyer, 1907; Rütimeyer, 1881). Our data also show that this variability cannot be related to cervid systematics, either to their ecology or behavior. Lastly, we found that the lacrimal facial facet scales allometrically with skull size.

The overlap in size (PC1 in Figure 4e) and size-independent shape (PC2 and PC3 in Figure 4e,f) seen for the lacrimal facial facet of Cervidae, Moschidae, and the two cervid subfamilies contrasts with the clear phylogenetic and systematic separation of these (sub-) families (see, e.g., Hassanin et al., 2012; Heckeberg, Erpenbeck, Wörheide, & Rössner, 2016; Pitra, Fickel, Meijaard, & Groves, 2004). Thus, the extensive overlap between *A alces* (Capreolinae) and *R eldii* (Cervinae) in shape space indicates that the shape of the lacrimal facial facet is not a trait conserved within systematic relationship. The shape overlap of *C capreolus* and *M gouazoubira* with the remaining cervid species (except *M muntjak)* further supports that shape is not systematically informative. From a technical point of view, one may note that the relatively small sample sizes for all species except *C capreolus* and *M gouazoubira*, may result in an underestimation of variability and hence, interspecific overlap in size and shape of the lacrimal facial facet.

Still, the form of the lacrimal facial facet that is, its size and shape (Figure 4c,d), especially when combined with traits of the preorbital fossa (Figure 7), can be used to identify species. This is in line with previous observations and conclusions based on qualitative traits of the lacrimal facial facet (Gregory, 1920; Knottnerus-Meyer, 1907; Rütimeyer, 1881). In fact, our data show that size-independent shape (i.e., PC2 and PC3; see Figure 4c,d) alone is sufficient to discriminate some cervid species, for example, *Pudu* from both *Hydropotes* and *Rangifer* as well as *Dama* from *Rangifer* (PC2 in Figure 4c) and both *Hydropotes* and *Pudu* from *Rangifer* (PC3 in Figure 4d).

As the morphology of the lacrimal facial facet could not be related to cervid systematics, we investigated its potential relationships with cervid habitat, social behavior, and head weapons. Size and shape varied also extensively within any of the ecological or behavioral categories considered (Figure 4g–l). This documents that none of these conditions imposes strict constraints on the size and shape of the lacrimal facial facet in the species investigated.

A salient finding of the present investigation is that the facial facet of the cervid lacrimal bone scales allometrically with skull length (Figure 3, Table 3), and thus body size (Cardini & Polly, 2013). As body size is a selected trait, the form of the lacrimal facial facet could be the result of "indirect selection" (Hansen, 2014, p. 355). Thus, whatever mechanisms influence body size, could eventually also impact on the morphology of the lacrimal facial facet.

The allometric scaling of the lacrimal facial facet implies that changes in its size go along with changes in its shape. Large cervids (*Alces*, *Cervus*, *Dama*, *Rucervus*, *Rangifer*) tend to have elongated and rather narrow lacrimal facial facets. In smaller-sized cervid species (*Capreolus* and *Hydropotes*; and also *Pudu* and *Mazama*, which probably have reduced their body size secondarily [Eisenberg, 1987]), as well as in the small-sized outgroups *Tragulus* and *Moschus*, the lacrimal facial facet is rather higher than long, with a more prominent lacrimal height.

A consequence of these size-related changes in shape and hence, the relative length of individual sutures, is that any change in size alters the integration of the lacrimal facial facet with the skull bones directly surrounding it. Interestingly, elongation of the lacrimal facial facet goes along with a disproportional elongation of the lacrimojugal length. In contrast, the lacrimomaxillar length, which may be viewed as the rostral continuation of the lacrimojugal length, expands only isometrically with skull length (Figure 5, Table 5). This effectively results in the intercalation of an increasingly longer part of the jugal between the lacrimal facial facet and the maxillary bone. The allometric scaling of the lacrimal facial facet does not appear to be an "inevitable" consequence of skull elongation in herbivore mammals. Thus, in horses, which have a long face, the lacrimal facial facet is more or less square, rather than elongated (Gregory, 1920).

We do not know why the lacrimojugal length should scale differently from the lacrimomaxillar length. A still plausible explanation is that "…the form and size of the lacrymal of mammals are conditioned […] by several external factors, such as the […] special development of the maxillary and the jugal […]", as already proposed by Gregory (1920, p. 217).

As discussed above, the lacrimal facial facet apparently did not adapt directly in cervids. Following the argument of Gregory (1920) cited above, it seems reasonable to assume that the cervid lacrimal facial facet primarily fills the space created when its surrounding bones change as the skull gets longer or shorter (see also Cox, 2008). In cervids, the lacrimal facial facet may have subsequently been exapted sensu Gould and Vrba (1982). That is, it may have "evolved for other usages (or for no function at all), and later"coopted" for [its] current role (p. 6)". Thus, within the context of the architectural changes occurring with the evolution of the cervid skull, the lacrimal facial facet may be termed a "spandrel" sensu Gould (1997), that is, "a nonadaptive architectural byproduct of definite and necessary form—a structure of predictable size and shape that then becomes available for later and secondary utility (p. 10751)". Gould (1997) further continues "…any primary adaptation must generate **a set of** architecturally enjoined side consequences or spandrels". So what could this secondary utility of the lacrimal facial facet be? And which other spandrels may be identified in the cervid skull? It is well-known that antler size grows allometrically with body (and skull) size in cervids (Gould, 1974). Thus, large cervids are capable to produce larger antlers. This begs the question whether and how the allometric growth of antlers relates to that of the lacrimal facial facet observed presently. One possibility may be that a large lacrimal may serve to strengthen the skull to support antlers. This echoes a hypothesis previously stated for bovids with large horns (Gregory, 1920). Like horns, antlers are outgrowths of the frontal bone, which is in direct contact with the lacrimal facial facet, and through the jugal, also in indirect contact with it. Stress originating from antlers during intraspecific fights will be certainly modulated, but not abolished, by intrinsic stress- and impact dampening properties of antlers (i.e., their intrinsic elasticity and mineral content; see, for example, Currey et al., 2009; Picavet & Balligand, 2016). The remaining stress will be dissipated along the craniofacial sutures (Maloul, Fialkov, & Whyne, 2013) and we expect that longer sutures are more efficient in stress dissipation than shorter ones. Bones move along sutures (Bright, 2012 and see further references therein; Persson, 1995; Pritchard, Scott, & Girgis, 1956) to dissipate stress. In cervids, the ethmoidal gap could work as a crash-collapsible zone, giving space to the movements of frontal, jugal, and maxilla and, hence, buffering the mechanical loads originating from antlers.

The shift toward longer lacrimojugal sutures and the ethmoidal gap could be all components of a set of spandrels created by skull elongation in cervids. Both components may have developed proper functions, unrelated to the functions of the other one. Together, these spandrels can interact to dissipate antler-related stress and are thus functionally well integrated into the cervid skull. Thus, the size-dependent growth of the lacrimal facial facet suggests that variation in its size and shape may best be seen within the context of the integration of stress resulting from antlers used for intraspecific sexual competition and selection (Clutton-Brock, Guinness, & Albon, 1982; Kodric-Brown & Brown, 1984). This is supported by the observation that the length difference between the lacrimojugal and lacrimomaxillar length seen across large, antlered species quite nicely follows the known size-pattern of their antlers (*A alces*, 108/0.363; *Cervus elaphus*, 93.6/0.260; *R tarandus*, 117.2/0.493; *R eldii*, 94.3/0.233; *D dama*, 72.9/0.110; the numbers give antler length in cm as taken from Clutton-Brock, Albon, & Harvey, 1980 and the length differences, respectively; $R^2 = 0.95$).

Furthermore, even *deviations* of individual species from the common allometric line conform for analyses of antlers (Gould, 1974; his Figure 1) and the lacrimal facial facet. The two species common to both studies, that is, *A alces* and *D dama*, fall conspicuously below (*A alces*) or above (*D dama)* the lines describing allometric scaling.

We could not ascertain any systematic relationships of the measures characterizing the lacrimal facial facet with skull measures beyond immediate contact sites or distinct skull modules (Haber, 2014; Porto et al., 2009). This is consistent with the observation by Cox (2008), who, using a different (and smaller) set of measurements than used here, noted that the size of the lacrimal facial facet correlates rarely with other skull measures. However, we would like to point out that these data should not be interpreted to indicate that such integration does not exist. Rather, the presently observed variability inherent in these measures documents that a much larger dataset would be needed to detect such integration, or in fact to exclude it with an acceptable degree of certainty.

Finally, we could not ascertain any systematic relationships between the lacrimal facial facet and the size and position of the preorbital depression. The size of the lacrimal facial facet and the size of the preorbital depression appear to be unrelated or to evolve independently. Contrary to what one might expect, a large preorbital depression is not exclusively found in large cervids and large lacrimal facial facets (see e.g., *Pudu*, Figure 7a) and large cervids do not necessarily have large preorbital depressions (e.g., *Alces*, Figure 7a). Large preorbital depressions are also seen in cervids from the Miocene, for example, *Procervulus dichotomus* (Gervais, 1849) (Rössner, 1995), *Euprox* (Hou, 2015), *Eostyloceros* (Deng, Wang, Shi, Li, & Li, 2014) and their direct ancestors, for example, *Dremotherium* (Janis & Scott, 1987) and therefore seems to be a plesiomorphic character. The large preorbital depression in the small *Pudu* could be a plesiomorphic condition, not affected by the secondary size reduction. This hypothesis would be in line with reversals previously proposed to explain the species' spiked antlers and the suture closure in dwarfed fossil cervids from the island of Crete (Randi, Mucci, Pierpaoli, & Douzery, 1998; Sánchez-Villagra, 2010). We cannot exclude though, that it is a random or labile character, as *Mazama*, which also is considered to have reduced its body size secondarily, does not show the same pattern.

Whether and how the size and topography of the preorbital depression might affect the mechanical stability of the lacrimal facial facet cannot be addressed with the present data. A better understanding of the functional and/or ecologic relevance of the size (and, eventually, shape) and the exact position of the preorbital depression will require an approach that allows studying internal bone structure together with that of the preorbital gland and its associated muscles and soft tissue (Barrette, 1976; Ozaki, Suzuki, & Ohtaishi, 2004).

5 | CONCLUSIONS

We quantified the size and shape variation in the cervid lacrimal facial facet in 10 species covering genera from the major evolutionary lineages and tested potential systematic or ecological / behavioral relationships. Neither systematics nor any of the ecological categories tested in itself may be used to explain the variability of the lacrimal facial facet in cervids. Thus, the lacrimal facial facet may be viewed as an evolutionary flexible structure that may adjust readily to adaptive changes in its surrounding bones. One consequence of this situation is that the lacrimal facial facet may not be used to infer evolutionary relationships among cervid genera. This contrasts with the utility of this structure to differentiate taxa at or above the family level.

The allometric scaling of the cervid lacrimal facial facet with skull size is reminiscent of the size-dependent scaling of antlers (cf. Gould, 1974). It results in changes of its integration of the lacrimal facial facet with its surrounding bones that, secondarily, may have been exapted to reduce mechanical loads originating from increasingly larger antlers. The identification and characterization of force trajectories in the cervid skull, for example, by analysis of the trabecular architecture (e.g., Ruff, Holt, & Trinkaus, 2006; Schilling, Tofanelli, Hublin, & Kivell, 2014) should help to find out whether the lacrimal facial facet is indeed subjected to mechanical stress as suggested here.

ACKNOWLEDGMENTS

We are grateful to Dr. Anneke van Heteren (ZSM), Michael Hiermeier (ZSM), Britta Möllenkamp (SAPM), Dr. Henriette Obermaier (SAPM), PD Dr. Frank Zachos (NHMW), Alexander Bibl (NHMW), Christiane Funk (ZMB) and Steffen Bock (ZMB) for providing access to specimens.

AMS received an LMU TravelGrant 2015. We thank Jonathan Guzman and Nicola Heckeberg for helpful comments and input. We also thank the anonymous reviewers and the editor for their constructive criticism on earlier drafts of the manuscript, which helped much to improve it.

CONFLICT OF INTEREST

The authors declare that they do not have any conflict of interest.

AUTHOR CONTRIBUTIONS

AMS collected data, designed and performed statistical analyses, wrote the paper, revised the paper. GER supervised study design and performance, reviewed drafts of the paper. MCCC collected data.

ORCID

Ann-Marie Schilling https://orcid.org/0000-0002-3176-6792

REFERENCES

Bärmann, E. V., & Sánchez-Villagra, M. R. (2012). A phylogenetic study of late growth events in a mammalian evolutionary radiation-the cranial sutures of terrestrial artiodactyl mammals. *Journal of Mammalian Evolution*, *19*(1), 43–56. http://doi.org/10.1007/s10914-011-9176-8

Barrette, C. (1976). Musculature of facial scent glands in the muntjac. *Journal of Anatomy*, *122*(1), 61–66.

Barrette, C. (1977). Fighting behavior of muntjac and the evolution of antlers. *Evolution*, *31*(1):169–176.

Bright, J. A. (2012). The importance of craniofacial sutures in biomechanical finite element models of the domestic pig. *PLoS ONE*, *7*(2), e31769. http://doi.org/10.1371/journal.pone.0031769

Brown, C. M., Arbour, J. H., & Jackson, D. A. (2012). Testing of the effect of missing data estimation and distribution in morphometric multivariate data analyses. *Systematic Biology*, *61*(6), 941–954. http://doi.org/10.1093/sysbio/sys047

Cardini, A., & Polly, P. D. (2013). Larger mammals have longer faces because of size-related constraints on skull form. *Nature Communications*, *4*, 1–7. http://doi.org/10.1038/ncomms3458

Clutton-Brock, T. H., Albon, S. D., & Harvey, P. H. (1980). Antlers, body size and breeding group size in the Cervidae. *Nature*, *285*(5766), 565–567. http://doi.org/10.1038/285565a0

Clutton-Brock, T. H., Guinness, F. E., & Albon, S. D. (1982). *Red deer: Behavior and ecology of two sexes*. Chicago: University of Chicago press.

Cobb, W. M. (1943). The cranio-facial union and the maxillary tuber in mammals. *American Journal of Anatomy*, *72*(1), 39–111. http://doi.org/10.1002/aja.1000720104

Cox, P. G. (2008). A quantitative analysis of the eutherian orbit: Correlations with masticatory apparatus. *Biological Reviews*, *83*(1), 35–69. http://doi.org/10.1111/j.1469-185X.2007.00031.x

Currey, J. D., Landete-Castillejos, T., Estevez, J., Ceacero, F., Olguin, A., Garcia, A., & Gallego, L. (2009). The mechanical properties of red deer antler bone when used in fighting. *Journal of Experimental Biology*, *212* (24), 3985–3993. http://doi.org/10.1242/jeb.032292

Darroch, J. N., & Mosimann, J. E. (1985). Canonical and principal component of shape. *Biometrika*, *75*(2), 241–252.

Deng, T., Wang, S. Q., Shi, Q. Q., Li, Y. K., & Li, Y. (2014). A new species of Eostyloceros (Cervidae, Artiodactyla) from the late Miocene of the Linxia Basin in Gansu, China. *Zootaxa*, *3893*(3), 363–381. http://doi.org/10.11646/zootaxa.3893.3.3

Eisenberg, J. F. (1987). The evolutionary history of the Cervidae with special reference to the south American radiation. In C. M. Wemmer (Ed.), *Biology and Management of the Cervidae* (pp. 60–64). Washington, DC: Smithsonian Institution Press.

Emery, M. M. (2016). *Assessment of character variation in the cranial and teeth of modern artiodactyls for better species diagnosis in the fossil record*. (ProQuest Dissertations and Theses). University of Oregon.

Falsetti, A. B., Jungers, W. L., & Cole, T. M. (1993). Morphometrics of the Callitrichid forelimb - A case study in size and shape. *International Journal of Primatology*, *14*(4), 551–572.

Geist, V. (1998). *Deer of the world: Their evolution, behaviour, and ecology*. Mechanicsburg, Pennsylvania: Stackpole Books.

Geist, V., & Bayer, M. (1988). Sexual dimorphism in the Cervidae and its relation to habitat. *Journal of Zoology*, *214*(1), 45–53. http://doi.org/10.1111/j.1469-7998.1988.tb04985.x

Gould, S. J. (1974). The origin and function of "bizarre" structures: Antler size and skull size in the "Irish elk," Megaloceros giganteus. *Evolution*, *28*(2), 191–220.

Gould, S. J. (1997). The exaptive excellence of spandrels as a term and prototype. *Proceedings of the National Academy of Sciences*, *94*(20), 10750–10755.

Gould, S. J., & Vrba, E. S. (1982). Exaptation-a missing term in the science of form exaptation-a missing term in the science of form. *Paleobiology*, *8*(1), 4–15.

Gregory, W. K. (1920). Studies in comparative myology and osteology: No. IV. -A review of the evolution of the lacrymal bone of vertebrates with special reference to that of mammals. *Bulletin of the American Museum of Natural History*, *XLII*, 95–263.

Groves, C., & Grubb, P. (2011). *Ungulate Taxonomy* (Vol. 1). Baltimore: John Hopkins Universtiy Press.

Groves, C. P. (2007). Family Cervidae. In D. R. Prothero & S. E. Foss (Eds.), *The evolution of artiodactyls* (pp. 249–256). Baltimore: John Hopkins University Press.

Haber, A. (2014). The evolution of morphological integration in the ruminant skull. *Evolutionary Biology*, *42*(1), 99–114. http://doi.org/10.1007/s11692-014-9302-7

Hansen, T. F. (2014). Use and misuse of comparative methods in the study of adaptation. In L. Z. Garamszegi (Ed.), *Modern phylogenetic comparative methods and their application in evolutionary biology* (pp. 351–379). Berlin: Springer.

Hassanin, A., Delsuc, F., Ropiquet, A., Hammer, C., Jansen Van Vuuren, B., Matthee, C., … Couloux, A. (2012). Pattern and timing of diversification of Cetartiodactyla (Mammalia, Laurasiatheria), as revealed by a comprehensive analysis of mitochondrial genomes. *Comptes Rendus Biologies*, *335*(1), 32–50. http://doi.org/10.1016/j.crvi.2011.11.002

Heckeberg, N. S., Erpenbeck, D., Wörheide, G., & Rössner, G. E. (2016). Systematic relationships of five newly sequenced cervid species. *PeerJ*, *4*, e2307. http://doi.org/10.7717/peerj.2307

Heintz, E. (1970). Les Cervidés Villafranchiens de France et d'Espagne. *Memoires Du Museum National D'Histoire Naturelle Nouvelle Serie, Serie C, Sciences de La Terre*, *22*, 1–303.

Hervé, M. (2015). R package 'RVAideMemoire': Diverse Basic Statistical and Graphical Functions. Version: 0.9,45–2.

Hou, S. (2015). A new species of *Euprox* (Cervidae, Artiodactyla) from the upper Miocene of the Linxia Basin, Gansu Province, China, with interpretation of its paleoenvironment. *Zootaxa*, *3911*(1), 43–62. http://doi.org/10.11646/zootaxa.3911.1.2

Janis, C. M., & Scott, K. M. (1987). The interrelationships of higher ruminant families with special emphasis on the members of the Cervoidea. *American Museum Novitates*, *2893*, 1–85.

Jolicoeur, P. (1963). 193. Note: The multivariate generalization of the Allometry equation. *Biometrics*, *19*(3), 497. http://doi.org/10.2307/2527939

Klingenberg, C. P. (2016). Size, shape, and form: Concepts of allometry in geometric morphometrics. *Development Genes and Evolution*, *226*(3), 113–137. http://doi.org/10.1007/s00427-016-0539-2

Knottnerus-Meyer, T. C. B. (1907). Über das Tränenbein der Huftiere: Vergleichend -anatomischer Beitrag zur Systematik der Rezenten Ungulata. *Archiv Für Naturgeschichte*, *73*, 1–153.

Kober, J. (1880). Vergleichend-anatomische Beiträge zur Geschichte des Thränenbeins. *Jahreshefte des Vereins Für Vaterländische Naturkunde in Württemberg*, *36*, 118–154.

Kodric-Brown, A., & Brown, J. H. (1984). Truth in advertising: The kinds of traits favored by sexual selection. *The American Naturalist*, *124*(3), 309–323. http://doi.org/10.1086/284275

Langguth, A., & Jackson, J. (1980). Cutaneous scent glands in pampas deer *Blastoceros bezoarticus* (L., 1758). *Zeitschrift Für Säugetierkunde*, *45*, 82–90.

Logan, M. (2011). *Biostatistical design and analysis using R: A practical guide*. Chicester, UK: John Wiley & Sons. http://doi.org/10.1086/662500

Mallon, J. C. (2017). Recognizing sexual dimorphism in the fossil record: Lessons from nonavian dinosaurs. *Paleobiology*, *43*(03), 495–507. http://doi.org/10.1017/pab.2016.51

Maloul, A., Fialkov, J., & Whyne, C. M. (2013). Characterization of the bending strength of craniofacial sutures. *Journal of Biomechanics*, *46*(5), 912–917. http://doi.org/10.1016/j.jbiomech.2012.12.016

Mangiafico, S. (2017). rcompanion: Functions to Support Extension Education Program Evaluation. *R Package Version 1.5. 0. The Comprehensive R Archive Network*.

Marroig, G., & Cheverud, J. M. (2001). A comparison of phenotypic variation and covariation patterns and the role of phylogeny, ecology, and ontogeny during cranial evolution of New World monkeys. *Evolution*, *55*(12), 2576–2600. http://doi.org/10.1554/0014-3820(2001)055

Mattioli, S. (2011). Family Cervidae (deer). In D. E. Wilson & R. A. Mittermeier (Eds.), *Handbook of the mammals of the world* (Vol. 2, pp. 350–428). Barcelona: Lynx Ediciones.

McDonald, J. N., & Ray, C. E. (1989). The autochthonous north American musk oxen Bootherium, Symbos, and Gidleya (Mammalia: Artiodactyla: Bovidae). *Smithsonian Contributions to Paleobiology*, *66*, 1–77.

Meijaard, E. (2011). Family Tragulidae (Chevrotains). In D. E. Wilson & R. A. Mittermeier (Eds.), *Handbook of the mammals of the world*. (Vol. 2, pp. 320–334). Barcelona: Lynx Ediciones.

Meijaard, E., & Groves, C. (2004). Morphometrical relationships between Southeast Asian deer (Cervidae, tribe Cervini): Evolutionary and biogeographic implications. *Journal of Zoology*, *263*(2), 179–196. http://doi.org/10.1017/S0952836904005011

Mennecart, B., & Métais, G. (2015). *Mosaicomeryx* gen. nov., a ruminant mammal from the Oligocene of Europe and the significance of "gelocids.". *Journal of Systematic Palaeontology*, *13*(7), 581–600. http://doi.org/10.1080/14772019.2014.948505

Mitteroecker, P., Gunz, P., Windhager, S., & Schaefer, K. (2013). A brief review of shape, form, and allometry in geometric morphometrics, with applications to human facial morphology. *Hystrix*, *24*(1), 1–8. http://doi.org/10.4404/hystrix-24.1-6369

Mosimann, J. E. (1970). Size allometry: Size and shape variables with characterizations of the lognormal and generalized gamma distributions. *Journal of the American Statistical Association*, *65*(330), 930–945.

Oba, S., Sato, M. -a., Takemasa, I., Monden, M., Matsubara, K. -i., & Ishii, S. (2003). A Bayesian missing value estimation method for gene expression profile data. *Bioinformatics*, *19*(16), 2088–2096. http://doi.org/10.1093/bioinformatics/btg287

Oh, J., Kim, Y. K., Yasuda, M., Koyabu, D., & Kimura, J. (2017). Cranial suture closure pattern in water deer and implications of suture evolution in cervids. *Mammalian Biology*, *86*, 17–20. http://doi.org/10.1016/j.mambio.2017.03.004

Ozaki, N., Suzuki, M., & Ohtaishi, N. (2004). Histological variations in myoepithelial cells and arrectores pilorum muscles among caudal, metatarsal and preorbital glands in Hokkaido sika deer (*Cervus nippon yesoensis* Heude, 1884). *Journal of Veterinary Medical Science*, *66*(3), 283–285. http://doi.org/10.1111/j.1461-0248.2011.01694.x

Persson, M. (1995). The role of sutures in normal and abnormal craniofacial growth. *Acta Odontologica Scandinavica*, *53*(3), 152–161. http://doi.org/10.3109/00016359509005965

Picavet, P. P., & Balligand, M. (2016). Organic and mechanical properties of Cervidae antlers: A review. *Veterinary Research Communications*, *40*(3–4), 141–147. http://doi.org/10.1007/s11259-016-9663-8

Pitra, C., Fickel, J., Meijaard, E., & Groves, C. P. (2004). Evolution and phylogeny of old world deer. *Molecular Phylogenetics and Evolution*, *33*(3), 880–895. http://doi.org/10.1016/j.ympev.2004.07.013

Porto, A., de Oliveira, F. B., Shirai, L. T., de Conto, V., & Marroig, G. (2009). The evolution of modularity in the mammalian skull I: Morphological integration patterns and magnitudes. *Evolutionary Biology*, *36*(1), 118–135. http://doi.org/10.1007/s11692-008-9038-3

Pritchard, J. J., Scott, J. H., & Girgis, F. G. (1956). The structure and development of cranial and facial sutures. *Journal of Anatomy*, *90*(Pt 1), 73–86.3. http://doi.org/10.1007/BF02968480

R Core Team. (2018). R: A Language and Environment for Statistical Computing. Vienna, Austria.

Randi, E., Mucci, N., Pierpaoli, M., & Douzery, E. (1998). New phylogenetic perspectives on the Cervidae (Artiodactyla) are provided by the mitochondrial cytochrome b gene. *Proceedings. Biological Sciences/The Royal Society*, *265*(January), 793–801. http://doi.org/10.1098/rspb.1998.0362

Rehorek, S. J., Hillenius, W. J., Kennaugh, J., & Chapman, N. (2005). The gland and the sac — The preorbital apparatus of muntjacs. In *Chemical signals in vertebrates 10* (pp. 152–158). New York: Springer. http://doi.org/10.1007/0-387-25160-X_19

Rössner, G. E. (1995). Odontologische und schädelanatomische Untersuchungen an Procervulus (Cervidae, Mammalia). *Münchner Geowissenschaftliche Abhandlungen Reihe A Geologie Und Palaeontologie*, *29*, 1–127.

Ruff, C., Holt, B., & Trinkaus, E. (2006). Who's afraid of the big bad Wolff?: "Wolff's law" and bone functional adaptation. *American Journal of Physical Anthropology: The Official Publication of the American Association of Physical Anthropologists*, *129*(4), 484–498.

Rütimeyer, L. (1881). Beiträge zu einer natürlichen Geschichte der Hirsche. *Abhandlungen Der Schweizerischen Paläontologischen Gesellschaft*, *VIII*, 1–268. http://doi.org/10.5962/bhl.title.101995

Salibián-Barrera, M., Van Aelst, S., & Willems, G. (2006). Principal components analysis based on multivariate MM estimators with fast and robust bootstrap. *Journal of the American Statistical Association*, *101*(475), 1198–1211. http://doi.org/10.1198/016214506000000096

Sánchez-Villagra, M. R. (2010). Suture closure as a paradigm to study late growth in recent and fossil mammals: A case study with giant deer and dwarf deer skulls. *Journal of Vertebrate Paleontology*, *30*(6), 1895–1898. http://doi.org/10.1080/02724634.2010.521218

Schilling, A. M., & Rössner, G. E. (2017). The (sleeping) beauty in the beast – A review on the water deer, *Hydropotes inermis*. *Hystrix*, *28*(2), 121–133. http://doi.org/10.4404/hystrix-28.2-12362

Schilling, A. M., Tofanelli, S., Hublin, J. J., & Kivell, T. L. (2014). Trabecular bone structure in the primate wrist. *Journal of Morphology*, *275*(5), 572–585. http://doi.org/10.1002/jmor.20238

Scott, K. M., & Janis, C. M. (1987). Phylogenetic relationships of the Cervidae, and the case for a superfamily "Cervoidea.". In C. M. Wemmer (Ed.), *Biology and Management of the Cervidae* (pp. 3–20). Washington: Smithsonian Institution Press.

Sharp, A. C. (2015). Comparative finite element analysis of the cranial performance of four herbivorous marsupials. *Journal of Morphology*, *276*(10), 1230–1243. http://doi.org/10.1002/jmor.20414

Simonelli, V. (1908). Mammiferi quaternari dell'Isola di Candia-Memorie R. *Accademia Di Scienze Dell'Istituto Di Bologna (4)*, *5*, 456–470.

Stacklies, W., Redestig, H., Scholz, M., Walther, D., & Selbig, J. (2007). pcaMethods—A bioconductor package providing PCA methods for incomplete data. *Bioinformatics*, *23*(9), 1164–1167. http://doi.org/10.1093/bioinformatics/btm069

Todorov, V., & Filzmoser, P. (2009). An object-oriented framework for robust multivariate analysis. *Journal of Statistical Software*, *32*(3), 1–47.

Ungerfeld, R., González-Pensado, S., Bielli, A., Villagrán, M., Olazabal, D., & Pérez, W. (2008). Reproductive biology of the pampas deer

(*Ozotoceros bezoarticus*): A review. *Acta Veterinaria Scandinavica*, *50*(1), 16. http://doi.org/10.1186/1751-0147-50-16

van Aelst, S., & Willems, G. (2013). Fast and robust bootstrap for multivariate inference: The R package FRB. *Journal of Statistical Software*, *53*(3), 1–32. http://doi.org/10.18637/jss.v053.i03

von den Driesch, A. (1976). A guide to the measurement of animal bones from archaeological sites: As developed by the Institut für Palaeoanatomie, Domestikationsforschung und geschichte der Tiermedizin of the university of Munich. *Peabody Museum Bulletin*, *1*, 136.

Wang, X., & Hoffmann, R. S. (1987). Pseudois nayaur and *Pseudois schaeferi*. *Mammalian Species*, *278*, 1–6. http://doi.org/10.2307/3503993

Warton, D. I., Duursma, R. A., Falster, D. S., & Taskinen, S. (2012). Smatr 3-an R package for estimation and inference about allometric lines. *Methods in Ecology and Evolution*, *3*(2), 257–259. http://doi.org/10.1111/j.2041-210X.2011.00153.x

Warton, D. I., Wright, I. J., Falster, D. S., & Westoby, M. (2006). Bivariate line-fitting methods for allometry. *Biological Reviews*, *81*(02), 259. http://doi.org/10.1017/S1464793106007007

Whitlock, M., & Schluter, D. (2015). *The analysis of biological data* (2nd ed.). Greenwood Village, Colorado: Roberts and Company Publishers.

Wilson, D. E., & Mittermeier, R. A. (Eds.). (2011). *Handbook of the mammals of the world - volume 2. Hoofed mammals*. Barcelona: Lynx Edicions.

SUPPORTING INFORMATION

Additional supporting information may be found online in the Supporting Information section at the end of this article.

How to cite this article: Schilling A-M, Calderón-Capote MC, Rössner GE. Variability, morphometrics, and co-variation of the *os lacrimale* in Cervidae. *Journal of Morphology*. 2019;280: 1071–1090. https://doi.org/10.1002/jmor.21002

APPENDIX 1

Non-lacrimal skull measurements, collected for *Tragulus javanicus* and *Tragulus kanchil*, *Moschus moschiferus*, *Muntiacus muntjak*, *Hydropotes inermis*, and *Capreolus capreolus*. All sagittal measurements were taken along the skull midline. The 41 measures used for correlation analysis are in regular print, those excluded due to missing data are in italics. Data of the original measurements may be found in Table S3.

Index	Description	Distance	Distance defined by	Skull module[a]
1	Most caudal point of the occipital bone (Akrokranion, A) to most rostral point of the premaxillae (Prosthion, P); maximal skull length	AP	Driesch, 1976	None
2	Occipital angle (Lambda, L) to prosthion; skull length 1	LP	Driesch, 1976	None
3	Lambda to the most rostral point of nasal bone (Rhinion, Rh); skull length 2	LRh	Driesch, 1976	None
4	Lambda to nasofrontal suture (Nasion, N); frontoparietal length	LN	Driesch, 1976	Vault
5	Dorsal length of the nasal bone	NRh	Driesch, 1976	Nasal
6	Length of the supraoccipital bone	AL	This study	Vault
7	Lambda to the frontoparietal suture; length of parietal bone:	LF	This study	Vault
8	Length of the frontal bones	FN	Haber, 2014	Vault
9	Meeting point between the dorsal nasofrontal suture to the most caudal point of the frontal bone	NFcaud	This study	Vault
10	Most rostral to the most caudal point of frontal bone	FrostFcaud	This study	Vault
11	Maximal skull width		This study	None
12	Maximal interdistance between foramina supraorbitale		This study	Vault
13	Skull width at the rostral lacrimofrontal suture		This study	Vault
14	Nasal width at nasopremaxillar suture	NiNi	Haber, 2014	Nasal
15	Nasal width at the nasomaxillar suture	SNaSNa	Haber, 2014	Nasal
16	Premaxillar width at the palatine suture		This study	Oral
17	*Maxillar width over the canine protuberance*		*This study*	
18	Maximal distance between foramina infraorbitalia	IOF—IOF	Haber, 2014	Nasal
19	*Maximal width of the canine alveola*		*This study*	
20	*Maximal length of the canine alveola*		*This study*	
21	*Maximal width of the canine*		*This study*	
22	*Maximal length of the canine*		*This study*	
23	*Height of the canine from tip to protuberance in the maxilla*		*This study*	
24	*Height of the canine from tip to maxillar border*		*This study*	
25	*Length of maxilla between canine protuberance and IOF*		*This study*	
26	*Distance between canines at maxillar border*		*This study*	
27	*Distance between canines at tips*		*This study*	
28	*Condylobasal length*	*CBL*	*Driesch, 1976*	
29	Anterior margin of the foramen magnum (Basion, B) to prosthion; basal length	BP	Driesch, 1976	None
30	Most caudal part of the palate (Staphylion, St) to prosthion; median palatal length	StP	Driesch, 1976	Oral
31	Staphylion to palatomaxillary suture (palatino-orale, Po); length of palatine	StPo	Driesch, 1976	Oral
32	Length of the cheek tooth row	P^2M^3	Driesch, 1976	Oral
33	*Diastema length between P^2 and canine*	*This study*	*This study*	

(Continues)

Index	Description	Distance	Distance defined by	Skull module[a]
34	*Diastema length between P^2 and posterior point of the canine alveola*	*This study*	*This study*	
35	Prostion to the horizontal line, rostral to P^2 (premolare, pm); Oral snout length	Ppm	Driesch, 1976	Oral
36	Minimal width of diastema	HH‘	Meijaard & Groves, 2004	Oral
37	Distance between the foramina palatina majores		This study	Oral
38	Greatest breadth of occipital condyles	maxOC	Driesch, 1976	Base
39	Greatest breadth at the bases of the paraoccipital processes	maxPP	Driesch, 1976	Base
40	Anteriour snout length	PRh, horizontal distance	This study	Nasal
41	Anteriour snout height	PRh, vertical distance	This study	Nasal
42	Facial length	$P\text{-}M^3$	This study	Oral
43	Length of braincase	Braincase at the height of the orbital rim-A; this study, horizontal distance	This study	Vault
44	Greatest braincase width (Euryon, Eu)	Eu-Eu	Driesch, 1976	Vault
45	Braincase height	AB, vertical distance	Driesch, 1976	Vault
46	Maximal height braincase	Maximal vertical expansion of the cranial part of the skull.	This study	None
47	Occipital nucal height	AOMF	This study	Vault
48	Length of the foramen magnum	BOMF	Haber, 2014	Base
49	Dorsoventral occipital condyle length		This study	Base
50	*Length of the paraoccipital process*		*This study*	*Base*
51	Length of the nasomaxillar rim	NiSNa;	Haber, 2014	Nasal
52	*Dorsal length of the ethmoid gap*	*Frontolacrimal-ethmoid to frontal-nasal-ethmoid*	*This study*	*Nasal*
53	Anteriour height of the ethmoidal gap	Frontal-nasal-ethmoid to nasal-maxilla-ethmoid	This study	Nasal
54	Ventral length of the ethmoidal gap	Nasal-maxilla-ethmoid to maxilla-lacrimal-ethmoid	This study	Nasal
55	*Maximal skull width at the zygomatic arches*	**ZyZy*	*Driesch, 1976*	*Jugal*
56	Length of the jugal arch	Caudal rim of orbit to rostral rim of facet of insertion mandibular arch	This study	Jugal
57	Frontal width at its most caudal extension	Fcaud, this study	This study	Vault

[a]Measurement assignment to skull modules is based on Porto et al. (2009) and Haber (2014). If a measurement spanned more than one module, it was not assigned to any module (“none”).

Chapter 3

The size and shape of the lacrimal facial facet in *Candiacervus* and *Megaloceros,* two cervids from the Pleistocene

Author contributions:

Ann-Marie Schilling collected data, designed and performed statistical analyses, and wrote the chapter. Gertrud E. Rössner supervised the study and contributed the photographic documentation

The size and shape of the lacrimal facial facet in *Candiacervus* and *Megaloceros,* two cervids from the Pleistocene

3.1 Abstract

The vertebrate skull provides a protective structure for the brain, a platform for the large sense organs, and an entry point to the digestive and respiratory systems. In many species, notably ruminants, it also supports sexually selected bony and/or keratinized appendages used as ornaments or weapons. The integration of these diverse functions is based on an intricate set of bones. Among these, the lacrimal bone has an exceptionally large facial facet in cervids. Results obtained in a study on extant cervids, presented in **Chapter 2** of this thesis, led us to suggest that the lacrimal facial facet might be involved in mitigating stress resulting from antlers. Here, we follow up on this issue and analyze the size, the allometric scaling, and the shape of the lacrimal facial facet in two extinct cervids, well known for large and small body height, respectively, in combination with their large and distinctive antlers. In *Megaloceros* and *Candiacervus*, the lacrimal facial facet is relatively small when compared to extant cervids. It also differs in shape from that seen in extant cervids. This is primarily due to distinctively long lacrimofrontal and lacrimojugal lengths, and rather short lacrimoethmoidal lengths, that can be observed in both extinct species. These findings are discussed within the context of the size and structure of the antlers of the two species and their use in intraspecific combat or for "show-off".

3.2 Introduction

In ruminants, the lacrimal bone, in particular its facial facet, forms a considerable part of the facial skull. It has a central position between the braincase and facial skeleton, making contact with the maxilla, the frontal, the jugal, the nasal, or, when present, bordering the ethmoidal gap. Thus, one may ask how the size and shape of the lacrimal bone are integrated with the diverse functions of its neighbouring bones.

Despite the extensive variability of the lacrimal bone across ruminants (Bärmann & Sánchez-Villagra, 2012; Schilling, Calderón-Capote, & Rössner, 2019), and indeed mammals (Rütimeyer, 1881; Knottnerus-Meyer, 1907; Gregory, 1920), the functional significance of this bone is far from understood. Concerning headgear bearing artiodactyls, i.e. pecoran ruminants, the hypothesis of Cobb (1943) that the large lacrimal facial facet is part of the stress-bearing region of the face, is particularly

interesting. This perspective is also supported by a recent analysis of the size and shape of the lacrimal facial facet in extant cervids (Schilling *et al.*, 2019).

The data presented in this publication suggest that the lacrimal facial facet is an evolutionary flexible structure that may adjust readily to adaptive changes in its surrounding bones. The study also revealed that the cervid lacrimal facial facet scales allometrically with skull size, as do antlers (Gould, 1973). One of the conclusions of that study was that the resultant change of integration of the lacrimal facial facet with its surrounding bones helped to reduce mechanical loads originating from increasingly larger antlers, hence, being a further example of exaptation.

Megaloceros (Gould, 1974; Lister, 1994; Lister *et al.*, 2005; Hughes *et al.*, 2006), popularly known as the "Irish Elk", is among the largest deer that ever lived and bore the largest antlers ever observed (Gould, 1973, 1974). In contrast, *Candiacervus* was a small cervid that lived on the island of Crete which probably descended from (a) larger mainland cervid(s) (Azzaroli, 1952; Kuss, 1975; de Vos, 1979, 1984; van der Geer, Dermitzakis, & de Vos, 2006; van der Geer, 2018). Its antlers were quite large but simple (Strasser *et al.*, 2018; van der Geer, 2018). As it is true for so many fossils, these two extinct cervids allow studying (extreme) morphotypes no longer found among extant deer (**Fig. 3.1**). The goal of the present study is to describe the size and shape of the lacrimal facial facets of *Megaloceros* and *Candiacervus* and relate them to data found in extant cervids.

3.3 Materials and Methods

We sampled 20 skulls of adult *Megaloceros* and *Candiacervus* individuals, including both males and females for our analyses. We considered a specimen as "adult" when the third upper molar had erupted. The determination of the relative biological age of our specimens was based on the wear patterns of the upper molars (Bemmel, 1949; de Vos, 1984). Sex determination was based on the presence or absence of pedicles and antlers. For a specimen list, see the Appendix; for raw data of both extant and extinct species, see Supplement 1 given in **Chapter 7.2.1**. Data for extant species are taken from Schilling *et al.* (2019).

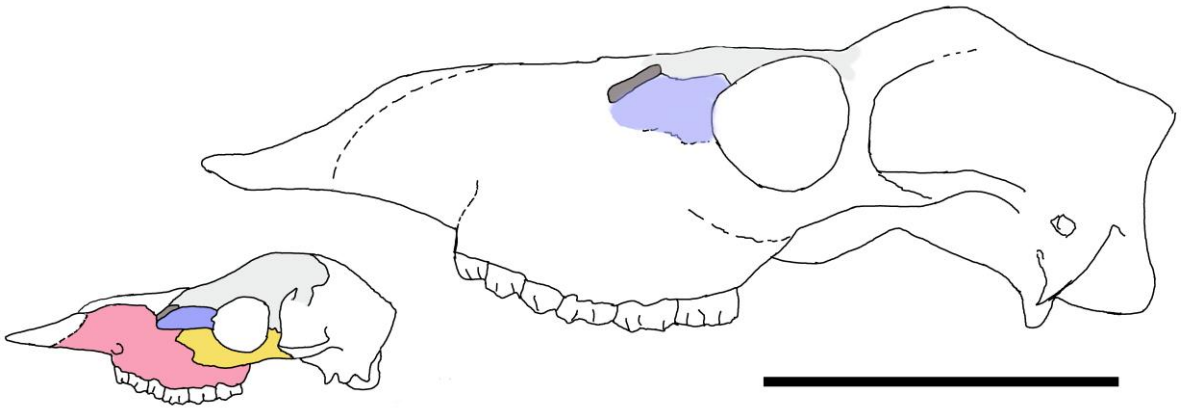

Figure 3.1 A schematic view of the skulls (without mandibulae) of *Megaloceros* and *Candiacervus*. Sketches are based on female specimens described by Reynolds (1929) and Schilling & Rössner (2021; Chapter 4), respectively. They are scaled to be representative of the average skull length known for these groups (see Fig. 3.3). For *Candiacervus* (left), bones are coloured as follows: blue, the lacrimal facial facet; red, maxilla; ochre, jugal; light grey, frontal bone. The ethmoidal gap is indicated in dark grey. For *Megaloceros*, only the lacrimal facial facet, the part of the frontal contacting the lacrimal facial facet, and the ethmoidal gap are coloured, as the borders between other bones are mostly ossified and hard to delineate in typical samples. Scale bar = 20 cm.

The *Megaloceros* specimens analyzed are housed in the Staatliches Museum für Naturkunde Stuttgart (SMNS), Germany; the *Candiacervus* specimens are housed in the SNSB-Bayerische Staatssammlung für Paläontologie und Geologie (SNSB-BSPG), München, Germany. Specimens of extant cervids are housed in the Naturhistorisches Museum Wien (NHMW), Austria; Museum für Naturkunde (MfN) Berlin, Germany; Zoologische Staatssammlung München (ZSM), Germany; and Staatssammlung für Anthropologie und Paläoanatomie München (SAPM), Germany.

For a morphometric analysis, we selected landmarks and the measurements of the lacrimal facial facet of *Megaloceros* and *Candiacervus* as described in Schilling *et al*. (2019; see **Chapter 2,** Table 2 and Figure 2). In this way, we obtained six inter-landmark distances for each of the 20 specimens. In addition, we could obtain the maximal skull length, measured from the prosthion (P) to akrokranion (A), for seven *Megaloceros* specimens and one *Candiacervus* specimen, to which we refer as "skull length", or more technically, as "AP-distance" in the following (see **Supplement 7.1.1** for landmarks). The remaining specimens were incomplete and did not allow to measure skull length.

Inter-landmarks distances describing the lacrimal facial facet were taken with a digital caliper (0-150 mm); the one skull length of *Candiacervus* was taken with a mechanical calliper (0-300 mm). Measurements were recorded to the nearest 0.1 mm. The skull lengths of *Megaloceros* were taken with a yardstick and rounded to the nearest 1.0 mm.

Since we could obtain an exact measure for skull length for only one of our *Candiacervus* specimens, we used the range of skull sizes reported by de Vos (1984) to estimate the skull lengths of the remaining seven specimens. De Vos (1984) reported for his specimens the basilar length, the linear distance from the basion to the prosthion.

In the one *Candiacervus* specimen (SNSB-BSPG 1972 XIX 1) from which we could obtain both the basilar length and the skull length, these measures differed by a factor of 0.8804. Consequently, we derived an estimate of the skull length for the de Vos specimens by dividing the basilar length he reported by this factor. A critical issue here is the reliability of this factor calculated from the one complete specimen we had at hand. Cleary, data from one specimen does not allow estimating variability. Hence, we derived an estimate of this variability by comparing the basilar length with the AP-distance observed in a larger sample of living cervids (for data, see Schilling *et al.*, 2019). This data set yielded a ratio of 0.8745 $\pm$ 0.0023 (mean $\pm$ 1 SEM; n=143 from 10 species). That is, the variability as expressed by the standard error of the mean (SEM) amounts to 0.26% of the measured value.

The statistical approach used to assess the size and shape of the lacrimal facial facet is described in detail in Schilling *et al.* (2019). Briefly, in a first step, all original measurements were log10-transformed. We defined the size of the lacrimal facial facet as the mean of the log10-transformed measurements obtained from this bone, i.e., the log10 of the geometric mean of the original measurements. To size-correct the data, the mean was subtracted from individual measurements (Darroch & Mosimann, 1985; Falsetti, Jungers & Cole, 1993). Skull length was taken as a proxy for skull size (see Klingenberg (2016) and Mosimann (1970) for a rationale for this approach). All statistical procedures were performed in R software (R Core Team 2018, version 3.5.1). The R code used may be found in **Chapter 7.2.2**.

3.4 Results

All of the *Megaloceros* specimens analyzed here had a small, but well-delineated ethmoidal gap and the lacrimal facial facet did not contact the nasal bone. In males, the sutures tended to be ossified (**Fig. 3.2A, B**). In female specimens, the sutures of the lacrimal facial facet could be readily recognized (**Fig. 3.2C**). An

unexpected observation in some specimens was that the part of the lacrimal facial facet where the two lacrimal orifices come to lie was separated from the remainder of this bone (**Fig. 3.2A**). This was observed in two male skulls and one female skull. For the male specimen shown in **Fig. 3.2A**, this separation could hardly be recognized on the left side. In the second male (SMNS 6316.2.9.73.3) the separation could be recognized on the right side. The left lacrimal was broken along this line. Finally, in the female skull (SMNS 6616.5.5.84.14), this line could be recognized on the left side but the bone was continuous.

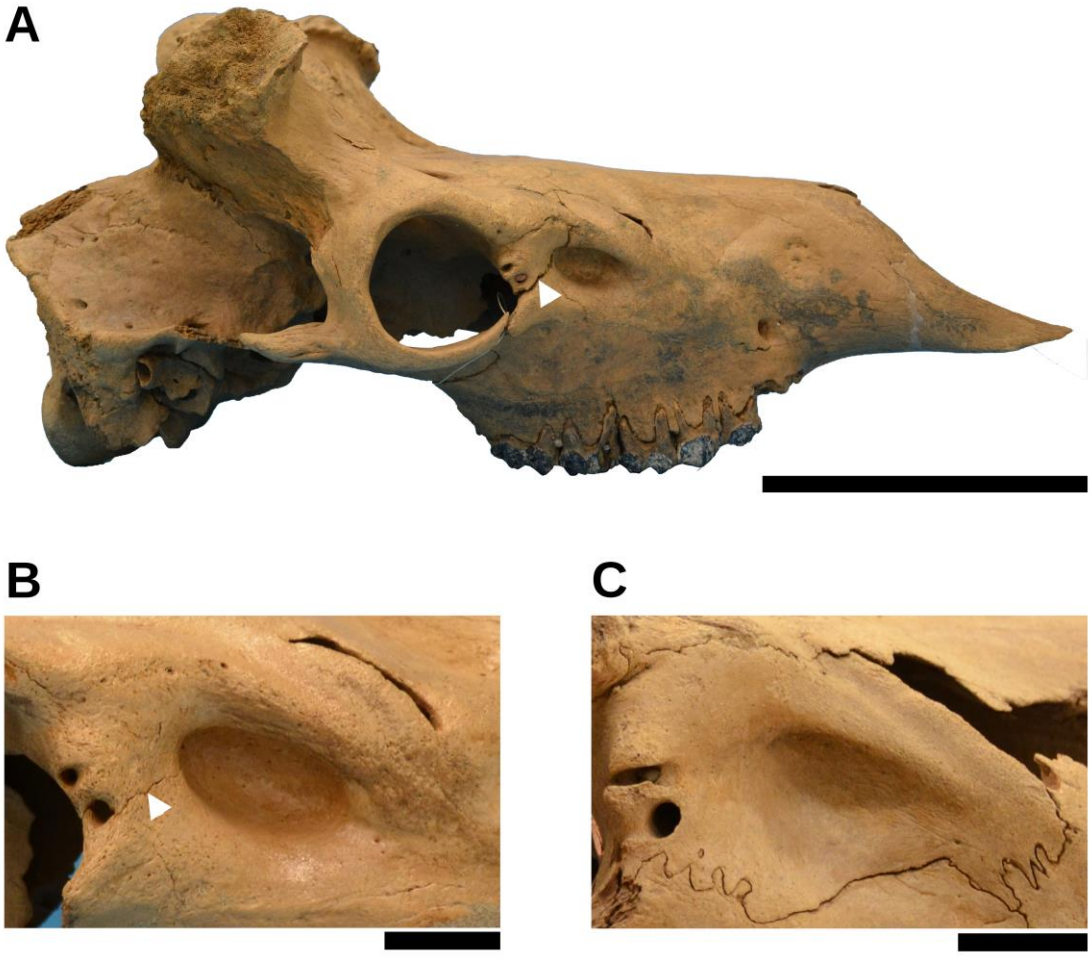

Figure 3.2 Examples of the lacrimal facial facet in *Megaloceros*. **A,** lateral view of a male skull of *Megaloceros sp.* (SMNS 6616.17.11.80.37). Note that the sutures of the lacrimal facial facet can be rather well recognized, which is exceptional for males in the sample we had at hand. **B**, the lacrimal facial facet of a male *M. giganteus (*SMNS 6316.2.9.73.3). Sutures of the lacrimal facial facet are largely fused and therefore hard to recognize. **C**, the lacrimal facial facet in a female *Megaloceros sp*. (SMNS 6616.10.10.66.4). The sutures of the lacrimal facial facet with the adjacent bones are well recognizable. Scale bars are 10 cm in panel **A** and 2 cm in panels **B** and **C**. The rostral part is to the right in all three

panels. The structure separating the lacrimal facial facet described in the main text is marked with white arrowheads

First, we wanted to know how the size of the lacrimal facial facet of fossil cervids relates with skull length, and how this fits the allometric scaling observed in extant cervids. For seven *Megaloceros* specimens, both skull length and size of the lacrimal facial facet could be obtained. These measurements are shown in colour in **Fig. 3.3.** The allometric line shown in **Fig. 3.3** is based on measurements obtained from extant cervids (see also Schilling *et al.*, 2019, fig. 3) reproduced in grey here. **Figure 3.3** also allows for comparison of the variability seen in *Megaloceros* with that in extant species. For those *Megaloceros* specimens for which we could not obtain the skull length, the size of the lacrimal facial facet is in the same range (1.548 – 1.590, n = 5) as those for which the skull length is preserved (1.548 – 1.659, n = 7) and which are depicted in **Fig. 3.3**.

Photographic documentation of the lacrimal facial facet in *Candiacervus* may be found in **Figs. 1-4** of **Chapter 4.** For this cervid, the skull length could be obtained only for one female skull (Schilling & Rössner, 2021; **Chapter 4**). Therefore, we used data reported by de Vos (1984) to delineate the region where measured sizes of their lacrimal facial facets should come to lie in **Fig. 3.3,** assuming that their skull sizes fall in the range defined by that reported by de Vos (1984).

As may be seen in **Fig. 3.3**, the region defined by the range of skull lengths based on de Vos (1984) (vertical lines) and the range of the sizes of the lacrimal facial facets we measured (horizontal lines) is located largely below the allometric line. This indicates that *Candiacervus* tends to have small lacrimal facets relative to skull length.

We recall that the allometric line shown in **Fig. 3.3** is based exclusively on male specimens of extant cervids. Therefore, strictly speaking, only measurements obtained from male *Megaloceros* and *Candiacervus* should be related to this line. However, for both genera, we also include specimens of females and specimens of unknown sex, given the scarcity of the data, especially for *Candiacervus*.

The two female *Megaloceros* skulls for which we could obtain skull length were the smallest in our *Megaloceros* sample. As may be taken from **Fig. 3.3**, the female with the smallest skull (SMNS 6617.5.9.64) also had the smallest lacrimal facial facet of all *Megaloceros* specimens. The other female SMNS 6617.1.12.81.33) had a relatively large facial facet, which was indeed larger than that of four of the five males available.

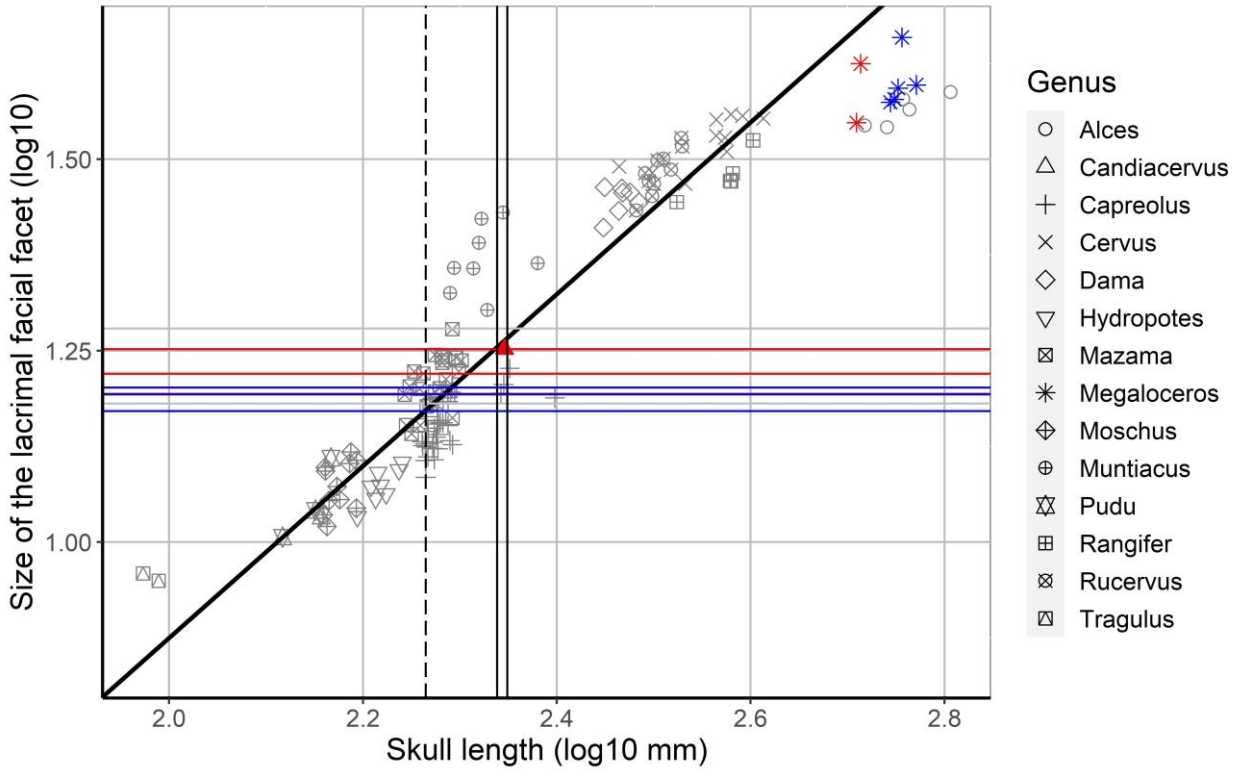

Figure 3.3 Relationships between skull length and size (geometric mean) of the lacrimal facial facet. In extant cervids, the size of the lacrimal facial facet shows positive interspecific allometry, as indicated by the solid line. The solid vertical lines indicate the estimated range of skull length for *Candiacervus* based on de Vos (1984). The dashed vertical line indicates the lower range of skull sizes that may be estimated based on the observed sizes of the lacrimal facial facet. The upper limit of this range coincides with the lower skull length estimate based on de Vos (1984). The horizontal lines indicate the size of the lacrimal facial facet obtained for our sample of *Candiacervus* specimens. The one *Candiacervus* female for which we could obtain skull length is shown as a red triangle. Data for extant species were taken from Schilling *et al.*, (2019) and plotted in grey. Data for fossil specimens are colour-coded according to sex (red, females; blue, males; grey, unknown sex). Note that all *Megaloceros* specimens plot underneath the allometric line. The area where we expect the *Candiacervus* data is also largely below the allometric line (see also text). Note also that the data of two *Megaloceros* males overlap extensively and can hardly be told apart.

Apart from size, the shape of the lacrimal facial facet and hence its interactions with adjacent bones reflect its potential functions. Among extant cervids, shape, as defined by the relative length of distances describing the lacrimal facial silhouette and the maximal lacrimal length, varies considerably (Schilling *et al.*, 2019). In **Fig. 3.4**, we present parallel coordinates plots (Simonelli, 1908; Heintz, 1970) for *Megaloceros* and *Candiacervus*, which allow us to assess the shape of the lacrimal facial facet and compare it with that of extant cervids.

In *Megaloceros* (**Fig. 3.4A**), the lacrimofrontal length is on average the longest measure of the silhouette of the lacrimal facial facet. The lacrimojugal length also tends to be relatively large, whereas the lacrimoethmoidal length is quite short. However, this pattern appears more nuanced, when male and female skulls are considered separately. In females, the lacrimojugal length is particularly long and the lacrimomaxillar length is rather short. Moreover, the graphs describing lacrimal silhouettes for three of the four females run closely together and almost in parallel, suggesting low variability among females in our sample. In contrast, in males, the lacrimal height, the lacrimojugal length, and the lacrimomaxillar length are on average of the same size. The relative length of these three measures differs considerably for single individuals. Thus, the shape of the lacrimal facial facet of males is much more variable than that of females in our sample.

In *Candiacervus* (**Fig. 3.4B**), again, the lacrimofrontal length is on average the longest measure of the silhouette of the lacrimal facial facet. The lacrimojugal length is longer than the lacrimal height and the lacrimomaxillar length. The lacrimoethmoidal length is small and about the same size as the lacrimomaxillar length. The limited dataset available to us and presented here does not allow delineating clear sex-related differences for *Candiacervus*. The lacrimal facial facet of the one *C. reumeri* specimen (SNSB-BSPG 1972 XIX 201) is next to the smallest of our sample. Its lacrimoethmoid length is rather long, and its lacrimofrontal length is rather short when compared to the other specimens of our sample (black arrowheads in **Fig. 3.4B**). Interestingly, in this *C. reumeri* specimen, the maxilla just touches the frontal dorsal to the small ethmoidal gap (Schilling & Rössner, 2021, figs. 3G, H; **Chapter 4**).

In **Figs. 3.4C** and **3.4D**, we plotted lacrimal measurements obtained from male and female fossil cervids together with measurements from those extant cervids for which data for both sexes were available. This allows for direct comparison between sexes and between species. These findings may be described briefly as follows: *Megaloceros* and *Candiacervus* have similar shapes of the lacrimal facial facet that differ, however, from those seen in extant deer. This is particularly obvious in males (**Fig. 3.4C**). Specifically, in males, the lacrimoethmoid length in the two fossil species is smaller than its neighbouring measures, whereas in extant cervids the lacrimoethmoid length is larger than its neighbouring measures. This pattern is reminiscent of that observed in the out-group, *Tragulus*. In three of the four female *Megaloceros*, the lacrimoethmoid length is longer than the lacrimomaxillar length but shorter than the lacrimofrontal length and thus differs from the relative lengths of these measures seen in females of extant cervids. We could not observe an unambiguous sexual dimorphism of the lacrimal facial facet in any of the extant species analyzed.

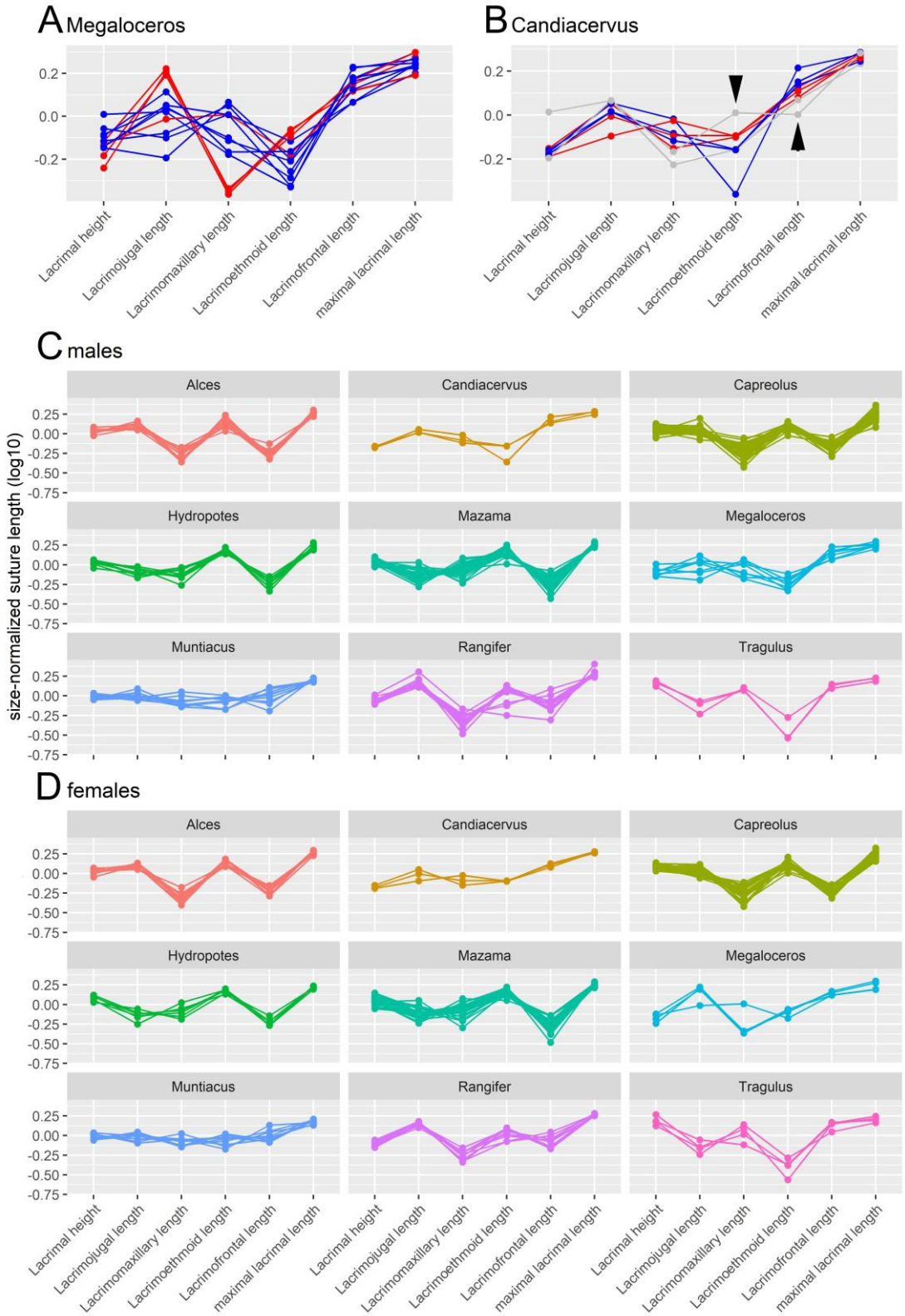

Figure 3.4 Legend see next page.

Figure 3.4 (see previous page). The shape of the lacrimal facial facet in fossil and extant cervids. Variables are size-corrected, and the relative length of any individual lacrimal suture can thus be compared across specimens and species. Lacrimal measures are depicted in their anatomical order. **A**, The shape of the lacrimal facial facet in *Megaloceros*. Note the higher variability in males (blue) and that three females (red) show very long lacrimojugal lengths and rather short lacrimomaxillar lengths. **B**, The shape of the lacrimal facial facet in *Candiacervus*. Females are red, males are blue and specimens of unknown sex are shown in grey. The general pattern resembles that of *Megaloceros*. Sex differences could not be recognized in the small *Candiacervus* sample at hand. Black arrowheads point to the curve representing the lacrimal facial facet of *C. reumeri* (SNSB-BSPG 1972 XIX 201). **C**, The shape of the lacrimal facial facet of fossil males in comparison with some extant male cervids. **D**, The shape of the lacrimal facial facet of fossil females in comparison with some extant female cervids.

3.5 Discussion

In this manuscript, we analyzed the size, shape, and variability of the lacrimal facial facet of two extinct cervids from the Pleistocene, *Megaloceros,* and *Candiacervus*. When compared with extant species, the lacrimal facial facet of these fossils is small relative to skull length. The shape of this facial bone is similar in *Megaloceros* and *Candiacervus* but differs from the patterns observed in extant cervids. Finally, the shape data obtained raise the question of whether the lacrimal facial facet might be sexually dimorphic in *Megaloceros*.

As in the previous chapter, we will relate the size and the shape of the lacrimal facial facet to skull length and discuss these data, among others, with a view on antler size. While it is well known that antler size scales allometrically with body size given as shoulder height (e.g., Gould, 1973, 1974; Clutton-Brock, Albon, & Harvey, 1980), the allometric scaling of antler size with skull length has gained less attention. Yet it is well documented in the literature, if exclusively for intraspecific allometry (Gould, 1973, 1974; Hayden, Lynch, & O'Corry-Crowe, 1994). The data of Clutton-Brock et al. (1980) and Ceacero (2016), when combined with the skull length data reported by Haber (2016), allow deriving also an estimate of interspecific allometric scaling of antler size with skull length. These datasets, which comprise 20 and 26 species, respectively, yield scaling factors of 3.25 (95% confidence interval, 2.48-4.60) and 3.67 (95% CI, 2.93-4.84). The scaling factors for antler size *vs.* shoulder height for these two samples are 2.39 (95% CI, 1.88-3.19) and 2.84 (95% CI, 2.26-3.77). While the two datasets yield somewhat different scaling factors, which might be expected, they unambiguously establish that antler length scales positively with skull length, just as it does with shoulder height. The numerical data from which these values were calculated are given in **Chapter 7.2.3.**

A critical technical point when positioning the size data of the lacrimal facial facet of *Candiacervus* relative to the allometric line of extant cervids is that we could measure the skull length only for one specimen. To overcome this issue, we used the range of skull lengths reported by de Vos (1984) for specimens from Gerani 4. This seems justified for the following reasons: first, our sample was collected close to the Gerani 4 cave and comprises the same two species as described for this site (de Vos, 1984; Schilling & Rössner, 2021; **Chapter 4**). Second, a skull length reported by Kuss (1975) and the one skull length we could measure, fall within the range based on de Vos (1984). Lastly, the one skull from Liko for which de Vos (1984) gives the skull length is clearly longer, by about 12%. We would like to point out that if we underestimated the skull lengths for the present specimens, the size data of the lacrimal facial facet would plot even further below the allometric line. On the other hand, as may be seen in **Fig. 3.3**, if we utilized the size of the lacrimal facial facet to estimate the skull lengths of the *Candiacervus* specimens used here, we would obtain skull lengths much shorter than those previously reported. Thus, it seems justified to conclude that in *Candiacervus*, as in *Megaloceros*, the size of the lacrimal facial facet is smaller relative to skull size than in extant deer.

Most *Megaloceros* have lacrimal facial facets comparable in size with those of *Alces* and indeed, the data points of the size of the lacrimal facial facet of *Megaloceros* fall below the allometric line, as do those of *Alces* (**Fig. 3.3**). The lacrimal facial facets of two *Megaloceros* specimens in our sample, one male and one female are rather large and lie close to the allometric line. In contrast, the data points representing the larger part of our sample essentially overlap with those obtained from *Alces*.

Thus, *Megaloceros* and *Alces* differ from other cervids bearing large antlers (*Rangifer*, *Cervus*, *Dama*, and *Rucervus*) by having a relatively small lacrimal facial facet. For *Megaloceros*, this is somewhat unexpected, if we consider that one of the functions of the lacrimal facial facet might be to support forces originating from antlers (Schilling *et al.*, 2019) and that *Megaloceros* arguably had the largest antlers ever known.

Yet the lacrimal facial facet is not only relatively small in *Megaloceros*, it also differs in shape, and by the fact that it is also largely fused with its surrounding bones, at least in males. The shape differences are mainly due to a reduced lacrimoethmoid length and a concomitant increase in the lacrimofrontal length. One consequence is the reduction of the ethmoidal gap. Moreover, in *Megaloceros*, the lacrimomaxillar length gains in length at the expense of the lacrimojugal length. This is particularly evident when compared with large-antlered extant cervids, e.g., *Rangifer* and *Alces*.

Both the small size of the lacrimal facial facet and the fact that the relative length of its individual sutures differs from that observed in extant (large-antlered) cervids suggest that the mechanical loading and force transmission might have been different in *Megaloceros.* This is also suggested by the extensive ossification of these sutures in *Megaloceros.* Thus, ossified sutures have been reported to better withstand compressive and static forces. Open sutures allow for the dampening and dissipation of dynamic and tensile stress (Jaslow & Biewener, 1995; Herring, 2008; Bärmann & Sánchez-Villagra, 2012; Curtis *et al.*, 2013) as may arise with the use of antlers in intraspecific fights typical for extant deer. Conversely, mechanical loading has been implied as a driving force of suture closure or patency (see references above). The observed specifics of the lacrimal facial facet in *Megaloceros* raise the question of whether this cervid used its antlers differently than extant cervids, as previously proposed by Gould (1974). He argued that *Megaloceros* antlers served as ornaments and for display rather than as weapons. Consequently, the type of loads originating from antlers and operating on the skull, including the lacrimal facial facet, should have been primarily static rather than dynamic. Hence, the way the lacrimal facial facet is integrated with its surrounding bones might be an exaptation well suited for this condition.

Based on a finite element analysis of *Megaloceros* antlers, Klinkhamer *et al.* (2019, p. 8) suggested that *Megaloceros* may well have been "capable of withstanding some fighting loads […] provided that their antlers interlocked proximally". In other words, these authors suggest that the effective antler size used in fighting must have been smaller than the actual antler size to withstand fighting stress. Assuming that this hypothesis is correct, dynamic forces originating from the antlers and loading on the skull of *Megaloceros* should have been smaller than suggested by actual antler size. The relatively small lacrimal facial facet observed would still be in agreement with the hypothesis that this bone is involved in supporting stress originating from antlers. Finally, we recall that the thickened frontal bone between the pedicles has also been suggested to contribute to shock absorption in *Megaloceros* (Lister, 1994, fig. 14). This interpretation of the *Megaloceros* data would be consistent with the observation that *Alces* has antlers of a rather small spread (Clutton-Brock *et al.*, 1980; Klinkhamer *et al.*, 2019), and also a comparatively small lacrimal facial facet (Schilling *et al.*, 2019). Both the relatively short antlers of *Alces* and the effective antler size of *Megaloceros* as suggested by Klinkhamer *et al.* (2019) should have relatively low leverage on the skull. Consistently, they have been predicted to generate only a relatively modest loading on the facial skull (Klinkhamer *et al.*, 2019). However, no data on biomechanical properties of the skulls and antlers are available for *Alces*.

Megaloceros females are known to have somewhat shorter skulls than males (~ 10%; Aaris-Sørensen & Liljegren, 2004) and accordingly, the skull lengths of our female specimens were shorter than those of our male samples. However, we could not detect sexual dimorphism in the size of the lacrimal facial facets. This may reflect the small sample size or the variability due to the inclusion of specimens belonging to unknown species, rather than a true absence of sexual dimorphism. The differences observed in the shape of the lacrimal facial facet of male *Megaloceros* compared with female *Megaloceros* might suggest such a sex difference. Yet again, the variability of these data and the small number of specimens preclude an unambiguous explanation. Lastly, we note that the largely fused sutures in male specimens may have affected the recognition and exact positioning of landmarks, and hence, the precision, with which inter-landmark distances could be taken.

The shape of the lacrimal facial facet in *Candiacervus* is similar to that seen in *Megaloceros,* and as in the latter, differs from that of extant cervids. This is mainly due to a reduced lacrimoethmoid length and a concomitant increase in the lacrimofrontal length. One consequence is the reduction of the ethmoidal gap, as also seen in *Megaloceros*. Moreover, in the fossil cervids, the lacrimomaxillar length gains in length at the expense of the lacrimojugal length. This is particularly evident when compared with extant cervids bearing large antlers, e.g., *Rangifer* and *Alces* (**Fig.3.4C**) or *Cervus* and *Rucervus* (Schilling *et al.*, 2019, fig. 5; **Chapter 2**).

Candiacervus generally had extremely long, but also uniquely simple antlers. This is especially true for *Candiacervus ropalophorus* de Vos, 1984 (van der Geer, 2018), the species to which five of the seven specimens analyzed here could be referred (Schilling & Rössner, 2021; **Chapter 4**). Except for a small tine emanating about 10 cm distant from the skull, the antlers of these fossil deer consisted of a single unbranched beam. Only one of our specimens was assigned to *Candiacervus reumeri* van der Geer, 2018. This specimen had somewhat branched, but rather short antlers. As proposed by van der Geer, the highly simplified antlers of *Candiacervus* resulted from "evolution towards show-off" (*idem*, p. 20). If so, the same argument as proposed above for the skull load by antlers of *Megaloceros* can be made. Moreover, the structure of *Candiacervus* antlers suggests that if they were indeed used in intraspecific fighting, they may have interlocked only close to the skull. Thus, if used for combat, the effective antler size was again small, as is the lacrimal facial facet in *Candiacervus*.

If we compare the shapes of the lacrimal facial facet in the two fossils analysed here (**Fig.3.4A-C**) and that of extant cervids (Schilling *et al.*, 2019, fig. 5, **Chapter 2)** the fossils are clearly distinct from extant cervids with large antlers. This seems true also for *Dama*, a putative close relative of both *Candiacervus* and *Megaloceros* (Lister *et al.*, 2005; van der Geer, 2018). As the exact phylogenetic relationships

between these three species are still unclear, it may be tempting to consider the similarity in the shape of the lacrimal facial facet (**Fig. 3.4A-C**) as support for a close phylogenetic relationship between *Megaloceros* and *Candiacervus* and a more distant relationship to *Dama* (Schilling *et al.*, 2019, fig. 5, **Chapter 2**). However, we cannot exclude a convergent evolution (Wake, Wake, & Specht, 2011). A striking example of convergent morphological evolution of genetically diverse cervids has been reported for South American brocket deer, *Mazama* (Duarte, González, & Maldonado, 2008; for further discussion, see also: Heckeberg *et al.*, 2016; Heckeberg, 2020). Geist (1998) also attributed the similarities between the musk deer, *Moschus*, and cervids to convergent evolution. As pointed out in the previous chapter, for cervids, the shape of the lacrimal facial facet does not show a phylogenetic signal in cervids in general. Thus, it must remain open whether the similarities between the lacrimal facial facets seen in *Megaloceros* and *Candiacervus* attest to their purported close phylogenetic relationship (Capasso Barbato, 1989, 1990, 1995; Caloi & Palombo, 1995; Croitor, 2016).

In summary, our analyses showed that the lacrimal facial facets of fossil *Megaloceros* and *Candiacervus* differ from those observed in extant cervids. Yet, the relative size and shape are comparable in these two extinct cervids. These data are consistent with the view that both cervids might have used their peculiar antlers primarily for show-off or, alternatively, for a highly ritualistic mode of intraspecific combat.

3.6 Acknowledgements

I am grateful to M.C. Calderón-Capote for her diligent help with collecting data for recent cervids. I thank G.E. Rössner for the photographic documentation of the *Megaloceros* skulls and valuable comments on a previous version of this chapter. I also thank Dr Reinhard Ziegler for providing access to the Paleontology Collection of the Staatliches Museum für Naturkunde Stuttgart, Germany, enabling the study of *Megaloceros* skulls.

3.7 References

AARIS-SØRENSEN, K. & LILJEGREN, R. (2004) Late Pleistocene remains of giant deer (*Megaloceros giganteus* Blumenbach) in Scandinavia: chronology and environment. *Boreas* **33**, 61–73.

AZZAROLI, A. (1952) La sistematica dei cervi giganti e i cervi nani delle isole. *Atti della Società Toscana di Scienze Naturali, Memorie (A)* **59**, 119–127.

BÄRMANN, E. V. & SÁNCHEZ-VILLAGRA, M.R. (2012) A Phylogenetic Study of Late Growth Events in a

Mammalian Evolutionary Radiation-The Cranial Sutures of Terrestrial Artiodactyl Mammals. *Journal of Mammalian Evolution* **19**, 43–56.

BEMMEL, A.C.V. VAN (1949) Revision of the rusine deer in the Indo-Australian Archipelago. *Treubia* **20**, 191–262.

CALOI, L. & PALOMBO, M.R. (1995) Functional aspects and ecological implications in Pleistocene endemic cervids of Sardinia, Sicily and Crete. *Geobios* **28**, 247–258.

CAPASSO BARBATO, L. (1989) Cervidi endemici del Pleistocene di Creta. Università Consortiziate, Modena, Bologna, Firenze, Roma.

CAPASSO BARBATO, L. (1990) Les cervidés endémiques de Crète. *Quaternaire* **1**, 265–270.

CAPASSO BARBATO, L. (1995) Un tentativo di analisi cladistica applicata ad un cervide endemico del Pleistocene di Creta. *Geologica Romana* **31**, 243–248.

CEACERO, F. (2016) Long or Heavy? Physiological Constraints in the Evolution of Antlers. *Journal of Mammalian Evolution* **23**, 209–216.

CLUTTON-BROCK, T.H., ALBON, S.D. & HARVEY, P.H. (1980) Antlers, body size and breeding group size in the Cervidae. *Nature* **285**, 565–567.

COBB, W.M. (1943) The cranio-facial union and the maxillary tuber in mammals. *American Journal of Anatomy* **72**, 39–111.

CROITOR, R. (2016) Systematical position and paleoecology of the endemic deer *Megaceroides algericus* Lydekker, 1890 (Cervidae, Mammalia) from the late Pleistocene-early Holocene of North Africa. *Geobios* **49**, 265–283.

CURTIS, N., JONES, M.E.H., EVANS, S.E., O'HIGGINS, P. & FAGAN, M.J. (2013) Cranial sutures work collectively to distribute strain throughout the reptile skull. *Journal of the Royal Society Interface* **10**, 20130442.

DARROCH, J.N. & MOSIMANN, J.E. (1985) Canonical and principal components of shape. *Biometrika* **72**, 241–252.

DUARTE, J.M.B., GONZÁLEZ, S. & MALDONADO, J.E. (2008) The surprising evolutionary history of South American deer. *Molecular Phylogenetics and Evolution* **49**, 17–22.

FALSETTI, A.B., JUNGERS, W.L. & COLLE, T.M. (1993) Morphometrics of the callitrichid forelimb: A case study in size and shape. *International Journal of Primatology* **14**, 551–572.

VAN DER GEER, A. (2018) Uniformity in variety: Antler morphology and evolution in a predator-free environment. *Palaeontologia Electronica* **21**, 1–31.

VAN DER GEER, A., DERMITZAKIS, M. & DE VOS, J. (2006) Crete Before the Cretans : the Reign of Dwarfs. *Pharos* **13**, 119–130.

GEIST, V. (1998) *Deer of the World: Their Evolution, Behaviour, and Ecology*, 1st edition. Swan Hill Press,

Shrewsbury.

GOULD, S.J. (1973) Positive allometry of antlers in the "Irish Elk", *Megaloceros giganteus*. *Nature* **244**, 375–376.

GOULD, S.J. (1974) The Origin and Function of "Bizarre" Structures: Antler Size and Skull Size in the "Irish Elk," *Megaloceros giganteus*. *Evolution* **28**, 191.

GREGORY, W.K. (1920) Article II. - Studies in Comparative Myology and Osteology: No. IV. - A Review of the Evolution of the Lacrymal Bone of Vertebrates with Special Reference to That of Mammals. *Bulletin of the American Museum of Natural History* **XLII**, 95–263.

HABER, A. (2016) Phenotypic Covariation and Morphological Diversification in the Ruminant Skull. *The American Naturalist* **187**, 576–591.

HAYDEN, T.J., LYNCH, J.M. & O'CORRY-CROWE, G. (1994) Antler growth and morphology in a feral sika deer *Cervus nippon* population in Killarney, Ireland. *Journal of Zoology* **232**, 21–35.

HECKEBERG, N.S. (2020) The systematics of the Cervidae: A total evidence approach. *PeerJ* **8**, e8114.

HECKEBERG, N.S., ERPENBECK, D., WÖRHEIDE, G. & RÖSSNER, G.E. (2016) Systematic relationships of five newly sequenced cervid species. *PeerJ* **4**, e2307.

HEINTZ, E. (1970) Les cervidés villafranchiens de France et d'Espagne. *Mémoires du Muséum national d'histoire naturelle. Série C, Sciences de la terre* **22**, 1–303.

HERRING, S.W. (2008) Mechanical influences on suture development and patency. In *Frontiers of Oral Biology* (ed D.P. RICE), pp. 41–56. Karger, London.

HUGHES, S., HAYDEN, T.J., DOUADY, C.J., TOUGARD, C., GERMONPRÉ, M., STUART, A., LBOVA, L., CARDEN, R.F., HÄNNI, C. & SAY, L. (2006) Molecular phylogeny of the extinct giant deer, *Megaloceros giganteus*. *Molecular Phylogenetics and Evolution* **40**, 285–291.

JASLOW, C.R. & BIEWENER, A.A. (1995) Strain patterns in the horncores, cranial bones and sutures of goats (*Capra hircus*) during impact loading. *Journal of Zoology* **235**, 193–210.

KLINGENBERG, C.P. (2016) Size, shape, and form: concepts of allometry in geometric morphometrics. *Development Genes and Evolution* **226**, 113–137.

KLINKHAMER, A.J., WOODLEY, N., NEENAN, J.M., PARR, W.C.H., CLAUSEN, P., SÁNCHEZ-VILLAGRA, M.R., SANSALONE, G., LISTER, A.M. & WROE, S. (2019) Head to head: The case for fighting behaviour in *Megaloceros giganteus* using finite-element analysis. *Proceedings of the Royal Society B* **286**, 20191873.

KNOTTNERUS-MEYER, T.C.B. (1907) Über das Tränenbein der Huftiere: Vergleichend -anatomischer Beitrag zur Systematik der rezenten Ungulata. *Archiv für Naturgeschichte* **73**, 1–152.

KUSS, S.E. (1975) Die pleistozänen Hirsche der ostmediterranen Inseln Kreta, Kasos, Karpathos und Rhodos (Griechenland). *Berichte der Naturforschenden Gesellschaft zu Freiburg im Breisgau* **65**, 25–

79.

LISTER, A.M. (1994) The evolution of the giant deer, *Megaloceros giganteus* (Blumenbach). *Zoological Journal of the Linnean Society* **112**, 65–100.

LISTER, A.M., EDWARDS, C.J., NOCK, D.A.W., BUNCE, M., VAN PIJLEN, I.A., BRADLEY, D.G., THOMAS, M.G. & BARNES, I. (2005) The phylogenetic position of the "giant deer" *Megaloceros giganteus*. *Nature* **438**, 850–853.

MOSIMANN, J.E. (1970) Size allometry: Size and shape variables with characterizations of the lognormal and generalized gamma distributions. *Journal of the American Statistical Association* **65**, 930–945.

R CORE TEAM (2018) A Language and Environment for Statistical Computing. Vienna, Austria.

REYNOLDS, S.H. (1929) A Monograph on the British Pleistocene Mammalia Vol. III. Part III the Giant Deer. *Monographs of the Palaeontographical Society* **81**, 1–62. Taylor & Francis.

RÜTIMEYER, L. (1881) Beiträge zu einer natürlichen Geschichte der Hirsche. *Abhandlungen der Schweizerischen Paläontologischen Gesellschaft* **VIII**, 1–268. Zürcher und Furrer, Zürich.

SCHILLING, A.-M., CALDERÓN-CAPOTE, M.C. & RÖSSNER, G.E. (2019) Variability, morphometrics, and co-variation of the *os lacrimale* in Cervidae. *Journal of Morphology* **280**, 1071–1090.

SCHILLING, A.-M. & RÖSSNER, G.E. (2021) New skull material of Pleistocene dwarf deer from Crete (Greece). *Comptes Rendus Palevol* **20**, 141–164.

SIMONELLI, V. (1908) Mammiferi quaternari dell'isola di Candia. *Memorie della Reale Accademia delle Scienze dell'Istituto di Bologna* **5**, 456–470.

STRASSER, T.F., MURRAY, S.C., VAN DER GEER, A., KOLB, C. & RUPRECHT, L.A. (2018) Palaeolithic cave art from Crete, Greece. *Journal of Archaeological Science: Reports* **18**, 100–108.

DE VOS, J. (1979) The endemic Pleistocene deer of Crete. I. *Proceedings of the Koninklijke Nederlandse Akademie van Wetenschappen, Series B* **82**, 59–90.

DE VOS, J. (1984) The endemic Pleistocene deer of Crete. *Verhandelingen der Koninklijke Nederlandse Akademie van Wetenschappen* **31**, 1–100.

WAKE, D.B., WAKE, M.H. & SPECHT, C.D. (2011) Homoplasy: From detecting pattern to determining process and mechanism of evolution. *Science* **331**, 1032–1035.

3.8 Appendix

List of specimens used in this study. A detailed description of the *Candiacervus* specimens will be presented in **Chapter 4**. For raw data, see Supplement 1 in **Chapter 7.2.1**. Abbreviations: Sex: m, male; f, female; u, unknown. Collections; SMNS, Museum für Naturkunde Stuttgart; SNSB-BSPG, Bayerische Staatssammlung für Paläontologie und Geologie, München.

Genus	Species	Sex	Site	Catalogue No.	Collection
Megaloceros	*sp.*	f	Otterstadt, Angelhofer Altrhein, Germany	6616.10.10.66.4	SMNS
Megaloceros	*sp.*	f	Otterstadt, Auriegel, Germany	6616.5.5.84.14	SMNS
Megaloceros	*giganteus*	m	Mannheim-Rheinau, Lanzgelände, Germany	6517.2.7.72.8	SMNS
Megaloceros	*giganteus*	m	Altrip, Germany	6516.4.8.70.7	SMNS
Megaloceros	*giganteus*	m	Altisheim, Allmendwiesen, Germany	6717.2.7.64.1	SMNS
Megaloceros	*giganteus*	m	Lampertheim in der Tann, Germany	6316.2.9.73.3	SMNS
Megaloceros	*sp.*	f	Brühl, Edingen, Edinger Ried, Germany	6617.1.12.81.33	SMNS
Megaloceros	*sp.*	f	Kelsch, Rheinwald, Germany	6617.5.9.64	SMNS
Megaloceros	*sp.*	m	Brühl, Mannheim, Germany	6617.5.9.73.4	SMNS
Megaloceros	*giganteus*	m	Rheinhausen, Osterwiesen, Germany	6717.7.6.62.5	SMNS
Megaloceros	*sp.*	m	Brühl (Koller), Schlangenwinkel, Germany	6616.17.11.80.37	SMNS
Megaloceros	*sp.*	m	Brühl, Spieswiesen-Ost, Germany	6617.3.6.66.54	SMNS
Candiacervus	*ropalophorus*	f	Cave near Gerani, Rethymnon, Crete, Greece	1972 XIX 204	SNSB-BSPG
Candiacervus	*sp.*	m	Cave near Gerani, Rethymnon, Crete, Greece	1972 XIX 7	SNSB-BSPG
Candiacervus	*sp.*	u	Cave near Gerani, Rethymnon, Crete, Greece	1972 XIX 5	SNSB-BSPG
Candiacervus	*ropalophorus*	f	Cave near Gerani, Rethymnon, Crete, Greece	1972 XIX 1	SNSB-BSPG
Candiacervus	*ropalophorus*	m	Cave near Gerani, Rethymnon, Crete, Greece	1972 XIX 203	SNSB-BSPG
Candiacervus	*ropalophorus*	f	Cave near Gerani, Rethymnon, Crete, Greece	1972 XIX 202	SNSB-BSPG
Candiacervus	*ropalophorus*	m	Cave near Gerani, Rethymnon, Crete, Greece	1972 XIX 200	SNSB-BSPG
Candiacervus	*reumeri*	u	Cave near Gerani, Rethymnon, Crete, Greece	1972 XIX 201	SNSB-BSPG

Chapter 4

New skull material of Pleistocene dwarf deer from Crete (Greece)

Research article published in *Comptes Rendus Palevol 20: 141-164, 2021*

© Publications Scientifiques du Muséum national d'Histoire naturelle, Paris

Author contributions:

Ann-Marie Schilling collected data, designed and performed statistical analyses, wrote and revised the paper.
Gertrud E. Rössner gave access to specimens, organised meeting with Dr. H.-J. Gregor, supervised study design and performance and reviewed drafts of the paper.

comptes rendus palevol

2021 • 20 • 9

New skull material of Pleistocene dwarf deer from Crete (Greece)

Ann-Marie SCHILLING & Gertrud E. RÖSSNER

art. 20 (9) — Published on 8 March 2021
www.cr-palevol.fr

PUBLICATIONS SCIENTIFIQUES

Directeurs de la publication / *Publication directors* :
Bruno David, Président du Muséum national d'Histoire naturelle
Étienne Ghys, Secrétaire perpétuel de l'Académie des sciences

Rédacteurs en chef / *Editors-in-chief* : Michel Laurin (CNRS), Philippe Taquet (Académie des sciences)

Assistante de rédaction / *Assistant editor* : Adeline Lopes (Académie des sciences ; cr-palevol@academie-sciences.fr)

Mise en page / *Page layout* : Fariza Sissi & Audrina Neveu (Muséum national d'Histoire naturelle; fariza.sissi@mnhn.fr)

Rédacteurs associés / *Associate editors* (***, took charge of the editorial process of the article*/a pris en charge le suivi éditorial de l'article) :

Micropaléontologie/*Micropalaeontology*
Maria Rose Petrizzo (Università di Milano, Milano)

Paléobotanique/*Palaeobotany*
Cyrille Prestianni (Royal Belgian Institute of Natural Sciences, Brussels)

Métazoaires/*Metazoa*
Annalisa Ferretti (Università di Modena e Reggio Emilia, Modena)

Paléoichthyologie/*Palaeoichthyology*
Philippe Janvier (Muséum national d'Histoire naturelle, Académie des sciences, Paris)

Amniotes du Mésozoïque/*Mesozoic amniotes*
Hans-Dieter Sues (Smithsonian National Museum of Natural History, Washington)

Tortues/*Turtles*
Juliana Sterli (CONICET, Museo Paleontológico Egidio Feruglio, Trelew)

Lépidosauromorphes/*Lepidosauromorphs*
Hussam Zaher (Universidade de São Paulo)

Oiseaux/*Birds*
Éric Buffetaut (CNRS, École Normale Supérieure, Paris)

Paléomammalogie (mammifères de moyenne et grande taille)/*Palaeomammalogy (large and mid-sized mammals)*
Lorenzo Rook* (Università degli Studi di Firenze, Firenze)

Paléomammalogie (petits mammifères sauf Euarchontoglires)/*Palaeomammalogy (small mammals except for Euarchontoglires)*
Robert Asher (Cambridge University, Cambridge)

Paléomammalogie (Euarchontoglires)/*Palaeomammalogy (Euarchontoglires)*
K. Christopher Beard (University of Kansas, Lawrence)

Paléoanthropologie/*Palaeoanthropology*
Roberto Macchiarelli (Université de Poitiers, Poitiers)

Archéologie préhistorique/*Prehistoric archaeology*
Marcel Otte (Université de Liège, Liège)

Couverture / *Cover* :
Lateral and dorsal views of *Candiacervus* sp. (photo: Manuela Schellenberger, SNSB-Bayerische Staatssammlung für Paläontologie und Geologie, Germany).

Comptes Rendus Palevol est indexé dans / Comptes Rendus Palevol *is indexed by:*
– Cambridge Scientific Abstracts
– Current Contents® Physical
– Chemical, and Earth Sciences®
– ISI Alerting Services®
– Geoabstracts, Geobase, Georef, Inspec, Pascal
– Science Citation Index®, Science Citation Index Expanded®
– Scopus®.

Les articles ainsi que les nouveautés nomenclaturales publiés dans *Comptes Rendus Palevol* sont référencés par / *Articles and nomenclatural novelties published in* Comptes Rendus Palevol *are registered on:*
– ZooBank® (http://zoobank.org)

Comptes Rendus Palevol est une revue en flux continu publiée par les Publications scientifiques du Muséum, Paris et l'Académie des sciences, Paris
Comptes Rendus Palevol *is a fast track journal published by the Museum Science Press, Paris and the Académie des sciences, Paris*

Les Publications scientifiques du Muséum publient aussi / *The Museum Science Press also publish:*
Adansonia, ***Geodiversitas***, ***Zoosystema***, ***Anthropozoologica***, ***European Journal of Taxonomy***, ***Naturae***, ***Cryptogamie*** **sous-sections** ***Algologie***, ***Bryologie***, ***Mycologie***.

L'Académie des sciences publie aussi / *The Académie des sciences also publishes:*
Comptes Rendus Mathématique, ***Comptes Rendus Physique***, ***Comptes Rendus Mécanique***, ***Comptes Rendus Chimie***, ***Comptes Rendus Géoscience***, ***Comptes Rendus Biologies***.

Diffusion – Publications scientifiques Muséum national d'Histoire naturelle
CP 41 – 57 rue Cuvier F-75231 Paris cedex 05 (France)
Tél. : 33 (0)1 40 79 48 05 / Fax : 33 (0)1 40 79 38 40
diff.pub@mnhn.fr / https://sciencepress.mnhn.fr

Académie des sciences, Institut de France, 23 quai de Conti, 75006 Paris.

© Publications scientifiques du Muséum national d'Histoire naturelle / © Académie des sciences, Paris, 2021
ISSN (imprimé / *print*) : 1631-0683/ ISSN (électronique / *electronic*) : 1777-571X

New skull material of Pleistocene dwarf deer from Crete (Greece)

Ann-Marie SCHILLING
Gertrud E. RÖSSNER
SNSB-Bayerische Staatssammlung für Paläontologie und Geologie,
Richard-Wagner-Str. 10, 80333 Munich (Germany)
and Department of Earth and Environmental Sciences, Ludwig-Maximilians-Universität
München, Richard-Wagner-Str. 10, 80333 Munich (Germany)
roessner@snsb.de
schilling.annmarie@gmail.com

Submitted on 7 November 2019 | Accepted on 6 March 2020 | Published on 8 March 2021

urn:lsid:zoobank.org:pub:CDEF7B73-BB00-4603-BDEC-57F36ED3D9F5

Schilling A.-M. & Rössner G. E. 2021. — New skull material of Pleistocene dwarf deer from Crete (Greece). *Comptes Rendus Palevol* 20 (9): 141-164. https://doi.org/10.5852/cr-palevol2021v20a9

ABSTRACT
In the Pleistocene faunas of the island of Crete, Cervidae was one of the most abundant taxa. Respective species vary in body size, including dwarfs, and skeletal morphology; however, the number of species and the identity of the mainland ancestor(s) are still debated. In this paper, we morphologically and morphometrically describe and analyze eight skulls of Cretan deer from a so far little known fossil site near Gerani, Rethymnon, Greece. The recorded character suite allows for affiliation to dwarfed *Candiacervus* Kuss, 1975, *Candiacervus ropalophorus* de Vos, 1984 and *C. reumeri* van der Geer, 2018. It comprises previously unknown unique traits, some of them hinting to sexual dimorphism. Comparisons of the *Candiacervus* skulls presented here with those of cervids belonging to Megalocerotini Brooke, 1828, *s.s.* and *s.l.* stress certain similarities; yet more material is needed to reconstruct *Candiacervus*' phylogenetic position. The newly detected craniodental specifics allow for more insights into island adaptation of *Candiacervus*; at the same time, they blur the morphological heritage of their mainland ancestors.

KEY WORDS
Candiacervus, craniodental morphology, morphometrics, island evolution.

RÉSUMÉ
Nouveau matériel crânien de cerfs nains du Pléistocènes de Crète (Grèce).
Au sein de la faune du Pléistocène de l'île de Crète, les Cervidae sont l'un des taxons les plus abondants. Les différentes espèces se différencient par leur taille, incluant des formes naines, et par la morphologie de leur squelette ; cependant, le nombre d'espèces et l'identité de leur(s) ancêtre(s) continental(aux) sont encore débattus. Dans cet article, nous décrivons et analysons de manière morphologique et morphométrique huit crânes de cerfs crétois d'un site fossilifère peu connu, proche de Gerani, Réthymnon, en Grèce. L'ensemble des caractères observés permet une affiliation aux espèces naines de *Candiacervus* Kuss, 1975, *Candiacervus ropalophorus* de Vos, 1984 et *C. reumeri* van der Geer, 2018. De nouveaux caractères morphologiques uniques sont à relier au dimorphisme sexuel. Les comparaisons de ces crânes de *Candiacervus* avec ceux d'autres Cervidae appartenant au Megalocerotini Brooke, 1828, *s.s.* et *s.l.* pointent des similarités. Cependant, du matériel additionnel est nécessaire pour reconstruire la position phylogénétique de *Candiacervus*. Les nouvelles données cranio-dentaires permettent un éclairage sur l'adaptation de *Candiacervus* au milieu insulaire, mais brouillent également l'héritage morphologique de leurs ancêtres continentaux.

MOTS CLÉS
Candiacervus,
morphologie
cranio-dentaire,
morphométrie,
évolution insulaire.

INTRODUCTION

Pleistocene fossils from the Mediterranean island of Crete provide a fascinating view into island evolution. Mammals colonized this island during the early Pleistocene, probably by sweepstake route, i.e., swimming, floating, or rafting (Simpson 1940) and the fossil record indicates that the Pleistocene faunas of Crete were highly unbalanced (de Vos 1984), as typical for island faunas (Carlquist 1974; Losos & Ricklefs 2009). The mammalian fauna of the late middle to late Pleistocene was characterized by giant mice (*Mus bateae* Mayhew, 1977, *M. minotaurus* Bate, 1942), the still existent Cretan shrew (*Crocidura zimmermanni* Wettstein, 1953), a dwarf elephant (*Palaeoloxodon creutzburgi* (Kuss, 1965)), several species of deer (*Candiacervus* Kuss, 1975) and an otter (*Lutrogale cretensis* Symeonides & Sondaar, 1975) (Strasser *et al.* 2018).

Cervidae, typically referred to as *Candiacervus,* are one of the most abundant taxa (Sondaar 1971) in Cretan Pleistocene faunas. Remains of *Candiacervus* have been found at several sites, mainly in karst caves along the Cretan coastline (Lax 1996; Iliopoulos *et al.* 2010). Most of the studied material of *Candiacervus* comes from the Simonelli Cave (Accordi 1972; Malatesta 1980; Caloi & Palombo 1995; Palombo *et al.* 2008), the Bate Cave (Raia & Meiri 2006; Kolb *et al.* 2015), the Liko Cave, and the Gerani caves (de Vos 1984; Raia & Meiri 2006; van der Geer *et al.* 2006a, b, c, 2014; Vislobokova 2013; Kolb *et al.* 2015; van der Geer 2018). Post-cranial and cranial remains, including antlers, as well as dental remains have been obtained from these sites (see references given above and also Simonelli 1908; Kuss 1965, 1975; de Vos 1979; Capasso Barbato & Petronio 1986), and were dated to the late Pleistocene.

Post-cranial material of *Candiacervus* has been utilized to investigate, among other aspects, bone growth and skeletal adaptations to the palaeoenvironment, as well as for comparative studies (Caloi & Palombo 1990; van der Geer *et al.* 2006b; van der Geer 2008, 2014; Attard & Reumer 2009; Mazza 2013; Kolb *et al.* 2015; Amson & Kolb 2016; Mazza *et al.* 2016). Moreover, size differences of post-cranial remains have been interpreted to indicate the existence of six distinct size groups (cf. de Vos 1979, 1984) ranging from about 40 cm to 165 cm height at withers (de Vos 1979; van der Geer *et al.* 2006a). Analyses of skull specimens (see de Vos 1984) and of antlers (van der Geer 2018 and references therein) allowed the distinction of four types, referred to as skull types a-d by de Vos (1984). Up to now, it has not been possible to unambiguously link post-cranial with cranial remains, including antlers. However, de Vos (1984: 46) presented a well-reasoned suggestion "that there are at least eight groups of fossil deer [on Crete], each one representing a species". He maintained the view that all of these belonged to one genus, *Candiacervus*, and referred to them, from smallest to largest, as *Candiacervus ropalophorus* de Vos, 1984*, Candiacervus* sp. IIa, IIb, and IIc, *Candiacervus cretensis* (Simonelli, 1908)*, Candiacervus rethymnensis* Kuss, 1975, *Candiacervus* sp. V, and *Candiacervus* sp. VI , respectively (Table 1).

In contrast, Capasso Barbato & Petronio (1986) and Capasso Barbato (1989, 1990) argued in favor of five distinct species (Table 1), which they assigned to two different genera. According to their classification: 1) *Candiacervus ropalophorus* de Vos, 1984 and *Candiacervus* sp. IIa, IIb, and IIc are conspecific – *Megaceros* (*Candiacervus*) *ropalophorus* (de Vos, 1984) – later referred to as *Megaloceros* (*Candiacervus*) *ropalophorus*; 2) *Candiacervus cretensis* (Simonelli, 1908) was revised as *Megaceroides* (*Candiacervus*) *cretensis* (Simonelli, 1908). *Candiacervus rethymnensis* Kuss, 1975 as well as the larger species *Candiacervus dorothensis* (Capasso Barbato, 1990) and *Candiacervus major* (Capasso Barbato & Petronio, 1986), were revised to belong to a newly established subgenus of *Cervus* (*Leptocervus*) Capasso Barbato, 1990*,* and classified into; 3) *Cervus* (*Leptocervus*) *rethymnensis* (Kuss, 1975); 4) *Cervus* (*Leptocervus*) *dorothensis* Capasso Barbato, 1990; and 5) *Cervus* (*Leptocervus*) *major* Capasso Barbato & Petronio, 1986, respectively. In a more recent publication, Capasso

TABLE 1. — Diversity and taxonomical history of Cretan deer.

Morphotype or "species" (de Vos 1979, 1984)	Available material	Description based on element	Type material	Type locality	Other occurrences	Revision			
						Capasso Barbato (1990)	Capasso Barbato (1995)	Caloi & Palombo (1996)	van der Geer (2018)
Candiacervus ropalophorus de Vos, 1984; Size group 1	cranial	skulls	male skull, Ge4-46, holotype (de Vos 1984, plate. 10)	Gerani 4, uppermost 40 cm	Gerani 2,3,6; Mavro Mouri 4c; Sourida, Simonelli Cave, Rethymnon fissure; Kalo Chorafi	*Megaceros* (*Candiacervus*) *ropalophorus*	*Megaceroides* (*Candiacervus*) *ropalophorus*	*Megaceroides* (*Candiacervus*) "*ropalophorus*"	*Candiacervus ropalophorus*
–	post-cranial	metacarpi, metatarsi	–	–	Gerani 4, Rethymnon fissure	–	–	–	–
Candiacervus sp. IIa; Size group 2	cranial	skulls, antlers	male skull, AMPG(V) 1734, holotype (de Vos 1984, plate 12)	Liko, uppermost 75 cm	Gerani 1, 2, 4; Grida Avlaki; Gumbes B; Kalo Chorafi; Mavromuri 3 and 4; Peristeri 2, Sifanos, Simonelli Cave	*Megaceros* (*Candiacervus*) *ropalophorus*	*Megaceroides* (*Candiacervus*) *ropalophorus*	*Megaceroides* (*Candiacervus*) "*ropalophorus*"	*Candiacervus listeri*
Candiacervus sp. IIb; Size group 2	cranial	skulls, antlers	male skull, AMPG(V) 1735, holotype (de Vos 1984, plate 13)	Liko, uppermost 75 cm	Mavromuri 4	*Megaceros* (*Candiacervus*) *ropalophorus*	*Megaceroides* (*Candiacervus*) *ropalophorus*	*Megaceroides* (*Candiacervus*) "*ropalophorus*"	*Candiacervus devosi*
Candiacervus sp. IIc; Size group 2	cranial	skulls, antlers	AMPG(V) 1736, holotype (de Vos 1984, plate 14)	Liko, uppermost 75 cm	Peristeri 2; Simonelli Cave; Kalo Chorafi; Mavromuri 3	*Megaceros* (*Candiacervus*) *ropalophorus*	*Megaceroides* (*Candiacervus*) *ropalophorus*	*Megaceroides* (*Candiacervus*) "*ropalophorus*"	*Candiacervus reumeri*
Candiacervus cretensis (Simonelli, 1908); Size group 3	Cranial	skulls, antlers	–	Gerani 4	Simonelli cave	*Megaceros* (*Candiacervus*) *cretensis*	*Megaceros* (*Candiacervus*) *cretensis*	*Megaceroides* (*Candiacervus*) *cretensis*	*Candiacervus cretensis*
–	post-cranial	right metacarpal	metacarpal, lectotype (Simonelli 1908, fig. 24,25)	Unknown site, possibly near Grida Avlaki	Liko, Mavro Mouri 4c, Rethymnon fissure; Kharoumes 2	–	–	–	–
Candiacervus rethymnensis Kuss, 1975; Size group 4	post-cranial	metacarpi, metatarsi	right metacarpal, holotype (Kuss 1975, plate IV, fig. o)	Mavro Mouri 4	Gerani 2, Mavro Mouri 4c, Sourida, Rethymnon fissure, Liko, ?Simonelli Cave	*Cervus* (*Leptocervus*) *rethymnensis*	*Pseudodama* (*Leptocervus*) *rethymnensis*	*?Pseudodama rethymnensis*	*Candiacervus rethymnensis*
Candiacervus sp. V; Size group 5	post-cranial	radius, metacarpi, metatarsi	right radius, MPUR 25, holotype (Capasso Barbato 1992: fig. 4)	Bate Cave	–	*Cervus* (*Leptocervus*) *dorothensis*	*Pseudodama* (*Leptocervus*) *dorothensis*	?*Pseudodama* (*Leptocervus*) *dorothensis*	*Candiacervus dorothensis*
Candiacervus sp. VI; Size group 6	post-cranial	metapodial	metatarsus, MPUR 30, holotype (Capasso Barbato & Petronio 1986, Tav. II.)	Bate Cave	Liko	*Cervus* (*Leptocervus*) *major*	*Pseudodama* (*Leptocervus*) *major*	?*Pseudodama* (*Leptocervus*) *major*	*Candiacervus major*

Barbato (1995) revised the latter three species to *Pseudodama* (*Leptocervus*) *rethymnensis* (Kuss, 1975), *Pseudodama* (*L.*) *dorothensis* (Capasso Barbato, 1990), and *Pseudodama (L.) major* (Capasso Barbato & Petronio, 1986), respectively, without further clarifications. Moreover, Capasso Barbato (1995) revised *Megaloceros* (*Candiacervus*) *ropalophorus* to *Megaceroides* (*Candiacervus*) *ropalophorus*. Recently, van der Geer (2018) proposed to assign all six size groups of Cretan deer to the genus *Candiacervus* and specifically, to rename de Vos' *Candiacervus* sp. IIa, IIb, and IIc as *Candiacervus listeri*, *C. devosi*, and *C. reumeri*, respectively.

Thus, the assignment of the smaller species of *Candiacervus* to *Megaceros* Owen, 1844 / *Megaloceros* Brookes, 1828 / *Megaceroides* Joleaud, 1914 (Caloi & Palombo 1996; Capasso Barbato 1989, 1990, 1995) indicates consideration of *C. ropalophorus, C. listeri, C. devosi, C. reumeri*, and *C. cretensis* (Simonelli, 1908) as dwarfed members of giant deer. In fact, this implies that these *Candiacervus* species belong to Megalocerotini Brookes, 1828 *s.s.*, which comprises the genera *Megaloceros*, *Megaceroides*, and *Dama,* and which constitutes a phylogenetic branch (as outlined by Croitor 2016). This holds also for the views presented by

other authors (e.g. Radulescu & Samson 1967; Sondaar & Boekschoten 1967; Caloi & Palombo 1994). Van der Geer (2018) favored a close relationship of *Candiacervus* with the fallow deer, *Dama,* based on antler morphology. As *Dama* is more closely related to *Megaloceros* than to *Cervus* (Hughes *et al.* 2006; Immel *et al.* 2015; Mennecart *et al.* 2017) and has actually been considered to be the last living member of giant deer (Lister *et al.* 2005), this again supports a close relationship of *Candiacervus* with Megalocerotini *s.s.*

Vislobokova (2013) presented a reassessment of some of the cranial material described originally by de Vos (1984), compared it with material from giant deer, and also concluded that *Candiacervus* is a member of this group. However, it should be noted that her study comprises material of Megalocerotini *s.l.*, which is considered a polyphyletic group of giant cervids (Croitor 2014, 2016).

The presumptive mainland relatives, or ancestors, of the medium-sized and larger morphotypes of *Candiacervus,* i.e., *Candiacervus rethymnensis* Kuss, 1975*, Candiacervus dorothensis* and *Candiacervus major* (Table 1) remain enigmatic, as do their relationships with the smaller species of *Candiacervus*. Whatever ancestor(s) gave rise to the Cretan deer, it has been criticized that none of the genera suggested "share synapomorphologies with *Candiacervus* that are not shared with other genera" (de Vos & van der Geer 2002: 400).

Thus, despite the extensive studies cited above, the biological systematics of Cretan deer is still subject of debate (Table 1). Clearly, this discussion should profit from additional morphological data. Accordingly, in this study, we present undescribed, exquisitely preserved *Candiacervus* skull remains from Gerani, west of Rethymnon, Crete. We provide a detailed morphological and morphometric description, discuss it within the existing qualitative and quantitative framework and give a systematic assessment of the studied specimens. Our intentions are: 1) to complement previous character lists and species diagnoses; and 2) to highlight hitherto unknown traits and to interpret them in the context of island evolution and dwarfing in Cervidae.

Abbreviations

Institutional Abbreviations

AMPG	Museum of Paleontology and Geology of the University of Athens, Athens;
MPUR	Museo di Paleontologia, Università degli Studi di Roma 'La Sapienza', Rome;
NNML	National Natuurhistorisch Museum, Leiden;
SNSB-BSPG	Staatliche Naturwissenschaftliche Sammlungen Bayerns – Bayerische Staatssammlung für Paläontologie und Geologie, Munich.

MATERIAL AND METHODS

Eight skulls of Cretan deer or fragments thereof, stored at the SNSB-BSPG are described (SNSB-BSPG identification see Appendix 1). In the following text, we refer to specimens by their specific ID only, e.g. "SNSB-BSPG 1972 XIX 201" will be abbreviated to "1972 XIX 201', or simply by the last number of the ID, e.g. "201". The material comes from a cave near the village Gerani, to the west of Rethymnon; it was collected by H.-J. Gregor in 1971. The exact location of the cave remains unknown. However, according to H.-J. Gregor (pers. communication, September 28, 2018), the cave entrance is at about five meters above sea level. The fossil site itself could be reached by crawling through a small tunnel and it extended approximately two meters in height and seven meters in length. Its sidewalls consisted of gravel and conglomerate, in which bones were embedded. H.-J. Gregor also noted that the material comes from the same cave he introduced to S. E. Kuss (Freiburg im Breisgau, Germany), in May 1971, and which the latter briefly mentioned in his paper of 1973 (Kuss 1973: 58). The description of the cave, however fragmentary, allows concluding that the material presented here does not come from one of the better-described sites (de Vos 1984; Lax 1991). Both H.-J. Gregor (pers. communication) and S. E. Kuss (1973) reported that they did not find bones of any other taxon than cervids at this location.

The precise geological age of our specimens is unclear. Kuss (1973) suggested that fossils from the respective layer were younger than the Grida-Avlaki-Fauna, which he previously correlated with the Riss/Würm Interglacial (Eem Interglacial, Tarantian, late Pleistocene) (Kuss 1970). Molars of *Candiacervus ropalophorus* from the nearby sites Gerani V and Gerani VI (Lax 1991) were dated by electron spin resonance dating to a corresponding age (Reese *et al.* 1996).

Specimens were covered with a layer of brownish calcareous sinter, typically formed in karst caves, as already noted by Kuss (1973), who visited the site in summer 1971. The sinter was removed mechanically in 2017, just when we started the study.

Methodologically, we first undertook an extensive morphological comparison based on previous descriptions of Cretan deer (Simonelli 1908; Kuss 1975; Malatesta 1980; de Vos 1984) and described the studied material in detail. The relative biological age of our specimens was determined based on the wear patterns of the upper molars (van Bemmel 1949; de Vos 1984) and developmental stages of antlers.

Next, we obtained 37 skull and 4 dental variables that had been established in previous publications to describe Cretan deer (Simonelli 1908; Malatesta 1980; de Vos 1984; Vislobokova 2013) and allow us to integrate our findings with these seminal publications. These variables and their definitions are listed in Table 2. Linear measurements were taken with digital and mechanical calipers (150 mm and 300 mm, respectively). Angles were measured with a mechanical protractor/goniometer (resolution: 1°). Angles between lines to which the available goniometer could not be applied (because of its size) were measured in appropriately oriented and magnified photographs, using the "Measure"-tool implemented in Gimp v.2.8.16 (http://www.gimp.org). Raw data are reported in Appendix 1. Relative sizes are given as percentages of the condylobasal length.

Basic descriptive statistics are reported in Table 3. For the coefficient of variation, values between 2 and 8 are indicative for individuals of a single population (Simpson *et al.* 1960; de Vos 1984).

FIG. 1. — *Candiacervus ropalophorus* de Vos, 1984: **A**-**E**, SNSB-BSPG 1972 XIX 1; **F**-**I**, SNSB-BSPG 1972 XIX 200. The species typically has an interfrontal crest, visible in A and F; thick dorsal orbital rims, no contact between frontals and maxillae (**B**, **G**); and protocone and metaconule of similar size (**D**). SNSB-BSPG 1972 XIX 200 has weak rims on the left pedicle and bony pearls on a minimal burr (H). Its left M3 is in eruption (I). **A**, **F**, rostral view; **B**, **G**, left lateral view; **C**, **H**, dorsal view; **D**, **I**, ventral views; **E**, occipital view. **A**, **B**, **E**-**G**, dorsal to the top; **B**-**D**, **G**-**I**, rostral to the left. Scale bars: 1 cm.

We compared the values of descriptive measures of teeth with those previously published and taken from specimens from Simonelli Cave and Gerani IV (Simonelli 1908; de Vos 1984; Appendix 1). In doing so, we exclude data of one specimen Simonelli (1908) reported on, as he could not reliably assign the isolated maxilla fragment with cheek teeth to any of his skull remains with sex-specific characters ("mascellare superiore appartenuto verosimilmente al teschio rappresentato dalle figures 1-4", p. 9 [the upper jaw belonged probably to the skull represented by figures1-4]). We then compared the ranges of variation of our data with that of Simonelli (1908) and de Vos (1984).

We follow Croitor (2016) and refer to Megalocerotini *s.l.* as a polyphyletic group of giant forms of cervids, and Megalocerotini *s.s.* as comprising the genera *Megaloceros*, *Megaceroides*, and

Dama (see also Introduction). In order to assess to which degree the adaptation to the insular environment has affected skull morphology of Cretan deer, we applied diagnostic, qualitative and quantitative traits defined by Vislobokova (2013) for Megalocerotini *s.l.*

SYSTEMATIC PALEONTOLOGY

Order ARTIODACTYLA Owen, 1848
Suborder RUMINANTIA Scopoli, 1777
Infraorder PECORA Flower, 1883
Family CERVIDAE Goldfuss, 1820
Subfamily *Cervinae* Goldfuss, 1820

Genus *Candiacervus* Kuss, 1975

TYPE SPECIES. — *Anoglochis cretensis* (Simonelli, 1908) from the late Pleistocene of Rethymnon Area (Crete, Greece), unknown site, possibly near Grida Avlaki (de Vos 1984) by subsequent designation of Kuss (1975).

Candiacervus ropalophorus de Vos, 1984
(Figs 1; 2; 3A-E)

Candiacervus ropalophorus de Vos 1984: 43. — van der Geer 2018: 5, fig. 3.

Megaceros (*Candiacervus*) *ropalophorus* – Capasso Barbato 1990: 268, fig. 2; 1992: 192.

Megaceroides (*Candiacervus*) *ropalophorus* – Capasso Barbato 1995: 243, fig. 1. — Caloi & Palombo 1996: 136, figs 10.5-10.7, 10.9-10.13.

HOLOTYPE. — Male skull Ge4-46 from the Late Pleistocene (van der Geer *et al.* 2006b); Gerani 4, 40 uppermost centimeters of cave filling (de Vos 1979, 1984).

REFERRED MATERIAL. — 1972 XIX 1, 1972 XIX 200, 1972 XIX 202, 1972 XIX 203, 1972 XIX 204.

SPECIMENS

1972 XIX 1 (Fig. 1A-E)
The skull is complete, with the exception of the rostral part of the left frontal, and from a female, because pedicles and antlers are not developed. The basal M3s have fully erupted. The occlusal surfaces show medium wear. The paracone and metacone and the protocone and metaconule of M2 are separated by enamel ridges (van Bemmel 1949) This indicates that the animal is likely older than an early adult and younger than a middle-aged adult *sensu* de Vos (1984).

1972 XIX 200 (Fig. 1F-I)
The specimen comes from a male because pedicles are present. On the left pedicle, there is a partial burr, i.e., a ring of bony pearls at the proximal end of the antler. The rest of the left antler is broken. The right pedicle is broken close to its base. The part of the occipital bone situated below the linea nuchae, the petrosals, and the snout are missing. Left P3 to M2 and right P4 to M3 are present. P4, M1, and M2 are little worn. The P3 is unworn. In addition, the alveola of the right P3 are preserved. The paracone and protocone of M2 are not in contact with the dentine of the metacone and metaconule, respectively. The right M3 is only halfway erupted, indicating that we deal with an early adult. Caudal to the left foramen supraorbitale, a weakly developed bony rim can be identified and runs towards the lateral margin of the left pedicle. The axis of the pedicle and the midline of the frontal bone form an angle of 35°.

1972 XIX 202 (Fig. 2A-E)
This is a female skull. There are neither pedicles nor antlers present. The left and right premaxilla, the left orbital rim, and both zygomatic arches are missing. The tooth rows are complete with P2 to M3 and M3s are fully erupted. Their occlusal surface is medium worn, but more heavily than in specimen 1. The dentine of the paracone and metacone of M2 are in contact, while the dentine of protocone and metaconule are not yet in contact. Therefore, the individual was an older middle-aged adult at the time of its death.

1972 XIX 203 (Fig. 2F-J)
The male skull has pedicles and, on the left one, the distal part may represent the proximal portion of a first generation, unbranched spike-like antler without burr (details on antler development see e.g. Davis *et al.* (2011)). The pedicle is slightly bent to lateral and bears the most proximal portion of a yearling antler without burr. The rest of the antler is broken and missing. The right pedicle is broken close to its base. Most of the rostral facial skull is missing, except for most caudal nasal and maxilla portions and the lacrimal bones. The left premolar row, the left M3 and the zygomatic arch are not preserved. The right P2 and P3 are also missing. The right M3 is in eruption. The teeth are little worn, hence the dentine of the paracone and protocone are not in contact with the dentine of the metacone and metaconule, respectively. The latter, the not fully erupted M3, and the presence of a first generation antler indicate that the specimen is from a relatively young or early adult. Bony rims at the base of the pedicles could not be discerned, contrary to what has been identified in specimen 200 (see above). The axis of the pedicle and midline of the frontal form an angle of 41°.

1972 XIX 204 (Fig. 3A-E)
A female skull without pedicles and antlers. The premaxilla and right zygomatic arch are not preserved. The dentition is complete with left and right P2 to M3; the left P2 is slightly damaged. The occlusal surface is heavily worn; the right P2, both P3 and both M1 are worn down to the crown base, enamel islets almost disappeared. The dentition status indicates an old animal.

DESCRIPTION

Overall, these five skulls are gracile; they are widest at the caudal orbital border. Their facial part is longer than their cranial part, in particular; the snout is long and slender (Fig. 1B). The orbits are located at about the same distance from the snout

TABLE 2. — Measurements, their abbreviations and definitions. Abbreviation: **na**, character ID not given in the reference.

	Measurement, abbreviation	Landmarks or definition	Taken from	Character ID in reference
1	Basilar length, BL	Prosthion-basion	de Vos (1984)	1
2	Width bizygomatic, ZyZy	Zygion-zygion	de Vos (1984)	2
3	Skull height, BLnsup	Linea nuchae superior-basion	de Vos (1984)	3
4	Width of the occipital, OtOt	Otion-otion	de Vos (1984)	4
5	Orbital width, DRC	Rostrocaudal diameter in the horizontal plane	de Vos (1984)	5
6	Orbital height, DDV	Dorsoventral diameter in the vertical plane	de Vos (1984)	6
7	Orbital shape	DVV/DRC	de Vos (1984)	Index 2
8	Relative orbit size	(M2 length + M3 length, measured on the occlusal surface) /DRC	Vislobokova (2013)	General character, 16
9	Skull flexion	Angle between the forehead and the dorsal surface of the braincase	Vislobokova (2013)	General character, 1
10	Inclination of the braincase roof relative to the braincase axis	Angle between dorsal surface of the braincase and the horizontal basicranium	Vislobokova (2013)	General character, 9
11	Greatest skull width	Width at the caudal orbital border	Vislobokova (2013)	General character, 12
12	Inclination of the skull roof and the occipital plane	Angle between the upper and lower part of the squama occipitalis (above and below the linea nuchae superior)	Vislobokova (2013)	General character, 4
13	Greatest width of the supraorbital groove, maxWSG	Maximal mediolateral extension of the groove	Vislobokova (2013)	Generic character, 1.2
14	Horizontal diameter of the supraorbital foramen, DSF	Maximal mediolateral extension of the foramen	Vislobokova (2013)	Generic character, 1.2
15	Proportion of supraorbital foramen to groove	maxWSG/ DSF	Vislobokova (2013)	Generic character, 1.2
16	Length of the foramen ovale	Rostrocaudal extension of the f. ovale	Vislobokova (2013)	Generic character, 6.4
17	Width of the foramen ovale	Mediolateral extension of the f. ovale	Vislobokova (2013)	Generic character, 6.4
18	Shape of the foramen ovale	Length/Width of the f. ovale	This study	
19	Position of the foramen ovale	Angle between the greatest axis of the f. ovale and the sagittal skull plane	Vislobokova (2013)	Generic character, 6.4
20	Length of the occipital	Lambda-Inion	Simonelli (1908)	na
21	Length of the parietal	Lambda-Bregma	Simonelli (1908)	na
22	Length of the frontal	Bregma-Nasion	Simonelli (1908)	na
23	External distance between foramina supraorbitalia	Maximal diameter between the foramina supraorbitalia	Simonelli (1908)	na
24	Inclination of the tympanic bullae relative to the meatus acusticus	Angle between the major axis of the tympanic bullae and the transversal axis of the external meatus acusticus	Vislobokova (2013)	Generic character, 7.2
25	Position of the external meatus acusticus	Angle between the transversal axis of the external meatus acusticus and the median plane	Vislobokova (2013)	Generic character, 7.2
26	Orientation of the orbit	Angle between the left and right anteroposterior orbital diameter in a horizontal plane	Vislobokova (2013)	na
27	Klinorhynchy	Angle between the horizontal basicranium and the palatine plane	Starck (1979)	
28	Frontal breadth 1	Frontal breadth at the constriction in males	Croitor (2018)	18
29	Frontal breadth 2	Frontal breadth behind the pedicles in males	Croitor (2018)	19
30	Facial length	Anterior edge of orbit to prosthion	Croitor (2018)	11
31	Condylobasal length, CBL	Posterior edges of the occipital condyles to prosthion	Croitor (2018)	1
32	Relative facial length	Facial length/CBL		
33	Muzzle length	P2 to prosthion	Croitor (2018)	5
34	Relative muzzle length	Muzzle length/ CBL		
35	Length of the braincase	Bregma to opisthion	Croitor (2018)	7
36	Greatest width of braincase	Euryon-Euryon		
37	Relative length of braincase	Length of braincase/greatest width of braincase		
38	Length of the premolar row, P2P4	Distance between P2 and P4 taken at the level of the gum	Simonelli (1908)	na
39	Length of the molar row, M1M3	Distance between M1 and M3 taken at the level of the gum pad	Simonelli (1908)	na
40	Relationship between molar and premolar row	M1M3/P2P4	This study	
41	Length of tooth row, P2M3	Distance between the P2 and M3 taken at the level of the gum pad	Simonelli (1908)	na

tip and the occiput (Fig. 1B). The skulls are klinorhynchic (Starck 1979), i.e., the palatine plane is inclined downwards in relation to the horizontal basicranium. The angle encompassed by the two bones is about 170° (Table 3).

The facial skull

From a lateral and rostral view, the facial skeleton shows a clear flexion of the frontal between the orbits. The interfrontal suture is slightly prominent in both males and females (Figs 1A, B, F, G; 2F, G; 3A, B). Since the prominence is equally developed in both the early (200, 203) and the old (204) adults, it does not seem to be an age-dependent trait. Malatesta identified the same "crest" (1980, p. 21) in male specimens of *Candiacervus reumeri* (van der Geer, 2018) from Simonelli cave. While this crest continues caudally in females up to the point where antlers develop in males, such eminence is not discernible in the two males (Figs 1F; 2F). The supraorbital grooves are weakly developed in all specimens. The foramen supraorbitale is large (*c.* 50% of the width of the supraorbital groove, Appendix 1) and circular. The two foramina lie at a greater transversal distance than the ethmoidal gaps, such that straight lines connecting the foramina and ethmoidal gaps transversally and rostrocaudally form a trapezium.

The orbits are roundish, quantified by the ratios of the dorsoventral and rostrocaudal diameters equaling one (Appendix 1). The orbits are small, with the rostrocaudal orbital diameter as long as the length of M2 + M3 (Appendix 1). The caudal orbital rims (= postorbital bar) are triangular in cross-section and robust; with the robust zygomatic arch, they form an angle of approximately 90°. The dorsal orbital rim is roundish and thick, rising slightly above the frontal bones (Figs 1A, F; 2A; 3A) and conforms to the description by de Vos (1984). The rostral orbital border is above M2 (Figs 1G; 2G) or above the border between M2 and M3 (Figs 1B; 2B; 3B).

Rostrally to the orbit extends the lacrimal bone. Its facial facet makes up part of the orbital rim, contacts the jugal and the maxilla ventrally and the frontal bone dorsally, as in living cervid species. It forms a pentagon, narrow in the dorsoventral direction and elongated in the rostral-caudal direction. The angle between the lacrimojugal and the lacrimomaxillar sutures is approximately 180°. Two lacrimal orifices, as typical for cervids (Leinders & Heintz 1980), can be recognized in all specimens. One is located on the orbital rim, the other one is located slightly more rostrally. In specimens 1 and 203, a little protuberance is preserved and separates these two orifices (Figs 1A; 2F). There is no preorbital depression in the lacrimal facial facet. A relatively small, clear, and triangular ethmoidal gap can be recognized in all specimens.

The nasals are cruciform, having their widest lateral extension at the level of the ethmoidal gap. Caudally, the nasal bones converge to an apex. The latter and the nasofrontal suture are located rostrally to the level of the rostral orbital border (Figs 1C, H; 2C, H; 3C). From the rostral view, the shape of the nasal cavity is arched, narrow and high. The nasal septum does not completely divide the nasal cavity in a dorsoventral direction (Figs 1A; 3A).

The maxilla presents a bulge instead of a facial crest and the maxillary tubercle is discernible. A small tuber above M1 can be identified. The premaxillae are slightly widened caudally; the outline of its most rostral part is rectangular (Fig. 1C, D). Ventrally, the sinistral and dextral margo interalveolaris between P2 and the praemaxillo-maxillar suture run in parallel to each other.

The maxillopalatine suture has a rectangular outline. The rostrocaudal portion of the suture runs in parallel to the molars; the other one runs straight in a transversal direction (see e.g. Fig. 1D). The ventral position of the transversal part is quite variable. In specimens 1 and 200, this suture meets M1 right between the protocone and the metaconule. In specimen 202, the suture is at the height of the anterior border of M2. In specimen 204, this suture meets M2 right between the protocone and the metaconule. The foramina palatinae are located either in the corners, where the rostrocaudal and transversal parts of the maxillopalatine suture meet, or slightly shifted rostrally or caudally to the transversal part of this suture.

The spina nasalis caudalis of the palate, if present at all, is very weakly developed (Figs 1D; 2D; 3D). The location of the pterygopalatine fossae relative to the molars is variable: they are located at the level of the caudal border of M3 (Figs 1D; 2J; 3D) or half of M2 (Figs 1I; 3D). If present at all, a ventral projection on the pterygoid (hamulus pterygoideus) is only partially preserved (Fig. 1D).

The neurocranium

The braincase is, on average, as long as wide (Table 3). In dorsal view, the shape of the braincase is oval, i.e., it does not expand caudally (Figs 1C, H; 2C, H; 3C). The temporal lines converge from the linea nuchae superior towards the lambdoid suture and then diverge to the base of the pedicles in one of the males (Fig. 1H) and until the base of the zygomatic process in females (Figs 1C; 3C). In specimens 202 and 203, the lines are less developed. An interparietal prominence can be tactually, but hardly visually recognized. Fossae located laterally to the interparietal eminence are absent, with the possible exception of weakly developed ones in specimen 204. A parietal foramen cannot be discerned. The frontoparietal suture is straight. Specimen 204 has a slight depression at the junction of the dorsal midline and the frontoparietal suture (Fig. 3C). The linea nuchae superior is well developed and slightly arched, in both males and females. The latter is even more pronounced in the older specimens of our sample. The upper and lower portions of the squama occipitalis comprise either a right or an obtuse angle when seen from lateral (Appendix 1) and the occipital condyles do not protrude beyond the caudal border of the occiput (Figs 1B; 2B, G; 3B). Due to its size, the foramen ovale can be easily identified at the basisphenoid.

In all four specimens in which the occiput is preserved (Figs 1E; 2E, J; 3E), it consists of a single bone with a weakly developed protuberantia occipitalis externa. The latter occupies approximately half of the dorsoventral height of the occiput (Fig. 1E). While the shape of the protuberantia cannot be assessed in the male specimen (Fig. 2J), it is rhomboid in the remaining three, female specimens. The median occipital crest,

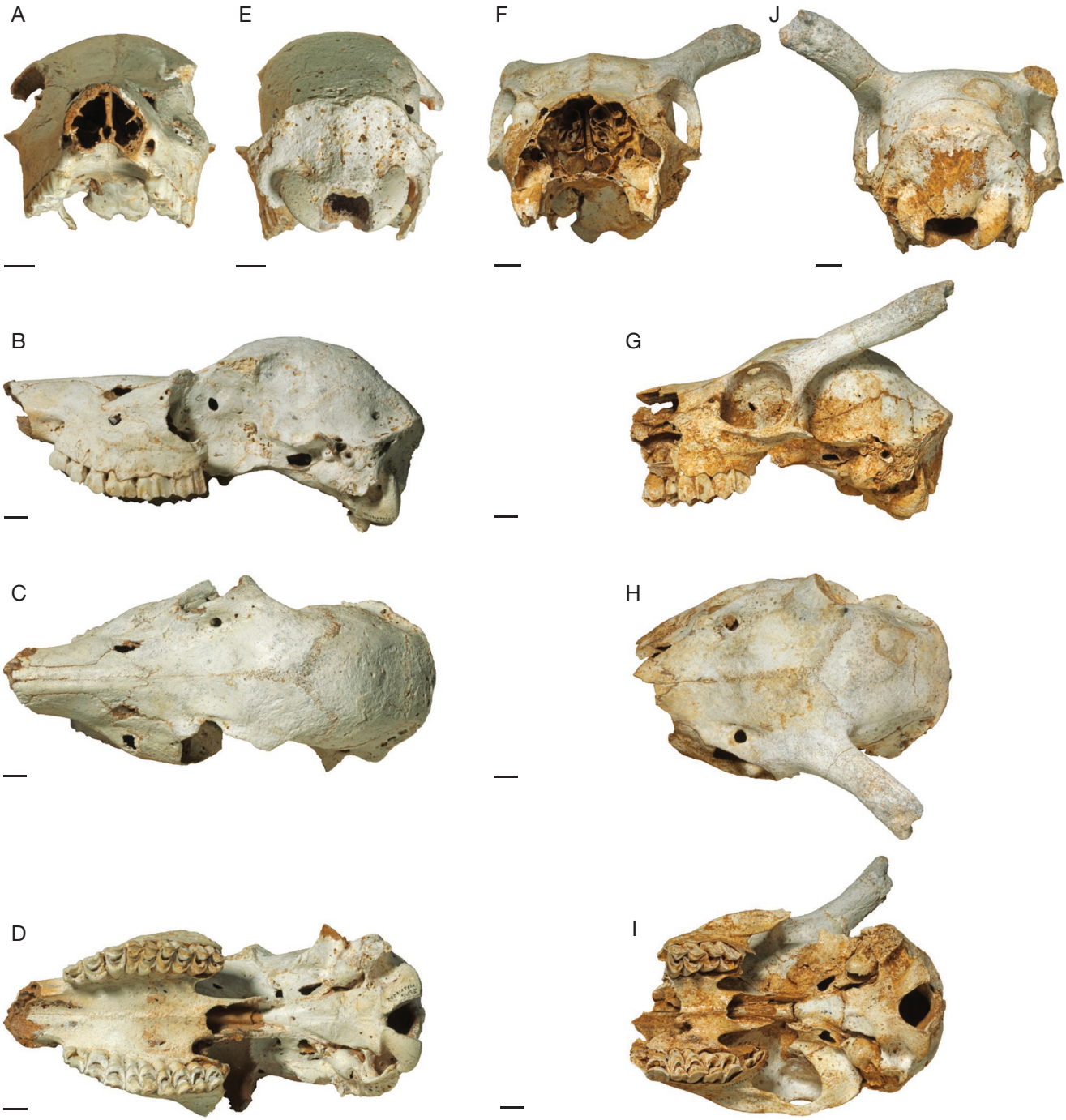

FIG. 2. — *Candiacervus ropalophorus* de Vos, 1984: **A**-**E**, SNSB-BSPG 1972 XIX 202; **F**-**J**, SNSB-BSPG 1972 XIX 203. Right M3 is in eruption (I). **A**, **F**, rostral view; **B**, **G**, left lateral view; **C**, **H**, dorsal view; **D**, **I**, ventral view; **E**, **J**, caudal view. **A**, **B**, **E**-**G**, **J**, dorsal to the top; **B**-**D**, **G**-**I**, rostral to the left. Scale bars: 1 cm.

despite being sharp-edged, is still quite delicate (Figs 1E; 2E, J; 3E). At the dorsocaudal end of the occiput, the nuchal fossae on either side of this crest are wide and arched. Laterally, the petrosal part of the temporal bone flanks the occiput, extending to about the middle of the occipital height. The processus paracondylaris descends in parallel to the lateral edge of the condyles and extend a bit more ventrally (Figs 1E; 2E).

The braincase roof is generally in an acute angle to the braincase axis (Appendix 1). The external auditory canal is round with a longitudinal groove (Figs 1B; 2B, G; 3B). From a ventral view, the tympanic bullae are inflated; in specimen 1 and 204, they are less inflated than in other specimens (Figs 1D; 3D *vs.* Fig. 2D, I). The bullae present a long rostral process (Fig. 2I) and their ventral surfaces do not descend below the ventral surface of the basioccipital. The pyramidal petrosal part of the temporal bone is pressed to the basioccipital. It separates the lacerate foramen from the jugular foramen. The basioccipital is wide, narrowing rostrally, with sharp, lateral

TABLE 3. — Summary statistics for 36 craniodental variables for all the specimens described here. If the values of the coefficient of variation are between 2 and 8, then individuals are from a single population (de Vos 1984; Simpson *et al.* 1960). Variables for which only one specimen is available have been omitted. Lengths in mm, angles in degree. Abbreviations: **Sd**, Standard deviation; **CV**, coefficient of variation, given in percent; **CV***, coefficient of variation, for which specimen -201 has been excluded, given in percent; **Min**, minimum; **Max**, Maximum.

	n	Mean	Sd	Median	CV	CV*	Min	Max
2. Width bizygomatic	2	92.31	7.76	92.31	8.40	8.40	86.82	97.79
3. Skull height	4	48.48	1.08	48.50	2.23	2.23	47.15	49.76
4. Width of the occipital	4	68.54	5.20	70.29	7.58	7.58	61.00	72.60
5. Orbital width	7	29.38	0.94	29.38	3.19	3.49	28.00	30.93
6. Orbital height	7	28.52	1.53	28.16	5.38	5.70	26.56	31.23
7. Orbital shape	7	0.97	0.06	0.95	5.79	6.18	0.90	1.04
8. Relative orbit size	7	0.90	0.08	0.92	8.89	3.15	0.79	0.97
9. Skull flexion	5	103.70	5.72	101.50	5.52	5.52	99.80	112.00
10. Inclination of the braincase roof relative to the braincase axis	4	16.55	1.13	16.08	6.84	6.84	15.44	18.09
11. Greatest skull width	6	111.49	1.76	111.47	1.58	1.58	109.83	114.00
12. Inclination of the skull roof and the occipital plane	4	93.05	4.32	94.45	4.64	4.64	87.00	96.30
13. Greatest width of the supraorbital groove	6	9.81	1.08	9.88	11.00	9.84	8.55	11.38
14. Horizontal diameter of the supraorbital foramen	6	5.14	0.48	5.12	9.26	9.26	4.46	5.79
15. Proportion of supraorbital foramen to groove	6	0.53	0.05	0.53	9.47	8.27	0.45	0.59
16. Length of the foramen ovale	5	8.76	2.18	8.58	24.91	24.91	6.48	11.10
17. Width of the foramen ovale	5	5.28	1.24	5.02	23.37	23.37	4.12	6.84
18. Shape of the foramen ovale	5	1.67	0.27	1.62	16.19	16.19	1.35	2.08
19. Position of the foramen ovale	5	33.72	2.42	34.50	7.19	7.19	29.85	35.80
20. Length of the occipital	5	18.31	1.71	18.25	9.36	9.36	16.44	20.32
21. Length of the parietal	5	45.88	2.48	45.60	5.41	5.41	42.67	49.31
22. Length of the frontal	5	61.57	3.83	61.63	6.22	6.22	57.04	66.36
23. External distance between foramina supraorbitalia	5	52.26	4.49	53.20	8.60	9.43	45.79	57.34
24. Inclination of the tympanic bullae relative to the meatus acusticus	4	128.47	2.78	128.40	2.16	2.16	125.91	131.19
25. Position of the external meatus acusticus	4	92.98	2.44	94.13	2.63	2.63	89.32	94.36
26. Orientation of the orbit	6	59.98	2.78	59.20	4.63	4.66	57.61	65.45
27. Klinorhynchy	3	169.65	2.09	169.63	1.23	1.23	167.58	171.75
28. Frontal breadth 1	2	55.72	2.33	55.72	4.16	4.16	54.07	57.36
29. Frontal breadth 2	2	80.39	1.49	80.39	1.85	1.85	79.33	81.44
35. Length of the braincase	5	62.82	1.7	62.37	2.71	2.71	61.03	65.01
36. Greatest width of braincase	5	62.78	1.35	62.6	2.15	2.15	61.3	65
37. Relative length of braincase	5	100.09	3.44	98.58	3.44	3.44	97.49	106.05
38. Length of the premolar row	5	28.02	1.23	28.05	4.38	4.94	26.20	29.29
39. Length of the molar row	7	38.85	3.25	40.41	8.36	6.46	33.75	42.11
40. Relationship between molar and premolar row	5	0.75	0.07	0.75	9.18	9.06	0.65	0.82
41. Length of tooth row	5	64.04	3.65	63.75	5.70	6.45	58.68	67.73

edges. Its surface is slightly concave or flat, with a median crest and large fossae caudal to muscular tubercles. Muscular tubercles are weakly developed in females and in one of our male specimens (203). They cannot be assessed in the other male specimen (200), as there is no basioccipital preserved. The foramen ovale of the sphenoid is large and ovate, no vascular foramen rostral to the foramen ovale could be discerned in any of our specimens.

DENTITION

Specimen 1972 XIX 1 is characterized by a complete and well-preserved upper dentition. Hence, it offers itself as a reference for *C. ropalophorus* (Fig. 1D). We could not identify any trace of upper canines or their alveolae (Fig. 1D). M3 is the last tooth to erupt, even after premolars have erupted (see early adult males; Figs 1I; 2I). Whereas the molar row runs essentially in parallel to the midline of the skull, the premolars form a slightly curved row that rostrally gets closer to the midline. (Figs 1D; 2D; 3D). The premolar row is shorter than the molar row (Appendix 1). For specimen 1, M3 is slightly smaller than M2 (Fig. 1D).

In P2, the protocone and metaconule are of the same size and thus, this premolar can be classified as morphotype 1 according to de Vos (1984). In P3 and P4, the lingual wall consists of the protocone only. In the P3, the two cusps are equally developed, while in the P4, the protocone is better developed than the metaconule. Specimen 202 presents a cingulum on the left P3 (Fig. 2D).

In M1 and M2, the posterior lobe is of the same length and width as the anterior lobe; in M3, the posterior lobe is narrower and shorter than the anterior one, as typical for Megalocerotini *s.l.* (Vislobokova 2013). Styles on the upper molars are of the same width at the base and in the apical half of the crown.

Individual dental wear of the upper premolars and molars allows for the following ordering of the specimens according to their ontogenetic stage, from younger to older: 203 < 200 < 1 < 202 < 5 < 201 < 204.

FIG. 3. — **A**-**E**, *Candiacervus ropalophorus* de Vos, 1984, SNSB-BSPG 1972 XIX 204; **F**-**J**, *Candiacervus reumeri* van der Geer, 2018, SNSB-BSPG 1972 XIX 201. *C. reumeri* lacks an interfrontal crest (F), has thin dorsal orbital rims (H), and the protocone is smaller than the metaconule (I). Also note the differently sized foramina supraorbitalia and the strong sinus of the frontal bones caudally (H). The frontals touch the maxilla above the ethmoidal gap (G, H). **A**, **F**, rostral view; **B**, **G**, left lateral view; **C**, **H**, dorsal view; **D**, **I**, ventral view; **E**, caudal view. **A**, **B**, **E**-**G**, dorsal to the top; **B**-**D**, **G**-**I**, rostral to the left. Scale bars: 1 cm.

Candiacervus reumeri
van der Geer, 2018
(Fig. 3F-I)

Candiacervus reumeri van der Geer, 2018: 12.

Candiacervus sp. IIc – de Vos 1984: 44, pl. 14. — Dermitzakis & de Vos 1987: 393, fig. 10d.

Megaceros (*Candiacervus*) *ropalophorus* – Capasso Barbato 1990: 268, fig. 2; 1992: 192; 1995: 243.

Candiacervus sp. IIc – de Vos 1996: 113; 2000: 127. — van der Geer *et al.* 2006: 120; 2010: 54, 58.

Holotype. — Male skull AMPG(V) 1736 from the Late Pleistocene; Liko Cave, 75 uppermost cm of the cave filling (Likotinara, Crete, Greece) (van der Geer 2018).

Referred material. — 1972 XIX 201.

Specimen
1972 XIX 201
The skull belongs to a specimen of unknown sex, possibly male, as the right part of the skull seems to continue into a pedicle. The neurocranium and the premaxillae are missing. Both tooth rows are complete with P2 to M3, with M3 broken on the right side. The occlusal surfaces are heavily worn, both M1s and M3s and the left P4 are worn down to the gum pad. Enamel islets have disappeared, except for P2s. This indicates the specimen stems from a rather old animal.

Description
This species is very similar to *Candiacervus ropalophorus.* In particular, from a ventral view, canine alveolae in the maxilla are absent. The transversal part of the maxillopalatine suture is at the height of the anterior border of M2. The spina nasalis caudalis of the palate is very weakly developed. The pterygopalatine fossae are located at the level of the caudal border of M3 (Fig. 3I).

C. reumeri differs from *C. ropalophorus* in having a thinner dorsal orbital rim (Fig. 3H) and its rostral orbital border is above M2 (Fig. 3G). The orbits appear to be smaller than in *C. ropalophorus* because the length of M2 + M3 is shorter in *C. reumeri*.

At the caudal portion of the interfrontal suture, the frontal bones present a strong sinus and at the rostral portion, the skull lacks the crest which is typical in the above described *C. ropalophorus* specimens. The supraorbital foramina are of different size, with the right one being the larger (Fig. 3H). The supraorbital grooves are deeper than in *C. ropalophorus* with sharp edges and the nasofrontal contact is shorter than in specimen 1. Moreover, contrary to *C. ropalophorus*, the frontal bones touch the maxilla above the ethmoidal gap; consequently, the nasals do not form part of the ethmoidal gap rim. The metaconule of the right P2 is larger than the protocone. For the left P2, these two cones are not well separated.

Candiacervus sp.
(Fig. 4)

Referred material. — 1972 XIX 5, 1972 XIX 7.

Specimens
1972 XIX 5 (Fig. 4A-D)
The specimen comprises two fragments of the facial skull. One fragment consists of a small part of the maxilla with the still attached left tooth row (P2 to M3) (Fig. 4A, C). The other fragment comprises the right tooth row (P2 to M3), part of the palate, the lacrimal bone and the rostral part of the right orbit (Fig. 4B, D). The lacrimal bone is damaged. The sex is unknown. The occlusal surfaces of teeth are heavily worn; the dentine of the paracone and metacone of M2 are in contact and so is the dentine of protocone and metaconule. The latter indicates an old animal, elder than specimen 1, but younger than specimen 201. The premolars and M1 are more heavily worn than M2 and M3.

1972 XIX 7 (Fig. 4E, F)
The fragment comprises the left facial skull, i.e., part of the maxilla, the lacrimal bone, the orbita, the jugal and part of the frontal bone. The skull fragment comes from a male, as left pedicle and a short, spike-like antler with a burr are present. The tooth row is completely missing. Age determination on dental wear is not possible. However, cranial sutures are hardly recognizable, the pedicle has a larger diameter than that of the other two males in our sample and the left antler is degenerated. Taken together, this indicates that we deal with a rather old individual.

Description
Overall, given the fragmentary status of the two specimens, little can be added to what has been already described for *C. ropalophorus*. The dorsal orbital rim is roundish and thick (Fig. 4E) and conforms to the description by de Vos (1984). The rostral orbital border is above M2 (Fig. 4B, E). In contrast to *C. ropalophorus,* the gracile zygomatic arch and caudal orbital rim form an acute angle (Fig. 4E). The transversal part of the maxillopalatine suture meets M2 right between the protocone and the metaconule (Fig. 4C, D). The dental characters (Fig. 4C, D) do not differ from those described for *C. ropalophorus*. There are a protocone and metaconule on both P3 and P4. Both the right and the left P4 have a cingulum, well developed in the former and less developed in the latter tooth. The M3s of this specimen are slightly smaller than M2s. An entostyle is present on M2s and M3s. M1s are too worn to be specific on that area.

QUANTITATIVE ANALYSES

Basic summary statistics (Table 3) indicate that the variability of most measures obtained is low to moderate, as documented by their rather narrow range, and also by their coefficient of variation. Exceptions to this are the length and width of

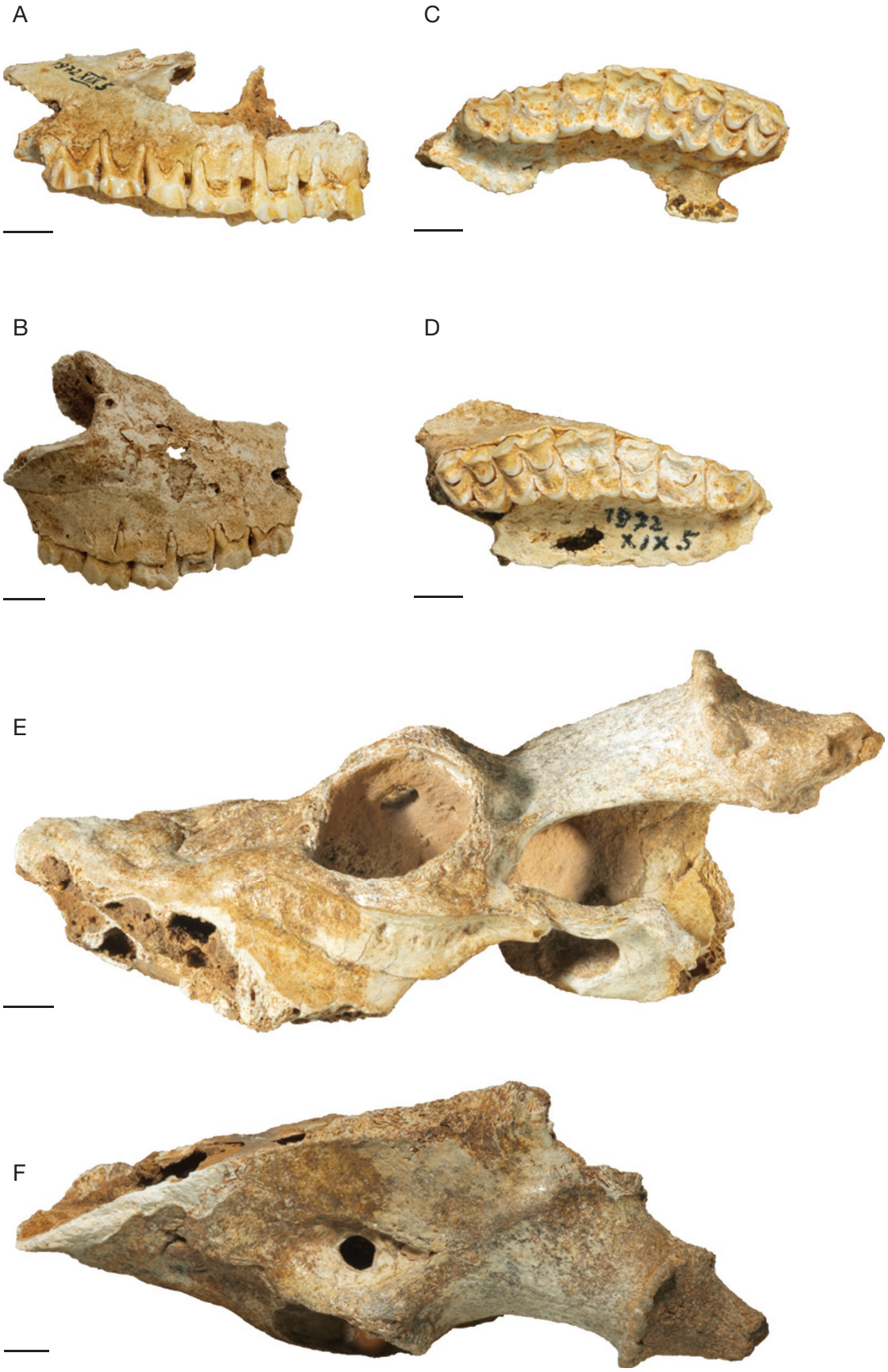

FIG. 4. — *Candiacervus* sp.*;* **A**-**D**, SNSB-BSPG 1972 XIX 5; **E**-**F**, SNSB-BSPG 1972 XIX 7. **A**, **C**, **E**, fragment of the left facial skull; rostral to the left; **B**, **D**, fragment of the right facial skull with cheek tooth row; rostral to the right; **A**, **B**, **E**, lateral views; **C**, **D**, occlusal views; **F**, dorsal view. Scale bars: 1 cm.

TABLE 4. — Application of binary characters for Megalocerotini Brooke, 1828 *s.l.* (= Megacerini, Viret 1961) and *s.s.* (= *Dama, Megaloceros* and *Megaceroides*), according to Croitor (2016), to the dwarf *Candiacervus*. Data for Megalocerotini are taken from Vislobokova (2013). Mean data from Table 3 are reported to facilitate comparison.

Vislobokova 2013			Results for *Candiacervus* in this study
Character ID	**Character**	**Description or values**	
1	Skull bend	> 130°…Megacerini; 120°…*Candiacervus listeri; Cervus elaphus* 110°…*Dama dama*	103.7°, *Dama dama;* Megalocerotini *s.s.*
1	Angle between braincase roof and braincase base	< 25°…Megacerini > 30°…Cervini	16.55°, Megalocerotini *s.l.*
2	Position of the anterior orbital rim	over M2/M3 or M3…*Megaloceros giganteus* over M2…other Megacerini	At most over M2/M3, Megalocerotini *s.l.*
4	Greatest skull width at the posterior orbital rim	46.9-59.1% of skull length…*Megaloceros giganteus*	48.93%; *Megaloceros giganteus*, Megalocerotini *s.s.*
6	Foramen parietale	Present…some Megacerini (e.g. *Praemegaceros*, *Orchonoceros*, some *Megaloceros giganteus)*, also *Dama dama*	Absent, Megalocerotini *s.l.* which lack the foramen parietale
8	Linea nuchae superior (= "Occipital crest")	Well-developed, arched between supraotic tubercules from dorsal view…Megacerini Trapezoid from dorsal view…Cervini	Well-developed and slightly arched, Megalocerotini *s.l.*
9	Angle between skull roof and occipital plane	> 90°…Megacerini < 90°…Cervini	93.05°, Megalocerotini *s.l.*
11	Length of the paraoccipital processes relative to occipital condyles	Shorter or slightly longer…Megacerini Much longer…Cervini	Slightly longer, Megalocerotini *s.l.*
14.2	Bend of braincase baseline between the basioccipital and basisphenoid	> 90°…Megacerini = 180°/0°…Cervini	Obtuse, Megalocerotini *s.l.*

the foramen ovale, the length of the occipital, and measures obtained from the supraorbital region.

For 24 out of 36 measures, the coefficient of variation is below 8% (Table 3). This also holds for all but one variable, if we exclude the data of specimen 201, which, based on its distinct skull morphology (see description above), was classified as *Candiacervus reumeri*, whereas the five other rather complete skulls were classified as *Candiacervus ropalophorus*. For the relative orbit size, the exclusion of specimen 201 results in a reduction of the value of the coefficient of variation and the range of this variable becomes particularly homogeneous.

In Figure 5A, we contrast the six quantitative measures described by de Vos (1984: table 7) for his sample from Gerani 4 with the corresponding values obtained from our samples. Our data fall well within the range recorded by de Vos, although they tend to be on the smaller side, except for the two orbital measures DRC and DDV.

The length of the premolar and molar rows of the present specimens fall within the ranges defined by de Vos for his samples from Gerani 4 and Mavro Mouri 4c, i.e., the minima and maxima for these two sites are both smaller and larger, respectively, than those for our sample (Appendix 2). The length of the complete tooth row (P2M3) of the present specimens falls within the range defined by de Vos (1984) for a sample from Gerani 4.

In Figure 5B, we present the ratios of the length of the premolar rows and the molar rows of our sample and compare them with the ones reported by de Vos (1984: Fig. 2). The ratios of P2-P4/M1-M3 of specimens 201 and 5 (Appendix 1) fall just outside the 99% confidence interval as defined by the data shown in figure 2 of de Vos (1984), and reflect the relative small P2-P4 length.

When we compare the ranges of variation of the lengths of the premolar and molar tooth rows with the means of the respective variables reported by Simonelli (1908), we find that the premolar rows of our sample tend to be somewhat shorter, i.e., the mean of Simonelli's data does not fall within the range defined by the present measurements. In contrast, the molar rows of both samples seem to be of comparable length, i.e., the means of Simonelli's data are included in the ranges defined by our data (Appendix 2).

Finally, we performed a comparative analysis of our specimens along the lines of Vislobokova (2013). In her morphological characterization and classification of Megalocerotini Brookes, 1828 *s.l.*, she had also included one specimen of Candiacervus IIb (de Vos 1984 or *Candiacervus listeri* van der Geer 2018; specimen AMPG (V)1734), and two specimens of *Candiacervus ropalophorus* (one from the MPUR, the other one from the NNML; specimen numbers are not reported). In Table 4, we summarize those characteristics defined by Vislobokova (2013) that could be measured or assessed in our sample. For most traits (13 out of 15), we find that the studied specimens of *Candiacervus ropalophorus* and *C. reumeri* resemble giant forms of cervids; specifically, nine characters, resemble Megalocerotini Brookes, 1828 *s.l.* and four other traits resemble Megalocerotini Brookes, 1828 *s.s.* When we scrutinize our sample for characters that had been used to differentiate various giant forms of cervids, we find that some traits are present in both, our sample and *Praemegaceros;* others traits present in our sample are identified also in *Megaloceros*, or even *Cervus elaphus*; for still other traits, no similarity could be reliably established (Table 5). Thus, we cannot identify any trend towards one specific member of Megalocerotini Brookes, 1828 neither *s.l.* nor *s.s.*

DISCUSSION

In the present study, we describe some exquisitely preserved new skull remains of smaller-sized Cretan deer, i.e., *Candiacervus ropalophorus* de Vos, 1984 (= size 1, de Vos 1984), *Candiacervus reumeri* van der Geer, 2018 (= size 2, de Vos 1984), and *Candiacervus* sp.

Systematic assessment of the specimens studied

Notwithstanding the uncertainties about the exact geological age of our specimens, they all can be unambiguously assigned to *Candiacervus*. We base this conclusion on the comparison of morphological characters of our specimens with those described for deer remains found in Gerani IV (de Vos 1984; Kuss 1975) and the Simonelli Cave (Malatesta 1980). Specifically, our specimens can be diagnosed as *Candiacervus* based on the following characters: cruciform nasals that do not contact the lacrimal bone and terminate rostrally or at the level of the rostral orbital rim. Orbits are round, with a thick dorsal orbital rim which rises above the frontal bone (Malatesta 1980). Ethmoidal gaps are small and alveolae for upper canines are absent. Preorbital depressions are absent. This latter finding is in contrast with previous observations, where weakly developed preorbital depressions are described, if somewhat cautiously, in rare individuals of Cretan deer (de Vos 1984; Kuss 1975; Simonelli 1908); however, figures in the respective papers do not allow for a clear or unambiguous identification. Kuss (1975) noted that young females lacked a depression and that older females had weakly developed depressions. For young males, Kuss (1975) noted the absence of the preorbital depression. The absence of the depressions, as noted in our sample, sets *Candiacervus* apart from all extant cervids (Schilling *et al.* 2019), and also from members of the extinct giant forms of cervids (*Megaloceros*- and the *Praemegaceros*-group (Vislobokova 2013)). The most plausible explanation for these discrepancies is that *Candiacervus* lost the depression when adapting to the insular environment.

We could assign five of our specimens (1972 XIX 1, 1972 XIX 200, 1972 XIX 202, 1972 XIX 203, 1972 XIX 204) to the smallest size group defined by de Vos (1984), i.e., *Candiacervus ropalophorus* (Figs 1; 2; 3A-E). These five specimens, as all members of this size group, have a skull type "a" as defined by de Vos (1984), with round orbits, a thick dorsal orbital rim, an at most weakly developed interfrontal crest and a P2 of "morphotype 1", i.e., protocone and metaconule are of similar size (de Vos 1984). Our quantitative analyses support this latter classification. We used the same variables as de Vos (1984: table 7), and our data fall within those of his specimens from Gerani IV (Figure 9) – a site, where apparently nearly all individuals belonged to *Candiacervus ropalophorus* (99% of the material; de Vos 1984). Both males are early adults as confirmed by dentition status (early to no wear and M3s in eruption). 1972 XIX 203 is from a yearling, because it lacks a burr at the proximal end of its left antler. Crests at the base of the pedicles could not be discerned, which contrasts with previous findings on adult, mature specimens, where such crests are strongly developed (Kuss 1975; Vislobokova 2013).

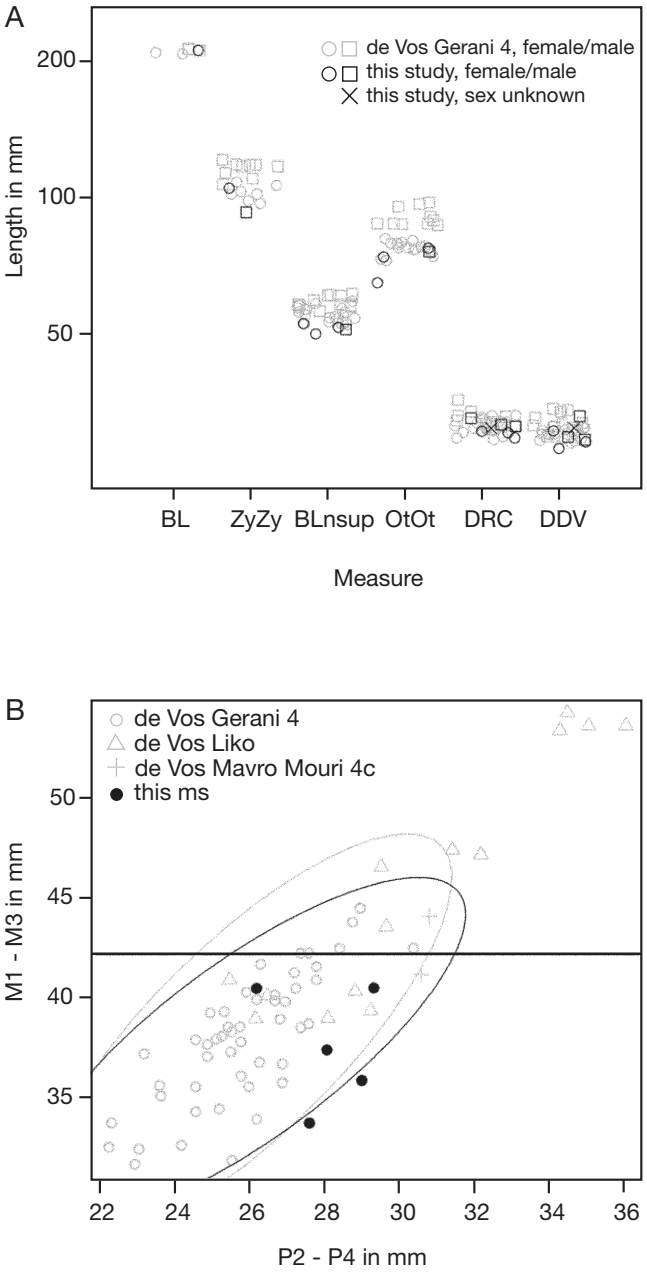

Fig. 5. — **A**, Skull measurements obtained with the present sample (in **black**) compared to those reported by de Vos (1984) (in **grey**). The skull measures defining our sample lie within the range of the sample from Gerani 4 of de Vos, although they tend to be on the smaller side. Abbreviations: **BL**, basilar length; **ZyZy**, bizygomatic width; **BLnsup**, height of the linea nuchae superior to the basion; **OtOt**, width of the occipitale; **DRC**, rostrocaudal diameter of the orbit; **DDV**, dorsoventral diameter ('height') of the orbit. Data of de Vos (1984) are taken from his table 7. **B**, The relation between the length of premolar rows (P2-P4) and the length of the molar rows (M1-M3) in our sample (in **black**), contrasted with those reported by de Vos (1984) for different sites (in **grey**). Data of de Vos are extrapolated from his figure 2 and taken from his table 2. The horizontal line represents cases for which P2-P4 are not available, and the data for M1-M3 are so similar that lines coincide. The ellipses show the 99% confidence interval (CI) for our sample (in **black**) and the *C. ropalophorus* de Vos, 1984 sample from Gerani 4 described by de Vos (in **grey**). The ellipses were calculated based on standard deviations. Three specimens fall within the space where the two CIs intersect and could be identified as *C. ropalophorus*. SNSB-BSPG 1972 XIX 201 and SNSB-BSPG 1972 XIX 5 (*C. reumeri* van der Geer, 2018 and *Candiacervus* sp., respectively) fall just outside the given CIs.

In 1972 XIX 200, the right distal pedicle plus antler as well as largest portion of left antler are missing; however, a minimal burr with some pearls is preserved. The burr indicates that 1972 XIX 200 is somewhat older than 1972 XIX 203. This interpretation is also supported by the finding that in 1972 XIX 200, the eruption stage of the 3rd molar is a later one than in 1972 XIX 203. Still, the small size and the simplicity of the burr – which is hardly more than a ring of bony pearls – suggest, in addition to eruption stage of the right 3rd molar, that 1972 XIX 200 is also from a quite young individual with a second antler generation. In fact, the structure of the burr observed here is even simpler than that of the most immature burrs described for *Candiacervus* (Kuss 1975): This author defined four stages of antler development, with a well-developed burr composed of bony pearls present already in the first stage.

Based on our quantitative measures, the two early adult males (Figs 1F-I; 2F-I) cannot be told apart from older adult females (Fig. 5A). An exception to this is the bizygomatic width (ZyZy): For one early adult male, 1972 XIX 203, this distance is smaller than that of one older adult female of our sample and that of the adult males and females of the sample of de Vos (1984).

1972 XIX 201 differs from the five *C. ropalophorus* specimens. Its thin dorsal orbital rims and a P2 characterized by unequally sized protocone and metaconule ("morphotype 2", de Vos (1984)), indicate that this specimen is probably of skull type "d" (= *Candiacervus* IIc, de Vos 1984) or *Candiacervus reumeri* van der Geer, 2018. Another notable difference of this *C. reumeri* specimen compared with *C. ropalophorus* is that in the former the maxilla directly contacts the frontal bone above the ethmoidal gap. Differently sized foramina supraorbitalia, as observed in this *C. reumeri* specimen, have been noted before in specimens of *Candiacervus cretensis*. Thus, this appears to be a quite labile character in Cretan deer. The quantitative measures we could obtain for *C. reumeri* are less diagnostic than its qualitative characters described above. For example, the length of the molar tooth row of the present *C. reumeri* specimen (62.9 mm) falls within the overlap between size A, typical for *C. ropalophorus* and size B, typical for *Candiacervus II*. i.e., *C. listeri, C. devosi* or *C. reumeri* (62.7 – 71.7 mm; de Vos 1984: table 10).

The fact that the site close to Gerani, where our sample was collected, yielded *C. ropalophorus* and *C. reumeri* is in line with previous reports of better-known sites, i.e., Gerani IV, Mavro Mouri 4c, Rethymnon fissure, Sourida, and Kalo Chorafi (see e.g. de Vos 1984), where the two species also coexisted. While qualitative, morphological characters allow distinguishing these sympatric species, our quantitative data, even when considered together with those of de Vos (1984: tables 2 and 7), are not discriminative. Potential exceptions might be the relative orbit size, which is clearly smaller for the one *C. reumeri* than for the *C. ropalophorus* specimens analyzed here, and the relative length of the molar and premolar tooth rows. The ranges of variation of the premolar and molar row of our specimens fall within the ranges for samples from Gerani IV and Mavro Mouri 4c (de Vos 1984) (Appendix 2). However, when we consider the relationship between the premolar and the molar row length (Fig. 5B), *C. reumeri* falls outside the confidence interval defining *C. ropalophorus* specimens, together with one of the specimens for which a species assignment was not possible, *Candiacervus sp*. (SNSB-BSPG 1972 XIX 5). In contrast, all three of our *C. ropalophorus* specimens for which this ratio could be obtained fall well within the confidence interval defined by the *C. ropalophorus* specimens from Gerani 4 (de Vos 1984). That said, we add that this observation is based essentially on a single specimen of *C. reumeri*. Thus, it is at best a clue for further studies, but certainly does not yet define a unique feature to tell apart *Candiacervus* species.

The conclusion that, so far, quantitative data do not allow to discriminate *C. ropalophorus* from *C. reumeri* is also supported by the few quantitative measures that are common to our analysis and those of Malatesta (1980) and Simonelli (1908) for skull specimens from Simonelli Cave, which were identified as *Praemegaceros cretensis* by Malatesta (1980), and as *Candiacervus reumeri* by van der Geer (2018). These include the orbital width and height and the greatest skull width (Malatesta's variables "i", "n" and "o" in his table 1; our variables 5, 6 and 10; Table 2). The ranges for the orbital measure fully overlap. The greatest skull diameter reported by Malatesta is somewhat smaller (102-106 mm; n = 4) than that observed for *C. ropalophorus* presently (110-114 mm; Table 3). The comparison of these data is limited by the fact that Malatesta's report allows to extract information on the sex from only four specimens he studied: these bear pedicles and thus can be identified as males. Further, the age of the specimens analyzed by Malatesta has not been reported, but may be tentatively discussed as follows: the four figured specimens are adults, for one specimen (Malatesta 1980: plate II) none of the cheek teeth is preserved and the developmental stage can only be inferred by the presence of alveolae of permanent teeth. The remaining three specimens have an erupted M3, occlusal surfaces are generally more heavily worn than in our two early adult males and specifically, the dentine of the paracone of M2 is in contact with the dentine of the protocone (Malatesta 1980: plate III; IV), indicating a more advanced age of the specimens from Simonelli Cave. Hence, our males and those of Malatesta (1980) do not allow for direct comparison and a (supporting) assessment of our *C. ropalophorus* specimens.

The comparison of our data on the premolar and molar rows with that of Simonelli does not allow for any sound interpretation given the extremely small sample sizes, especially for Simonelli's data (2 specimens).

Cranial character states of Megalocerotini Brookes, 1828 *s.l.* in Candiacervus

Our results also confirm previous findings (e.g. Azzaroli 1852; Caloi & Palombo 1994; Radulescu & Samson 1967; Sondaar & Boekschoten 1967) that the *Candiacervus* skull shares several character states with Megalocerotini Brookes, 1828 *s.l.* Four of these general characters need particular attention (character IDs according to Vislobokova (2013) are given in brackets; see also Table 4):

TABLE 5. — Diagnostic traits to discriminate members of Megalocerotini, Brookes, 1828 *s.l.* (Croitor 2016) applied to Candiacervus. Traits were taken from Vislobokova (2013).

Vislobokova 2013			
Character ID	Character name/ description	Discrimination	Results for *Candiacervus* in this study
1.1	Forehead structure and position of pedicles	Convex forehead, interantler eminence distinct, interfrontal suture strongly developed, pedicles directed posterolaterally, angle between the aboral edge of the pedicle and skull roof < 90°… *Megaloceros*-group Flat forehead, interantler eminence indistinct, interfrontal suture weakly developed; pedicles diverging, directed laterally, and widely spaced, angle between the aboral edge of the pedicle and skull roof *c.* 90°… *Praemegaceros*-group	*Praemegaceros*-group
1.2	Shape of the supraorbital foramen and supraorbital groove	Large supraorbital foramen, irregularly rounded, deep supraorbital groove with the supraorbital foramen at its external edge, diameter foramen /width of groove *c.* 0.5 … *Megaloceros* Supraorbital foramen smaller and shallower supraoccipital groove than in *Megaloceros* … *Praemegaceros* Supraorbital groove deep and widened in the middle part, large foramen at the external edge… *Candiacervus*	*Megaloceros?* *Praemegaceros?*
2.1	Angle between skull roof and occiput	> 90°… ancestral megacerines (*Arvernoceros, Orchonoceros*) = 90°… advanced megacerines (*Praemegaceros, Megaloceros*)	Ancestral megacerins
3	Fossae lateral to interantler eminence	Weakly developed… *Megaloceros*; Well-developed… *Praemegaceros*, *Orchonoceros*, *Arvernoceros*	*Megaloceros*
4.1	Position of the occipital condyles	Occipital condyles project strongly posteriorly… *Praemegaceros, Orchonoceros* Occipital condyles project moderately posteriorly… *Megaloceros*	none

(1) Angle between the forehead and the dorsal surface of the braincase

Our *C. ropalophorus* specimens have steeper foreheads than Megalocerotini Brookes, 1828 *s.l.* and with respect to this character, are most similar to *Dama* (Linnaeus, 1758). Similarities with this genus have been proposed based on the antler morphology of the smaller-sized *Candiacervus* species, to which *C. ropalophorus* belongs (van der Geer 2018). In contrast to our data, Vislobokova (2013) reports the angle for *C. listeri* (120°), a species assigned to size group 2 *sensu* de Vos (1984) (Table 1). For the present *C. reumeri*, another species of size group 2, this character cannot be assessed.

(2) Position of the rostral orbital rim

In small and short-faced living cervid species (e.g. *Muntiacus, Capreolus, Mazama,* and *Pudu*), the rostral orbital rim is positioned above M1/M2. In larger cervids with longer faces (e.g. *Alces* and *Cervus*, but also *Megaloceros*), the rostral orbital rim is positioned above M3. In our specimens that are from rather small animals, the rostral orbital rim is located above M2 or M2/M3. Thus, we may infer that they tended to have relatively long faces compared with small, extant cervids. This is also indicated by the rather long face (55.7% of the condylobasal length) of SNSB-BSPG 1972 XIX 1, the only one in which the snout is preserved. Relative to the condylobasal length, the face is thus longer than that of *Praemegaceros cazioti*, the dwarfed cervid from Sardinia (49.7%; Croitor 2016: Table 2). However, *Candiacervus* had a shorter face than the large-sized *Cervus elaphus, Praemegaceros obscurus* and *Megaloceros giganteus* (> 57%; Croitor 2016: Table 2).

(4) Greatest skull width

For the one complete skull of *C. ropalophorus* we could analyze (SNSB-BSPG 1972 XIX 1), the skull width is 48.9% of the skull length and falls within the range defined for Megalocerotini Brookes, 1828 *s.s.* The greatest skull width of our specimens was found to be at the caudal orbital border (Figs 1A, F; 2F; 3A, F). This contrasts with Vislobokova (2013), who states that the greatest skull width of *Candiacervus* is at the orbital center and that this distinguishes *Candiacervus* from other giant forms of cervids, where it is at the caudal orbital border. Thus, our data add yet another morphological similarity between *Candiacervus* and giant forms. However, we would like to stress that this finding may be interpreted as a habitat-related apomorphic character, as the position of the widest skull breath relates to the inclination of the orbits in the sagittal plane (see below, 5.3, discussion on the inclination of the orbits). Finally, we would like to point out that the location of the greatest skull width in *Candiacervus* at the caudal orbital border may also be recognized in figure 11c of Vislobokova (2013).

(14.2) Bend of the braincase baseline between the basioccipital and basisphenoid

The angle is obtuse in our sample from older females, as it is also in Megalocerotini Brookes, 1828 *s.l.* In the one early adult male (1972 XIX 203) where we could measure it, the two bones are in one plane, as diagnosed by Vislobokova (2013) for *Cervus* and close relatives. This may reflect a developmental phenomenon, as Meunier (1963) observed that the bend is absent in reindeer calves and develops postnatally. Alternatively, it might be a sex difference reflecting the greater load on the atlanto-occipital joint that should result from antlers (cf. Vislobokova 2013).

For other characters, our sample may be compared with members of Megalocerotini *s.l.*, but also, with some restrictions, to Megalocerotini *s.s.* For instance, for *C. ropalophorus*, the ratio between the diameter of the foramen supraorbitale and the supraorbital groove (character ID 1.2, Table 5) observed in our *C. ropalophorus* specimens is comparable with that seen in *Megaloceros* (*c.* 0.5, Appendix 1; Vislobokova (2013)). In contrast, the supraorbital groove of *C. ropalophorus* is relatively shallow, reminiscent of *Praemegaceros*. Despite the larger ratio between the diameter of the foramen supraorbitale and the supraorbital groove, the present *C. reumeri* specimen resembles *Megaloceros* in having deep, sharp-edged orbital grooves. In the two males of our sample, the relatively weakly developed muscular tubercles of the basioccipital (Fig. 2I) and the more rostral extension of the pterygopalatine fossa (Figs 1I; 2I) might be linked to their relatively young age.

While the comparison of our sample with that described by Vislobokova (2013) is somewhat limited due to e.g. specimen incompleteness, our data confirm, for most of the traits (Table 5), similarities between *Candiacervus* and Megalocerotini Brookes, 1828 *s.l.* This observation is based on a larger sample set than that of Vislobokova, as we include *C. reumeri*, which had not been analyzed along the lines defined by Vislobokova before. However, we think that such similarities cannot be confidently interpreted in a phylogenetic context; hence, the mainland relatives, or ancestors, of *Candiacervus* remain elusive. We propose that the most plausible explanation of the ambiguous nature of some traits may have resulted from the secondary size reduction of *Candiacervus ropalophorus* and *C. reumeri.*

In fact, distinct variations of a number of morphological traits in the *Candiacervus* skull, or rather its predecessor(s), resulting from insular dwarfing on Crete, may have "obscure[d] affinities with any other known taxon; many such groups [that have undergone dwarfism] are taxonomic enigmas" (Hanken & Wake 1993: 510).

Morphological consequences of dwarfing are, among others: 1) a reduction and structural simplification; and 2) an increased morphological variability (Hanken & Wake 1993). The first consequence can manifest itself as a reduced development or even a complete loss of structures or organs. Thus, the lack of preorbital depressions as observed presently in both *C. reumeri* and *C. ropalophorus* results from a simplification of the lacrimal bone housing this depression. A reduction of the preorbital depression has also been noted in *Praemegaceros cazioti* from Sardinia (Croitor *et al.* 2006). In extant cervids, the preorbital depression hosts the preorbital gland, which is used for intraspecific communication (Mattioli 2011). The absence of the depression in *Candiacervus* (and presumably in *Praemegaceros,* see e.g. Vislobokova (2013: figs 54, 55); Croitor *et al.* (2006: fig. 2)) suggests that also the preorbital glands were likely reduced in these species, maybe even lacking. Indeed, it has been argued that the reduction of the preorbital depression might be correlated with decreased olfactory capacities of island deer (Croitor *et al.* 2006).

In most, if not all, extant cervids, the braincase is longer than wide. This holds also for cervid fossils (Croitor 2018). If this was also so in the unknown ancestor of *Candiacervus*, any changes in braincase length and width during dwarfing must have occurred to different degrees, as these two measures are about equal in *Candiacervus.* This is fully consistent with the observation of Palombo et al (2008), that brain size in *Candiacervus* is little affected by dwarfing: as the side lengths of its braincase approach equality, its overall volume gets optimized with respect to its surface size to house a brain of "minimal size needed according to environmental conditions" (Palombo *et al.* 2008: p. 178). The relatively short braincase, together with the rostrally displaced occipital condyles also result in a mechanical optimization to carry the long antlers present in *Candiacervus* (Strasser *et al.* 2018; van der Geer 2018).

The lack of upper canine alveolae, and consequently the upper canine teeth, is another structural reduction. The second consequence of dwarfing, i.e., an increased morphological variability, is manifested, in our sample, by a variety of traits (see those with a CV > 8 in Table 3), notably the morphology of the supraorbital foramen and groove. This variability is yet another factor that limits the use of these traits for the reconstruction of phylogenetic relationships between *Candiacervus* and mainland deer.

The habitat of *Candiacervus* revealed by skull characteristics

Other cranial particularities described presently for Cretan deer and discussed in the light of its relationship with mainland deer give hints on the ecology of *C. ropalophorus*. For instance, the rectangular outline of the premaxilla, observed in specimen 1 (Fig. 1D), has been reported previously for *Candiacervus* IIb *sensu* de Vos (1984) (now *Candiacervus devosi* van der Geer, 2018)) and linked to a large proportion of herbs in the diet (Vislobokova 2013). In addition, a slightly obtuse angle between the skull roof and the occiput (Appendix 1) as well as the rostrally displaced occipital condyles relative to the most caudal point of the occiput has also been observed in *Praemegaceros verticornis* (Dawkins, 1872) and *Megaloceros* and has been interpreted as an adaptation to mixed feeding (Vislobokova 2013).

The inclination of the orbits relative to the median skull plane has been used to infer habitat preferences in cervids. Specifically, large angles, as found in *Candiacervus* (Appendix 1), have been suggested as indicative for open habitats (Vislobokova 2013), but also as a reduced need to avoid predators (Welker *et al.* 2014). The better stereoscopic view, afforded by the more anterior orientation of the eyes, has been interpreted as secondarily derived trait typical for island dwellers (van der Geer 2005). It also implicates a reduced field of view. The rather small size of the orbits (their widths equal 13.6% of the condylobasal length, Table 3) is reminiscent of what has been described for the insular *Praemegaceros cazioti* (14.7%, Croitor 2016: table 2). The concurrence of this finding in these two insular cervids suggests that this may be yet another adaptation to the insular environment. The probable changes in the sense of smell (see above) and vision in *Candiacervus* would be well in line with the notion that this cervid was living in a predator-free environment (Palombo *et al.* 2008; van der Geer 2018; van der Geer *et al.* 2014).

Finally, the relative timing of the eruption of the third molar might give insights into habitat preferences. In cervids, the lower premolars typically erupt after the third molar (Veitschegger & Sánchez-Villagra 2016). This has been said to be also true for *Candiacervus* (van der Geer *et al.* 2014), although it is not clear how this conclusion was arrived at. Our material allows, for the first time, to directly time the eruption of the third molar in the *maxilla*. Systematic data on the eruption sequences of maxillary teeth are not available yet, but Smith (2000: p. 213) noted that the "eruption order [of the permanent dentition in eutherians] is similar in the maxilla and mandible. This is also supported by the present understanding of principles of mammalian dentition and the functional morphology of the mastication apparatus (e.g. Ungar 2010). Specifically, the timing of eruption of upper and lower teeth has been observed to be very similar in cervids (Seo *et al.* 2017; Severinghaus 1949), as also in other ruminants (Hemming 1961; Dow & Wright 1962; Węgrzyn & Serwatka 1984). Thus, it seems justified to assume that the eruption sequence in the maxilla is the same as in the mandibula in cervids. The fact that M3 is the last tooth to erupt in the maxilla of *Candiacervus ropalophorus* sets it apart from most other cervids, except for a Spanish population of red deer (*C. elaphus* Linnaeus, 1758), where a similar pattern has been described (Azorit *et al.* 2002), and Newfoundland caribou, in which m3 and the premolars erupt about simultaneously (Bergerud 1970). More intriguingly, this trait parallels the pattern observed in some bovid caprines (*Capra* Linnaeus, 1758, *Hemitragus* Hodgson, 1833, *Nilgiritragus* Ropiquet & Hassanin, 2005, and *Ovis* Linnaeus, 1758), where m3 erupts after p4 in the lower jaw. This has been interpreted as an adaptation to resource availability in high elevation habitats (Monson & Hlusko 2018). Lastly, we caution that we cannot exclude that the eruption of M3 as last tooth in the two *Candiacervus* males in our sample is a case of intraspecific variability. Yet no data are available to follow up on this idea.

The dental eruption pattern is yet another trait of *Candiacervus* reminiscent of goats. Previously, the limb morphology and also the relatively simple antlers have led to comparisons with goats and functionally, this has been interpreted as indicating that *C. ropalophorus* and *C. devosi* probably occupied a rocky environment, as does the Cretan wild goat, *Capra aegagrus* (van der Geer *et al.* 2006a). Our data are fully in line with this and show that *Candiacervus* adapted also towards the rather poor diet that goats may typically live on.

CONCLUSIONS

Our detailed morphological and morphometric study on some new, exquisitely preserved craniodental material of Cretan deer reveal affiliations to the two smaller-sized *Candiacervus* species, *C. ropalophorus* and *C. reumeri* (size group I and II, respectively, according to de Vos (1984)), documenting a further record of sympatry of both species. In addition, our data show for the first time a specific tooth replacement pattern and the absence of a preorbital depression, both extremely rare within Cervidae, as well as a clearly longer snout than in other small cervids; taken together, these particularities might constitute distinctive character states of *Candiacervus* specimens. Moreover, we can document that the basioccipital and basisphenoid are arranged in different angles, on the one hand, in females and, on the other hand, in the one male available.

Morphological comparison to assess the relatedness of *Candiacervus* within Megalocerotini Brookes, 1828 *s.l.* and *s.s.* provide an extended evidence that *Candiacervus* and extinct giant forms of cervids share many similarities. However, more material is needed to interpret characters in terms of intraspecific variation, development, and sexual dimorphism; a multivariate cluster analysis might help to put the morphological comparison of *Candiacervus* with its suspected relatives and/or ancestors on a more formal footing.

Our data complement the previous findings on morphometric specifics in *Candiacervus* that match what has been called the "island dwarfing syndrome" (Croitor *et al.* 2006, p. 35-36). Particularly, our data strengthen the hypothesis that small-sized *Candiacervus* species adapted to niches specific to goats. Finally, we have to conclude that, while the adaptive characteristics of *Candiacervus* described here provide more insight into its life in harsh, insular environment, they also blur ancestral traits and constitute a major impediment for reliably relating this cervid to its ancestors and mainland relatives.

Acknowledgements
We are grateful to Judith Braukämper (SNSB-BSPG), Elisabeth Lange (SNSB-BSPG), and Stefan Sonyi (SNSB-BSPG) for specimen preparation, Manuela Schellenberger (SNSB-BSPG) for photographs, Dr H.-J. Gregor (Olching) for describing and discussing details of the site from where he collected the specimens. Bastien Mennecart (Basel) provided French translation. We would like to thank two anonymous reviewers for their constructive comments that helped us to improve the manuscript. We also would like to thank the associate editor, L. Rook. This research did not receive any specific grant from funding agencies in the public, commercial, or not-for-profit sectors.

REFERENCES

Accordi B. 1972. — *Lo scavo della "Grotta Simonelli" con cervi nani del Quaternario, effettuato a Creta nel 1971 dall'Istituto di Geologia e Paleontologia dell'Università di Roma con il finanziamento dell'Accademia Nazionale dei Lincei*. Quaderno dell'Accademia nazionale dei Lincei 167: 1-17.

Amson E. & Kolb C. 2016. — Scaling effect on the mid-diaphysis properties of long bones-the case of the Cervidae (deer). *The Science of Nature* 103: 58. https://doi.org/10.1007/s00114-016-1379-7

Attard I. R. & Reumer J. 2009. — Taphonomic reinterpretation of a bone sample of endemic Pleistocene deer from Crete (Greece): osteoporosis versus regurgitation. *Palaeodiversity* 2: 379-385.

Azzaroli A. 1952. — La sistematica dei cervi giganti e i cervi nani delle isole. *Atti della Società Toscana di Scienze Naturali, Memorie (A)* 59: 119-127.

AZORIT C., ANALLA M., CARRASCO R., CALVO J. A. & MUNOZ-COBO J. 2002. — Teeth eruption pattern in red deer (*Cervus elephus hispanicus)* in southern Spain. *Anales de Biologia* 24: 107-114.

BERGERUD A. 1970. — Eruption of Permanent Premolars and Molars for Newfoundland Caribou. *The Journal of Wildlife Management* 34: 962-963. https://doi.org/10.2307/3799172

CALOI L. & PALOMBO M. R. 1990. — Gli Erbivori Pleistocenici Delle Isole Del Mediterraneo: Adattamenti. *Hystrix* 2: 87-100.

CALOI L. & PALOMBO M. R. 1994. — Functional Aspects and Ecological Implications in Pleistocene Endemic Herbivores of Mediterranean Islands. *Historical Biology* 8: 151-172. https://doi.org/10.1080/10292389409380475

CALOI L. & PALOMBO M. R. 1995. — Functional aspects and ecological implications in Pleistocene endemic cervids of Sardinia, Sicily and Crete. *Geobios* 28: 247-258. https://doi.org/10.1016/S0016-6995(95)80231-2

CALOI L. & PALOMBO M. R. 1996. — Functional aspects and ecological implications in Hippopotami and cervids of Crete, *in* REESE D. S. (ed.), *Pleistocene and Holocene Fauna of Crete and Its First Settlers*. *Monographs in World Archeology* 28: 125-151. https://doi.org/10.1080/10292389409380475

CAPASSO BARBATO L. 1989. — *Cervidi endemici del Pleistocene di Creta*. Unpublished PhD thesis, Modena, Bologna, Firenze, Roma, 214 p.

CAPASSO BARBATO L. 1990. — Les cervidés endémiques de Crète. *Quaternaire* 1: 265-270. https://doi.org/10.3406/quate.1990.1943

CAPASSO BARBATO L. 1992. — *Nuova specie di Cervide del Pleistocene di Creta*. Atti della Accademia Nazionale dei Lincei. Classe di Scienze Fisiche, Matematiche e Naturali 1: 183-220.

CAPASSO BARBATO L. 1995. — Un tentativo di analisi cladistica applicata ad un cervide endemico del Pleistocene di Creta. *Geologica Romana* 31: 243-248.

CAPASSO BARBATO L. & PETRONIO C. 1986. — *Cervus major* n. sp. *of the Bate Cave (Rethymnon, Crete).* Atti della Accademia Nazionale dei Lincei, Memorie 18: 59-100.

CARLQUIST S. J. 1974. — *Island Biology*, First edition. Columbia University Press, New York: 660 p. https://doi.org/10.5962/bhl.title.63768

CROITOR R. 2014. — Deer from late Miocene to Pleistocene of western Palearctic: Matching fossil record and molecular phylogeny data. *Zitteliana B, 32*: 115-153. https://doi.org/10.5282/UBM/EPUB.22391

CROITOR R. 2016. — Systematical position and paleoecology of the endemic deer *Megaceroides algericus* Lydekker 1890 (Cervidae, Mammalia) from the late Pleistocene-early Holocene of North Africa. *Geobios* 49: 265-283. https://doi.org/10.1016/j.Geobios.2016.05.002

CROITOR R. 2018. — Plio-Pleistocene Deer of western Palearctic: Taxonomy, Systematics, Phylogeny. *Institute of Zoology of the Academy of Sciences of Moldova*, Chișinău, 140 p.

CROITOR R., BONIFAY M.-F. & BONIFAY E. 2006. — Origin and evolution of the Late Pleistocene island deer *Praemegaceros (Nesoleipoceros) cazioti* (Depéret) from Corsica and Sardinia. *Bulletin du Musée d'Anthropologie préhistorique Monaco* 46: 35-68.

DAVIS E. B., BRAKORA K. A. & LEE A. H. 2011. — Evolution of ruminant headgear: A review. *Proceedings of the Royal Society B. Biological Science* 278: 2857-2865. https://doi.org/10.1098/rspb.2011.0938

DE VOS J. 1979. — The endemic Pleistocene deer of Crete. *Proceedings of the Koninklijke Nederlandse Akademie van Wetenschappen, B* 82: 59-90.

DE VOS J. 1984. — The endemic Pleistocene deer of Crete. *Verhandelingen der Koninklijke Nederlandse Akademie van Wetenschappen* 31: 1-100.

DE VOS J. 2000. — Pleistocene Deer Fauna in Crete: Its Adaptive Radiation and Extinction. *Tropics* 10: 125-134. https://doi.org/10.3759/tropics.10.125

DE VOS J. & VAN DER GEER A. A. E. 2002. — Major Patterns and Processes in Biodiversity: taxonomic diversity on islands explained in terms of sympatric speciation, *in* WALDREN B. & ENSENYAT J. A. (eds), *World Islands in Prehistory, International Insular Investigations*, *V Deia International Conference of Prehistory*. British Archaeological Reports (BAR) International Series 1095, Oxford: 395-405.

DOW S. A. & WRIGHT P. L. 1962. — Changes in Mandibular Dentition Associated with Age in Pronghorn Antelope. *The Journal of Wildlife Management* 26: 1-18. https://doi.org/10.2307/3798162

FLOWER W. H. 1883. — On the arrangement of the orders and families of existing Mammalia. *Proceedings of the Zoological Society of London* Vol. 51: 178-186. https://www.biodiversitylibrary.org/page/28679980

GOLDFUSS G. A. 1820. — *Handbuch der Zoologie; Erste Abteilung*. J. L. Schrag, Nürnberg, 696 p.

HANKEN J. & WAKE D. B. 1993. — Miniaturization of body size: Organismal consequences and evolutonary significance. *Annual Review of Ecology and Systematics* 24: 501-519. https://doi.org/10.1146/annurev.es.24.110193.002441

HEMMING J. E. 1961. — *Mandibular dentition and horn development as criteria of age in the Dall sheep* Ovis dalli *Nelson 1884*. Master thesis, University of Montana, Missoula. https://scholarworks.umt.edu/etd/6503

HUGHES S., HAYDEN T. J., DOUADY C. J., TOUGARD C., GERMONPRÉ M., STUART A., LBOVA L., CARDEN R. F., HÄNNI C. & SAY L. 2006. — Molecular phylogeny of the extinct giant deer, *Megaloceros giganteus*. *Molecular Phylogenetics and Evolution* 40: 285-291. https://doi.org/10.1016/j.ympev.2006.02.004

ILIOPOULOS G., EIKAMP H. & FASSOULAS C. 2010. — A new Late Pleistocene mammal locality from western Crete. *Bulletin of the Geological Society of Greece* 43: 1-7. https://doi.org/10.12681/bgsg.11257

IMMEL A., DRUCKER D. G., BONAZZI M., JAHNKE T. K., MÜNZEL S. C., SCHUENEMANN V. J., HERBIG A., KIND C. J. & KRAUSE J. 2015. — Mitochondrial genomes of giant deers suggest their late survival in central Europe. *Scientific Reports* 5: 1-9. https://doi.org/10.1038/srep10853

KOLB C., SCHEYER T. M., LISTER A. M., AZORIT C., DE VOS J., SCHLINGEMANN M. A. J., RÖSSNER G. E., MONAGHAN N. T. & SÁNCHEZ-VILLAGRA M. R. 2015. — Growth in fossil and extant deer and implications for body size and life history evolution. *BMC Ecology and Evolution* 15: 19. https://doi.org/10.1186/s12862-015-0295-3

KUSS S. E. 1965. — Eine pleistozäne Säugetierfauna der Insel Kreta. *Berichte der Naturforschenden Gesellschaft zu Freiburg im Breisgau* 55: 271-348.

KUSS S. E. 1970. — Abfolge und Alter der pleistozänen Säugetierfaunen der Insel Kreta. *Berichte der Naturforschenden Gesellschaft zu Freiburg im Breisgau* 60: 35-83.

KUSS S. E. 1973. — Die pleistozänen Säugetierfaunen der ostmediterranen Inseln. Ihr Alter und ihre Herkunft. *Berichte der Naturforschenden Gesellschaft zu Freiburg im Breisgau* 63: 49-71.

KUSS S. E. 1975. — Die pleistozänen Hirsche der ostmediterranen Inseln Kreta, Kasos, Karpathos und Rhodos (Griechenland). *Berichte der Naturforschenden Gesellschaft zu Freiburg im Breisgau* 65: 25-79.

LAX E. M. 1991. — A Gazetteer of Pleistocene Paleontological Sites on Crete Island, Greece. *The University of Arizona*. http://hdl.handle.net/10150/558152

LAX E. M. 1996. — A gazetteer of Cretan paleontological localities, *in* REESE D.S. (ed.), *Pleistocene and Holocene Fauna of Crete and Its First Settlers*. Prehistory Press, Madison (Wisconsin): 1-32.

LEINDERS J. J. M. & HEINTZ E. 1980. — The configuration of the lacrimal orifices in Pecorans and Tragulids (Artiodactyla, Mammalia) and its significance for the distinction between Bovidae and Cervidae. *Beaufortia* 30: 155-160.

LISTER A. M., EDWARDS C. J., NOCK D. A. W., BUNCE M., VAN PIJLEN I. A., BRADLEY D. G., THOMAS M. G. & BARNES I. 2005. — The phylogenetic position of the "giant deer" *Megaloceros giganteus*. *Nature* 438: 850-853. https://doi.org/10.1038/nature04134

LOSOS J. B. & RICKLEFS R. E. 2009. — Adaptation and diversification on islands. *Nature* 457: 830-836. https://doi.org/10.1038/nature07893

MALATESTA A. 1980. — Dwarf Deer and Other Late Pleistocene Fauna of the Simonelli Cave in Crete. *Accademia nazionale dei Lincei* 1: 1-128. https://doi.org/10.1145/2505515.2507827

MATTIOLI S. 2011. — Family Cervidae (Deer), *in* WILSON D. E. & MITTERMEIER R. A. (eds), *Handbook of the Mammals of the World*. Lynx Ediciones, Barcelona: 350-428.

MAZZA P., ROSSI M. A., RUSTIONI M., AGOSTINI S., MASINI F. & SAVORELLI A. 2016. — Observations on the postcranial anatomy of *Hoplitomeryx* (Mammalia, Ruminantia, Hoplitomerycidae) from the Miocene of the Apulia Platform (Italy). *Palaeontographica A (Paleozoology, Stratigraphy)* 307: 105-147.

MAZZA P. P. A. 2013. — The systematic position of Hoplitomerycidae (Ruminantia) revisited. *Geobios* 46: 33-42. https://doi.org/10.1016/j.Geobios.2012.10.009

MENNECART B., DE MIGUEL D., BIBI F., RÖSSNER G. E., MÉTAIS G., NEENAN J. M., WANG S., SCHULZ G., MÜLLER B. & COSTEUR L. 2017. — Bony labyrinth morphology clarifies the origin and evolution of deer. *Scientific Reports* 7: 1-11. https://doi.org/10.1038/s41598-017-12848-9

MEUNIER K. 1963. — Die Knickungsverhältnisse des Cervidenschädels. Mit Bemerkungen zur Systematik. *Zoologischer Anzeiger* 172: 184-216.

MONSON T. A. & HLUSKO L. J. 2018. — The Evolution of Dental Eruption Sequence in Artiodactyls. *Journal of Mammalian Evolution* 25: 15-26. https://doi.org/10.1007/s10914-016-9362-9

OWEN R. 1848. — Description of teeth and portions of jaws of two extinct anthracotherioid quadrupeds (*Hyopotamus vectianus* and *Hyopotamus bovinus)* discovered by the Marchioness of Hastings in the Eocene deposits on the N.W. coast of the Isle of Wight. Contrib. to Hist. Br. Foss. Mamm. 7: 30-71. https://doi.org/10.1144/GSL.JGS.1848.004.01-02.21

PALOMBO M. R., KOHLER M., MOYA SOLA S. & GIOVINAZZO C. 2008. — Brain versus body mass in endemic ruminant artiodactyls: A case studied of *Myotragus balearicus* and smallest Candiacervus species from Mediterranean Islands. *Quaternary International* 182: 160-183. https://doi.org/10.1016/j.quaint.2007.08.037

RADULESCU C. & SAMSON P.-M. 1967. — Sur un nouveau cerf mégacérin du Pléistocène moyen de la dépression de Brasov (Roumanie). *Geologica Romana* 6: 317-344.

RAIA P. & MEIRI S. 2006. — The Island Rule in Large Mammals: Paleontology Meets Ecology. *Evolution* (N. Y) 60: 1731-1742 https://doi.org/10.1554/05-664.1

REESE D. S., BELLUOMINI G. & IKEYA M. 1996. — Absolute dates for the Pleistocene fauna of Crete, *in* REESE D. S. (ed.), *Pleistocene and Holocene Fauna of Crete and Its First Settlers*. Prehistory Press, Philadelphia: 47-51.

SCHILLING A.-M., CALDERÓN-CAPOTE M. C. & RÖSSNER G. E. 2019. — Variability, morphometrics, and co-variation of the os lacrimale in Cervidae. *Journal of Morphology* 280: 1071-1090. https://doi.org/10.1002/jmor.21002

SCOPOLI G. A. 1777. — Introductio ad historiam naturalem sistens genera lapidum, plantarum et animalium: hactenus detecta, caracteribus essentialibus donata, in tribus divisa, subinde ad leges naturae. Apud Wolfgangum Gerle, Prag, 506 p. https://doi.org/10.5962/bhl.title.10827

SEO H., KIM J., SEOMUN H., HWANG J. J., JEONG H. G., KIM J. Y., KIM H. J. & CHO S. W. 2017. — Eruption of posterior teeth in the maxilla and mandible for age determination of water deer. *Archives of Oral Biology* 73: 237-242. https://doi.org/10.1016/j.archoralbio.2016.10.020

SEVERINGHAUS C. W. 1949. — Tooth Development and Wear as Criteria of Age in White-Tailed Deer. *The Journal of Wildlife Management* 13: 195-216. https://doi.org/10.2307/3796089

SIMONELLI V. 1908. — Mammiferi quaternari dell'Isola di Candia. *Memorie della Accademia delle Scienze dell'Istituto di Bologna* 4: 456-470.

SIMPSON G. G. 1940. — Mammals and land bridges. *Journal of the Washington Academy of Sciences* 30: 137-163.

SIMPSON G. G., ROE A. & LEWONTIN R. C. 1960. — *Quantitative Zoology*, Revised Ed. Ed. Harcourt, Brace, New York, 440 p.

SMITH B. H. 2000. — Schultz's rule' and the evolution of tooth emergence and replacement patterns in primates and ungulates, *in* TEAFORD M. F., SMITH M. M. & FERGUSON M. W. J., *Development, Function and Evolution of Teeth.* Cambridge University Press, Cambridge, New York, Melbourne, Madrid, Cape Town, Singapore, São Paulo: 212-227. http://hdl.handle.net/2027.42/106593

SONDAAR P. Y. 1971. — Paleogeozoography of the Pleistocene mammals from the Aegean. *Opera Bot*: 30: 65-70.

SONDAAR P. Y. & BOEKSCHOTEN G. J. 1967. — Quaternary mammals in the south Aegean island arc with notes on other mammals from the coastal regions of the Mediterranean, I/ II. *Proceedings of the Koninklijke Nederlandse Akademie van Wetenschappen* 70: 556-576.

STARCK D. 1979. — *Vergleichende Anatomie der Wirbeltiere auf evolutionsbiologischer Grundlage: Band 2: Das Skelettsystem.* Springer-Verlag, Berlin, Heidelberg, 776 p.

STRASSER T. F., MURRAY S. C., VAN DER GEER A., KOLB C. & RUPRECHT L. A. 2018. — Palaeolithic cave art from Crete, Greece. *Journal of Archaeological Science: Reports* 18: 100-108. https://doi.org/10.1016/j.jasrep.2017.12.041

UNGAR P. S. 2010. — *Mammal teeth: origin, evolution, and diversity*, 1st ed. John Hopkins University Press, Baltimore, 304 p.

VAN BEMMEL A. C. V. 1949. — Revision of the Rusine Deer in the Indo-Australian Archipelago. *Treubia* 20: 191-262. https://doi.org/10.14203/treubia.v20i2.2625

VAN DER GEER A. A. E. 2005. — Island ruminants and parallel evolution of functional structures. *Quaternaire* 2: 231-240.

VAN DER GEER A. A. E. 2008. — The effect of insularity on the Eastern Mediterranean early cervoid *Hoplitomeryx*: The study of the forelimb. *Quaternary International* 182: 145-159. https://doi.org/10.1016/j.quaint.2007.09.021

VAN DER GEER A. A. E. 2014. — Systematic revision of the family Hoplitomerycidae Leinders 1984 (Artiodactyla: Cervoidea), with the description of a new genus and four new species. *Zootaxa* 3847: 1-32. https://doi.org/10.11646/zootaxa.3847.1.1

VAN DER GEER A. A. E. 2018. — Uniformity in variety: Antler morphology and evolution in a predator-free environment. *Palaeontologia Electronica* 21.1.9A: 1-31. https://doi.org/10.26879/834

VAN DER GEER A. A. E., DERMITZAKIS M. & VOS J. DE 2006a. — Crete Before the Cretans: the Reign of Dwarfs. *Pharos* 13: 119-130.

VAN DER GEER A. A. E., DERMITZAKIS M. & DE VOS J. 2006b. — Relative growth of the metapodals in a juvenile island deer: *Candiacervus* (Mammalia, Cervidae) from Pleistocene of Crete. *Hellenic Journal of Geoscience* 41: 119-125.

VAN DER GEER A. A. E., DE VOS J., LYRAS G. A. & DERMITZAKIS M. 2006c. — New data on the Pleistocene Cretan deer *Candiacervus sp. II* (Cervinae, Mammalia). *CFS Courier Forschungsinstitut Senckenberg* 256: 131-137.

VAN DER GEER A. A. E., LYRAS G. A., MACPHEE R. D. E., LOMOLINO M. & DRINIA H. 2014. — Mortality in a Predator-free Insular Environment: the Dwarf Deer of Crete. *American Museum Novitates* 3807: 1-26. https://doi.org/10.1206/3807.1

VEITSCHEGGER K. & SÁNCHEZ-VILLAGRA M. R. 2016. — Tooth Eruption Sequences in Cervids and the Effect of Morphology, Life History, and Phylogeny. *The Journal of Mammalian Evolution* 23: 251-263. https://doi.org/10.1007/s10914-015-9315-8

VISLOBOKOVA I. A. 2013. — Morphology, taxonomy, and phylogeny of megacerines (Megacerini, Cervidae, Artiodactyla). *Paleontological Journal* 47: 833-950. https://doi.org/10.1134/S0031030113080017

WĘGRZYN M. & SERWATKA S. 1984. — Teeth eruption in the European bison. *Acta Theriologica (Warsz)* 29: 111-121. https://doi.org/10.4098/at.arch.84-9

WELKER F., DUIJM E., VAN DER GAAG K. J., VAN GEEL B., DE KNIJFF P., VAN LEEUWEN J., MOL D., VAN DER PLICHT J., RAES N., REUMER J. & GRAVENDEEL B. 2014. — Analysis of coprolites from the extinct mountain goat *Myotragus balearicus*. *Quaternary Research* 81: 106-116. https://doi.org/10.1016/j.yqres.2013.10.006

Submitted on 7 November 2019;
accepted on 6 March 2020;
published on 8 March 2021.

APPENDICES

APPENDIX 1. — Raw data for 41 craniodental measurements taken for eight new specimens of *Candiacervus* Kuss, 1975. Length measures are given in millimeters and relative lengths in percent, angles are given in degrees. Abbreviation: **na**, not applicable.

	SNSB-BSPG 1972 XIX 1	**SNSB-BSPG 1972 XIX 5**	**SNSB-BSPG 1972 XIX 7**	**SNSB-BSPG 1972 XIX 200**	**SNSB-BSPG 1972 XIX 201**	**SNSB-BSPG 1972 XIX 202**	**SNSB-BSPG 1972 XIX 203**	**SNSB-BSPG 1972 XIX 204**
Sex	female	na	male	male	na	female	male	female
Developmental stage based on dental wear	early-middle aged adult	old adult	na	early adult	old adult	middle-aged adult	early adult	old adult
1. Basilar length	195.37	na	na	na	na	na	na	na
2. Width bizygomatic	97.79	na	na	na	na	na	86.82	na
3. Skull height	49.76	na	na	na	na	47.15	48.26	48.73
4. Width of the occipital	72.60	na	na	na	na	61.00	71.17	69.40
5. Orbital width	28.96	na	29.96	30.93	29.38	28.77	29.66	28.00
6. Orbital height	27.47	na	31.23	27.76	29.47	26.56	28.16	29.00
7. Orbital shape	0.95	na	1.04	0.90	1.00	0.92	0.95	1.04
8. Relative orbit size	0.93	na	na	na	0.79	0.97	na	0.91
9. Skull flexion	100.00	na	na	na	na	99.80	103.00	112.00
10. Inclination of the braincase roof relative to the braincase axis	16.08	na	na	18.09	na	15.44	17.38	15.77
11. Greatest skull width	111.47	na	na	114.00	na	109.83	109.86	112.30
12. Inclination of the skull roof and the occipital plane	96.30	na	na	96.00	na	na	87.00	92.90
13. Greatest width of the supraorbital groove	10.16	na	na	10.45	8.55	8.72	9.59	11.38
14. Horizontal diameter of the supraorbital foramen	5.07	na	na	5.79	5.06	4.46	5.27	5.12
15. Proportion of supraorbital foramen to groove	0.50	na	na	0.55	0.59	0.51	0.55	0.45
16. Length of the foramen ovale	6.77	na	na	6.48	na	10.85	8.58	11.10
17. Width of the foramen ovale	5.02	na	na	4.16	na	6.28	4.12	6.84
18. Shape of the foramen ovale	1.35	na	na	1.56	na	1.73	2.08	1.62
19. Position of the foramen ovale	35.80	na	na	33.00	na	29.85	35.47	34.50
20. Length of the occipital	18.25	na	na	16.44	na	20.32	19.71	16.81
21. Length of the parietal	47.03	na	na	45.60	na	49.31	42.67	44.80
22. Length of the frontal	58.66	na	na	61.63	na	66.36	64.15	57.04
23. External distance between foramina supraorbitalia	57.34	na	na	54.93	50.02	na	53.20	45.79
24. Inclination of the tympanic bullae relative to the meatus acusticus	131.19	na	na	na	na	126.25	125.91	130.54
25. Position of the external meatus acusticus	94.36	na	na	na	na	94.19	94.06	89.32
26. Orientation of the orbit	58.92	na	na	58.74	57.61	59.48	65.45	59.68
27. Klinorhynchy	169.63	na	na	na	na	171.75	na	167.58
28. Frontal breadth 1	na	na	na	54.07	na	na	57.36	na
29. Frontal breadth 2	na	na	na	81.44	na	na	79.33	na
30. Facial length	118.79	na	na	na	na	na	na	na
31. Condylobasal length, CBL	213.3	na	na	na	na	na	na	na
32. Relative facial length	55.69	na	na	na	na	na	na	na
33. Muzzle length	63.01	na	na	na	na	na	na	na
34. Relative muzzle length	29.54	na	na	na	na	na	na	na
35. Length of the braincase	64.08	na	na	61.03	na	65.01	61.60	62.37
36. Greatest width of braincase	65	na	na	62.6	na	61.3	62.6	62.4
37. Relative length of braincase	98.58	na	na	97.49	na	106.05	98.4	99.94
38. Length of the premolar row, P2P4	29.29	28.97	na	na	27.59	26.20	na	28.05
39. Length of the molar row, M1M3	40.43	35.84	na	42.07	33.75	40.41	42.11	37.35
40 Relationship between molar and premolar row	0.72	0.81	na	na	0.82	0.65	na	0.75
41. Length of tooth row, P2M3	67.73	63.75	na	na	62.90	67.13	na	58.68

APPENDIX 2. — Comparative dataset for the descriptive statistics on dental variables. Data for Mavro Mouri 4c and Gerani 4 are taken from de Vos (1984: table 2), data for Simonelli Cave are taken from Simonelli (1908: 9; specimens II and III). Abbreviations: **Sd**, standard deviation; **CV**, coefficient of variation, given in percent; **Min**, minimum; **Max**, maximum. All measurements are given in mm.

	Site	n	Mean	Sd	CV	Min	Max
39. Length of the premolar row, P2P4	Mavro Mouri 4c	7	28.89	1.98	6.85	25.1	30.8
40. Length of the molar row, M1M3		5	38.6	3.47	8.98	34.8	43.4
42. Length of tooth row, P2M3		2	70.90	2.4	3.38	69.2	72.6
39. Length of the premolar row, P2P4	Gerani 4	58	25.96	1.89	7.28	22.3	31.4
40. Length of the molar row, M1M3		75	37.38	2.8	7.49	31.3	43.9
42. Length of tooth row, P2M3		70	62.79	3.67	5.84	53.2	71.7
39. Length of the premolar row, P2P4	Simonelli Cave	2	30.5	1.06	3.47	29	32
40. Length of the molar row, M1M3		2	39	1.41	3.61	37	41
42. Length of tooth row, P2M3		2	67.25	3.36	4.99	62.5	72

Chapter 5

The (Sleeping) Beauty in the Beast – A review on the water deer, *Hydropotes inermis*

Review article published in Hystrix 28: 121-133, 2017

© The authors and Associazione Teriologica Italiana ((CC BY-NC 4.0)

Author contributions:
Ann-Marie Schilling conceived the manuscript; viewed, collected, and organized the literature; drafted and wrote the manuscript, and prepared the figures.
Gertrud E: Rössner conceived the concept of the study, supervised the study, and reviewed drafts of the manuscript

Published by Associazione Teriologica Italiana
Hystrix, the Italian Journal of Mammalogy
Online first – 2017
OPEN ACCESS
Available online at:
http://www.italian-journal-of-mammalogy.it/article/view/12362/pdf
doi:10.4404/hystrix-28.2-12362

Commentary

The (sleeping) Beauty in the Beast – a review on the water deer, *Hydropotes inermis*

Ann-Marie Schilling[1,2,*], Gertrud E. Rössner[1,2,3]

[1] *SNSB Bayerische Staatssammlung für Paläontologie und Geologie, Richard-Wagner-Str. 10, 80333 Munich, Germany*
[2] *Department of Earth and Environmental Sciences, Ludwig-Maximilians-Universität München, Richard-Wagner-Str. 10, 80333 Munich, Germany*
[3] *GeoBio-Center LMU, Ludwig-Maximilians-Universität München, Richard-Wagner-Str. 10, 80333 Munich, Germany*

Keywords:
biogeography
morphology
phenotype
ecology
behaviour genetics
phylogeny
Cervidae
fossil record
conservation

Article history:
Received: 5 June 2016
Accepted: 21 March 2017

Acknowledgements
M. Hiermeier (Zoologische Staatssammlung München), H. Obermaier (Staatssammlung für Anthropologie und Paläoanatomie München), F. Zachos (Naturhistorisches Museum Wien) and L. Costeur (Naturhistorisches Museum Basel) gave access to Hydropotes specimens. R. Huang (Bonn) helped with the translation of a paper from Chinese. N. Heckeberg (München) provided photographs and helped with photo editing. B. Mennecart (Basel) provided information on (semi-)free ranging *H. inermis* populations in France. M. Clauss taught mammal anatomy and large mammal dissection. We are grateful to an anonymous reviewer for her/his most constructive and encouraging comments on a previous version of the manuscript. AMS received travel grants for 2015 and 2016 from the LMU GraduateCenter. GER received travel grants from Deutsche Forschungsgemeinschaft (project RO 1197/7-1).

Abstract

The water deer, *Hydropotes inermis* (Cervidae, Mammalia), is a small, solitary cervid. It is native to China and Korea, but some feral populations also live in Europe. In contrast to other deer species, where males are characterized by antlers and small/no upper canines, *H. inermis* lacks antlers, but grows long upper canines. For this phenotype and particularities of its biology, the species holds considerable potential not only for our understanding of cervid biology, but also for important questions about basic developmental and regenerative biology. However, *H. inermis* populations are decreasing, and many of the pressing scientific questions motivated by this peculiar species are still open. Here, we review the most different aspects of the species' biology and discuss scientific publications ranging from the year of the species' first description in 1870 until 2015. We briefly sketch its state of conservation, and we discuss the current understanding of its phylogeny. Lastly, the present overview identifies areas that deserve future research available.

Introduction

Hydropotes inermis, the water deer, is native to China and the Korean peninsula. It was first described in the scientific literature by Swinhoe (Swinhoe, 1865), who assigned it as a new genus and species to Cervidae (Swinhoe, 1870). Traditionally *H. inermis* is considered to comprise two subspecies, which are distinguished by their geographic distribution and body colour: the Chinese *H. inermis inermis* (Swinhoe, 1870) and the Korean *H. inermis argyropus* (Heude, 1884) (e.g., Allen, 1940; Lee et al., 2011). We address the issue of whether it is indeed justified to distinguish subspecies towards the end of this paper.

H. inermis differs from all other deer because males lack antlers; instead they have long, sabre-like canines in the upper jaw (Fig. 1A, B). This peculiar phenotype, which resembles that of non-cervid ruminants, created problems with the systematic classification of *H. inermis* early on. It was repeatedly included with Moschidae, rather than Cervidae (e.g. Gray, 1872; Bubenik, 1983 fig. 17, 1990). Alternatively, it has been classified as a "primitive" cervid sister to antlered deer (Pocock, 1923). More recent molecular analyses generally posit *H. inermis* within Cervidae (e.g., Randi et al., 1998; Hassanin et al., 2012). However, the exact phylogenetic relationships with other deer remain unclear and it cannot be overlooked that there persist considerable discrepancies between phylogenetic hypotheses.

These issues go well beyond the question of the systematic classification of *H. inermis*. Rather, *H. inermis* interests primarily because a better understanding of the biology of this peculiar small animal holds the potential to yield novel insights into the phylogeny of deer and antler development. Thus, resolution of the systematic position of *H. inermis* is substantial for answering the question whether its lack of antlers is a derived trait or not. In turn, this should eventually allow drawing on *H. inermis* to probe the (phylo-) genetic basis of the origin and development of antlers. A better location of *H. inermis*' phylogenetic position would also be of interest for our understanding of karyotype evolution (Neitzel, 1987; Makunin et al., 2016) and its significance for the diversification of cervids.

From a conservational point of view, a better understanding of water deer biology seems also most desirable. Except for a population of *H. inermis* in France, accurate estimates of the population sizes are not available. However, the Chinese water deer is categorized as "vulnerable" since 2008, according to the IUCN Red List. It is hard to judge whether the situation in Korea is any better, as Korean water deer are classified as being "data deficient" on the IUCN Red List (Lee et al., 2011). Habitat fragmentation and extensive illegal hunt (e.g., Sheng and Lu, 1985b; Ohtaishi and Gao, 1990; Cooke and Farrel, 1998) pose a serious threat to the populations (Harris and Duckworth, 2015), which is supposed to be in steady decline, although dependable data are missing. Ongoing efforts to conserve this species are critically dependent on an in-depth understanding of its biology.

As a contribution towards its status, we set out to summarize and critically review the scientific literature on this extraordinary animal (Fig. 2). While some reviews on this species are available (Allen, 1940; Cooke and Farrel, 1998; Qiong, 2013), these mostly cover selected as-

*Corresponding author
Email address: AnnMarie.Schilling@campus.lmu.de (Ann-Marie Schilling)

©2017 Associazione Teriologica Italiana
doi:10.4404/hystrix-28.2-12362

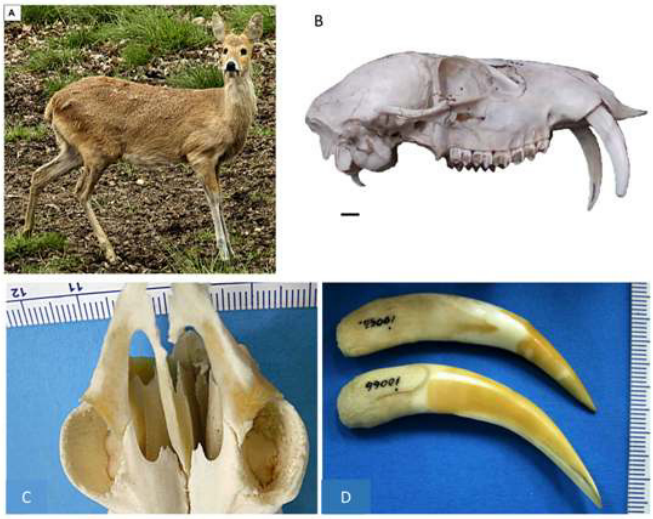

Figure 1 – Morphological characteristics of *Hydropotes inermis*. A: External appearance of a male. Antlers are absent, long upper canines present. The hindlimbs are longer than the forelimbs; the tail is short. Except for the long canines, females have a very similar appearance. Photograph: Nicola S. Heckeberg. B: Skull of male *H. inermis*, with impressive upper canines. Antlers, as well as pedicles, are lacking. Specimen-ID 1977/4438, Zoologische Staatssammlung München. Scale bar: 1 cm. C: Canine alveola of a male *H. inermis*. Ventral view of the snout, rostral pointing to the top. Note the trabecular cushion and the smooth inner alveolar walls. D: Male canine tooth with closed roots. C, D: Specimen il066 from Naturhistorisches Museum Basel. Photographs: Gertrud E. Rössner.

pects of *H. inermis* biology, or regional subgroups of this species. Here, we attempt to integrate this previous work with an extensive search of literature and data of more recent vintage. This review is meant to be a compact but also broad guide for anyone interested in cervid biology.

The rest of this paper is organized as follows: in section 2, we describe aspects of the species' biogeography; section 3 is dedicated to the external and internal morphology. In section 4, we cover aspects of the biology and ecology of *H. inermis*, and we relate them to the fossil record. Section 5 summarizes genetic studies and discusses how genetic data complement or contrast with phylogeography, phylogeny and systematics of the species. Finally, we highlight open questions and issues that need further research.

Biogeography

As mentioned above, *H. inermis* is native to the Korean peninsula and China, where historically it was found in all territories bordering the Yellow Sea and in wetlands all down China's eastern coast to the South China Sea (Fig. 3A). This is supported both by early descriptions of this species (see Swinhoe, 1865, 1870; Brooke, 1872; Swinhoe, 1873; for an overview, see Ohtaishi and Gao, 1990) and also by the fossil record, although the latter is rather scarce. Well-characterized fossils attributed to *H. inermis* have been found at Anyang (Henan), Choukoutien (Beijing) (Young, 1932; Teihard de Chardin and Young, 1936) and Tangshan (Hebei) (Pei, 1930; Young, 1932). The historical geographic distribution of *H. inermis* that may be reconstructed from these fossils is complemented by finds originating from archaeological excavations, or associated with anthropological remains (Aigner, 1981; Liu et al., 2010; Wu et al., 2011). Yet, as these are mentioned typically in faunal lists and not described in detail, their identification and association with *H. inermis* is less dependable. Similarly, fauna lists associated with archaeological remains from Misong-ni cave (Pyongyang) and the Haisang cave (Kangwon) in North Korea contain *H. inermis swinhoe* (Henthorn, 1966; Ayres and Rhee, 1984).

Today, the distribution of *H. inermis* in its native lands is much more restricted. In China, remaining animals are found primarily in the eastern half of Guangxi Zhuang autonomous region, and along the eastern Yangtze basin, in the Anhui, Hubei, Jiangsu, Jiangxi, and Zhejiang provinces, and also on the islands at the coast close to the mouth of the Yangtze river Province (Ohtaishi and Gao, 1990). The last available census from 1985 accounted for about 3300 individuals in Zhoushan Islands, the coasts, Poyang Lake and Anhui Province (Ohtaishi and Gao, 1990; Min, 2012). In North Korea, Won and Smith (1999) reported *H. inermis* to be present in the Taebak and Nagrim Mountains, Kangwon Province, and the adjacent South Hamgyong Province. In South Korea, *H. inermis* occurs in all provinces except Seoul and Jeju (Kim and Cho, 2005; Kim et al., 2013b). Kim and Cho (2005) recorded *H. inermis* in the demilitarized zone in Korea, specifically in the forest wetlands and river habitats of the provinces Paju, Yeoncheon, Cheorwon, and in the Donghae coast. For its abundance and damage to crops, the species has been considered a wildlife pest by the Korean Ministry of Environment (Kim et al., 2013a; Kim and Park, 2015). Actual numbers on its prevalence, however, are not available (Kim and Park, 2015).

In the 19^{th} century, *H. inermis* was introduced to England. A captive *H. inermis* population was recorded in the London Zoo in 1873. The Duke of Bedford then introduced the species to Woburn Park in 1900, and finally to Whipsnade Zoo in 1929/1930 (Lister, 1984; Hofmann et al., 1988; Corbet and Harris, 1991). Escapes and deliberate releases of the deer resulted in feral populations, which may be found in the Norfolk Broads, Cambridgeshire, Whipsnade, Hertfordshire, Berkshire, and Suffolk (Arnold, 1993; Harris et al., 1995; Wilson, 2003; Ward, 2005) (Fig. 3B). Over time, these feral *H. inermis* seem to have adapted well to the local conditions. In 2004, their population counted approximately 2000 individuals (Battersby, 2005; Macdonald and Burnham, 2011). More recent data are not available because the species is thought to have a low environmental and socio-economic impact (Nentwig et al., 2010; Kumschick et al., 2015); thus, monitoring is limited (Newson et al., 2012).

Lastly, in France, a population of 80–100 animals lives under semi-free conditions in the 12 ha-sized Zoological Park of Branféré (Bretagne). The founders of this population have been introduced in the 1970's from Whipsnade Park, England (Kay, 1987; Axmacher and Hofmann, 1988; Cooke and Farrel, 1998; Dubost et al., 2008). Yet another semi-free ranging population exists in the Haute Touche Zoological Park of Obterre (Centre-Val de Loire) (Bastien Mennecartart, Basel, written notification). A third population ranges around Saint Jean de Ligour (Nouvelle-Aquitaine) and Le Vigen (Occitanie). This population originated from escapes from a local park. Its size is not known, but it is considered as not expanding (Sand and Klein, 1995; Maurin and Gavazzi, 1997).

Given the precarious and endangered status of *H. inermis* in its native habitat, several attempts of conservation are in place. In China, legal hunt is regulated since 1988 (Liang et al., 2011). Further, *H.*

Table 1 – Aggressive behaviour in *Hydropotes inermis*. Behaviours are ranked from low (first row) to highly aggressive, according to Stadler (1991).

Behaviour	Action
Aggressive approach	Stiff walk towards the opponent, head and neck hold in 90° angle, ritualized.
Parallel walk	Stiff walk side-by-side, ca. 10–20 meters apart, head and neck hold in 90°angle. Stadler (1991) interpreted this behaviour as an ancient, broadside display, because it is found also in other Cervidae, Ruminantia (including Tragulidae), Artiodactyla, Canidae and Rodentia. It is absent in the musk deer. The behaviour might be either interrupted by defecation, territory marking or feeding or extended into a parallel run.
Chase with front-leg-strike	Males chase one another. The dominant male tries to hit the intruder with both front-legs at a time.
Dance	Males are in front of each other, head-to-head or neck-to-neck contact. They try to press to the ground the opponent's neck (Scherpe, 1971). Males jump back and forth, presence of front-leg-strike.

Table 2 – Reproductive traits of *Hydropotes inermis* compared with those of other cervids and ruminants without cranial appendages. Source: Scherpe (1971); Dubost et al. (2011) and references therein.

Species	GL (days)	LS	AW (weeks)	AM_1 (months)	AM_2 (months)	AM_3 (months)	SM (months) m–f
Non-cervid ruminants							
Tragulus javanicus	140	1	11.5	?	?	?	?–4.5
Tragulus napu	150	1	10	?	?	?	?–5.5
Hyemoschus acquaticus	225	1	12	4	10	20	?–6
Moschus moschiferus	188	1.5	14	?	?	?	?–18
Cervids							
Hydropotes inermis	**168.5**	**2.5**	**3**	**2**	**5**	**10–12**	**?–6**
Muntiacus reevesi	214.5	1	8	4.75	9.75	23	9–11
Capreolus capreolus	157.5	1.9	12	5	8	16.5	21–13

GL Gestation length
LS Litter size
AW Age at weaning
AM_1 Age at eruption of first lower molar
AM_2 Age at eruption of second lower molar
AM_3 Age at eruption of third lower molar
SM Sexual maturity in males (m) and females (f)

inermis is now included in the Category II of the Chinese State Key Protected Wildlife list (Fang and Wan, 2002). This category embraces wildlife under special local protection. Also, attempts to reintroduce populations near Shanghai have been successful (Min, 2013; Yabin, 2013; Chen et al., 2015). A breeding centre exists on the Zhoushan Island, and similar centres have been proposed for the mainland (Hu et al., 2006). In 1994, North and South Korea ratified the Convention on Biological Diversity, which, among others, led to regulation of the hunt of *H. inermis* (Won and Smith, 1999).

H. inermis from head to toe — Aspects of external appearance and morphology

External appearance

H. inermis of both sexes reach approximately 50 cm height at withers (Scherpe, 1971; Cooke and Farrel, 1998) and weigh up to 15 kg (Kay, 1987; Axmacher and Hofmann, 1988; Cooke and Farrel, 1998; Dubost et al., 2008; Hofmann et al., 1988; Zhang, 2000). Both males and females show chestnut-coloured hair tips of the topcoat. The under-fur is black in summer and greyish in winter (Bützler, 1988). The belly and throat are white (Swinhoe, 1870; Garrod, 1877a) or at least paler than the rest of the body (Cooke and Farrel, 1998). Unlike other deer, *H. inermis* has no white patch on the ventral side of the short tail (Cooke and Farrel, 1998). White coloured patches placed along lines that run from neck to tail (Garrod, 1877a) are characteristic of fawns. These patches are lost around the age of two months and replaced by the adult coat (Cooke and Farrel, 1998). Males are typically dark-coloured around the nose, whereas females are light-coloured around the nose. Males also have thicker necks than females (Cooke and Farrel, 1998).

The skull

The skull of *H. inermis* has been described and compared to other deer and *Moschus* early on, in studies made at the end of the 19^{th} century (Swinhoe, 1870; Brooke, 1872; Swinhoe, 1873; Rütimeyer, 1881). Generally, females have slightly larger heads than males (Kim et al., 2013c).

Distinctive characters of the *H. inermis* skull noted include small orbits (Rütimeyer, 1881), small lacrimal fossae confined to the lacrimal bones (Swinhoe, 1870) with two lacrimal ducts, and an ethmoidal gap (Rütimeyer, 1881). *H. inermis* has no supraorbital ridges. The supraorbital foramen is in a groove (Swinhoe, 1870). The basioccipital bone is narrow and slightly grooved (Brooke, 1872).

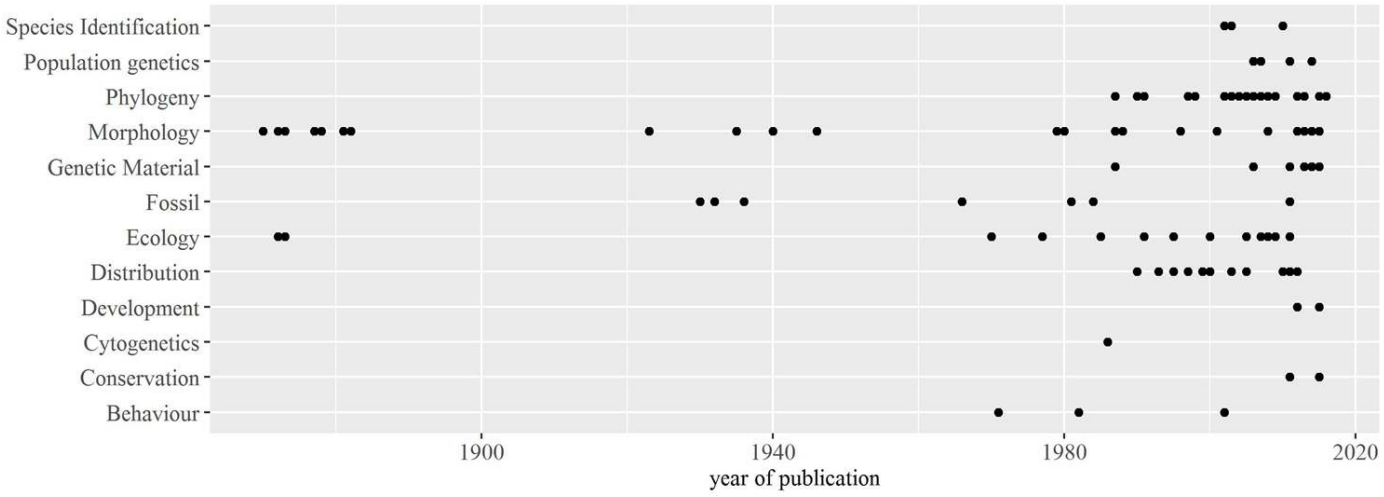

Figure 2 – Years of publication for scientific papers on *Hydropotes inermis*, published in English, German and French from 1870 to 2015. Each dot in the plot corresponds to one publication. The plot highlights research areas where most research has been performed, i.e. morphology, phylogeny and ecology, as well as areas that are weakly covered. The category "fossil" also includes studies, where *H.inermis* is mentioned in faunal lists. On the China Knowledge Resource Integrated Database more publications (n∼80), published in Chinese with an English abstract, are available. The titles and the abstracts of these papers indicate that these are mainly on behaviour, ecology and current species distribution, including fossil findings. We apologize to our Chinese and Korean colleagues that for obvious shortcomings of our language capabilities, we could not appropriately cover their work. Plot made with R (R Core Development Team, 2013) and `ggplot2` package (Wickham, 2009).

Table 3 – Gene sequences available on GenBank for *Hydropotes inermis*. Only few nuclear genes have been sequenced. Mitochondrial sequences sequenced independently and used for phylogenetic analyses are also given in Tab. 4. cds, coding sequence.

Gene name	Sequence	Accession number GenBank	Reference
Mitochondrial genome	Complete	EU315254.1 JN632649.1 KP203884.1 JX254914.2 JF802125.1 NC_018032.1 NC_011821.1	Liu and Huang, direct submission; Hassanin et al. (2012); Yu and Kwak, direct submission; Kim and Park (2015); Kim et al., direct submission
Satellite III	Complete	DQ085265.1	Lin and Li (2006)
Zinc finger protein 238 (ZNF238) gene	Partial cds	GU045457.1	Kim et al. (2010)
ZFX gene	Partial cds, exons 7 and 8	DQ179233.1	Han et al. (2005); direct submission
		FJ866606.1	Kim et al. (2009); direct submission
SRY gene	Complete cds	EF100132.1	Han et al. (2006), direct submission
Aromatase cytochrome P450 (Cyp19)	Partial, 3'untranslated region	AY122006	Hassanin and Douzery (2003)
Lactoferrin	Promotor region	AY122039	
alpha-lactalbumin	Intron 2	AY122020	
12 microsatellites		GU480080-GU480091	Lee et al. (2011)
Multiple microsatellites		HQ876092-HQ876170	Yu et al. (2011b)

The premaxillae are short and broad (Brooke, 1872) and the median palatal processes of the premaxilla have been described as spindle-shaped (Garrod, 1877b), though they rather impress as slender and equally wide. A rather distinctive feature of *H. inermis* are its large and inflated auditory bullae (Rütimeyer, 1881; Groves and Grubb, 1987).

The dental formula of *H. inermis* is I 0/3, C 1/1, P 3/3, M 3/3 and thus follows the general pattern present in Cervidae (Putman, 1988) and indeed ruminants, with the notable exception of an upper canine. In the mandible, *H. inermis* has three incisors and one incisiform canine, as typical for ruminants (McKenzie, 1990). The median incisor is larger than the two lateral, equally wide incisors (Swinhoe, 1870; Pocock, 1935; Groves and Grubb, 1987). Boué (1970) noted that the former had the form of a spatula, whereas the latter were lanceolate. Kim et al. (2013b) found that the premolar row in *H. inermis* was shorter than the molar row, both in the mandible and the maxilla.

Clearly, one of the most distinctive characteristics of *H. inermis* is the presence of upper canines (Fig. 1D). In males, these may reach a length of up to six centimetres. In females, they rarely exceed one centimetre length (Aitchison, 1946; Cooke and Farrel, 1998; personal observations). Rütimeyer (1881) described in detail the shape of the male canine. A convex outer surface and a concave inner one converged posteriorly to a sharp cutting edge and formed a pointed tip, pointing downwards and backwards. In the maxillary alveola, the canine is inserted vertically; of note, the alveola is much larger than the canine root, in both length and breadth, offering space for an extensive, soft-tissue holding apparatus. The alveolar walls are smooth on the inner side, and a cushion of trabecular bone builds up the alveolar roof (Fig. 1C). The canine can move back and forth and from side to side quite extensively (Swinhoe, 1873; Aitchison, 1946). Aitchison (1946) suggested that *H. inermis* could move its canines actively, allowing a successful canine blow and preventing tooth breakage or displacement. Specifically, he proposed that levator muscles in the upper lip, the so-called snarling muscles, controlled the erection of the canines. He noted that when the animals snarled and the muscle contracted, the tusk moved forward; when the muscle relaxed, the tusk returned into its original position. However, it is still unclear whether the canine can really be actively moved and if so, to which extent. Swinhoe (1873) noted that only fully-grown canines were mobile. This correlates with the fact that juvenile *H. inermis* have an open pulp cavity in the upper canines, whereas it is closed in fully developed canines (Brooke, 1872) (Fig. 1D). Yet whether there is causal relationship is not known. With ongoing development, the root of the upper canines also protrudes gradually to the ventral border of the maxilla (Brooke, 1872). An important physiological consequence of the root closure is that canines are not continuously growing.

In passing, it should be mentioned here that Sasaki et al. (2013) observed a weakly developed tendon of the *M. maxillo-mandibularis* in *H. inermis*. The authors speculated whether this may facilitate wide mouth opening, and thus effective use of the upper canines, as had previously been suggested for Bactrian camels, which also have conspicuous upper canines. These authors studied only female water deer. If their conjecture stands up, one would expect an even weaker *maxillo-mandibularis* tendon in males, which effectively use their much larger canines in fights.

The dental eruption sequence in the lower jaw of *H. inermis* follows that observed in other deer, notably *Axis*, *Odocoileus* and *Capreolus* (Veitschegger and Sànchez-Villagra, 2015). For the upper jaw, the eruption sequence in Cervidae is still unknown.

Besides the upper canines, the complete absence of antlers in both sexes is a diagnostic characteristic of the skull of *H. inermis*. Kim et al. (2013b) pointed out that neither sex showed the slightest tendencies to develop pedicles. This is a clear difference to, e.g., *Capreolus capreolus* and *Muntiacus* species. Thus, even most *Capreolus* females have small outgrowths on the homologous sites of the frontal bones, where males develop pedicles. Female *Muntiacus* have a prolongation of the frontal ridges, although to a lesser extent than males. The absence of antlers also correlates with the structure of the frontoparietal suture. As Li and Suttie (2012) pointed out, in antlered deer the frontal overlaps the parietal bone in the region where antlers develop, whereas in *H. inermis* the parietal overlaps the frontal bone in the homologous region. The brain case of *H. inermis* is long and narrow and its shape is similar to that of *Moschus* (Swinhoe, 1870; Brooke, 1872). It houses a quite convoluted brain (Garrod, 1877b; Forbes, 1882), as typical for Cervidae (Pillay and Manger, 2007), which is considered, though, as small and light (∼53 g) compared with body weight (Kruska, 1970).

Post-cranial Skeleton

The post-cranial axial and appendicular skeleton of *H. inermis* has been studied to a much lesser extent than the skull. Here, we focus on the appendicular skeleton, given its importance for the diagnosis and classification of Ruminantia.

An already externally obvious skeletal characteristic of *H. inermis* is that its hindlimbs are longer than its forelimbs, and that consequently, its back is arched dorsally. In the forelimb, the wrist is composed of seven carpal bones, four in the proximal row (lunate, scaphoid, triquetral, pisiform) and three in the distal row (trapezium, trapezoid-

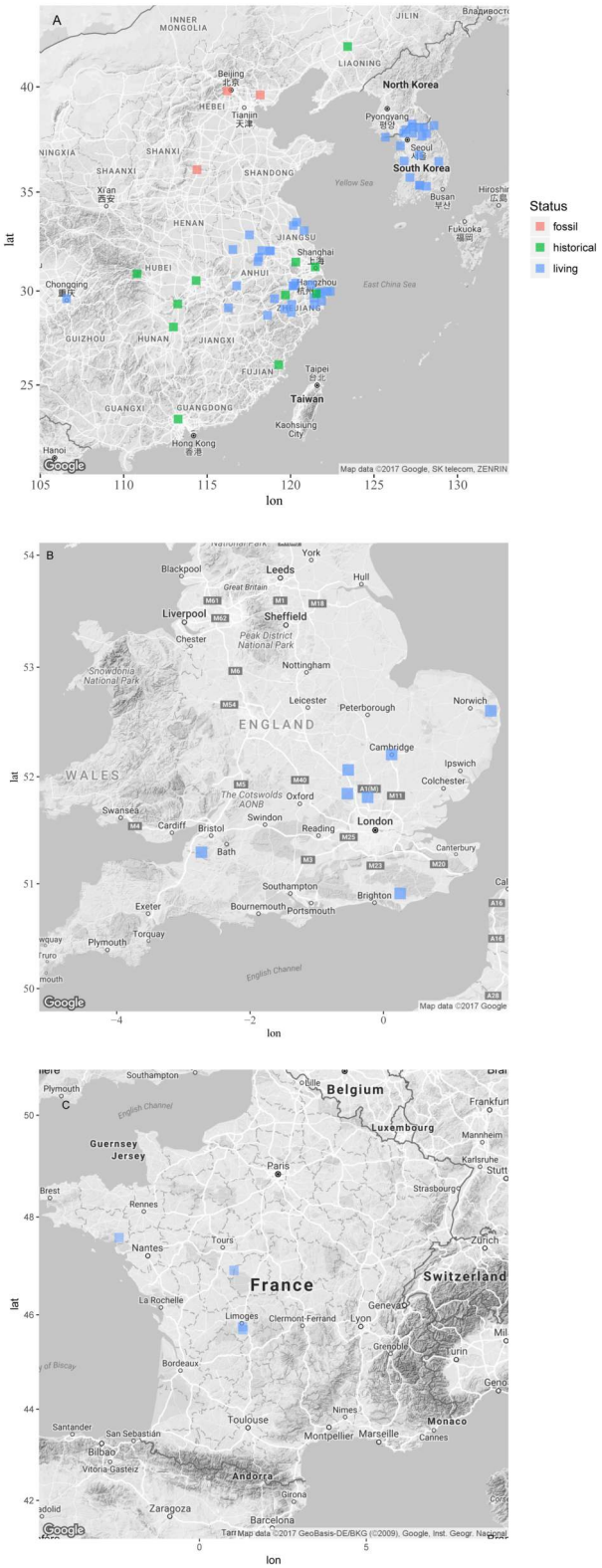

Figure 3 – The geographical distribution of free-ranging *Hydropotes inermis*. A: Native habitat in China and Korea. B: *H. inermis* in England. C: *H. inermis* in France. Points approximately mark regions of occurrences. To obtain these, sampling sites and sighting reports were extracted from the literature and transformed into latitudes (lat) and longitudes (lon). Fossils from archaeological sites are only included if a description or drawing of the fossil specimen is available. Literature used: China: Pei (1930); Young (1932); de Chardin and Young (1936); Allen (1940); Ohtaishi and Gao (1990); Sun and Xiao (1995); Sun et al. (2000); Kim and Cho (2005); Rhim and Lee (2007); Xi et al. (2010); Kim and Lee (2011); Min (2012); Kim et al. (2015a); He et al. (2015). England: Arnold (1993); Harris et al. (1995); Wilson (2003); Ward (2005). France: Dubost et al. (2011). All maps made with R and ggmap package (Kahle and Wickham, 2013).

magnum, hamate) (Ahn, 2008). Except for the trapezium, this arrangement is found also in other deer and ruminants (Nickel et al., 1992; Morejohn et al., 2005; Smart, 2009; Hillson, 2016). In the metacarpus, the distal part of the degenerated second and fifth metacarpal bones persist, whereas the proximal part is reduced, a pattern observed also in *Capreolus*, *Alces*, *Rangifer*, and other deer genera known as "Telemetacarpi" (Brooke, 1878) or Capreolinae (Gilbert et al., 2006; Hassanin et al., 2012).

For the hindlimb, it was observed that the median and lateral trochal ridges of the femur are rather symmetric. This morphology is typical for several small ruminants which share a preference for closed or mixed habitat (like *Hyemoschus acquaticus*, *Muntiacus reevesi*, *Odocoileus hemionus*, *Ourebia ourebi*, *Cephalophus silvicultur*, *Tragelaphus scriptus*, *T. imberbis*, *Antilocapra americana*, *Aepyceros melampus*) and is thought to be the result of convergent evolution (Janis et al., 2012).

The tarsus of *H. inermis* is composed of five bones, as commonly observed in pecoran ruminants. The proximal tarsal row consists of the talus and calcaneus. The second tarsal row consists of the *Os centroquartale* (= *Os naviculocuboideum*), the *Os tarsale* I (= *Os cuneiforme mediale*) and fused *Os tarsale* II and III (= *Os cuneiforme intermediolaterale*) (König and Liebich, 2005; Ahn, 2008; Morlat, 2010).

Finally, it may be noted that the obturator canal in the pelvic girdle of *H. inermis* usually is clearly separated from the foramen obturatorium by a bony bridge or marked bony spines (Tae et al., 2014). Based on the morphology and variability of this characteristic, *H. inermis* may be grouped with Capreolinae, rather than Cervinae (Tae et al., 2014).

Soft-tissue anatomy

As typical for Cervidae, and indeed Ruminantia, the aortic arch of *H. inermis* gives off a common brachiocephalic trunc, which then branches somewhat variably. Ahn (2008) analysed 23 animals and described the most common (19/23) pattern as follows: the brachiocephalic trunc gives first off the left subclavian artery; then the left common carotid artery; and then it trifurcates into the right common carotid artery, the right costocervical trunk and the right subclavian artery. He also noted that there was no bicarotid trunc. This latter finding in particular is identical to what has been observed in *Axis axis* (3 specimens) and *Ozotoceros bezoarticus* (8 specimens) (Pérez and Erdoğan, 2014). In contrast, a bicarotid trunc seems to be the rule in many domesticated ruminants, *Mazama gouazoubira* (Ahn et al., 2008; Pérez and Erdoğan, 2014) and the Siberian roe deer (Ahn et al., 2014, abstract).

The digestive system of *H. inermis* comprises a quadruplicate omasum, a liver without gall bladder and an intestine wanting the ileocecal gland (Garrod, 1877a; Forbes, 1882). The testis and the accessory reproductive glands are similar to those of other ruminants for shape, location and histology (Sohn and Kimura, 2012). Forbes (1882) described the penis as an "elongated tapering compressed cone, with the urethral opening subterminal" (p. 82). Furthermore, he could not identify a Cowper's gland in an adult *H. inermis* male.

H. inermis lacks a metatarsal gland (Garrod, 1877a), while an interdigital gland in the hind limbs, and inguinal glands are present (Pocock, 1923). The latter glands are specific to *H. inermis* within Cervidae (Pocock, 1923).

Biology and Ecology

Habitat

In its native lands, *Hydropotes inermis* is often found in mixed habitats rather than closed forests. It prefers meadows with shrubs to hide (Dubost et al., 2008) or forests interspersed with clearings (Rhim and Lee, 2007). Connectivity and proximity of forest patches seem to be important factors favouring the abundance of *H. inermis* (Jung et al., 2011). From observations made in Korea, it has been concluded that *H. inermis* prefers altitudes below 300 m. However, droppings found on mountain slopes of different degrees indicate that it did not avoid steeper slopes (Kim et al., 2011b). From a Korean sample of four feral animals, the home range of *H. inermis* has recently been estimated to

be about two to four km^2 (Kim and Lee, 2011, estimated with the minimum convex polygon (MCP) method). Based on a sample of 10 animals in a reintroduced population in the Nanhui Wildlife Sanctuary near Shanghai, the home range has been estimated to be about 0.7–6.7 km^2 (Chen et al., 2015; MCP method). For this sample, the winter home ranges were reported to be about twice as large as the ranges reported for other seasons (He et al., 2015). In contrast, for the Korean sample, the summer home ranges were found larger (Kim and Lee, 2011). Interpretation of these data is qualified by the small sample sizes and by the fact that the Chinese sample was analysed shortly after reintroduction. Thus, it may not be representative of a truly feral population. In addition, two of the four Korean animals had been wounded before tagging (Kim and Lee, 2011). In England, *H. inermis* has a much more restricted home range (on average: 0.21 km^2) (Cooke and Farrel, 1998). These observations suggest differences in that home range size may vary with sex, season, and age; however, more data are needed to address these issues.

Diet

Molecular biological and microhistological analyses of plants extracted from the faeces and feeding signs revealed that in its native lands in China and Korea, *H. inermis* feeds mainly on forbs and woody plants such as Asteraceae, Leguminosae and Fagaceae (Guo and Zhang, 2005; Kim et al., 2011a). Boué (1970) noted that *H.inermis* selected the leaves and twigs to feed on. In England, the stomach contents of *H. inermis* consisted mainly of grasses, sedges and herbs; woody species made up only a small part of the ingested food (Cooke and Farrel, 1998). Clauss et al. (2008) classified individuals from the English Whipsnade population as intermediate feeders, based on the percentage of grass in their natural diet. Yet, as documented by Hofmann et al. (1988), food available to *H. inermis* in Whipsnade might be suboptimal, thus it does not represent their natural choices. Still, it should be stressed that the populations in Whipsnade and in the Bretagne were and are the main resource for studies on the behaviour and ecology of *H. inermis* under (semi-) feral conditions Dubost et al. (2008, 2011).

Sociality

Hydropotes inermis is a rather solitary deer, and especially males range alone. Outside the parturition/early-fawning period, individuals only occasionally form small, transient groups of two, rarely up to five individuals (Stadler, 1991; Sun, 2002). Individuals of both sexes are peaceful, living "unconcerned about the others" (Dubost et al., 2011, p. 196). In a semi-feral population, direct physical interactions were observed to be restricted to the strictly necessary. Adults did not groom each other; rarely licked another and 'partners' were not marked (Dubost et al., 2011). In alert situations, groups burst away, each individual in a different direction (Scherpe, 1971). When in danger, *H. inermis* flees in a leaping form (Bützler, 1988; Cooke and Farrel, 1998; Geist, 1998), commensurate to its rather longer hind-legs. Furthermore, *H. inermis* does not tail-flash, as other deer species do, in order to warn each other. More frequent and intensive body contacts among individuals occur during the mating season and the fawning period (Zhang, 2000; Dubost et al., 2011). Mating season lasts from November until January both in Asia and in Europe (Scherpe, 1971; Sheng and Lu, 1985a; Stadler, 1991; Sun and Dai, 1995; Dubost et al., 2008). During the mating season, some males establish and defend territories (Sun and Dai, 1995; Dubost et al., 2011). These territories are based on female distribution (Sun and Xiao, 1995), and female home ranges were observed to overlap with several male territories. Males mark their territories by pawing a hole and filling it with urine or faeces (used in 86.4% of all observations) or by rubbing their forehead, up to several minutes, against an inanimate object (13.6%; Sun and Dai, 1995). A particularly excited male may interrupt forehead rubbing and repeat it several times (Stadler, 1991). Head rubbing of females typically includes also rubbing of the ears and posterior parts of the head and it is considered a comfort, rather than a marking behaviour (Feer, 1982). (Dubost et al., 2011) noted that females and young could travel unhindered through male territories. In contrast, non-territorial males

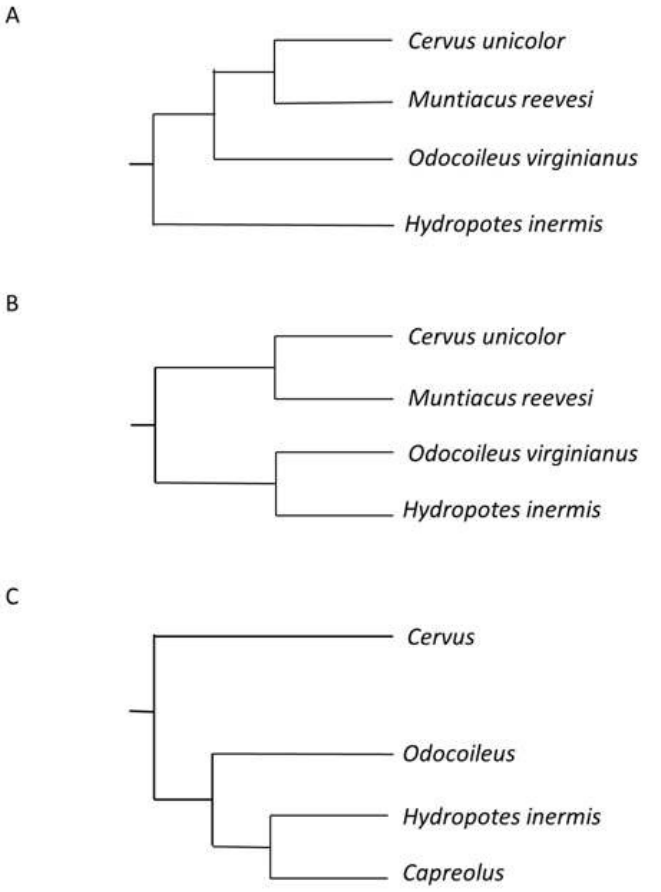

Figure 4 – Phylogenetic position of *H. inermis* within Cervidae as described by Kraus and Miyamoto (1991) (A, B) and Douzery and Randi (1997) (C). A: Phylogenetic relationships based on mitochondrial 12S and 16S rRNA genes and considering transversions, transitions and gaps. B: Result obtained considering only transversions. C: Phylogeny based on the cytochrome b sequence. The same phylogeny was obtained regardless of whether transitions or transitions and transversions were considered. Note the basic identity of the cladograms in B and C. *Muntiacus* was not included in the analysis of Douzery and Randi (1997), and Kraus and Miyamoto (1991) did not include *Capreolus*.

usually stayed between the territories, where they lived together peacefully. Moreover, non-territorial males were observed to conquer a territory only rarely, when challenging a territory holder (Stadler, 1991; Dubost et al., 2011).

In a combat for a territory and for females, *H. inermis* males prefer direct attacks (Feer, 1982). Threatening gestures are limited to an aggressive approach (Stadler, 1991, Tab. 1) and to stamping with the forefeet ("Drohstampfen", Scherpe, 1971). According to Stadler (1991), the fight in *H. inermis* typically consists of well-divided steps. Each step can be associated with a behavioural pattern (Tab. 1) and an increased level of aggressiveness, with the canine blow as last and most aggressive step. Canine-blows can cause serious injuries in captivity (Feer, 1982) and the wild, e.g., "ripped ears, long scars (5–30 centimetres) on virtually all parts of the body, or limping legs" (Stadler, 1991, p. 93). Thus, the canines are very effective weapons, with the potential to kill. For instance, Stadler (1991) reported on a dead male with two holes piercing its heart. The depth of the wound, the shape of each hole and the distance between them matched well with the morphology of water deer canines. In a way, the agonistic fighting behaviour of *H. inermis* finds parallels in that of *Moschus* (described by Zhang et al., 1979; see also: Sathyakumar et al., 2015). In contrast, *Muntiacus* males, which have antlers and canines, use both in intra-specific fights, but with a clear preference for antlers (Barrette, 1977).

Mating, reproduction, rearing fawns

H. inermis is a polygynous species and males herd the females present in their territory (Scherpe, 1971; Stadler, 1991). Only territory holders mate successfully with females. When approaching a female, the

male emits a mating call (Stadler, 1991; Cap et al., 2008; Dubost et al., 2011). It lowers its head, slaps the ears and sniffs either the female or the site where she was lying and then performs flehming to assess her sexual status (Stadler, 1991). Both unreceptive and receptive females withdraw from an approaching male, which follow-up receptive females, until these stop and copulation occurs. Copulation lasts only a couple of seconds (Stadler, 1991; Dubost et al., 2011). The gestation period is about six months (170 days, Dubost et al., 2011) and it is the shortest among cervids (Tab. 2). Most parturitions occur from May to June (Sheng and Lu, 1985a; Stadler, 1991; Dubost et al., 2011) and females do not select isolated places to give birth (Stadler, 1991). In captivity or under semi-free ranging conditions, *H. inermis* has a litter size of two to four, and occasionally up to eight fawns (Dobroruka, 1970; Scherpe, 1971; Sheng and Lu, 1985a; Stadler, 1991; Dubost et al., 2008). This latter number agrees with what has been observed in occasional dissections of pregnant females (Swinhoe, 1870; Hudson, 1872; Hamilton, 1873). Dubost et al. (2008) pointed out that litter sizes in parks in Europe are smaller than the Asian ones, and suggested that, as in other deer, it may vary with overall population density. This comparatively large litter size (see Tab. 2) has been interpreted as a derived condition (Jabbour et al., 1997; Mauget and Mauget, 2009). Thus, an explanation for the high foetus number based on early reports on the one hand and the few new-borns on the other hand, is still missing. Systematic studies that track females (and their foetus) from perception to birth and studies on protected, native populations, which are not exposed to hunting or high-density pressure, might be approaches to find solutions to this bias in *H. inermis* reproductive biology. Females interact with their fawns only for a short period and mother-fawn interaction decreases rapidly with weaning. Occasionally, females help to rear non-filial fawns (Scherpe, 1971; Stadler, 1991; Mauget and Mauget, 2009). Suckling fawns perform the so-called "milk-step" (Scherpe, 1971; Stadler, 1991). Fawns execute the step from bottom-to-top and Scherpe (1971) interpreted the movement to be proportional to the hunger of the fawn. Mothers wean their fawns after only a couple of weeks (Scherpe, 1971; Chaplin, 1977; Dubost et al., 2008). Fawns become independent after three to four months and are loners (Stadler, 1991). At six months, the young reach sexual maturity and at 18 months, they reach adult weight. In the wild, *H. inermis* has been reported to reach an age of eight years (Dubost et al., 2008), in captivity it reaches up to eleven years (Jones, 1977). Dubost et al. (2011) point out that among cervids, *H. inermis* is "the most precocious and the most prolific, even if one takes into account small ruminants like [the dikdik] *Madoqua kirki* or the roe deer *C. capreolus*…", and they note that for many characters of its reproduction, maturation and life cycle, it is rather reminiscent of large rodents.

Genetics

Overall, genetic characterization of *H. inermis* is still rather limited. Karyotype analyses revealed that *H. inermis* has 70 chromosomes (2n), comprising 68 autosomes and two sex chromosomes (Hsu and Benirschke, 1973). All chromosomes are acrocentric. Other cervids either have the same or lower numbers of chromosomes (Nietzel et al., 1986; Neitzel, 1987; Dementyeva et al., 2010), which led to the suggestion that the karyotype of *H. inermis* represents an ancestral state (Neitzel, 1987). In 1990, Miyamoto and colleagues published the first mitochondrial gene sequences for *H. inermis*, coding for 12S and 16S ribosomal RNAs. Since then, several authors have published additional mitochondrial sequences, which they used primarily to infer the phylogenetic position of *H. inermis*. Recently, the complete mitochondrial genome of *H. inermis* has been sequenced (Yu et al., 2011a; Hassanin et al., 2012; Liu, Z. and Huang, J., direct submission to GenBank), with sequences available in GenBank (see Tab. 3 for accession numbers). Today, only a handful of nuclear sequences have been published. These include ZNF238, ZFX, ZFY, lactoferrin, and, notably several (micro-) satellite sequences (for additional genes, accession numbers and references, see Tab. 3). In cervids, six satellite DNA families (I-VI) have so far been described (for a review, see Li and Lin, 2011; Hsieh et al., 2014). In *H. inermis* satellite I (Bogenberger et al., 1987; Lin and Li, 2006), II, III (Lin and Li 2006), and V (Li et al., 2005) families were identified. Satellite families I and II are found in many cervids (see Lin and Li 2006 and references therein). Family III satellite DNA was originally thought to be specific for the roe deer (*Capreolus capreolus*; Buntjer et al., 1998), but subsequently also identified in *H. inermis* (Lin and Li, 2006). The presence of family V satellite DNA, originally identified from the Y-chromosome of Indian muntjac (*Muntiacus muntjak vaginalis*), has been studied so far in only a few cervids and related species. It was found in males of Indian, Formosan and Chinese muntjac (*M. muntjak vaginalis*, *M. reevesi micrurus* and *M. reevesi*, respectively), sambar deer (*Cervus unicolor swinhoei*), and *H. inermis*. Moreover, it was identified in female Indian and Formosan muntjac and in female Chinese water deer. In *H. inermis*, it is found on both the Y and X chromosomes. No satellite V signal was detected in probes from caribou (*Rangifer tarandus caribou*) and black-tailed deer (*Odocoileus hemionus hemionus*) (Li et al., 2005). Finally, family VI satellite DNA was first isolated from chromosome 3+X of the Indian muntjac. In this species, the X-chromosome fused with the autosome 3 (Hartmann and Scherthan, 2004). Thus, females have 2n=6 (chromosome pairs 1, 2, 3+x) and males have 2n=7 (chromosome pairs 1, 2, unfused 3 and 3+X and Y) (**?**Li et al., 2005). Satellite VI was then also found in the Formosan sambar deer (*Rusa unicolor swinhoei*), in Formosan sika deer (*Cervus nippon taioanus*) and the Formosan muntjac. In contrast, this satellite was not detectable in black-tailed deer, caribou, water deer, roe deer, bull and goat (Hsieh et al., 2014). Given the role attributed to microsatellites for centromere function (see, e.g., Lin and Li, 2006; Ferguson-Smith and Trifonov, 2007; Makunin et al., 2016, it will be interesting to see whether, and how these data may be integrated with karyotype variability in cervids.

Besides application in phylogenetic studies (see the following section), genetic approaches have been used for species identification, forensic science, food safety (e.g., Fang and Wan, 2002; Wan and Fang, 2003; Kim et al., 2010), population genetics, and management (e.g., Hu et al., 2006, 2007; Kim et al., 2014; Shi et al., 2014). Thus, analyses of microsatellites (Hu et al., 2007; Shi et al., 2014) and the mitochondrial control region (Hu et al., 2006) led the authors to conclude that *H. inermis inermis* in China "has a relatively high-genetic diversity" when compared to other rare cervid species, such as the Chinese sika deer (*Cervus nippon*), Eld's deer (*Cervus eldi*), the black muntjac (*Muntiacus crinifrons*) (Hu et al., 2006), the forest musk deer (*Moschus berezovskii*), and the North American wapiti, (*Cervus elaphus*) (Shi et al., 2014). As expected, intraspecific genetic diversity was higher in feral populations living in mainland China and three islands of the Zhoushan archipelago than in zoo populations (Hu et al., 2007). Similarly, mainland populations had a greater haplotype diversity than island populations (Hu et al., 2006). The authors disagree whether there is no inbreeding (Shi et al. 2014), some inbreeding (Hu et al., 2006) or severe inbreeding (Hu et al., 2007) levels in populations from the Zhoushan Archipelago. The genetic diversity of a population of *H. inermis argyropus* living in South Korea was found to be lower than that of the Chinese populations of *H.inermis inermis* (Kim et al., 2014).

Passing the buck — Phylogenetic considerations

Morphological evidence

The resolution of the phylogenetic position of *H. inermis* is of considerable interest, arguably less for systematics than for the insight into fundamental biological processes, such as karyotype evolution (Neitzel, 1987; Ferguson-Smith and Trifonov, 2007; Makunin et al., 2016) and antlerogenesis evolution (DeMiguel et al., 2014; Ceacero, 2016; Heckeberg, 2017). Furthermore, antlerogenesis is considered a prime model for mammalian regenerative biology, and indeed medicine (Price et al., 2005a; Kierdorf et al., 2009). Its conspicuous cranial morphology, and in particular its tusk-like upper canines, long and narrow brain case and the absence of supraorbital ridges led Gray (1872) to classify *H. inermis* with Moschidae. However, early on, differences with *Moschus* were noted: Brooke (1872) pointed out that, among others, the premaxilla is shorter and broader and the basioccipital bone is narrower in *H. inermis* than in *Moschus*. He and Rütimeyer (1881), also

stressed that *H. inermis* had smaller orbits than *Moschus*, a lacrimal fossa and an ethmoidal gap. In a detailed study on *H. inermis*' internal organ anatomy (Garrod, 1877a) contrasted *H. inermis* with *Moschus moschiferus*, identifying the lack of a gall bladder and an ileocecal gland, the quadruplicate psalterium (dupliciplicate in *M. moschiferus*), differences in the numbers of colic coils (2.5 vs. 3.5, respectively), and finally, the considerably more convoluted brain of *H. inermis*. He summarised his observations sharply, stating, "In other words, *Hydropotes* is typically Cervine, whilst *Moschus* is anything but so", concluding "To what group of the Cervidae Hydropotes is most allied there is still considerable uncertainty" (Garrod, 1877a, p. 891). Further morphological studies done since then (see, e.g., Brooke, 1878; Forbes, 1882; Pocock, 1923; Heintz, 1963; Meunier, 1963; Leinders, 1979; Leinders and Heintz, 1980; Groves and Grubb, 1987; Scott and Janis, 1987; Bouvrain et al., 1989) have not really solved this conundrum. More recent studies suggest that additional anatomical structures such as the vascular branching pattern of the aorta (Ahn et al., 2008; Clauss, 2014) or the obturator canal (Tae et al., 2014) may hold significant phylogenetic

Table 4 – Overview of molecular studies concerning the phylogenetic position of *Hydropotes inermis*. Results are discussed in the text. Sequences sequenced for the first time in the studies listed are highlighted in bold.

Number in text	Reference	Research aim	Approaches	Material sequenced and/or analysed
1	Kraus and Miyamoto (1991)	Relationships among pecoran ruminants	Two step tree construction: Step 1: MP on transitions, transversions, gaps; Step 2: MP on transversions only; Indels included (=gaps)	**mtDNA; 12S, 16S rRNA and flanking regions 2.7 kilo kbp**
2	Douzery and Randi (1997)	Test for the postulated basal position of the antlerless Hydropotinae within Cervidae and for affinities between Odocoileinae and Hydropotinae	Two step tree construction: MP; all indels excluded; ML; NJ	**MtDNA; control region (1099 bp)**
3	Randi et al. (1998)	Phylogenetic position of *H. inermis*	MP; ML, quartet puzzling; NJ	**MtDNA; cytochrome b (1140 bp)**
4	Hassanin and Douzery (2003)	Phylogeny of ruminants, with special emphasis on the position of *Moschus*	MP, equal weights and differential weights; ML, standard and partitioned; NJ	MtDNA: 12S, 16S rRNA, cytochrome b, complete sequences; **nDNA: cytochrome oxidase P450 (193bp), lactoferrin promotor (325 bp), alpha-lactalbumin intron 2; k-casein exon 4 (401 bp)**
5	Pitra et al. (2004)	Phylogeny of Cervinae	MP, equally weighted; ML, quartet puzzling; NJ; BI	MtDNA: cytochrome b
6	Kuznetsova et al. (2005)	Phylogeny of Cervidae	MP, equally weighted; ML	MtDNA: 12S, 16S rRNA (2445 bp)
7	Hernández Fernández and Vrba (2005)	Phylogeny of Ruminantia	Supertree, Matrix representation parsimony	Combination of trees based on morphology, genetics, behaviour, physiology
8	Price et al. (2005b)	Phylogeny of Cetartiodactyla	Supertree, Matrix representation parsimony	Combination of different trees based on morphology, genetics, behaviour
9	Gilbert et al. (2006)	Phylogeny of Cervidae	ML; Bayesian	MtDNA: cytochrome b (1140bp), **CO2**; nDNA: alpha-lactalbumin, **PRKC1**
10	Lin and Li (2006)	Tracing rare cervid satellites in *H. inermis*		nDNA: Satellite DNA
11	Cap et al. (2002)	Phylogeny of Cervidae	MP, unweighted characters	Behavioural traits: resting, survey, type of locomotion, postures, feeding activities, interactions with the non-social environment, grooming activities, agonistic and affiliative acts, and play
12	Cap et al. (2008)	Phylogenetic coherence of behaviour with molecular data	MP	Male vocal behaviour
13	Marcot (2007)	Phylogeny of terrestrial artiodactyls	Super matrix	mtDNA: cytochrome b, 12S, 16S rRNA,alpha-lactalbumin, CYP19, lactoferrin
14	Agnarsson and May-Collado (2008)	Phylogeny of Artiodactyla	Bayesian analysis	MtDNA: cytochrome b
15	Zhang and Zhang (2012)	Phylogeny of Cervidae	NJ; Bayesian analysis	MtDNA: whole genome
16	Hassanin et al. (2012)	Phylogeny of Artiodactyla	ML	**MtDNA: whole genome**
17	Wang and Yang (2013)	Phylogeny of Cetartiodactyla	ML; Bayesian analysis	MtDNA: whole genome

MtDNA Mitochondrial DNA
nDNA Nuclear DNA
MP Maximum parsimony
ML Maximum likelihood
NJ Neighbourhood joining

signals. However, the variability of these traits (see also Pérez and Erdoğan, 2014; Ahn et al., 2014 (abstract)) and the relatively low numbers of specimens analysed so far, precluded its assessment.

Before the advent of molecular analysis, Pocock's idea that *H. inermis* is "the most primitive of all existing Cervidae" ((Pocock, 1923), p. 195), which implies that the lineage leading to *H. inermis* split off from all other cervids before antlers have evolved, seems to have been the predominant, but not uncontested view. For instance, Simpson (1945) and Ellerman and Morrison-Scott (1951) presented alternatives to Pocock's "primitive deer hypothesis", without, however, arguing their point. Simpson (1945) stressed, "the classification of the deer presents many difficult, and in large part unsolved, problems" (p. 266) — which sounds like an echo of Garrod's (1877a) conclusion cited above. A concise overview of the status and problems of the phylogenetic classification of *H. inermis* before molecular data became available is given by Bouvrain et al. (1989). For these authors, it is clear that *H. inermis* belongs to Cervidae, but less so whether it may be grouped with Odocoileinae or Cervinae, or whether it defines a sister group to both of these clades. On the weight of the morphological data available at that time, they favour the view that *H. inermis* either is a member of Odocoileinae or constitutes a sister group to them, and that Cervinae are a sister group to the lineage formed by *H. inermis* and Odocoileinae together. They also note, though, that this is not "satisfying" to them ("L'hypothèse (…) est, à notre avis, la plus vraisemblable, bien qu'elle ne soit pas vraiment satisfaisante", p. 89).

Considering our current molecular-based perspective of *H. inermis* phylogeny (see below, following section) it seems ironic that Pocock formulated his hypothesis focussing on differences between *Hydropotes* and *Capreolus*, notably the lacking antler and presence of tusks, preorbital and inguinal glands, and the absence of the metatarsal gland in *Hydropotes*. This focus on differences between the two species rapidly overshadowed the potential close relatedness of *H.inermis* and *Capreolus*, which was suggested by a set of morphological criteria, as pointed out early on, like skull morphology (Rütimeyer, 1881) and soft-tissue peculiarities, such as the brain, the absence of Cowper's glands, and the glans penis (Forbes, 1882), the latter being long, slender, cylindrical and with a subterminal opening in *C. capreolus* (Garrod, 1877b).

Molecular, genetic, and behavioural evidence

More recently, behavioural and molecular characters were increasingly used to probe the phylogeny of *H. inermis*. In behavioural studies, it was noted that the scent-marking behaviour in *H. inermis*, which uses urine or head rubbing resembles more that of antlered deer than that of other ruminants lacking cranial appendages like *Moschus*, which use their musk and caudal glands (Green, 1987; Green and Kattel, 1997), or *Tragulus napu*, which uses its intermandibular glands (Kalina and Adams, 1984). While it was noted that the forehead rubbing of *H. inermis* was reminiscent to that observed in *Capreolus capreolus* (Johansson and Liberg, 1996), yet another analysis, based on locomotion, feeding and non-social and social interactions did not allow resolving the phylogenetic relationships between *H. inermis* and antlered Cervidae (Cap et al., 2002) (Tab. 4, #11). Specifically, in that study, the bootstrap support for a clade encompassing *H. inermis* and *C. capreolus* remained underneath the 50% threshold of acceptance. In contrast, in a maximum parsimony analysis of male vocal behaviour, *H. inermis* and *C. capreolus* did cluster together (Cap et al., 2008) (Tab. 4, #12).

The era of DNA-based, molecular analysis of cervid phylogeny was heralded by Miyamoto et al. (1990), who sequenced the ribosomal RNA from the mitochondria to study the evolutionary relationship of antlered deer. In that study, the authors used *H. inermis* as outgroup. In subsequent studies, authors used additional mitochondrial DNA, different sample compositions and statistical methods to probe the phylogenetic position of *H. inermis*. This might have resulted in conflicting conclusions (Kraus and Miyamoto, 1991; Douzery and Randi, 1997; Randi et al., 1998) (Fig. 4).

The importance of methodology is impressively documented already in the first study providing molecular phylogenetic trees of *H. inermis* (Kraus and Miyamoto, 1991). Using Maximum parsimony (MP) analyses of a ∼2.7 kbp DNA fragment encompassing the mitochondrial 12S and 16S rRNA genes (Tab. 4, #1), these analyses placed *H. inermis* as a sister group to Cervidae when point mutations, i.e. transitions and transversions, and gaps in the sequence were considered. In contrast, when only transversions were considered, *H. inermis* was placed within Cervidae, specifically Odocoileinae/ Capreolinae, as sister to *Odocoileus virginianus*. Further, Douzery and Randi (1997) pointed out that use of a maximum likelihood method with the data of Kraus and Miyamoto (1991) "strongly favours the grouping of *Hydropotes* with *Odocoileus*" (p. 1163). In the same study, Douzery and Randi (1997) also provide an example how the influence of methodology on phylogenetic inference may depend on the particular sequence analysed. Thus, in contrast to the data used by Kraus and Miyamoto (1991), analysis of the phylogenetic signal in the mitochondrial control region (∼1kbp) consistently placed *H. inermis* within Odocoileinae, irrespective of whether transitions or conversions and transitions were considered (Tab. 4, #2). Importantly, it should be mentioned that the study of Douzery and Randi (1997) was the first to provide molecular support for a close relationship between *H. inermis* and *C. capreolus*, which had been suggested in older, but rather neglected, morphological studies (see above, and in particular Bouvrain et al., 1989). Subsequent analyses using additional mitochondrial and nuclear sequences, either from *H. inermis* or other cervids (Douzery and Randi, 1997; Randi et al., 1998; Pitra et al., 2004; Kuznetsova et al., 2005; Gilbert et al., 2006; Hassanin et al., 2012) (Tab. 4, #2,#3, #5, #6, #9, #16) concur to support the placement of *Hydropotes* in Capreolinae, and indeed as a sister to *Capreolus*. Furthermore, although the (statistical) support for this interpretation of the data predictably varies with the genes analysed and exact methods used, this is currently the most accepted interpretation of available data. We would also like to point out that even in the cytochrome b-based study by Agnarsson and May-Collado (2008), which placed *Capreolus* and *Hydropotes* in a clade closer to Muntiacinae and Cervinae than to Odocoileinae, the close association of *Hydropotes* with *Capreolus* was not questioned (Tab. 4, #14). Furthermore, in Heckeberg et al. (2016), *Hydropotes* and *Capreolus* species are placed in an unresolved trichotomy. Lastly, the fact that *H. inermis* and *C. capreolus* are the only cervids sharing family III satellite DNA III also supports a close relationship between these two genera (Lin and Li, 2006) (Tab. 4, #10).

Combined assessment of morphological, genetic and other evidence

Some of the studies just cited already combined information from more than one gene, or even genetic and morphological/paleontological information. For instance, Hassanin and Douzery (2003) (Tab. 4, #4) and Gilbert et al. (2006) (Tab. 4, #9) both analyzed several concatenated mitochondrial and nuclear genes together. Pitra et al. (2004) (Tab. 4, #5) present a cytochrome b-based phylogram that was fossil-constrained. Finally, Cap et al. (2008) combined molecular and behavioural data. A formalized technique that allows to combine different data types is the supertree approach (for reviews, see Sanderson et al., 1998; Bininda-Emonds et al., 2002). Key to this methodology is that instead of individual characters, topologies of phylogenetic trees constructed based on such characters are interpreted as phylogenetic evidence. Tree topologies are encoded as matrices, which then may be combined using a variety of algorithms. In a supertree analysis of Artiodactyla, Price et al. (2005b) found that *H. inermis* grouped with antlered deer, in agreement with the molecular genetic studies discussed above (Tab. 4, #8). This analysis employed a variant of the supertree approach referred to as matrix representation with parsimony (MRP). It was obtained by integrating 201 source trees from 141 publications. In contrast, Hernández Fernández and Vrba (2005) (Tab. 4, #7) applied this methodology to a set of 124 phylogenetic trees for Ruminantia from 158 publications, 67 of these publications overlapped with those used by Price et al. (2005b). They also used a MRP-based approach, which, however, seemed to differ in several aspects from the that used by Price et al. (2005b). Their results suggested that *H. inermis* does not belong to

antlered deer, but is sister group to the latter. Yet their data also show that the support for this conclusion, as measured by the Bremer decay index, remained low. Their significance of our understanding of Artiodactyla and Ruminantia phylogeny, notwithstanding these analyses, do not help to resolve the issue of the phylogenetic position of *H. inermis*. Their conflicting conclusions may be due to differences in the database or exact methodology used in these studies. Of note, both research groups point out a lack of data for lineages in the phylogeny that is particularly relevant to derive the position of *H. inermis*. Thus, Price et al. (2005b, p. 455) indicate that their analysis "highlights areas in need of further phylogenetic research and data collection (...) especially on (...) Cervidae (...), where very little phylogenetic information is currently available". And Hernández Fernández and Vrba (2005, p. 291) stress that "the most serious gaps in our knowledge concern the basal relationships of Odocoileini (...). This situation must be recognized and remedied...", which is supported by a recent study on Cervidae (Heckeberg et al., 2016). Hernández Fernández and Vrba (2005) also repeatedly point out the significant role of fossil evidence for reconstructing a dependable phylogeny. Indeed, the presence of fossils in a phylogenetic tree can change the topology, compared with analyses where only extant species are used (Gauthier et al., 1988; Axsmith et al., 1998). Among others, Scott and Janis (1987) and Gentry and Hooker (1988) already included ruminant fossils in cladistic analyses, while Lister et al. (2005) combined morphological and molecular approaches to determine the phylogenetic position of the giant deer, *Megaloceros giganteus*.

The rocky road of *Hydropotes inermis* — Fossil evidence

Overall, the fossil record that so far could be linked to *H. inermis* is exceedingly scarce. Specimens interpreted as possible direct predecessor to *H. inermis* or intermediate forms between *H. inermis* and other cervids (or ruminants) are still unknown. The rather short list of where *H. inermis*-related fossils have so far been found was already given above (see section "Biogeography"). The better diagnosed ones from Tangshan (Hebei), Choukoutien (Beijing) and Anyang (Henan province) include some upper canines and other teeth, lower jaws, one juvenile skull, and limb bones (Young, 1932; de Chardin and Young, 1936). The most ancient findings are those from Tangshan and Choukoutien, which are dated back to the Lower Pleistocene (de Chardin and Young, 1936). To the best of our knowledge, *H. inermis* fossils from Korea have not been described yet. To date, this age estimate seems the only evidence that may be linked with the genetic record. Considering that fossils available closely resemble contemporary animals — although, as noted by Young (1932), extinct *H. inermis* might have been somewhat larger than contemporary forms — it seems reasonable to speculate that the species originated well before the period for which fossils are available. Unfortunately, this rather vague estimate is not informative with respect to the affinity of *H. inermis*, as it does not allow to relate the fossil appearance of the species with any of the critical splits of the phylogenetic tree within Cervidae (see e.g., Pitra et al., 2004, fig. 3; Gilbert et al., 2006, fig. 4). No fossils are known that might be interpreted as transitional forms between *H. inermis* and its purported relatives.

From past to future

If what we know about the past of *H. inermis* is rather limited, what may we say about its future? As documented above (see section "Biogeography"), numbers of free living *H. inermis* are not really known, but rather small, and probably in decline (Harris and Duckworth, 2015). On the other hand, breeding under semi-feral conditions and in captivity seems rather straightforward, and conservation programs are under way, notably in China (Hu et al., 2006; Min, 2013; Yabin, 2013). Still, recommendations whether combine (Shi et al., 2014) or not combine (Hu et al., 2006, 2007) distinct Chinese subpopulations are conflicting, which reflects a deeper lack of scientific understanding of the internal structure of the species *H. inermis* and its subpopulations. Any conservation effort must confront and address these issues, which have been around since the early years of *H. inermis* description. We did not find active conservation programs for *H. inermis* in Korea. Traditionally, two subspecies of *H. inermis* are recognized: *H. i. inermis* occurs in China, and *H. i. argyropus* occurs in Korea. Today, these populations must be designated as allopatric due to habitat fragmentation; up to about hundred years ago, they were parapatric (Ohtaishi and Gao, 1990, fig. 4; Xu et al., 1997). The two subspecies are said to differ by pelage colour. This is so far the only criterion on which the diagnosis is based on, although information on pelage colour is still conflicting (Heude, 1884; Kori, 1922; Tate, 1947). Kori (1922) described differences regarding canines and the skull. However, he had access to only a single Korean specimen and some Chinese specimens. A more recent study aimed to investigate the geographical variation in the Hydropotes skull and test the validity of the traditional subspecies classification (Kim et al., 2015b). This study was based on a much larger sample size for both subspecies. It did not reveal any differences between the two allopatric populations. So far, both mitochondrial DNA and (nuclear) microsatellites have been used to study the population structure of *H. inermis* (e.g., Koh et al., 2009; Yu et al., 2011b; Kim et al., 2014, 2015a). While these studies yielded valuable insight in the genetic diversity of various populations both in China and in Korea (see above, section "Genetics"), they generally do not support the notion that Korean and Chinese populations of *H. inermis* might be genetically distinct. A notable exception is the microsatellite study described by Yu et al. (2011b), where it was found that allele sizes at three microsatellite loci were well separated in Chinese and Korean water deer gene pools. However, the authors also caution that "further studies using larger numbers of Korean water deer should be performed" (p. 6) before this lead might be sensibly interpreted. While the origin of species is ultimately due to a genetic process, just how much or which genetic changes allow to define a novel species is contentious, or plainly unknown. As Zachos (2016a) pointed out, species ranking is an arbitrary decision, as nature has fuzzy boundaries and we humans try to fit it into a binary system (for a detailed discussion of this issue, see, e.g., Zachos et al., 2013; Zachos, 2016a. What is clear, though, is that, genetic data available for *H. inermis* are far too few to seriously probe whether the two allopatric populations may be considered subspecies, or even different species, as has also been suggested (Heude, 1884; Tate, 1947). Zachos et al. (2013) proposed potential guidelines how to recognize species when few data are available. Accordingly, it would be best to "compare them to data from the same marker in better-studied closely related pairs of sister species...If no such data exist, then the single genetic finding maybe formulated as a two-species hypothesis that needs further testing" (Zachos et al., 2013, p. 4). Besides the two (sub-) species under investigation, there are no further sister species and therefore, it might be reasonable to apply the second criterion. We do not know whether the Korean and Chinese (or European) populations of *H. inermis* may or can crossbreed. At least we are not aware of any published studies addressing this issue. Thus, we cannot even test one of the more prominent species concepts, referred to as the Biological Species Concept, which posits that we may distinguish two species if these are reproductively isolated "due to intrinsic isolation mechanisms, not due to extrinsic factors such as a geographical barrier" (Zachos, 2016a, p. 110). Since most of the genetic data is based on mitochondrial sequences, mitochondrial introgression may pose a further problem blurring phylogenetic relationships "up to the point that in some populations most or even all animals carry mtDNA from a closely related but different species ("mitochondrial capture")" (p. 4, Zachos et al., 2013, see also: Bradley and Baker, 2001; Baker and Bradley, 2006). Therefore, for the time being, the question whether *Hydropotes* is monospecific cannot be answered. Clearly, there is an urgent need for more data before the population structure, and the subspecies structure, of *H. inermis* may be sensibly discussed. Recently, a taxonomic revision of the species has been proposed (Groves, 2016). An integrative approach, using both molecular and morphometric data, allowed to successfully identify squirrel species (Wauters et al., 2017) and thus, such an approach might help to clarify the taxonomic status

of the water deer. The species concept in taxonomy is currently under debate (Gippoliti and Groves, 2013; Zachos et al., 2013); a (new) taxonomic assignment to *H. inermis* allopatric populations will likely have impacts on rational efforts of conservation and wildlife management and therefore, these questions are also of eminent practical importance (see e.g., Gippoliti and Groves, 2013; Zachos, 2016b). Currently, protection seems to be biased towards the Chinese population of *H. inermis*.

Conclusions

In this review, we summarize the to-date available information on the biology of the water deer, *Hydropotes inermis* and highlight the potential for future research involving this species. Morphological studies mostly focused on the skull, while the skeleton and soft-tissues have been rather neglected. A deeper knowledge on its morphology, biology, ecology and genetics are required in order to manage and conserve the species. This also requires a more intense international collaboration between scientists and managing institutions from countries hosting the species. The weight of genetic evidence favours the placing of *Hydropotes* within Capreolinae/Odocoileinae, and indeed as closest relative to *Capreolus*. However, in the light of the limited raw material available and phylogenetic methods performed, the factual basis is still restricted, and its interpretation somewhat variable. Phylogenetic studies on ruminants and artiodactyls generally include *H. inermis* in the sample, but its phylogenetic positioning appears to be a by-product, rather than a principal research aim. Moreover, none of the genetic traits characterized so far are to the antlerless state of male *H. inermis*, or their prominent canines, i.e. the morphological characters defining their contested phylogenetic classification. The focus on mitochondrial genetic markers, i.e. the matrilineage, also limits our understanding of the population structure and dynamics of these animals. Moreover, the absence of described fossils of *Hydropotes* in Korea as well as the absence of diagnostic phenotypic traits between allopatric populations combined with their genetic and morphological conformity, question the conventional (sub-) species rank of *H. inermis*. The scarcity of fossil remains, and the complete lack of what may be considered transitory forms between *H. inermis* and its relatives, does not allow us to complement, and test results from molecular phylogenetic analyses. Yet, while the access to additional fossils can hardly be planned, further genetic studies might profit from genes involved in dental and bone development and antler induction. While for the latter process, genes are still to be discovered, genes involved in tooth growth might eventually be informative also for other mammals with excessive upper canines.

References

Agnarsson I., May-Collado L.J., 2008. The phylogeny of Cetartiodactyla: The importance of dense taxon sampling, missing data, and the remarkable promise of cytochrome b to provide reliable species-level phylogenies. Mol. Phylogenet. Evol. 48(3): 964–985.

Ahn D., 2008. Carpal bones and Tarsal bones in Korean Chinese water deer (*Hydropotes inermis argyropus*, Heude 1884). FASEB J. 22: 772.1.

Ahn D.C., Kim H.C., Tae H.J., Kang H.S., Kim N.S., Park S.Y., Kim I.S., 2008. Branching Pattern of Aortic Arch in the Korean Water Deer. J. Vet. Med. Sci. 70(10): 1051–1055.

Ahn D., Sim J.H., Park B.Y., Kim I.S., 2014. Various branching pattern of aortic arch in the Siberian roe deer. FASEB J. 28: 543.7.

Aigner J.S., 1981. Archaeological Remains in Pleistocene China. University of Michigan: Beck.

Aitchison J., 1946. Hinged Teeth in Mammals: A Study of the Tusks of Muntjacs (*Muntiacus*) and Chinese Water Deer (*Hydropotes inermis*). Proc. Zool. Soc. London 116(2): 329–338.

Allen G.M., 1940. The mammals of China and Mongolia, part 2. New York: American Museum of Natural History.

Arnold H., 1993. Atlas of mammals in Britain. 1st ed. London: Her Majesty's Stationery Office.

Axmacher H., Hofmann R.R., 1988. Morphological characteristics of the masseter muscle of 22 ruminant species. J. Zool. 215(3): 463–473.

Axsmith B.J., Taylor E.L., Taylor T.N., 1998. The limitations of molecular systematics: a palaeobotanical persective. Taxon 47: 105–108.

Ayres W.S., Rhee S.N., 1984. The Acheulean in Asia? A review of research on Korean Palaeolithic culture. Proc. Prehist. Soc. 50: 35–48.

Baker R.J., Bradley R.D., 2006. Speciation in mammals and the genetic species concept. J. Mamm. 87(4): 643–662.

Barrette C., 1977. Fighting Behavior of Muntjac and the Evolution of Antlers. Evolution 31(1): 169–176.

Battersby J., 2005. UK mammals: Species status and population trends. JNCC/Tracking Mammals Partnership, Peterborough.

Bininda-Emonds O., 2014. An introduction to supertree construction (and partitioned phylogenetic analyses) with a view toward the distinction between gene trees and species trees. In: Garamszegi L.Z. (Ed.) Modern Phylogenetic Comparative Methods and their Application in Evolutionary Biology. Berlin, Heidelberg: Springer Berlin Heidelberg. 19–48.

Bininda-Emonds O.R.P., Gittleman J.L., Steel M.A., 2002. The (Super)Tree of Life: Procedures, Problems, and Prospects. Annual Annu. Rev. Ecol. Syst. 33(1): 265–289.

Bogenberger J.M., Neitzel H., Fittler F., 1987. A highly repetitive DNA component common to all Cervidae: its organization and chromosomal distribution during evolution. Chromosoma 95(2): 154–161.

Boué C., 1970. Morphologie fonctionelle des dents labiales chez les ruminants. Mammalia 34: 696–711. [In French]

Bouvrain G., Geraads D., Jehenne Y., 1989. Nouvelles données relatives à la classification des Cervidae (Artiodactyla, Mammalia). Zool. Anz. 223(1–2): 82–90. [In French]

Bradley R.D., Baker R.J., 2001. A test of the genetic species concept: cytochrome-b sequences and mammals. J. Mammal. 82(4): 960–973.

Brooke V., 1872. On *Hydropotes inermis* and its Cranial Characters as compared with those of *Moschus moschiferus*. Proc. Zool. Soc. London 1872: 522–525.

Brooke V., 1878. On the classification of Cervidae with a synopsis of the existing species. Brooke V. 1872. On *Hydropotes inermis* and its Cranial Characters as compared with those of *Moschus moschiferus*. Proc. Zool. Soc. London 46(1): 883–928.

Bubenik A., 1983. Taxonomy of Pecora in relation to morphophysiology of their cranial appendices. In: Brown R. (Ed.) Antler development in Cervidae. Kingsville, Texas: Caesar Kleberg Wildlife Research Institute. 163–185.

Bubenik A.B., 1990. Epigenetical, morphological, physiological, and behavioral aspects of evolution of horns, pronghorns, and antlers. In: Bubenik G.A., Bubenik A.B. (Eds.) Horns, Pronghorns, and Antlers. New York.: Springer. 3–113.

Buntjer J.B., Nijman I.J., Zijlstra C., Lenstra J.A., 1998. A satellite DNA element specific for roe deer (*Capreolus capreolus*). Chromosoma 107(1): 1–5.

Bützler W., 1988. Wasserhirsche. In: Grzimek B. (Ed.) Grzimeks Enzyklopädie Säugetiere. 2. Auflage. München: Kindler Verlag. 198–199.

Cap H., Aulagnier S., Deleporte P., 2002. The phylogeny and behaviour of Cervidae (Ruminantia Pecora). Ethol. Ecol. Evol. 14(3): 199–216.

Cap H., Deleporte P., Joachim J., Reby D., 2008. Male vocal behavior and phylogeny in deer. Cladistics 24(6): 917–931.

Ceacero F., 2016. Long or Heavy? Physiological Constraints in the Evolution of Antlers. J. Mamm. Evol. 23(2): 209–216.

Chaplin R.E., 1977. Deer. Littlehampton Book Services Ltd: Blandford Press.

de Chardin P.T., Young C.C., 1936. On the mammalian remains from the archaeological site of Anyang. Nanking: Geological Survey of China.

Chen Y.J., Liu K.H., Chu W.L., 2016. New Record of Water Deer (*Hydropotes inermis*) from Iron Age Archeological Sites in Central Taiwan. Collect. Res. 29: 31–39.

Chen M., Pu A., He X., Zhang E., Ding Y., Wang T., Cai Y., Pei E., Yuan X., 2015. Chinese water deer (*Hydropotes inermis*) reintroduction in Nanhui, Shanghai, China. Pak. J. Zool. 47(5): 1499–1501.

Clauss M., 2014. Soft tissue characteristics for the reconstruction of ruminant phylogeny. Zitteliana 32: 33–46.

Clauss M., Hofmann R.R., Streich W.J., Fickel J., Hummel J., 2008. Higher masseter muscle mass in grazing than in browsing ruminants. Oecologia 157(3): 377–385.

Cooke A., Farrell L., 1998. Chinese Water Deer. The Mammal Society, London and The British Deer Society, Fordingbridge.

Corbet G.B., Harris S., 1991. The Handbook of British Mammals. 3rd ed. London: Blackwell Scientific Publications.

Dementyeva P.V., Trifonov V.A., Kulemzina A.I., Graphodatsky A.S., 2010. Reconstruction of the putative cervidae ancestral karyotype by chromosome painting of siberian roe deer (*Capreolus pygargus*) with dromedary probes. Cytogenet. Genome Res. 128(4): 228–235.

DeMiguel D., Azanza B., Morales J., 2014. Key innovations in ruminant evolution: A paleontological perspective. Integr. Zool. 9(4): 412–433.

Dobroruka L.J., 1970. Fecundity of the Chinese Water Deer *Hydropotes inermis* Swinhoe, 1870. Mammalia 34: 161–162.

Douzery E, Randi E., 1997. The mitochondrial control region of Cervidae: evolutionary patterns and phylogenetic content. Mol. Biol. Evol. 14(1): 1154–1166.

Dubost G., Charron F., Courcoul A., Rodier A., 2008. Population characteristics of a semi-free-ranging polytocous cervid, *Hydropotes inermis*. Mammalia 72(4): 333–343.

Dubost G., Charron F., Courcoul A., Rodier A., 2011. Social organization in the Chinese water deer, *Hydropotes inermis*. Acta Theriol. 56(2): 189–198.

Ellerman J.R., Morrison-Scott T.C.S., 1951. Checklist of Palaearctic and Indian mammals 1758 to 1946. London.

Fang S., Wan Q., 2002. A genetic fingerprinting test for identifying carcasses of protected deer species in China. Biol. Conserv. 103(3): 371–373.

Feer F., 1982. Quelques observations éthologiques sur l'Hydropote de Chine, *Hydropotes inermis* (Swinhoe, 1870) en captivité. Mamm. Biol. — Zeitschrift für Säugetierkunde 47: 175–185. [In French]

Ferguson-Smith M.A., Trifonov V., 2007. Mammalian karyotype evolution. Nat. Rev. Genet. 8(12): 950–62.

Forbes W.A., 1882. Supplementary Notes on the Anatomy of the Chinese Water-Deer (*Hydropotes inermis*). Proc. Zool. Soc. London 50(4): 636–638.

Garrod A.H., 1877a. Notes on the Anatomy of the Chinese Water Deer (*Hydropotes inermis*). Proc. Zool. Soc. London 1877: 789–792.

Garrod A.H., 1877b. Notes on the Visceral Anatomy and Osteology of the Ruminants, with a suggestion regarding a method of expressing the relations of species by means of formulae. Proc. Zool. Soc. London 1877: 2–18.

Gauthier J., Kluge A.G., Rowe T., 1988. Amniote Phylogeny and the Importance of Fossils. Cladistics 4(2): 105–209.

Geist V., 1998. Deer of the World: Their Evolution, Behaviour, and Ecology. Mechanicsburg, Pennsylvania: Stackpole Books.

Gentry A.W., Hooker J.J., 1988. The phylogeny of the Artiodactyla. In: The phylogeny and classification of the tetrapods, 2. Clarendon Press, Oxford. 235–272.

Gilbert C., Ropiquet A., Hassanin A., 2006. Mitochondrial and nuclear phylogenies of Cervidae (Mammalia, Ruminantia): Systematics, morphology, and biogeography. Mol. Phylogenet. Evol. 40(1): 101–117.

Gippoliti S., Groves C.P., 2013. "Taxonomic inflation" in the historical context of mammalogy and conservation. Hystrix 23(2): 8–11. doi:10.4404/hystrix-23.2-8685

Gray J.E., 1872. Catalogue of ruminant Mammalia (Pecora, Linnaeus) in the British Museum. London: Taylor and Francis.
Green M.J.B., 1987. Scent-marking in the Himalayan musk deer (*Moschus chrysogaster*). J. Zool. 1(4): 721–737.
Green M.J.B, Kattel B., 1997. Musk deer: little understood, even its scent. First International Symposium on Endangered Species Used in Traditional East Asian Medicine: Substitutes for Tiger Bone and Musk. Hongkong. 7–8.
Groves C., 2016. Systematics of the Artiodactyla of China in the 21st century. Zool. Res. 37(3): 119–125.
Groves C.P., Grubb P., 1987. Relationships of Living Deer. Biology and Management of the Cervidae. 20–59.
Guo G., Zhang E., 2005. Diet of the Chinese water deer (*Hydropotes inermis*) in Zhoushan Archipelago, China. Acta Theriol. Sin. 25(2): 122–130.
Hamilton E., 1873. May 20, 1873. Proc. Zool. Soc. London 41(1): 472–517.
Harris R.B., Duckworth J.W., 2015. *Hydropotes inermis*. IUCN Red List Threat. Species.
Harris S., Morris P., Wray S., Yalden D., 1995. A review of British mammals: population estimates and conservation status of British mammals other than cetaceans. Peterborough: The Joint Nature Conservation Committee.
Hartmann N., Scherthan H., 2004. Characterization of ancestral chromosome fusion points in the Indian muntjac deer. Chromosoma 112(5): 213–220.
Hassanin A., Delsuc F., Ropiquet A., Hammer C., Jansen Van Vuuren B., Matthee C., Ruiz-Garcia M., Catzeflis F., Areskoug V., Nguyen T.T., Couloux A., 2012. Pattern and timing of diversification of Cetartiodactyla (Mammalia, Laurasiatheria), as revealed by a comprehensive analysis of mitochondrial genomes. C. R. Biol. 335(1): 32–50.
Hassanin A., Douzery E.J.P., 2003. Molecular and morphological phylogenies of Ruminantia and the alternative position of the Moschidae. Syst. Biol. 52(2): 206–228.
He X., Chen M., Zhang E., 2015. Dispersal of reintroduced Chinese water deer after release in Nanhui East Shoal Wildlife Sanctuary of Shanghai, China. Ital. J. Zool. 82(4): 582–591.
Heckeberg N.S., 2017. Origination of antlerogenesis. J. Morphol. 278(2): 182–202.
Heckeberg N.S., Erpenbeck D., Wörheide G., Rössner G.E., 2016. Systematic relationships of five newly sequenced cervid species. PeerJ 4: e2307.
Heintz E., 1963. Les caractères distinctifs entre métatarses de Cervidae et Bovidae actuels et fossiles. Mammalia 27(2): 200–209. [In French]
Henthorn W.E., 1966. Recent archaeological activity in North Korea (I): The cave at Misong-ni. Asian Perspect. 73–78.
Hernández Fernández M., Vrba E.S., 2005. A complete estimate of the phylogenetic relationships in Ruminantia: a dated species-level supertree of the extant ruminants. Biol. Rev. Camb. Philos. Soc. 80(2): 269–302.
Heude P., 1884. Comptes rendus hebdomadaires des séances de l'Académie des science. Paris. [In French]
Hillson S., 2016. Mammal bones and teeth: an introductory guide to methods of identification. Routledge.
Hofmann R.R., Kock R.A., Ludwig J., Axmacher H., 1988. Seasonal changes in rumen papillary development and body condition in free ranging Chinese water deer (*Hydropotes inermis*). J. Zool. 216(1): 103–117.
Hsieh L.J., Cheng Y.M., Wang Y.C., Lin C.C., Li Y.C., 2014. Organization and evolution of a novel cervid satellite DNA with yeast CDEI-like repeats. Zool. Stud. 53(1): 25.
Hsu T.C., Benirschke K., 1973. *Hydropotes inermis* (Chinese water deer). In: An Atlas of Mammalian Chromosomes. New York: Springer. 213–215.
Hu J., Fang S.G., Wan Q.H., 2006. Genetic diversity of Chinese water deer (*Hydropotes inermis inermis*): Implications for conservation. Biochem. Genet. 44(3–4): 161–172.
Hu J., Pan H.J., Wan Q.H., Fang S.G., 2007. Nuclear DNA microsatellite analysis of genetic diversity in captive populations of Chinese water deer. Small Rumin. Res. 67(2–3): 252–256.
Hudson R., 1872. May 21, 1872. Proc. Zool. Soc. London 40(1): 635–680.
Jabbour H., Hayssen V., Bruford M., 1997. Conservation of deer: contributions from molecular biology, evolutionary ecology, and reproductive physiology. J. Zool. 243(3): 461–484.
Janis C.M., Shoshitaishvili B., Kambic R., Figueirido B., 2012. On their knees: distal femur asymmetry in ungulates and its relationship to body size and locomotion. J. Vertebr. Paleontol. 32(2): 433–445.
Johansson A., Liberg O., 1996. Functional Aspects of Marking Behavior by Male Roe Deer (*Capreolus capreolus*). J. Mammal. 77(2): 558–567.
Jones M.L., 1977. Longevity of mammals in captivity. Int. Zoo News 159: 16–19.
Jung J., Shimizu Y., Omasa K., 2011. Analysing Habitat Characteristics for Korean Water Deer (*Hydropotes inermis argyropus*) in Korea Using Remote Sensing and Landscape Metrics. Eco-Enginnering 23(3): 75–80.
Kahle D., Wickham H., 2013. Spatial Visualization with `ggplot2`. R J. 5(1): 144–161.
Kalina J., Adams M.A., 1984. Intermandibular Gland Secretions of Larger Malayan Mouse-Deer (*Tragulus napu*). J. Mammal. 65(4): 715–718.
Kay R.N.B., 1987. Weights of salivary glands in some ruminant animals. J. Zool. 211(3): 431–436.
Kierdorf U., Li C., Price J.S., 2009. Improbable appendages: Deer antler renewal as a unique case of mammalian regeneration. Semin. Cell Dev. Biol. 20(5): 535–542.
Kim B.J., Lee Y.S., Park Y.S., Kim K.S., Min M.S., Lee S.D., Lee H., 2014. Mitochondrial genetic diversity, phylogeny and population structure of *Hydropotes inermis* in South Korea. Genes Genet. Syst. 89(5): 227–235.
Kim B.J., Lee N.S., Lee S.D., 2011a. Feeding diets of the Korean water deer (*Hydropotes inermis argyropus*) based on a 202 bp rbcL sequence analysis. Conserv. Genet. 12(3): 851–856.
Kim B.J., Lee S.D., 2011. Home range study of the Korean water deer (*Hydropotes inermis agyropus*) using radio and GPS tracking in South Korea: comparison of daily and seasonal habitat use pattern. J. Ecol. F. Biol. 34(4): 365–370.
Kim B.J., Oh D.H., Chun S.H., Lee S.D., 2011b. Distribution, density, and habitat use of the Korean water deer (*Hydropotes inermis argyropus*) in Korea. Landsc. Ecol. Eng. 7(2): 291–297.
Kim E.K., Kim H.R., Jeon S.H., Park Y.C., 2013a. Complete mitochondrial genome of a water deer subspecies, *Hydropotes inermis argyropus* (Cervidae: Hydropotinae). Mitochondrial DNA 24(1): 17–18.
Kim H.R., Kim E.K., Jeon M.G., Park Y.C., 2015a. Intraspecific Phylogeny of the Korean Water Deer, *Hydropotes inermis argyropus* (Artiodactyla, Cervidae). Anim. Syst. Evol. Diversity 31(2): 118–121.
Kim H.R., Park Y.C., 2015. Intraspecific comparison of two complete mitogenome sequences from the Korean water deer (Cervidae: *Hydropotes inermis argyropus*). Mitochondrial DNA 1–3.
Kim K.G., Cho D.G., 2005. Status and ecological resource value of the Republic of Korea's De-militarized Zone. Landsc. Ecol. Eng. 1(1): 3–15.
Kim W., Kim S., Choi H., Truong N.D., Thong L.E.M., Kim J.H., Xiao R., Park K.K., Seo K., Lee H., Kim B.S., Yoo M.H., Park C., 2010. Discrimination of animal species using polymorphisms of the nuclear gene zinc finger protein 238. J. Agric. Food Chem. 58(4): 2398–2402.
Kim Y.K., Suzuki S., Na K.J., Lee H., Kimura J., 2013b. Skull Growth of the Korean Water Deer, *Hydropotes inermis argyropus*. J. Vet. Med. Sci. 75(7): 867–878.
Kim Y.K., Koyabu D., Lee H., Kimura J., 2013c. Sexual Dimorphism of Craniomandibular Size in the Korean Water Deer, *Hydropotes inermis argyropus*. J. Vet. Med. Sci. 75(9): 1153–1159.
Kim Y.K., Koyabu D., Lee H., Kimura J., 2015b. Cranial morphological homogeneity in two subspecies of water deer in China and Korea. J. Vet. Med. Sci. 77(11): 1427–1435.
Koh H.S., Lee B.K., Wang J., Heo S.W., Jang K.H., 2009. Two sympatric phylogroups of the Chinese water deer (*Hydropotes inermis*) identified by mitochondrial dna control region and cytochrome b gene analyses. Biochem. Genet. 47(11–12): 860–867.
König H.E., Liebich H.G., 2005. Anatomie der Haussäugetiere. 5th ed. Stuttgart: Schattauer GmbH. [In German]
Kori T., 1922. LXIV. — On some new mammals from Korea and Manchuria. J. Nat. Hist. Ser. 9 10(60): 607–614.
Kraus F., Miyamoto M.M., 1991. Rapid cladogenesis among the pecoran ruminants: evidence from mitochondrial DNA sequences. Syst. Zool. 40(2): 117–130.
Kruska D., 1970. Über die Evolution des Gehirns in der Ordnung Artiodactyla Owen, 1848, insbesondere der Teilordnung Suina Gray, 1868. Mamm. Biol. — Zeitschrift fur Saugetierkunde 35(4): 214–238. [In German]
Kumschick S., Bacher S., Evans T., Marková Z., Pergl J., Pyšek P., Vaes-Petignat S., van der Veer G., Vilà M., Nentwig W., 2015. Comparing impacts of alien plants and animals in Europe using a standard scoring system. J. Appl. Ecol. 52(3): 552–561.
Kuznetsova M.V., Kholodova M.V., Danilkin A.A., 2005. Molecular phylogeny of deer (Cervidae: Artiodactyla). Russian J. Genet. 41(7): 742–749.
Lee Y.S., Choi S.K., An J., Park H.C., Kim S.I., Min M.S., Kim K.S., Lee H., 2011. Isolation and characterization of 12 microsatellite loci from Korean water deer (*Hydropotes inermis argyropus*) for population structure analysis in South Korea. Genes Genomics 33(5): 535–540.
Leinders J.J.M., 1979. On the osteology and function of the digits of some ruminants and their bearing on taxonomy. Mamm. Biol. — Zeitschrift für Säugetierkd 44: 305–319.
Leinders J.J.M., Heintz E., 1980. The configuration of the lacrimal orifices in Pecorans and Tragulids (Artiodactyla, Mammalia) and its significance for the distinction between Bovidae and Cervidae. Beaufortia 30(7): 155–160.
Li C., Suttie J., 2012. Morphogenetic aspects of deer antler development. Front. Biosci. (Elite edition) 4: 1836–1842.
Li Y.C., Lin C.C., 2011. Cervid satellite DNA and karyotypic evolution of Indian muntjac. Genes Genomics 34(1): 7–11.
Li Y.C., Cheng Y.M., Hsieh L.J., Ryder O.A., Yang F., Liao S.J., Hsiao K.M., Tsai F.J., Tsai C.H., Lin C.C., 2005. Karyotypic evolution of a novel cervid satellite DNA family isolated by microdissection from the Indian muntjac Y-chromosome. Chromosoma 114(1): 28–38.
Liang W., Yu J., Li J., Wu H., Wu X.B., 2011. Development of a species-specific AFLP-based SCAR marker for authentication of black muntjac (*Muntiacus crinifrons*). Mol. Ecol. Resour. 11(1): 162–165.
Lin C.C., Li Y.C., 2006. Chromosomal distribution and organization of three cervid satellite DNAs in Chinese water deer (*Hydropotes inermis*). Cytogenet. Genome Res. 114(2): 147–154.
Lister A.M., 1984. Evolutionary and ecological origins of British deer. Proc. R. Soc. Edinburgh Sect. B-Biological Sci. 82(4): 205–229.
Lister A.M., Edwards C.J., Nock D.A.W., Bunce M., van Pijlen I.A., Bradley D.G., Thomas M.G., Barnes I., 2005. The phylogenetic position of the "giant deer" *Megaloceros giganteus*. Nature 438(7069): 850–853.
Liu W., Wu X., Pei S., Wu X., Norton C.J., 2010. Huanglong Cave: A Late Pleistocene human fossil site in Hubei Province, China. Quat. Int. 211(1–2): 29–41.
Macdonald D., Burnham D., 2011. The State of Britain's Mammals: a focus on invasive species. People's Trust for Endangered Species.
Makunin A.I., Kichigin I.G., Larkin D.M., O'Brien P.C.M., Ferguson-Smith M.A., Yang F., Proskuryakova A.A., Vorobieva N.V., Chernyaeva E.N., O'Brien S.J., Graphodatsky A.S., Trifonov V.A., 2016. Contrasting origin of B chromosomes in two cervids (Siberian roe deer and grey brocket deer) unravelled by chromosome-specific DNA sequencing. BMC Genomics 17(1): 618.
Marcot J.A., 2007. Molecular phylogeny of terrestrial artiodactyls: conflicts and resolution. In: Prothero D.R., Foss S.E. (Eds.) The evolution of artiodactyls. John Hopkins University Press. 4–18.
Mauget C., Mauget R., 2009. Maternal investment and reproductive success in Chinese water deer. Curr. Zool. 55(2): 102–110.
Maurin H., Gavazzi E., 1997. L'homme et les mammifères de France métropolitaine: évolution historique et introductions d'espèces dans les milieux humides et aquatiques. Bulletin français de la pêche et da la pisciculture 344–345: 117–132. [in French]
McKenzie A.A., 1990. The ruminant dental grooming apparatus. Zool. J. Linn. Soc. 99(2): 117–128.
Mennecart B., DeMiguel D., Bibi F., Rössner G.E., Métais G., Neenan J.M., Wang S., Schulz G., Müller B., Costeur L., 2017. Bony labyrinth morphology clarifies the origin and evolution of deer. Sci. Rep. 7(1): 13176.
Meunier K., 1963. Die Knickungsverhältnisse des Cervidenschädels. Mit Bemerkungen zur Systematik. Zool. Anz. 172: 184–216. [In German]
Min C., 2012. Preliminary survey on distribution of Chinese water deer in Hanshan and Chuzhou area, Anhui province, China. Deer Spec. Gr. Newsl. 24 224(3): 285–288.
Min H., 2013. City reintroduces Chinese water deer for eco-tourism. Shanghai Dly.
Miyamoto M.M., Kraus F., Ryder O.A., 1990. Phylogeny and evolution of antlered deer determined from mitochondrial DNA sequences. Proc. Natl. Acad. Sci. U.S.A. 87(16): 6127–6131.
Morejohn G.V., Hearst J., Dailey C., 2005. Postcranial carpalial support for the extinct cervid genus Bretzia with associated antler. J. Mammal. 86(1): 115–120.

Morlat S., 2010. Atlas radiographique et ostéologique du chevreuil (*Capreolus capreolus* L.). Toulouse. [In French]
Neitzel H., 1987. Chromosome Evolution of Cervidae: Karyotypic and Molecular Aspects. In: Obe G., Basler A. (Eds). Cytogenetics. Basic and applied aspects. 1st ed. Berlin: Springer. 90–112.
Neitzel H., Benedum U., Bogenberger J., Fittler F., Sperling K., 1986. Chromosomale und molekulare Evolution bei Cerviden. Verhandlungen der Dtsch. Zool. Gesellschaft 79: 149–159. [In German]
Nentwig W., Kühnel E., Bacher S., 2010. A generic impact-scoring system applied to alien mammals in Europe. Conserv. Biol. 24(1): 302–311.
Newson S.E., Johnston A., Renwick A.R., Baillie S.R., Fuller R.J., 2012. Modelling large-scale relationships between changes in woodland deer and bird populations. J. Appl. Ecol. 49(1): 278–286.
Nickel R., Schummer A., Seiferle E., 1992. Lehrbuch der Anatomie der Haustiere. Band I: Bewegungsapparat. 6th ed. Berlin, Hamburg: verlag Paul Parey.
Ohtaishi N., Gao Y., 1990. A review of the distribution of all species of deer (Tragulidae, Moschidae and Cervidae) in China. Mamm. Rev. 20(2–3): 125–144.
Pei W.C., 1930. On a Collection of Mammalian Fossils from Chiachiashan near Tangshan. Bull. Geol. Soc. China 9(4): 371–377.
Pérez W., Erdoğan S., 2014. Arterial Thoracic Vascularization in Some Deer Species: Pampas Deer (*Ozotoceros bezoarticus*), Brown Brocket Deer (*Mazama gouazoubira*) and Axis Deer (*Axis axis*). Anat. Histol. Embryol. 43(6): 490–494.
Pillay P., Manger P.R., 2007. Order-specific quantitative patterns of cortical gyrification. Eur. J. Neurosci. 25(9): 2705–2712.
Pitra C., Fickel J., Meijaard E., Groves C.P., 2004. Evolution and phylogeny of old world deer. Mol. Phylogenet. Evol. 33(3): 880–895.
Pocock R.I., 1923. On the External Characters of Elaphurus, Hydropotes, Pudu, and other Cervidae. Proc. Zool. Soc. London 93(2): 181–207.
Pocock R.I., 1935. 12. The Incisiform Teeth of European and Asiatic Cervidae. Proc. Zool. Soc. London 105(1): 179–194.
Price J.S., Allen S., Faucheux C., Althnaian T., Mount J.G., 2005a. Deer antlers: a zoological curiosity or the key to understanding organ regeneration in mammals? J. Anat. 207(5): 603–618.
Price S.A., Bininda-Emonds O.R.P., Gittleman J.L., 2005b. A complete phylogeny of the whales, dolphins and even-toed hoofed mammals (Cetartiodactyla). Biol. Rev. Camb. Philos. Soc. 80(3): 445–473.
Putman R., 1988. The Natural history of Deer. Neal E, editor. Ithaca: Comstock Publishing Associates.
Qiong L., 2013. The research progress of *Hydropotes inermis argyropus*. Territ. Nat. Resour. Study 2: 033
R Core Development Team, 2013. R: A language and environment for statistical computing. Vienna, Austria: R Foundation for Statistical Computing.
Randi E., Mucci N., Pierpaoli M., Douzery E., 1998. New phylogenetic perspectives on the Cervidae (Artiodactyla) are provided by the mitochondrial cytochrome b gene. Proc. Zool. Soc. London 265: 793–801.
Rhim S.J., Lee W.S., 2007. Influence of Forest Fragmentation on the Winter Abundance of Mammals in Mt. Chirisan National Park, South Korea. J. Wildl. Manage. 71(5): 1404–1408.
Rütimeyer L., 1881. Beiträge zu einer natürlichen Geschichte der Hirsche. Zürich: Zürcher und Furrer. [In German]
Sand E., Klein F., 1995. Les populations de daim, de cerf sika et d'hydropote en France. Office National de la Chasse et de la Faune Sauvage 205: 32–39. [In French]
Sanderson M.J., Purvis A., Henze C., 1998. Phylogenetic supertrees: Assembling the trees of life. Trends Ecol. Evol. 13(3): 105–109.
Sasaki M., Kimura J., Sohn J., Nasu T., Kitamura N., Yasuda M., 2013. The Lamination of the Masseter Muscle in the Water Deer (*Hydropotes inermis*). Mammal Study 38(2): 91–95.
Sathyakumar S., Gopal S.R., Johnsingh A.J.T., 2015. Musk deer. In: Johnsingh A.J.T., Manjrekar N. (Eds.) Mammals of South Asia. Univeristies Press. 159–175.
Scherpe W.P., 1971. Beobachtungen am Verhalten des chinesischen Wasserrehs (*Hydropotes inermis*, Swinhoe), des indischen Muntjaks (*Muntiacus muntjak muntjak*, Zimmermann) und des chinesischen Muntjaks (*Muntiacus muntjak reevesi*, Ogilby). Freie Universität. Berlin.
Scott K.M., Janis C.M., 1987. Phylogenetic relationships of the Cervidae, and the case for a superfamily "Cervoidea". Biology and Management of the Cervidae. 3–20.
Sheng H., Lu H., 1985a. Preliminary Study on the Chinese River Deer Population of Zhoushan Island and Adjacent Islets. In: Kawamichi T. (Ed.) Contemporary Mammalogy in China and Japan. Osaka: Mammalogical Society of Japan. 6–9.
Sheng H.L., Lu H.J., 1985b. Cervid resources in subtropical and tropical areas of China. J. Shanghai Norm. Univ. Nat. Sci. 1: 96–104.
Shi W., Wang Y., Bao Y., Shou L., Chen H., 2014. Genetic assessment of captive Chinese water deer populations in Zhoushan Archipelago, China. Biochem. Syst. Ecol. 54: 160–165.
Simpson G.G., 1945. The Principles of Classification and a Classification of Mammals. Bull. Am. Museum Nat. Hist. 85: 1–350.
Smart T.S., 2009. Carpals and tarsals of mule deer, black bear and human: an osteology guide for the archaeologist. Western Washington University.
Sohn J.H., Kimura J., 2012. Observation of male reproductive organ in Korean water deer (*Hydropotes inermis argyropus*). Asian J. Anim. Vet. Adv. 7(1): 30–37.
Stadler S.G., 1991. Behaviour and social organisation of Chinese water deer (*Hydropotes inermis*) under semi-natural conditions. Bielefeld, Germany.
Sun L.X., 2002. Anti-predation does not fully explain grouping in the Chinese water deer (*Hydropotes inermis*). Acta Zool. Sin. 48(3): 302–308.
Sun L., Dai N., 1995. Male and female association and mating system in the Chinese water deer (*Hydropotes inermis*). Mammalia 59(2): 171–178.
Sun L., Xiao B., 1995. The effect of female distribution on male territoriality in Chinese water deer (*Hydropotes inermis*). Mamm. Biol. — Zeitschrift für Säugetierkd 60(1): 33–40.
Sun M., Bao Y., Mengjun S., Yixin B., 2000. Investigation on distribution and resources of *Hydropotes inermis* in Zhejiang Province. J. Zhejiang For. Sci. Technol. 21(6): 20–24.
Swinhoe R., 1865. June 27, 1865. Proc. Zool. Soc. London 1865: 510.
Swinhoe R., 1870. On a new Deer from China. Proc. Zool. Soc. London 1870: 86–99.
Swinhoe R., 1873. On Chinese Deer, with the Description of an apparently new Species. Proc. Zool. Soc. London 1873: 572–578.
Tae H.J., Park B.Y., Kim I.S., Ahn D., 2014. Morphological Examination of the Obturator Notch and Canal in Cervidae. J. Vet. Med. Sci. 76(5): 767–771.
Tate G.H.H., 1947. Mammals of Eastern Asia. New York: The Macmillan Company.
Teihard de Chardin P., Young C.C., 1936. On the Mammalian Remains from the Archaeological Site of Anyang. Wong W.H., Chow T.C., Grabau A.W., Lee J.S., Sun Y., Young C.C., Yin T.H. (Eds) Nanking: Geological Survey of China.
Veitschegger K., Sànchez-Villagra M.R., 2015. Tooth Eruption Sequences in Cervids and the Effect of Morphology, Life History, and Phylogeny. J. Mamm. Evol. 1–13.
Wan Q.H., Fang S.G., 2003. Species-specific "fingerprints" of deer in China. Biodivers. Conserv. 12(6): 1253–1260.
Ward A.I., 2005. Expanding ranges of wild and feral deer in Great Britain. Mamm. Rev. 35(2): 165–173.
Wauters L.A., Amori G., Aloise G., Gippoliti S., Agnelli P., Galimberti A., Casiraghi M., Preatoni D., Martinoli A., 2017. New endemic mammal species for Europe: *Sciurus meridionalis* (Rodentia, Sciuridae). Hystrix 28(1): 1–8. doi:l0.4404/hystrix-28.l-l2015
Wickham H., 2009. `ggplot2`: Elegant Graphics for Data Analysis. New York: Springer-Verlag.
Wilson C., 2003. Current and future deer management options: a report on behalf of Defra European wildlife division. Department of the Environment, Food and Rural Affairs, Exeter, UK.
Won C., Smith K.G., 1999. History and current status of mammals of the Korean Peninsula. Mamm. Rev. 29(1): 3–33.
Wu X.J., Schepartz L.A., Liu W., Trinkaus E., 2011. Antemortem trauma and survival in the late Middle Pleistocene human cranium from Maba, South China. Proc. Natl. Acad. Sci. U.S.A. 108(49): 19558–19562.
Xi Z., WeiBin C., Jun W., 2010. Mammalian fauna and distribution of Putuoshan Island in Zhoushan. J. Zhejiang For. Coll. 27(1): 110–115.
Xu H., Zheng X., Lu H., 1997. Impact of human activities and habitat changes on distribution of Chinese water deer along the coast area in northern Jiangsu. Acta Theriol. Sin. 18(3): 161–167.
Yabin J., 2013. Shanghai rebuilding population of endangered deer. Glob. Times.
Yang F., Carter N.P., Shi L., Ferguson-Smith M.A., 1995. A comparative study of karyotypes of muntjacs by chromosome painting. Chromosoma 103(9): 642–652.
Young C., 1932. On the Artiodactyla from the Sinanthropus Site at Chouk'outien. Ting V.K., Chow T.C., Grabau A.W., Lee Y.S., Sun Y.C., Young C.C. (Eds.) Peking: Geological Survey of China.
Yu J.N., Jun J., Won C., Oh K., Kwak M., 2011a. Complete mitochondrial genome sequence of the Korean water deer *Hydropotes inermis argyropus* (Cervidae, Capreolinae). Mitochondrial DNA 22(4): 83–85.
Yu J.N., Won C., Jun J., Lim Y., Kwak M., 2011b. Fast and cost-effective mining of microsatellite markers using NGS technology: An example of a Korean water deer *Hydropotes inermis argyropus*. PLoS One 6(10): e26933.
Zachos F., 2016a. Species concepts in Biology - Historical Development, Theoretical Foundations and Practical Relevance. Springer International Publishing.
Zachos F.E., 2016b. The Practical Relevance of Species Concepts and the Species Problem. In: Species Concepts in Biology. Cham: Springer International Publishing. 163–174.
Zachos F.E., Apollonio M., Bärmann E.V., Festa-Bianchet M., Göhlich U., Habel J.C., Haring E., Kruckenhauser L., Lovari S., McDevitt A.D., Pertoldi C., Rössner G.E., Sánchez-Villagra M.R., Scandura M., Suchentrunk F., 2013. Species inflation and taxonomic artefacts — A critical comment on recent trends in mammalian classification. Mamm. Biol. — Zeitschrift für Säugetierkunde. 78(1): 1–6.
Zhang B.L., Dang F.M., Li B.S., 1979. The farming of musk deer. Agricultural Publishing Company, Peking. [In Chinese]
Zhang E., 2000. Daytime activity budgets of the Chinese water deer. Mammalia 64(2): 163–172.

Associate Editor: L.A. Wauters

Supplemental information

After acceptance of this Manuscript, the following relevant papers were published:

- Mennecart B., DeMiguel D., Bibi F., Rössner G.E., Métais G., Neenan J.M., Wang S., Schulz G., Müller B., Costeur L., 2017. Bony labyrinth morphology clarifies the origin and evolution of deer. Sci. Rep. 7(1): 13176.
- Chen Y.J., Liu K.H., Chu W.L., 2016. New Record of Water Deer (*Hydropotes inermis*) from Iron Age Archeological Sites in Central Taiwan. Collect. Res. 29: 31–39.

Chapter 6

General discussion

The previous chapters present a set of quantitative and descriptive data on the cranial morphology of living and extinct cervids. These contribute to our understanding of the particularities of the cervid skull, its functionality, adaptive significance and evolution. Yet, when viewed together, our data also bring up a couple of questions, which we address here. In particular, our data may be interrogated to address the following issues:

1. Are antlers and enlarged upper canines functionally equivalent in intraspecific competition?
2. What is known about the developmental and genetic relationship of antlers and enlarged upper canines in cervids?
3. How do antlers and enlarged upper canines impinge on the mechanical integration of the cervid skull?
4. What may we infer about *Candiacervus* given the data obtained for living cervids?
5. Still a Sleeping Beauty? – Revisiting the water deer, *Hydropotes inermis,* in the light of the most recent publications

6.1 Are antlers and enlarged upper canines functionally equivalent?

Sexually dimorphic structures, including antlers and enlarged upper canines, are often sexually selected, and they may be categorized into two extreme variants: (i) ornaments, which serve to impress potential mates or competitors, or (ii) weapons, used for intraspecific competition. Indeed, antlers are used in both ways – the larger and the more complex antlers are, the more they function as visual signals, while they are used for combat, preferably if competitors have similar body and antler sizes (Emlen, 2008). In contrast, enlarged upper canines have been suggested to be used primarily as weapons (Cabrera & Stankowich, 2020).

However, behavioural studies in the water deer, *Hydropotes inermis,* have shown that aggressive use of enlarged upper canines during territorial defence is a last resort. In *H. inermis*, the canine blow is typically preceded by a (short) ritualistic show-off, chase or direct attack with the front legs (Stadler, 1991; Schilling & Rössner, 2017). The idea that the ritualistic show-off, in particular, the parallel walk, serves to show the impressive canines received so far little attention. This suggested reinterpretations of canine use is supported by the observations that older female *H. inermis* often develop a characteristic white tuft of hair that mimics an upper canine (Guthrie & Petocz, 1970). This mimicry clearly underscores the ornamental character of canines. Interestingly, a widely- known threatening gesture that consists in lifting up the upper lip to show the much-reduced canines, is also known for *Cervus* (Wölfel, 1983). Of note, this threat is the last one before males attack each other

with their antlers (Wölfel, 1984). Thus, the usage of enlarged upper canines in *H. inermis* may parallel that of large antlers more than hitherto thought and may indeed be functionally equivalent.

As introduced in section 1.3, antlers are generally considered the evolutionary "successors" of enlarged upper canines. Members of the pecoran stem lineage lacked cranial appendages but had enlarged upper canines. The fossil record of ruminant artiodactyls dating back to the Middle Eocene (≈ 43 mya) (e.g., Vislobokova & Métais, 2007), shows that large upper canines were a plesiomorphic character. These teeth were successively reduced, and this evolutionary phenomenon correlates with the appearance of increasingly larger antlers (e.g., Scott & Janis, 1987; Gentry, 1994; Janis, 2007; Emlen, 2008; DeMiguel, Azanza, & Morales, 2014; for a recent assessment of the evolution of antler cycle, see Rössner, Costeur, & Scheyer, 2021). Whether (stem-) Pecora similarly used their upper canines as does *H. inermis* and thus resembled, in their courtship and mating behavior extant cervids, remains enigmatic.

6.2 The developmental and genetic relationship of antlers and enlarged upper canines in cervids

The evolutionary reduction of the canine size seen with the appearance of ever-larger antlers implies an "uncoupling" of canine development from the mechanism by which sexual selection is realized in antler-bearing deer. As both phenotypic traits must be coded in the DNA, this brings up the question of how antler development and canine growth are genetically regulated. A gene that attracted much attention due to its effects on the presence and type of horns in bovids is *Rxfp2* (see e.g., Johnston *et al.*, 2011, 2013; Allais-Bonnet *et al.*, 2013; Bowles, Carson, & Isaac, 2014; Wiedemar *et al.*, 2014). Recently, the lack of cranial appendages in *Moschus* spp. and *Hydropotes inermis* was also linked to variants in the sequence of the *Rxfp2* gene (Chen *et al.*, 2019; B. Wang, Chen, & Wang, 2019). Specifically, these authors suggested that the insertion or the deletion of a single nucleotide in the 5' region of the *Rxfp2* gene in *Moschus* spp. and *H. inermis*, respectively, each resulted in the conversion of this gene into a non-expressed pseudogene.

While the suggestion that sequence variants of *Rxfp2* observed in *H. inermis* and *Moschus* spp. may relate to the lack of cranial appendages in these species is certainly intriguing, the mechanism proposed deserves some comment. Of note, the sequence identified by Wang *et al.* (2019) as encoding a premature stop codon close to the translation start site of *Rxfp2* in *Hydropotes* and *Moschus* consistently maps to intron 1, about 100 bp upstream of the start of exon 2, in several species. These include the cow (*Bos taurus*, reference sequence: ENSBTAG00000015132), the American bison (*Bison*

bison bison, ENSBBBG00000012802), sheep (*Ovis aries***,** ENSOARG00020007829), goat (*Capra hircus*, ENSCHIG00000007689), the Siberian musk deer (*Moschus moschiferus,* ENSMMSG00000001942) and the Yarkand deer (*Cervus elaphus yarkandensi*, ENSCHYG00000026840). Unmistakably, an intronic sequence cannot code a stop codon. It could, however, affect tissue-specific regulation of gene expression or expression strength. The sequences referenced above were retrieved from the Ensembl database (Howe *et al.*, 2021) in January 2021.

There is another observation that puts pseudogenization of *Rxfp2* by expression of a premature stop codon into question. A number of Afrotherian species (the lesser hedgehog tenrec, the Cape golden mole, the cape elephant shrew, and the manatee; Sharma *et al.*, 2018) that do not express (intact) *Rxfp2* consistently show testicondy, i.e., their testes do not descend during embryogenesis and are found intraabdominally, near the kidney. Similarly, the knockout of *Rxfp2* in mice also leads to a failure of the testes to descent (Overbeek *et al.*, 2001). Lastly, *maldescensus testis* in humans has also been associated with sequence variants of *RXFP2*, e.g., Ayers *et al.* (2019). Neither *Hydropotes inermis* (Sohn & Kimura, 2012; for a review, see Schilling & Rössner, 2017; **Chapter 5**) nor *Moschus* (Green, 1987; Green & Kattel, 1997; JianMing *et al.*, 2018) show testicondy.

Therefore, it may be surmised that the sequence variants in *Rxfp2* of *Hydropotes inermis* and *Moschus spp.* described by Wang *et al.* (2019) affect tissue-specificity and regulation of its expression, rather than causing a null variant. Tissue-specific effects of genes, as would be required for *Rxfp2* to selectively affect antlers, and not testicular descend, are typically due to variants in non-coding regions (e.g., Long *et al.*, 2020). We note that in sheep, the majority of molecularly characterized mutants of *Rxfp2* affecting the presence of horns or their morphology, are due to changes in non-coding regions (Wang *et al.*, 2014; Lühken *et al.*, 2016).

While the expression of *Rxfp2* during the development of horns and antlers is well established, whether and how it is important for dental growth is still an open question. In embryonic mice, *Rxfp2* is expressed also in the maxilla, the mandibula, and tooth primordia (Duarte *et al.*, 2014). As mice have no canines, this does not allow addressing the question of whether these teeth might be directly affected by *Rxfp2*.

Beyond a direct, local effect of *Rxfp2* variants on antler and/or canine growth, a more general, systemic effect should also be considered. Humans with mutations in *Rxfp2* suffer from osteoporosis. Further, mice in which *Rxfp2* has been knocked out, show an abnormally low bone mass (Ferlin *et al.*, 2008). The annual regrowth of antlers requires rapid provisioning of calcium and phosphorus

(Goss, 1983; Kodric-Brown & Brown, 1984). In cervids, the build-up of antlers goes along with a loss of mass in non-weight-bearing bones, e.g., ribs (Brockstedt-Rasmussen *et al.*, 1987; Price *et al.*, 2005; Landete-Castillejos *et al.*, 2019). This phenomenon has been referred to as "cyclic physiological osteoporosis" and has been compared with human osteoporosis (Stéger *et al.*, 2010 and further references therein). Together, these observations raise the question of whether *Rxfp2* might also be involved in the rapid mobilization of calcium and phosphorus from the skeleton during antlerogenesis.

While antlers are re-grown regularly, the permanent upper canines of *Hydropotes inermis* are a 'one-time investment'. Even as they continue to grow over the years, they certainly burden the calcium and phosphate metabolism and its dynamics less than the regrowth of antlers. Moreover, we could observe, in an adult specimen of *H. inermis*, that the canine root was closed. This signifies that the canine must have stopped growing at some point in the adult stage (Schilling & Rössner, 2017, fig. 1D; **Chapter 5**). It is still unclear, however, at which age the canine is fully grown in *H. inermis*. Systematic, long-term studies are needed to follow up on this question. Alternatively, collection material could be studied if the exact age at death is known. In this case, non-destructive approaches, such as CT scanning, should be the preferred method (von Koenigswald, 2011). Another difference between antlers and enlarged upper canines in cervids is that antlers are continuous with pedicles and thus the frontal bones. In contrast, canines are connected to the maxilla by connective tissue that allows considerable mobility (Aitchison, 1946), as clearly shown by differences in the size of the canine root and its alveola. This needs to be considered if one assesses how canines or antlers load on the skull.

Besides *Rxfp2*, a number of other genes have been associated with both antlerogenesis and dental development and/or development of facial bones. These include *Runx2*, *Dlx5*, *Osx*, *Sox9*, *Bmp4,* and constituents of the canonical Wnt-signalling pathway (Mount *et al.*, 2006; Stéger *et al.*, 2010; Lee & Saint-Jeannet, 2011; Jheon *et al.*, 2013; Ba *et al.*, 2019). Yet whether any of these genes is involved in the development of canines is unknown. The reason for this is that the mammalian model organism to study the genetics of tooth development, the mouse, has no canines. However, a clue for candidate genes involved in the development of the upper canine may come from the analysis of human malformations and their associated mutants. Among the several gene variants identified in human patients with missing or malformed permanent teeth (for reviews, see e.g., Phan *et al.*, 2016; Frazier-Bowers & Vora, 2017; Fournier *et al.*, 2018), WNT10A - and possibly its paralogue, WNT10B - stands out as (a) particularly interesting candidate(s) (Kantaputra, Kaewgahya, & Kantaputra, 2014; Kantaputra *et al.*, 2018; Xu *et al.*, 2017). Several distinct mutations in this gene have consistently been linked to various forms of tooth agenesis in humans (van den Boogaard *et al.*, 2012; Yang *et*

al., 2015; Zeng *et al.*, 2021). Intriguingly, two mutations in WNT10A, each of which leads to the exchange of a single amino acid at positions 171 and 213, respectively, were associated with selective agenesis of maxillary canines (Kantaputra *et al.*, 2014). Beyond tooth agenesis, several mutations in WNT10A have been reported to cause a malformation of molars referred to as taurodontism (Yang *et al.*, 2015), literally meaning that these teeth, specifically their roots, were reminiscent of the situation seen in ruminants, i.e. the bull.

Taken together, these observations suggest that the Wnt-signalling pathway, specifically Wnt10A, might be a candidate involved in the evolutionary regulation of dentition patterns. As it is also expressed in antlers (and other ectodermal targets of Wnt10A (Xu *et al.*, 2017), it is a potential candidate to mediate the developmental coordination of antlers and/or canines in cervids. To test this idea, it will be interesting to compare the sequences of members of the Wnt-signalling pathways in *Hydropotes*, *Muntiacus*, *Elaphodus*, *Rangifer* and *Cervus,* and possibly other cervids, once their genomes become publically available.

6.3 How do antlers and upper canines impinge on the mechanical integration of the cervid skull?

Arguably, a major source of stress acting on the facial skeleton originates from teeth and the process of food acquisition, ingestion, and, in ruminants, rumination (e.g., Rafferty & Herring, 1999; Rafferty, Herring, & Marshall, 2003 and further references cited therein). The total work associated with these activities is influenced by multiple factors, which are only partly understood. The total metabolic need, which, following Kleiber's law scales to body weight by a factor of ¾, should be one important factor (see e.g., Gould, 1975). Other factors include the (effective) postcanine dental area, chewing frequency and time spent on chewing, and, importantly, the toughness and caloric quality of the food used (for a review and further references, see Ungar, 2014). While experimental analyses of mastication-associated stress across the facial skull have been obtained or modelled for some species (Rafferty & Herring, 1999; Chalk *et al.*, 2011; Sharp, 2015) no such data are available for cervids; nor does it seem advisable to extrapolate across species, given the multiple factors involved.

It seems obvious that antlers and enlarged upper canines load differently on the cervid skull. Antlers impinge on the skull by their weight alone as well as by the forces transmitted during intraspecific fights. Enlarged upper canines load on the skull during intraspecific combat; yet they are not used for feeding, as by carnivores. Our data presented in **Chapters 2** and **3** suggest a systemic variation of the size and the shape of the cervid lacrimal bone and the type and size of head weapons. In mammals in

which the lacrimal bone has no or a minuscule facial facet, the maxilla is typically in direct contact with the frontal (e.g., primates, carnivores, bats, elephants; for a classical overview, see Gregory, 1920). In cervids, where a large lacrimal facial facet is intercalated between the frontal and the maxilla, these bones are connected but also insulated by two sutures. These sutures may thus dampen stress transfer (Herring & Mucci, 1991; Jaslow & Biewener, 1995; Bright, 2012; Curtis *et al.*, 2013; Maloul, Fialkov, & Whyne, 2013), analogous to two serially connected resistors in an electrical circuit. Indeed, as the jugal extends more and more rostrally, the suture between the jugal and the lacrimal is yet another suture that may dampen stress transfer between the maxilla and the frontal bone. The longer the lacrimojugal suture gets at the expense of the lacrimomaxillar suture, the more effectively the stress transfer between these bones will be reduced. In extant cervids, the relative lengths of these two sutures correlate nicely with antler size. However, in *Candiacervus* and *Megaloceros* this is not so obvious. Possible causes, biomechanical consequences, and behavioural interpretation have already been discussed in **Chapter 3.**

Another point to be briefly addressed here is how the lacrimal facial facet and the maxilla relate to the ethmoidal gap (**Fig. 1.1** in **Chapter 1**). As just discussed, in cervids the frontal is well separated from the maxilla by the lacrimal facial facet. This is actually true only for antlered cervids. In contrast, in *Hydropotes inermis*, a process of the maxilla extends dorsally of the ethmoidal gap along the nasal bone to almost reaching or even touching the frontal (see e.g., Leinders & Heintz, 1980, fig. 3; Janis & Scott, 1987, fig. 4d; Kim *et al.*, 2015, fig. 2). In this respect, *H. inermis* is similar to Tragulidae (Gregory, 1920, fig. 152; Rössner, 2007, fig. 16.3A: *Hyemoschus acquaticus*; Guzmán & Rössner, 2018, figs. 1c, 6: *Moschiola indica*; Schilling, Calderón-Capote, & Rössner, 2019, fig. 1b; **Chapter 2**) and Moschidae (Costeur, Schulz, & Müller, 2014, fig. 1b; Schilling *et al.*, 2019, fig. 1d; **Chapter 2**; Digitized Research Collections of the Zoological Institute of Russian Academy of Sciences, St. Petersburg: photographs of collection numbers: 18138 and 1938, https://www.zin.ru/Collections/Mammalia/catalog_en.html?taxon_id=1030631114703997). Males of these ruminant families have, like *H. inermis,* enormous upper canines. As mentioned above, the loading of enlarged upper canines on the skull is dampened in first place by its mobile suspension in the maxilla (Aitchison, 1946; Schilling & Rössner, 2017, **Chapter 5**). In the two antlered cervids that resemble *H. inermis* in having impressive upper canines, i.e. *Muntiacus* and *Elaphodus*, the maxilla and the frontal are however clearly well-separated by the lacrimal facial facet (Schaller & Vrba, 1996, fig. 3,4; Leslie, Lee, & Dolman, 2013, fig. 3; Keneisenuo *et al.*, 2021, fig. 1; Rössner *et al.*, 2021, fig. 1i). Thus, in extant cervids, the presence of antlers seems to correlate with an intercalation of the lacrimal bone between the frontal and the maxilla. This is also true for the Pleistocene cervids analyzed in this thesis, *Megaloceros spp.* (**Chapter 3**, **Fig. 3.2B, C**) and *Candiacervus ropalophorus* (**Chapter 4**).

The one species that seemingly deviates from this regularity is *Candiacervus reumeri*. In this cervid from the late Pleistocene, which bore short and ramified antlers (van der Geer, 2018), the frontal just touches the maxilla dorsal to the small ethmoidal gap (Schilling & Rössner, 2021, figs. 3G, H; **Chapter 4**). However, whether this observation made in one specimen can be generalized for the species remains open to future discoveries.

Finally, the lack of a pronounced sexual dimorphism in the shape of the lacrimal facial facet in extant cervids deserves some comment (**Chapter 3**). It seems at odds with the mechanical function proposed for this bone as an "insulator" between the antler-bearing frontal and the maxilla. However, we note that our sample used for morphometric analyses is rather small and we cannot exclude subtle shape differences between sexes. On the other hand, it seems reasonable that the basic *bauplan* of the cervid skull is the same for males and females. After all, females and males share most if not all of the genes that regulate development and morphogenesis. This basic similarity between the skulls of male and female cervids has been observed early on by Rörig (1904). He pointed out that the peculiar curvature of the coronal suture he related to pedicles is present in male and female roe deer (*Capreolus*). That the basic structure of the male, as well as that of the female cervid skull, allows bearing and using antlers is supported by the presence of regularly antlered females – the extant reindeer, *Rangifer tarandus,* and the extinct *Dicrocerus elegans* from the Middle Miocene (Ginsburg & Azanza, 1991; Azanza, DeMiguel, & Andrés, 2011). Antlered females may also occur occasionally in other cervid species, if probably only under pathological conditions (Alston, 1879; Wislocki, 1954, 1956; Donaldson & Doutt, 1965).

Do these findings allow inferring the function of the lacrimal facial facet in stem cervids from the Miocene? Stem cervids had both antlers and enlarged upper canines (e.g., *Procervulus* Gaudry 1878, *Heteroprox* Stehlin 1928, and *Dicrocerus* Lartet 1837 (Janis & Scott, 1987; Rössner, 1995, 2010; Hou, 2015), as have living muntjacs and tufted deer. However, in stem cervids, the position and orientation of pedicles and antlers differ from those of crown cervids (Rössner *et al.*, 2021, fig. 1). The pedicles of the stem cervids are positioned more or less above, and not caudal to the orbita, as they are in living cervids. Moreover, in Miocene stem cervids, the pedicles form a rather acute angle with the silhouette of the muzzle defined by the nasal bone. In contrast, this angle is more obtuse in their living relatives. Consequently, it may be conjectured that loadings originating from antlers and their dissipation across the facial skull differed between stem and crown cervids. Our results suggest that the scaling of the sutures of the lacrimal facial facet with skull length and notably the relative lengths of the lacrimojugal and lacrimomaxillar sutures might be particularly informative in this respect (see also Discussion of **Chapter 2**).

6.4 What may we infer about *Candiacervus* given the data obtained for living cervids?

As described and discussed in **Chapter 3**, the relative suture length, i.e. the shape, of the lacrimal facet clearly tells apart the Pleistocene cervids *Candiacervus spp.* and *Megaloceros spp.* from extant species studied here (**Chapter 2**). Here, I would like to comment briefly on the striking similarity of the lacrimal facial facet of these two fossil cervids. This is striking because *Candiacervus* is generally seen as a dwarfed relative of *Megaloceros* (de Vos, 1979; Vislobokova, 2013; **Chapter 1, Fig. 1.3**). However, not only its lacrimal facial facet but also its general skull morphology differs from that of small dwarf deer like the South American *Pudu* and *Mazama* (**Chapter 2, Chapter 3**). *Candiacervus* has a relatively long and slender muzzle. In contrast, *Pudu puda*, *Mazama gouazoubira*, as well as the Old World *Capreolus capreolus* and *Muntiacus muntjac* all have relatively short muzzles (**Chapter 4**). Indeed, if we compare the width of the muzzle with that of the palate as proposed by Janis & Ehrhardt (1988, fig. 1), we note that the muzzle of *Candiacervus* is at best some 80% of the palate width. In contrast, in *Megaloceros giganteus*, the muzzle is as wide as, or even somewhat wider than the palate. Finally, in *Pudu puda*, taken as an example of a very small deer, the muzzle is about 50-60% as wide as the palate. On the other hand, the distance between the second premolar (P2) and the prosthion is almost as long as the upper tooth row (P2-M3) in *Candiacervus*, but only some 80% of it in *M. giganteus* and *P. puda*. The resulting shape differences are shown in the schematic views presented in **Figure 6.1**.

How may these differences between *Candiacervus* and other small-sized deer be understood? The shoulder height of *Candiacervus ropalophorus* has been estimated to be around 40 cm (Palombo *et al.*, 2008). Hence, it is indeed a small-sized deer, when compared with *Capreolus capreolus* (~ 75 cm), *Muntiacus muntjak* (~ 60 cm), *Mazama gouazoubira* (~ 58 cm), and *Pudu puda* (~35 cm) (Ceacero, 2016). However, if we consider body mass, it turns out that *C. ropalophorus* had at least twice the mass of the species just mentioned (*C. capreolus:* 25 kg, *M. muntjak:* 24 kg, *M. gouazoubira,* 22.5 kg, and *P. puda:* 9.5 kg; Ceacero, 2016). The mass of *C. ropalophorus* was estimated to be about 40-75 kg (Palombo *et al.*, 2008), which is comparable with the body mass of cervids standing at withers twice as high as *C. ropalophorus*, e.g., *Axis axis*; 90 cm/78 kg; *Capreolus pygargus*, 88 cm/47 kg; Ceacero, 2016).

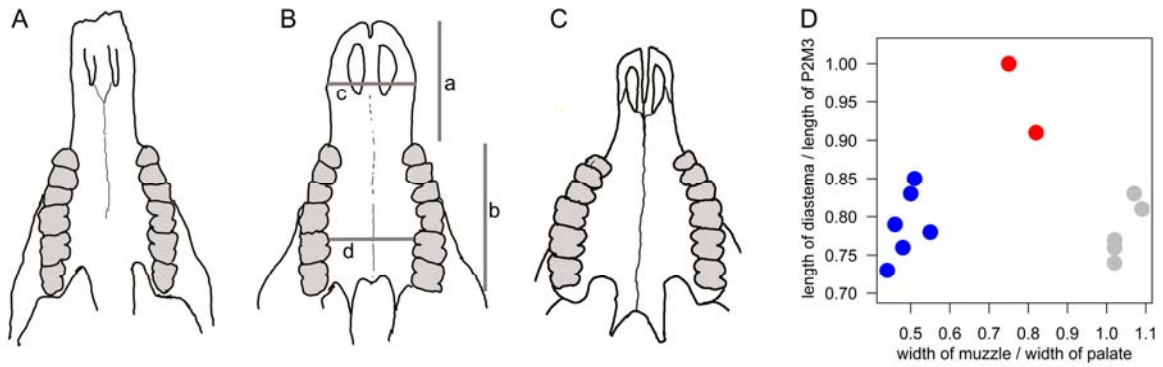

Figure 6.1 Outlines of the shape of the muzzle in *Candiacervus ropalophorus* (A), *Megaloceros giganteus* (Blumenbach, 1799) (B), and *Pudu puda* (C). In panel D, the relative length and width of the muzzle for samples of C*andiacervus* (red), *Megaloceros* (grey), and *Pudu puda* (blue) are depicted. The measures defining muzzle shape are the length of the maxillary diastema (a), the length of the premolar-molar tooth row (b), the muzzle width (c), and the palatal width (d). These are outlined in panel B. Panels A-C, which are not drawn to scale, are based on original images taken from Schilling & Rössner (2021, fig. 1d; **Chapter 4**), Vislobokova (2013, fig. 1e), and Pavez-Fox, Pino, & Corti (2015, fig. 1b). Data for panel D were obtained from images in Vislobokova (2013; figs. 1b, 1e, 1i, 2f, 4c), van der Geer *et al.*, (2006, fig. 2c), Schilling & Rössner (2021, fig. 1d; **Chapter 4**), Hershkovitz (1982, fig. 13), Saldivia & Villegas (2019, fig. 3), and Pavez-Fox, Pino, & Corti (2015, fig. 1b). In addition, three skulls of *P. puda* housed at the Bavarian State Collection of Zoology, Munich were photographed and measured (specimen numbers: AM/1067, 1954/447 and 1954/453).

Taken together, *C. ropalophorus* was certainly a small and lightweight cervid when compared with *Megaloceros*. However, it was quite heavy when compared with living cervids with similar shoulder heights. This short-legged, stocky stature is typical for island forms as has been repeatedly pointed out by van der Geer and colleagues (2006b; 2006a; 2011).

This relatively large body mass may offer one rationale for the relatively long facial skull in *Candiacervus*. Before we discuss this issue, it seems reasonable to briefly review the current estimate of the body mass in this species. This has been derived from skull size, specifically the distance between the occipital condyles (Palombo *et al.*, 2008).

I would like to suggest an independent approach to estimate the body mass of *C. ropalophorus*. In cervids, the rapid annual growth of antlers requires a transient, fast mobilization of calcium and phosphorus from the skeleton (Goss, 1983; Kodric-Brown & Brown, 1984). Heavy cervids have heavy skeletons, indeed the skeleton scales positively with body mass (Prange, Anderson, & Rahn, 1979). Now if we assume that the general bone metabolism in *C. ropalophorus* was comparable with that of living cervids, we could roughly estimate the body mass based on antler mass.

The antlers of *Candiacervus* have been described in detail by van der Geer (2018). Those of *C. ropalophorus* each measure some 70 cm in length and are essentially unbranched. The diameter can be estimated to be 2-3 cm (van der Geer, 2018, figs. 3, 4). Hence, the volume of each antler beam can

be calculated to range from 220 cm^3 to 495 cm^3. The specific weight of antlers of various cervid species has been determined to be about 1.4 g/cm^3 (Alvarez, 1994; Tsuboi *et al.*, 2020). Taking these values, the total weight of the antlers of *C. ropalophorus* may be estimated to range from 600 to 1400 g. Thus, it falls in-between the antler weights of *C. capreolus* and those of the white-tailed deer, *Odocoileus virginianus* (300 g and 1500 g, respectively; Ceacero, 2016). The body masses of the latter two species have been reported to be 25 kg and 80 kg, respectively (Ceacero, 2016). If we take the relationship between body mass and antler weight obtained by Ceacero (2016, fig. 2), an antler mass of 600-1400 g predicts a body mass of about 37.5 – 55 kg

These considerations strongly support the estimates of body mass provided by Palombo *et al.* (2008). I want to note again that the two congruent estimates were obtained independently. While the estimate of Palombo *et al.* (2008) is based primarily on biomechanical arguments (see also: Köhler & Moyà-Solà, 2004), the estimate presented here is based on considerations of bone metabolism. Thus, it follows the concept outlined in section 1.3 that skull size also reflects metabolic needs.

The relatively large body mass of *C. ropalophorus* compared with other small-sized cervids requires the space to allocate an appropriate dentition. In cervids, as in other mammals, the occlusal surface of postcanine teeth scales with body mass (Gould, 1975; Copes & Schwartz, 2010). Gould (1975) also pointed out that the reduction of tooth size during dwarfing is less pronounced than the reduction of total body size. This has also been observed in island dwarfs of red deer, *Cervus elaphus* (Lister, 1989). Here, we have a first explanation of why the facial skull of the dwarfed cervid, *C. ropalophorus,* should be quite long.

Like *Candiacervus*, *Pudu puda* is generally thought to be a descendant of a larger ancestor, although, as Hershkovitz (1982) argued, it may as well derive from a small deer. Osteological analyses that would allow testing whether *Pudu puda* is indeed dwarfed (e.g., Kolb *et al.*, 2015) are, to the best of my knowledge, not (yet) available. Given the scarce fossil record available (Saavedra & Simonetti, 1991, see also: Merino & Rossi, 2010; Gonzalez *et al.*, 2014), the phylogeny of *Pudu puda* (e.g., Heckeberg *et al.*, 2016; Heckeberg, 2020) is also non-informative in this respect. Whatever the eventual answer to this question, the specific appearance of *Pudu puda*, and in particular its short and pointed muzzle, are thought to indicate that it may have involved paedomorphic changes (Geist, 1987, 1998).

The situation in *Candiacervus ropalophorus* is quite different. Its muzzle does not impress as paedomorphic: quite to the contrary, it is long and narrow. Its molar tooth row is rather straight, which again contrasts with *Pudu*, which has a more curved molar tooth row, as typical for short-muzzled ruminant species. This character also sets *C. ropalophorus* apart from other small-sized insular ruminants (see, e.g., van der Geer, 2005, 2014). The short legs of *Candiacervus* have previously led Son-

daar to conclude that dwarfing of *Candiacervus* "cannot be considered as being due to […] paedomorphic changes" (*idem*, 1977, p. 682). The shape of the muzzle of *C. ropalophorus* adds additional support to this notion.

Lastly, the length of the face, and in particular, the shape of the muzzle, have been repeatedly associated with the feeding style and diet in various herbivores, including cervids (Tennant & MacLeod, 2014; Pavez-Fox *et al.*, 2015; Rex Mitchell *et al.*, 2018; Ercoli & Armella, 2021). A recurrent theme of these studies is that consumption of a tougher diet is associated with a blunt shape of the muzzle, whereas pointed muzzles are more typical for species living on softer and, notably, more selected diets.

Thus, the shape of the muzzle of *Candiacervus ropalophorus* may suggest some degree of selectivity in its feeding that in turn may relate to the diversification of these Cretan deer in the eight morphotypes currently recognized. A caveat for this interpretation comes from the work of Janis & Eberhardt (1988), who documented quite some variability and a strong influence of phylogeny when trying to relate muzzle shape and feeding behaviour. Likewise, Tennant & MacLeod (2014) noted a considerable overlap of muzzle shapes between feeding types. Still, these authors concluded that muzzle shape may "be used with a reasonable degree of confidence, especially if backed-up by additional information" (*idem*, p. 1) to infer feeding types. Such "additional information" may be taken from the peculiar dental eruption sequence of *Candiacervus* as described and discussed in **Chapter 4**. As indicated, this sequence is reminiscent of that in goats and has been explained as an adaptation to the diet available at high altitudes (Monson & Hlusko, 2018). Interestingly, the recent analysis of Gomes Rodrigues *et al.* (2019) suggests that this adaptation represents a reversal to the plesiomorphic dentition pattern. Based on the analysis of 63 extinct artiodactyl genera, these authors concluded that the plesiomorphic condition is indeed represented by the eruption of molars before permanent premolars, contrary to what had been surmised before (Monson & Hlusko, 2018) when only extant species were analysed. Unfortunately, as discussed in **Chapter 4**, known *Candiacervus* skulls cannot be unambiguously associated with the eight morphotypes defined primarily by postcranial material. Specifically, skulls of the larger phenotypes are not yet identified, which impedes follow-up on this issue. Considering the apparently slow growth of *Candiacervus* (Kolb *et al.*, 2015a, 2015b), the late eruption of M3 may also be seen as an example of "Schultz's rule" (Smith, 2009).

At this point, a very recent paper by Palombo & Zedda (2021) that became available only after **Chapter 4** (Schilling & Rössner, 2021) was published needs to be mentioned. In this publication, the authors suggest that *Candiacervus giganteus* (size group 6) suffered from pituitary gigantism, based on limb bone histology. This is true for both the holotype and the paratype. Consequently, they put into question whether *C. giganteus* is indeed an independent species. This would affect the classification

of *C. giganteus* as presented in **Table 1** of **Chapter 4**. However, we note that it would not affect the results and their interpretation presented in this thesis.

6.5 Still a Sleeping Beauty? – Revisiting the water deer, *Hydropotes inermis,* in the light of recent publications

As the discussion above has shown, the unique cranial phenotype of *Hydropotes inermis* is of considerable interest and significance for understanding the development, function, and adaptive character of cervid skulls. Since 2017, when our comprehensive review on biology, behaviour, and ecology was published (Schilling & Rössner, 2017, **Chapter 5**), a number of interesting studies about this species became available. Here, I would like to take the opportunity to summarize briefly key findings from these papers and discuss their relevance within the context of the present dissertation. I present them following the structure of **Chapter 5**.

Biogeography and conservation: Putman *et al.* (2020) studied the genetic structure and diversity of *H. inermis* populations in China, England, and France by analyzing variation in mitochondrial cytochrome b sequences and sequences of the control region. They concluded that British water deer may be genetically differentiated from the native Chinese populations. Specifically, they conjecture that "[…] Chinese water deer residing in the UK may be the descendants of a now-extinct Chinese mainland population – a reservoir of genetic variation that has been lost in the native range" (Putman *et al.*, 2020, p. 9). This implies that re-introductions of British water deer in their native ranges might be a means to increase the genetic variability of populations in Southeast Asia. Whether this is a sensible approach, remains an open question. After all, global warming, higher human population density, and habitat fragmentation were identified as the main causes of local extinction of this cervid species in China over the last three centuries (Wan *et al.*, 2019; Putman *et al.*, 2020). These developments might also have contributed to the fact that individuals of *H. inermis* have recently been sighted also in more northern regions, even in Russia, close to the Chinese and the Korean border (Darman, Storozhuk, & Sedash, 2019; Belyaev & Jo, 2021).

It is still unclear how many water deer are harvested yearly in Europe (Linnell *et al.*, 2020). In the UK, water deer is claimed to be "uncommon in the bag" (Aebischer, 2019, p. 6), with less than 100 killed individuals in 2004 and about 600 individuals killed in 2012 and 2016 each. "Uncommon" may sound reassuring, but it is based on a comparison with other mammals that are far more frequent in the UK. It sounds alarming if we consider that the most recent estimates put the population size of *H. inermis* in the UK at about 3500 individuals, although actual numbers may differ substantially from this estimate (Matthews, Kubasiewicz, & et al., 2018). Hence, we must conclude that the (effective) popula-

tion size and anthropogenic impact due to hunting remain still unclear (Schilling & Rössner, 2017; Aebischer, 2019).

In North and South Korea, *Hydropotes inermis* is still hunted legally and illegally, despite the efforts of the Korean governments to conserve it (Y. S. Jo, Baccus, & Koprowski, 2018). Furthermore, it is commonly the victim of road kills (Choi, 2016; Kim *et al.*, 2019) and killed because of its disrepute as vermin for agriculture (Eom *et al.*, 2018; Y.-S. Jo, Baccus, & Koprowski, 2018). Attempts to prevent road kills and proposals to avoid crop damage without killing the species are underway (Jung *et al.*, 2016; Park *et al.*, 2018). Recently, it has been concluded that the Korean water deer could be particularly useful in the dispersal of seeds and conserve the regional flora because it acts as a seed vector in lowland areas of the demilitarized zone (Lee & Lee, 2020). The Ministry of Environment and the National Institute of Biological Resources of Korea consider the population of the Korean water deer the "only healthy native population in the world" (Y.-S. Jo *et al.*, 2018, p. 295). However, the size of the *H. inermis* population in Korea remains obscure. Taken together, these recent publications suggest that the conservation status probably did not change significantly since 2017.

Fossil distribution: In the last years, new fossil material of *Hydropotes inermis* became available. Remains discovered in North Hwanghae Province (Choe *et al.*, 2020), where *H. inermis* is still living today, include a right mandible and several limb bones, dated to the Late Pleistocene. Further, fragments of upper canines and mandibles have been unearthed in Taiwan. These were dated to the Iron Age (Chen, Liu, & Chu, 2017). Finally, findings assigned to *H. inermis* and dated to the Late Pleistocene (ca. 80-100 kya) come from northern Vietnam: a left lower premolar (p4) was found in the Lang Trang Cave in Thanh Hóa Province (Lopatin *et al.*, 2021). Mandibles and maxillary canine fragments were found in the Hang Thung Binh 1 cave, located in the Ninh Bình Province, which borders the former province in the northeast (Stimpson *et al.*, 2021). These latter were dated to 13 000-16 000 years before present.

These latter two findings are currently the southernmost record of fossil *Hydropotes*. These three finds expand the range where prehistoric *H. inermis* once lived. The age of the material from Vietnam raises the question of whether, historically, *H. inermis* migrated from China towards more southern regions. The find from Taiwan (Chen *et al.*, 2017) might also offer the opportunity to probe whether these island animals differed from their contemporary mainland relatives, and/or from living species. Unfortunately, none of this new material informs us about the ancestor of the lineage, and whether the latter was antlered or not.

Systematics and evolution: Since the publication of our review (Schilling & Rössner, 2017), the whole genome of several deer species, including the *Hydropotes inermis* have been sequenced and assembled (Y. Wang *et al.*, 2019). This additional genetic material will eventually allow probing and refining

the current understanding of the phylogenetic relationships of the species. Mennecart *et al.* (2016), based on a detailed analysis of the inner ear, provided additional support for the close relationship of *H. inermis* with the roe deer, *Capreolus capreolus*. This view received further support by combined analyses of molecular and morphological traits (Heckeberg, 2020).

These two studies again support the view that *H. inermis* had lost its antlers secondarily. Even if there is more and more support for this evolutionary scenario, it is undoubtedly premature to consider it a fact, as some authors seem to do (Samejima & Matsuoka, 2020). As detailed above (section 6.2), the mechanism of evolutionary antler loss proposed so far (Y. Wang *et al.*, 2019) is questionable and the process(es) of antler induction remain also unknown.

Finally, in this context, the recent publication of Cabrera & Stankowich (2020) needs to be mentioned. These authors focused on the evolution and ecological significance of enlarged upper canines in artiodactyls and associated it with "a slinker lifestyle". Significantly, they suggest that enlarged upper canines of *Hydropotes*, but also those of the small-antlered *Muntiacus* "re-evolved". The same view has been held by Gilbert et al. (2006). Such an evolutionary scenario, again, implies a coordinated developmental gain and loss of upper canines and antlers, respectively. Yet, as discussed above, how the development of these cranial appendages is coordinated is still enigmatic. A more detailed understanding of the cervid facial skull, to which this dissertation attempts to contribute, might be one path towards solving this riddle of cervid evolution and ecology.

6.6 References

AEBISCHER, N.J. (2019) Fifty-year trends in UK hunting bags of birds and mammals, and calibrated estimation of national bag size, using GWCT's National Gamebag Census. *European Journal of Wildlife Research* **65**, 64.

AITCHISON, J. (1946) Hinged Teeth in Mammals: A Study of the Tusks of Muntjacs (*Muntiacus*) and Chinese Water Deer (*Hydropotes inermis*). *Proceedings of the Zoological Society of London* **116**, 329–338.

ALLAIS-BONNET, A., GROHS, C., MEDUGORAC, I., KREBS, S., DJARI, A., GRAF, A., ET AL. (2013) Novel Insights into the Bovine Polled Phenotype and Horn Ontogenesis in Bovidae. *PLoS ONE* **8**, e63512.

ALSTON, E.R. (1879) 2. On Female Deer with Antlers. *Proceedings of the Zoological Society of London* **47**, 296–299.

ALVAREZ, F. (1994) Bone Density and Breaking stress in relation to consistent fracture position in fallow deer antlers. *Doñana, Acta Vertebrata* **21**, 15–24.

AYERS, K., KUMAR, R., ROBEVSKA, G., BRUELL, S., BELL, K., MALIK, M.A., BATHGATE, R.A. & SINCLAIR, A. (2019) Familial bilateral cryptorchidism is caused by recessive variants in *RXFP2*. *Journal of Medical Genetics* **56**, 727–733.

AZANZA, B., DEMIGUEL, D. & ANDRÉS, M. (2011) The antler-like appendages of the primitive deer *Dicrocerus elegans*: Morphology, growth cycle, ontogeny, and sexual dimorphism. *Estudios Geologicos* **67**, 579–602.

BA, H., WANG, D., YAU, T.O., SHANG, Y. & LI, C. (2019) Transcriptomic analysis of different tissue layers in antler growth Center in Sika Deer (*Cervus nippon*). *BMC Genomics* **20**, 173.

BELYAEV, D.A. & JO, Y.S. (2021) Northernmost finding and further information on water deer *Hydropotes inermis* in Primorskiy Krai, Russia. *Mammalia* **85**, 71–73.

VAN DEN BOOGAARD, M.J., CRÉTON, M., BRONKHORST, Y., VAN DER HOUT, A., HENNEKAM, E., LINDHOUT, D., CUNE, M. & VAN AMSTEL, H.K.P. (2012) Mutations in wnt10a are present in more than half of isolated hypodontia cases. *Journal of Medical Genetics* **49**, 327–331.

BOWLES, D., CARSON, A. & ISAAC, P. (2014) Genetic distinctiveness of the Herdwick sheep breed and two other locally adapted hill breeds of the UK. *PLoS ONE* **9**, e87823.

BRIGHT, J.A. (2012) The importance of craniofacial sutures in biomechanical finite element models of the domestic pig. *PLoS ONE* **7**, e31769.

BROCKSTEDT-RASMUSSEN, H., SØRENSEN, P.L., EWALD, H. & MELSEN, F. (1987) The rhythmic relation between antler and bone porosity in Danish deer. *Bone* **8**, 19–22.

CABRERA, D. & STANKOWICH, T. (2020) Stabbing Slinkers: Tusk Evolution Among Artiodactyls. *Journal of Mammalian Evolution* **27**, 265–272.

CEACERO, F. (2016) Long or Heavy? Physiological Constraints in the Evolution of Antlers. *Journal of Mammalian Evolution* **23**, 209–216.

CHALK, J., RICHMOND, B.G., ROSS, C.F., STRAIT, D.S., WRIGHT, B.W., SPENCER, M.A., WANG, Q. & DECHOW, P.C. (2011) A finite element analysis of masticatory stress hypotheses. *American Journal of Physical Anthropology* **145**, 1–10.

CHEN, L., QIU, Q., JIANG, Y., WANG, K., LIN, Z., LI, Z., ET AL. (2019) Large-scale ruminant genome sequencing provides insights into their evolution and distinct traits. *Science* **364**, eaav6202.

CHEN, Y.-J., LIU, K.-H. & CHU, W.-L. (2017) New Record of Water Deer (*Hydropotes inermis*) from Iron Age Archeological Sites in Central Taiwan. *Collection and Research* **29**, 23–31.

CHOE, R.S., HAN, K.S., KIM, S.C., CHOL, U., HO, C.U. & KANG, I. (2020) Late pleistocene fauna from Chongphadae Cave, Hwangju County, Democratic People's Republic of Korea. *Quaternary Research* **97**, 42–54.

CHOI, T.-Y. (2016) Estimation of the Water deer (*Hydropotes inermis*) Roadkill Frequency in South Korea. *Ecology and Resilient Infrastructure* **3**, 162–168.

COPES, L.E. & SCHWARTZ, G.T. (2010) The scale of it all: postcanine tooth size, the taxon-level effect, and the universality of Gould's scaling law. *Paleobiology* **36**, 188–203.

COSTEUR, L., SCHULZ, G. & MÜLLER, B. (2014) High-resolution x-ray computed tomography to understand ruminant phylogeny. In *Proceedings of SPIE - The International Society for Optical Engineering* p. 921216. San Diego.

CURTIS, N., JONES, M.E.H., EVANS, S.E., O'HIGGINS, P. & FAGAN, M.J. (2013) Cranial sutures work collectively to distribute strain throughout the reptile skull. *Journal of the Royal Society Interface* **10**, 20130442.

DARMAN, Y.A., STOROZHUK, V.B. & SEDASH, G.A. (2019) *Hydropotes inermis* (Cervidae), a new species for the Russian fauna registered in the land of leopard national park (Russia). *Nature Conservation Research* **4**, 127–129.

DEMIGUEL, D., AZANZA, B. & MORALES, J. (2014) Key innovations in ruminant evolution: A paleontological perspective. *Integrative Zoology* **9**, 412–433.

DONALDSON, J.C. & DOUTT, J.K. (1965) Antlers in Female White-Tailed Deer: A 4-Year Study. *The Journal of Wildlife Management* **29**, 699–705.

DUARTE, C., KOBAYASHI, Y., KAWAMOTO, T. & MORIYAMA, K. (2014) Relaxin receptors 1 and 2 and nuclear receptor subfamily 3, group C, member 1 (glucocorticoid receptor) mRNAs are expressed in oral components of developing mice. *Archives of Oral Biology* **59**, 111–118.

EMLEN, D.J. (2008) The Evolution of Animal Weapons. *Annual Review of Ecology, Evolution, and Systematics* **39**, 387–413.

EOM, T.-K., HWANG, H.-S., LEE, J.-K. & RHIM, S.-J. (2018) Ecological factors influencing winter field sign

abundance of Korean water deer *Hydropotes inermis argyropus* in a temperate forest in South Korea. *Folia Zoologica* **67**, 173–178.

ERCOLI, M.D. & ARMELLA, M.A. (2021) Snout shape and masticatory apparatus of the rodent-like mesotheriid ungulates (Notoungulata, Typotheria): exploring evolutionary trends in dietary strategies through ancestral reconstructions. *Palaeontology*, 1–24.

FERLIN, A., PEPE, A., GIANESELLO, L., GAROLLA, A., FENG, S., GIANNINI, S., ZACCOLO, M., FACCIOLLI, A., MORELLO, R., AGOULNIK, A.I. & FORESTA, C. (2008) Mutations in the insulin-like factor 3 receptor are associated with osteoporosis. *Journal of Bone and Mineral Research* **23**, 683–693.

FOURNIER, B.P., BRUNEAU, M.H., TOUPENAY, S., KERNER, S., BERDAL, A., CORMIER-DAIRE, V., HADJ-RABIA, S., COUDERT, A.E. & DE LA DURE-MOLLA, M. (2018) Patterns of Dental Agenesis Highlight the Nature of the Causative Mutated Genes. *Journal of Dental Research* **97**, 1306–1316.

FRAZIER-BOWERS, S.A. & VORA, S.R. (2017) Genetic Disorders of Dental Development: Tales from the Bony Crypt. *Current Osteoporosis Reports* **15**, 9–17.

VAN DER GEER, A. (2018) Uniformity in variety: Antler morphology and evolution in a predator-free environment. *Palaeontologia Electronica* **21**, 1–31.

VAN DER GEER, A., DERMITZAKIS, M. & DE VOS, J. (2006a) Crete Before the Cretans : the Reign of Dwarfs. *Pharos* **13**, 119–130.

VAN DER GEER, A., LYRAS, G., DE VOS, J. & DERMITZAKIS, M. (2011) Patterns and Trends. In *Evolution of island mammals: adaptation and extinction of placental mammals on islands* (eds A. VAN DER GEER, G. LYRAS, J. DE VOS & M. DERMITZAKIS), pp. 358–366. John Wiley & Sons, West Sussex.

VAN DER GEER, A., DE VOS, J., LYRAS, G. & DERMITZAKIS, M. (2006b) New data on the Pleistocene Cretan deer *Candiacervus* sp. II (Cervinae, Mammalia). *Courier Forschungsinstitut Senckenberg* **256**, 131–137.

VAN DER GEER, A.A.E. (2005) Island ruminants and parallel evolution of functional structures. *Quaternaire* **2**, 231–240.

VAN DER GEER, A.A.E. (2014) Parallel patterns and trends in functional structures in extinct island mammals. *Integrative Zoology* **9**, 167–182.

GEIST, V. (1987) On speciation in Ice Age mammals, with special reference to cervids and caprids. *Canadian Journal of Zoology* **65**, 1067–1084.

GEIST, V. (1998) *Deer of the World: Their Evolution, Behaviour, and Ecology*, 1st edition. Swan Hill Press, Shrewsbury.

GENTRY, A.W. (1994) The Miocene Differentiation of Old World Pecora (Mammalia). *Historical Biology* **7**, 115–158.

GILBERT, C., ROPIQUET, A. & HASSANIN, A. (2006) Mitochondrial and nuclear phylogenies of Cervidae (Mammalia, Ruminantia): Systematics, morphology, and biogeography. *Molecular Phylogenetics*

and Evolution **40**, 101–117.

GINSBURG, L. & AZANZA, B. (1991) Presence de bois chez les femelles du cervide miocene *Dicrocerus elegans* et remarques sur le probleme de l'origine du dimorphisme sexuel sur les appendices frontaux des Cervides. *Comptes Rendus - Académie des Sciences, Serie II* **313**, 121–126.

GOMES RODRIGUES, H., LIHOREAU, F., ORLIAC, M., THEWISSEN, J.G.M. & BOISSERIE, J.-R. (2019) Unexpected evolutionary patterns of dental ontogenetic traits in cetartiodactyl mammals. *Proceedings of the Royal Society B* **286**, 20182417.

GONZALEZ, E., LABARCA, R., CHAVEZ-HOFFMEISTER, M. & PINO, M. (2014) First fossil record of the smallest deer cf. *Pudu* Molina, 1782 (Artiodactyla, Cervidae), in the late Pleistocene of South America. *Journal of Vertebrate Paleontology* **34**, 483–488.

GOSS, R.J. (1983) *Deer Antlers - Regeneration, Function and Evolution*. Academic Press, London.

GOULD, S.J. (1975) On the scaling of tooth size in mammals. *Integrative and Comparative Biology* **15**, 353–362.

GREEN, M.J.B. (1987) Scent-marking in the Himalayan musk deer (*Moschus chrysogaster*). *Journal of Zoology* **1**, 721–737.

GREEN, M.J.B. & KATTEL, B. (1997) Musk deer: little understood, even its scent. In *First International Symposium on Endangered Species Used in Traditional East Asian Medicine: Substitutes for Tiger Bone and Musk.* pp. 1–18. Hongkong.

GREGORY, W.K. (1920) Article II. - Studies in Comparative Myology and Osteology: No. IV. - A Review of the Evolution of the Lacrymal Bone of Vertebrates with Special Reference to That of Mammals. *Bulletin of the American Museum of Natural History* **XLII**, 95–263.

GUTHRIE, R.D. & PETOCZ, R.G. (1970) Weapon Automimicry Among Mammals. *The American Naturalist* **104**, 585–588.

GUZMÁN, J.A. & RÖSSNER, G.E. (2018) Skull morphometrics of *Tragulus* and *Moschiola* for an improved classification of tragulid collections. *Mammalian Biology* **90**, 78–88.

HECKEBERG, N.S. (2020) The systematics of the Cervidae: A total evidence approach. *PeerJ* **8**, e8114.

HECKEBERG, N.S., ERPENBECK, D., WÖRHEIDE, G. & RÖSSNER, G.E. (2016) Systematic relationships of five newly sequenced cervid species. *PeerJ* **4**, e2307.

HERRING, S.W. & MUCCI, R.J. (1991) In vivo strain in cranial sutures: The zygomatic arch. *Journal of Morphology* **207**, 225–239.

HERSHKOVITZ, P. (1982) Neotropical deer (Cervidae). Part I. Pudus, genus *Pudu* Gray. *Fieldiana, New Series* **11**, 1–86.

HOU, S. (2015) A new species of *Euprox* (Cervidae, Artiodactyla) from the upper Miocene of the Linxia Basin, Gansu Province, China, with interpretation of its paleoenvironment. *Zootaxa* **3911**, 43–62.

HOWE, K.L., ACHUTHAN, P., ALLEN, JAMES, ALLEN, JAMIE, ALVAREZ-JARRETA, J., RIDWAN AMODE, M., ET AL. (2021) Ensembl 2021. *Nucleic Acids Research* **49**, D884–D891.

JANIS, C.M. (2007) Evolutionary patterns and paleobiology. In *The Evolution of Artiodactyls* (eds D.R. PROTHERO & S.E. FOSS), pp. 292–302. John Hopkins University Press, Baltimore.

JANIS, C.M. & EHRHARDT, D. (1988) Correlation of relative muzzle width and relative incisor width with dietary preference in ungulates. *Zoological Journal of the Linnean Society* **92**, 267–284.

JANIS, C.M. & SCOTT, K.M. (1987) The Interrelationships of Higher Ruminant Families with Special Emphasis on the Members of the Cervoidea. *American Museum Novitates* **2893**, 1–85.

JASLOW, C.R. & BIEWENER, A.A. (1995) Strain patterns in the horncores, cranial bones and sutures of goats (*Capra hircus*) during impact loading. *Journal of Zoology* **235**, 193–210.

JHEON, A.H., SEIDEL, K., BIEHS, B. & KLEIN, O.D. (2013) From molecules to mastication: The development and evolution of teeth. *Wiley Interdisciplinary Reviews: Developmental Biology* **2**, 165–182.

JIANMING, W., DAYONG, F., CHENGLI, Z., LIE, Z. & HAIMEI, Z. (2018) Morphological structure and distribution of hair of forest musk deer. *Journal of Economic Animal* **22**, 142–149.

JO, Y.-S., BACCUS, J.T. & KOPROWSKI, J.L. (2018) *Mammals of Korea*, 1st edition. National Institute of Biological Resources, Incheon.

JO, Y.S., BACCUS, J.T. & KOPROWSKI, J.L. (2018) Mammals of Korea: A review of their taxonomy, distribution and conservation status. *Zootaxa* **4522**, 1–216.

JOHNSTON, S.E., GRATTEN, J., BERENOS, C., PILKINGTON, J.G., CLUTTON-BROCK, T.H., PEMBERTON, J.M. & SLATE, J. (2013) Life history trade-offs at a single locus maintain sexually selected genetic variation. *Nature* **502**, 93–95.

JOHNSTON, S.E., MCEWAN, J.C., PICKERING, N.K., KIJAS, J.W., BERALDI, D., PILKINGTON, J.G., PEMBERTON, J.M. & SLATE, J. (2011) Genome-wide association mapping identifies the genetic basis of discrete and quantitative variation in sexual weaponry in a wild sheep population. *Molecular Ecology* **20**, 2555–2566.

JUNG, J., SHIMIZU, Y., OMASA, K., KIM, S. & LEE, S. (2016) Developing and testing a habitat suitability index model for Korean water deer (Hydropotes inermis argyropus) and its potential for landscape management decisions in Korea. *Animal Cells and Systems* **20**, 218–227.

KANTAPUTRA, P., KAEWGAHYA, M. & KANTAPUTRA, W. (2014) WNT10A mutations also associated with agenesis of the maxillary permanent canines, a separate entity. *American Journal of Medical Genetics, Part A* **164**, 360–363.

KANTAPUTRA, P.N., HUTSADALOI, A., KAEWGAHYA, M., INTACHAI, W., GERMAN, R., KOPARAL, M., LEETHANAKUL, C., TOLUN, A. & KETUDAT CAIRNS, J.R. (2018) WNT10B mutations associated with isolated dental anomalies. *Clinical Genetics* **93**, 992–999.

KENEISENUO, K., CHOUDHARY, O.P., PRIYANKA, P., KALITA, P.C., KALITA, A., DOLEY, P.J. & CHAUDHARY, J.K.

(2021) Applied anatomy and clinical significance of the maxillofacial and mandibular regions of the barking deer (*Muntiacus muntjak*) and sambar deer (*Rusa unicolor*). *Folia Morphologica* **80**, 170–176.

KIM, K., WOO, D., SEO, H., PARK, T. & SONG, E. (2019) Korea Road-Kill Observation System: The First Case to Integrate Road-Kill Data in National Scale by Government. *Journal of Forest and Environmental Science* **35**, 281–284.

KIM, Y.K., KOYABU, D., LEE, H. & KIMURA, J. (2015) Cranial morphological homogeneity in two subspecies of water deer in China and Korea. *Journal of Veterinary Medical Science* **77**, 1427–1435.

KODRIC-BROWN, A. & BROWN, J.H. (1984) Truth in advertising: the kinds of traits favored by sexual selection. *American Naturalist* **124**, 309–323.

VON KOENIGSWALD, W. (2011) Diversity of hypsodont teeth in mammalian dentitions - Construction and classification. *Palaeontographica, Abteilung A: Palaozoologie - Stratigraphie* **294**, 63–94.

KÖHLER, M. & MOYÀ-SOLÀ, S. (2004) Reduction of Brain and Sense Organs in the Fossil Insular Bovid *Myotragus*. *Brain, Behavior and Evolution* **63**, 125–140.

KOLB, C., SCHEYER, T.M., LISTER, A.M., AZORIT, C., DE VOS, J., SCHLINGEMANN, M.A.J., RÖSSNER, G.E., MONAGHAN, N.T. & SÁNCHEZ-VILLAGRA, M.R. (2015a) Growth in fossil and extant deer and implications for body size and life history evolution. *BMC Evolutionary Biology* **15**, 19.

KOLB, C., SCHEYER, T.M., VEITSCHEGGER, K., FORASIEPI, A.M., AMSON, E., VAN DER GEER, A.A.E., VAN DEN HOEK OSTENDE, L.W., HAYASHI, S. & SÁNCHEZ-VILLAGRA, M.R. (2015b) Mammalian bone palaeohistology: A survey and new data with emphasis on island forms. *PeerJ* **2015**, e1358.

LANDETE-CASTILLEJOS, T., KIERDORF, H., GOMEZ, S., LUNA, S., GARCÍA, A.J., CAPPELLI, J., PÉREZ-SERRANO, M., PÉREZ-BARBERÍA, J., GALLEGO, L. & KIERDORF, U. (2019) Antlers - Evolution, development, structure, composition, and biomechanics of an outstanding type of bone. *Bone* **128**, 115046.

LEE, S.K. & LEE, E.J. (2020) Internationally vulnerable Korean water deer (*Hydropotes inermis argyropus*) can act as an ecological filter by endozoochory. *Global Ecology and Conservation* **24**, e01368.

LEE, Y.H. & SAINT-JEANNET, J.P. (2011) Sox9 function in craniofacial development and disease. *Genesis* **49**, 200–208.

LEINDERS, J.J.M. & HEINTZ, E. (1980) The configuration of the lacrimal orifices in Pecorans and Tragulids (Artiodactyla, Mammalia) and its significance for the distinction between Bovidae and Cervidae. *Beaufortia* **30**, 155–160.

LESLIE, D.M., LEE, D.N. & DOLMAN, R.W. (2013) *Elaphodus cephalophus* (Artiodactyla: Cervidae). *Mammalian Species* **45**, 80–91.

LINNELL, J.D.C., CRETOIS, B., NILSEN, E.B., ROLANDSEN, C.M., SOLBERG, E.J., VEIBERG, V., KACZENSKY, P., VAN MOORTER, B., PANZACCHI, M., RAUSET, G.R. & KALTENBORN, B. (2020) The challenges and

opportunities of coexisting with wild ungulates in the human-dominated landscapes of Europe's Anthropocene. *Biological Conservation* **244**, 108500.

LISTER, A.M. (1989) Rapid dwarfing of red deer on Jersey in the Last Interglacial. *Nature* **342**, 539–542.

LONG, H.K., OSTERWALDER, M., WELSH, I.C., HANSEN, K., DAVIES, J.O.J., LIU, Y.E., ET AL. (2020) Loss of Extreme Long-Range Enhancers in Human Neural Crest Drives a Craniofacial Disorder. *Cell Stem Cell* **27**, 765-783.e1-14.

LOPATIN, A. V., MASCHENKO, E.N., VISLOBOKOVA, I.A., SERDYUK, N. V. & DAC, L.X. (2021) Pleistocene Mammals from the Lang Trang Cave (Vietnam): New Data. *Doklady Biological Sciences* **496**, 1–4.

LÜHKEN, G., KREBS, S., ROTHAMMER, S., KÜPPER, J., MIOČ, B., RUSS, I. & MEDUGORAC, I. (2016) The 1.78-kb insertion in the 3'-untranslated region of RXFP2 does not segregate with horn status in sheep breeds with variable horn status. *Genetics Selection Evolution* **48**, 78.

MALOUL, A., FIALKOV, J. & WHYNE, C.M. (2013) Characterization of the bending strength of craniofacial sutures. *Journal of Biomechanics* **46**, 912–917.

MATTHEWS, F., KUBASIEWICZ, L.M. & ET AL. (2018) A Review of the Population and Conservation Status of British Mammals: Technical Summary. *Natural England Joint Publication* **JP025**, 1–72.

MENNECART, B., RÖSSNER, G.E., MÉTAIS, G., DEMIGUEL, D., SCHULZ, G., MÜLLER, B. & COSTEUR, L. (2016) The petrosal bone and bony labyrinth of early to middle Miocene European deer (Mammalia, Cervidae) reveal their phylogeny. *Journal of Morphology* **277**, 1329–1338.

MERINO, M.L. & ROSSI, R. V (2010) Origin, Systematics, and morphological radiation. In *Neotropical Cervidology: biology and medicine of Latin American deer* (eds J.M.B. DUARTE & S. GONZÁLEZ), pp. 2–11. Funep, Jaboticabal, Brazil.

MITCHELL, D.R., SHERRATT, E., LEDOGAR, J.A. & WROE, S. (2018) The biomechanics of foraging determines face length among kangaroos and their relatives. *Proceedings of the Royal Society B* **285**, 20180845.

MONSON, T.A. & HLUSKO, L.J. (2018) The Evolution of Dental Eruption Sequence in Artiodactyls. *Journal of Mammalian Evolution* **25**, 15–26.

MOUNT, J.G., MUZYLAK, M., ALLEN, S., ALTHNAIAN, T., MCGONNELL, I.M. & PRICE, J.S. (2006) Evidence that the canonical Wnt signalling pathway regulates deer antler regeneration. *Developmental Dynamics* **235**, 1390–1399.

OVERBEEK, P.A., GORLOV, I.P., SUTHERLAND, R.W., HOUSTON, J.B., HARRISON, W.R., BOETTGER-TONG, H.L., BISHOP, C.E. & AGOULNIK, A.I. (2001) A transgenic insertion causing cryptorchidism in mice. *Genesis* **30**, 26–35.

PALOMBO, M.R., KOHLER, M., MOYA SOLA, S. & GIOVINAZZO, C. (2008) Brain versus body mass in endemic ruminant artiodactyls: A case studied of *Myotragus balearicus* and smallest *Candiacervus* species from Mediterranean Islands. *Quaternary International* **182**, 160–183.

PALOMBO, M.R. & ZEDDA, M. (2021) The intriguing giant deer from the Bate cave (Crete): could paleohistological evidence question its taxonomy and nomenclature? *Integrative Zoology*, 1–24.

PARK, H., WOO, D., SONG, E.-G., LIM, A., LEE, B.-K., JANG, J.-D., PARK, T.-J. & CHOI, T.-Y. (2018) Assessment of Fence Height to Prevent Roadkill of Water Deer (*Hydropotes inermis*). *Journal of Environmental Impact Assessment (환경영향평가)* **27**, 232–239.

PAVEZ-FOX, M.A., PINO, M. & CORTI, P. (2015) Muzzle morphology and food consumption by pudu (*Pudu puda* Molina 1782) in south-central Chile. *Studies on Neotropical Fauna and Environment* **50**, 107–112.

PHAN, M., CONTE, F., KHANDELWAL, K.D., OCKELOEN, C.W., BARTZELA, T., KLEEFSTRA, T., VAN BOKHOVEN, H., RUBINI, M., ZHOU, H. & CARELS, C.E.L. (2016) Tooth agenesis and orofacial clefting: genetic brothers in arms? *Human Genetics* **135**, 1299–1327.

PRANGE, H.D., ANDERSON, J.F. & RAHN, H. (1979) Scaling of Skeletal Mass to Body Mass in Birds and Mammals. *The American Naturalist* **113**, 103–122.

PRICE, J.S., ALLEN, S., FAUCHEUX, C., ALTHNAIAN, T. & MOUNT, J.G. (2005) Deer antlers: A zoological curiosity or the key to understanding organ regeneration in mammals? *Journal of Anatomy* **207**, 603–618.

PUTMAN, R., DUNN, N., ZHANG, E., CHEN, M., MIQUEL, C. & SAVOLAINEN, V. (2020) Conservation genetics of native and European-introduced Chinese water deer (*Hydropotes inermis*). *Zoological Journal of the Linnean Society* **XX**, 1–11.

RAFFERTY, K.L. & HERRING, S.W. (1999) Craniofacial sutures: Morphology, growth, and in vivo masticatory strains. *Journal of Morphology* **242**, 167–179.

RAFFERTY, K.L., HERRING, S.W. & MARSHALL, C.D. (2003) Biomechanics of the rostrum and the role of facial sutures. *Journal of Morphology* **257**, 33–44.

RÖRIG, A. (1904) Das Wachstum des Schädels von *Capreolus vulgaris*, *Cervus elaphus* und *Dama vulgaris*. *Anatomischer Anzeiger* **26**, 17–25.

RÖSSNER, G.E. (1995) Odontologische und schädelanatomische Untersuchungen an *Procervulus* (Cervidae, Mammalia). *Münchner Geowissenschaftliche Abhandlungen. Reihe A: Geologie und Paläontologie* **29**, 1–128.

RÖSSNER, G.E. (2007) Family Tragulidae. In *The Evolution of Artiodactyls* pp. 214–220. Johns Hopkins University Press, Baltimore.

RÖSSNER, G.E. (2010) Systematics and palaeoecology of Ruminantia (Artiodactyla, Mammalia) from the Miocene of Sandelzhausen (southern Germany, Northern Alpine Foreland Basin). *Palaontologische Zeitschrift* **84**, 123–162.

RÖSSNER, G.E., COSTEUR, L. & SCHEYER, T.M. (2021) Antiquity and fundamental processes of the antler cycle in Cervidae (Mammalia). *Science of Nature* **108**, 3.

SAAVEDRA, B. & SIMONETTI, J.A. (1991) Archaeological evidence of *Pudu pudu* (Cervidae) in central Chile. *Zeitschrift für Säugetierkunde* **56**, 252–253.

SALDIVIA P., M. & VILLEGAS, F. (2019) Anatomical description of the bone segments that make up the skull of the *Pudu puda* species. *International Journal of Morphology* **37**, 167–173.

SAMEJIMA, Y. & MATSUOKA, H. (2020) A new viewpoint on antlers reveals the evolutionary history of deer (Cervidae, Mammalia). *Scientific Reports* **10**, 8910.

SCHALLER, G.B. & VRBA, E.S. (1996) Description of the giant muntjac (*Megamuntiacus vuquangensis*) in Laos. *Journal of Mammalogy* **77**, 675–683.

SCHILLING, A.-M., CALDERÓN-CAPOTE, M.C. & RÖSSNER, G.E. (2019) Variability, morphometrics, and co-variation of the *os lacrimale* in Cervidae. *Journal of Morphology* **280**, 1071–1090.

SCHILLING, A.-M. & RÖSSNER, G.E. (2017) The (Sleeping) Beauty in the Beast – A review on the water deer, *Hydropotes inermis*. *Hystrix* **28**, 121–133.

SCHILLING, A.-M. & RÖSSNER, G.E. (2021) New skull material of Pleistocene dwarf deer from Crete (Greece). *Comptes Rendus Palevol* **20**, 141–164.

SCOTT, K.M. & JANIS, C.M. (1987) Phylogenetic relationships of the Cervidae, and the case for a superfamily' Cervoidea'. In *Biology and management of the Cervidae* pp. 3–20. Smithsonian Institution Press, Washington.

SHARMA, V., LEHMANN, T., STUCKAS, H., FUNKE, L. & HILLER, M. (2018) Loss of RXFP2 and INSL3 genes in Afrotheria shows that testicular descent is the ancestral condition in placental mammals. *PLoS Biology* **16**, e2005293.

SHARP, A.C. (2015) Comparative finite element analysis of the cranial performance of four herbivorous marsupials. *Journal of Morphology* **276**, 1230–1243.

SMITH, B.H. (2009) 'Schultz's Rule' and the evolution of tooth emergence and replacement patterns in primates and ungulates. In *Development, Function and Evolution of Teeth* pp. 212–228, 1st edition. Cambridge University Press, Cambridge.

SOHN, J.H. & KIMURA, J. (2012) Observation of male reproductive organ in Korean water deer (*Hydropotes inermis argyropus*). *Asian Journal of Animal and Veterinary Advances* **7**, 30–37.

SONDAAR, P.Y. (1977) Insularity and Its Effect on Mammal Evolution. In *Major Patterns in Vertebrate Evolution* pp. 671–707. Springer, Boston.

STADLER, S.G. (1991) Behaviour and social organisation of Chinese water deer (Hydropotes inermis) under semi-natural conditions. Universität Bielefeld, Germany.

STÉGER, V., MOLNÁR, A., BORSY, A., GYURJÁN, I., SZABOLCSI, Z., DANCS, G., MOLNÁR, J., PAPP, P., NAGY, J., PUSKÁS, L., BARTA, E., ZOMBORSZKY, Z., HORN, P., PODANI, J., SEMSEY, S., LAKATOS, P. & OROSZ, L. (2010) Antler development and coupled osteoporosis in the skeleton of red deer *Cervus elaphus*: Expression dynamics for regulatory and effector genes. *Molecular Genetics and Genomics* **284**,

273–287.

STIMPSON, C.M., O'DONNELL, S., HUONG, N.T.M., HOLMES, R., UTTING, B., KAHLERT, T. & RABETT, R.J. (2021) Confirmed archaeological evidence of water deer in Vietnam: relics of the Pleistocene or a shifting baseline? *Royal Society Open Science* **8**, 210529.

TENNANT, J.P. & MACLEOD, N. (2014) Snout shape in extant ruminants. *PLoS ONE* **9**, e112035.

TSUBOI, M., KOPPERUD, B.T., SYROWATKA, C., GRABOWSKI, M., VOJE, K.L., PÉLABON, C. & HANSEN, T.F. (2020) Measuring Complex Morphological Traits with 3D Photogrammetry: A Case Study with Deer Antlers. *Evolutionary Biology* **47**, 175–186.

UNGAR, P.S. (2014) Dental allometry in mammals: A retrospective. *Annales Zoologici Fennici* **51**, 177–187.

VISLOBOKOVA, I. & MÉTAIS, G. (2007) Basal ruminants. In *The Evolution of Artiodactyls* (eds D.R. PROTHERO & S.E. FOSS), pp. 189–212. The Johns Hopkins University Press, Baltimore.

VISLOBOKOVA, I.A. (2013) Morphology, taxonomy, and phylogeny of megacerines (Megacerini, Cervidae, Artiodactyla). *Paleontological Journal* **47**, 833–950.

DE VOS, J. (1979) The endemic Pleistocene deer of Crete. I. *Proceedings of the Koninklijke Nederlandse Akademie van Wetenschappen, Series B* **82**, 59–90.

WAN, X., JIANG, G., YAN, C., HE, F., WEN, R., GU, J., LI, X., MA, J., STENSETH, N.C. & ZHANG, Z. (2019) Historical records reveal the distinctive associations of human disturbance and extreme climate change with local extinction of mammals. *Proceedings of the National Academy of Sciences of the United States of America* **116**, 19001–19008.

WANG, B., CHEN, L. & WANG, W. (2019) Genomic insights into ruminant evolution: from past to future prospects. *Zoological Research* **40**, 476–487.

WANG, X., ZHOU, G., LI, Q., ZHAO, D. & CHEN, Y. (2014) Discovery of SNPs in RXFP2 related to horn types in sheep. *Small Ruminant Research* **116**, 133–136.

WANG, Y., ZHANG, C., WANG, N., LI, Z., HELLER, R., LIU, R., ET AL. (2019) Genetic basis of ruminant headgear and rapid antler regeneration. *Science* **364**, eaav6335.

WIEDEMAR, N., TETENS, J., JAGANNATHAN, V., MENOUD, A., NEUENSCHWANDER, S., BRUGGMANN, R., THALLER, G. & DRÖGEMÜLLER, C. (2014) Independent *polled* mutations leading to complex gene expression differences in cattle. *PLoS ONE* **9**, e93435.

WISLOCKI, G.B. (1954) Antlers in Female Deer, with a Report of Three Cases in *Odocoileus*. *Journal of Mammalogy* **35**, 486–495.

WISLOCKI, G.B. (1956) Further Notes on Antlers in Female Deer of the Genus *Odocoileus*. *Journal of Mammalogy* **37**, 231–235.

WÖLFEL, H. (1983) Zur Jugendentwicklung, Mutter-Kind-Bindung und Feindvermeidung beim Rothirsch (*Cervus elaphus*). *Zeitschrift für Jagdwissenschaft* **29**, 143–162.

WÖLFEL, H. (1984) Zur Jugendentwicklung, Mutter-Kind-Bindung und Feindvermeidung beim Rothirsch (*Cervus elaphus*). *Zeitschrift für Jagdwissenschaft* **30**, 3–14.

XU, M., HORRELL, J., SNITOW, M., CUI, J., GOCHNAUER, H., SYRETT, C.M., ET AL. (2017) WNT10A mutation causes ectodermal dysplasia by impairing progenitor cell proliferation and KLF4-mediated differentiation. *Nature Communications* **8**, 15397.

YANG, J., WANG, S.K., CHOI, M., REID, B.M., HU, Y., LEE, Y.L., HERZOG, C.R., KIM-BERMAN, H., LEE, M., BENKE, P.J., KENT LLOYD, K.C., SIMMER, J.P. & HU, J.C.C. (2015) Taurodontism, variations in tooth number, and misshapened crowns in wnt10a null mice and human kindreds. *Molecular Genetics and Genomic Medicine* **3**, 40–58.

ZENG, Y., BAUGH, E., AKYALCIN, S. & LETRA, A. (2021) Functional Effects of WNT10A Rare Variants Associated with Tooth Agenesis. *Journal of Dental Research* **100**, 302–309.

Chapter 7

Supplements for Chapters 2 and 3

7.1 Supplementary data and code for Chapter 2

7.1.1 Chapter 2, Supplement 1: landmark positions

7.1.2 Chapter 2, Supplement 2: raw data of lacrimal measures

File: Chapter2_lacrimaldata.xlsx

7.1.3 Chapter 2, Supplement 3: summary statistics of lacrimal measures per species

File: Chapter2_SummaryStatistics_lacrimal.docx

7.1.4 Chapter 2, Supplement 4: raw data of skull measurements

File: Chapter2_livingdeer_data.csv

7.1.5 Chapter 2, Supplement 5: R-code for Chapter 2

File: Chapter2_Rcode.Rmd

The data and code are available online.

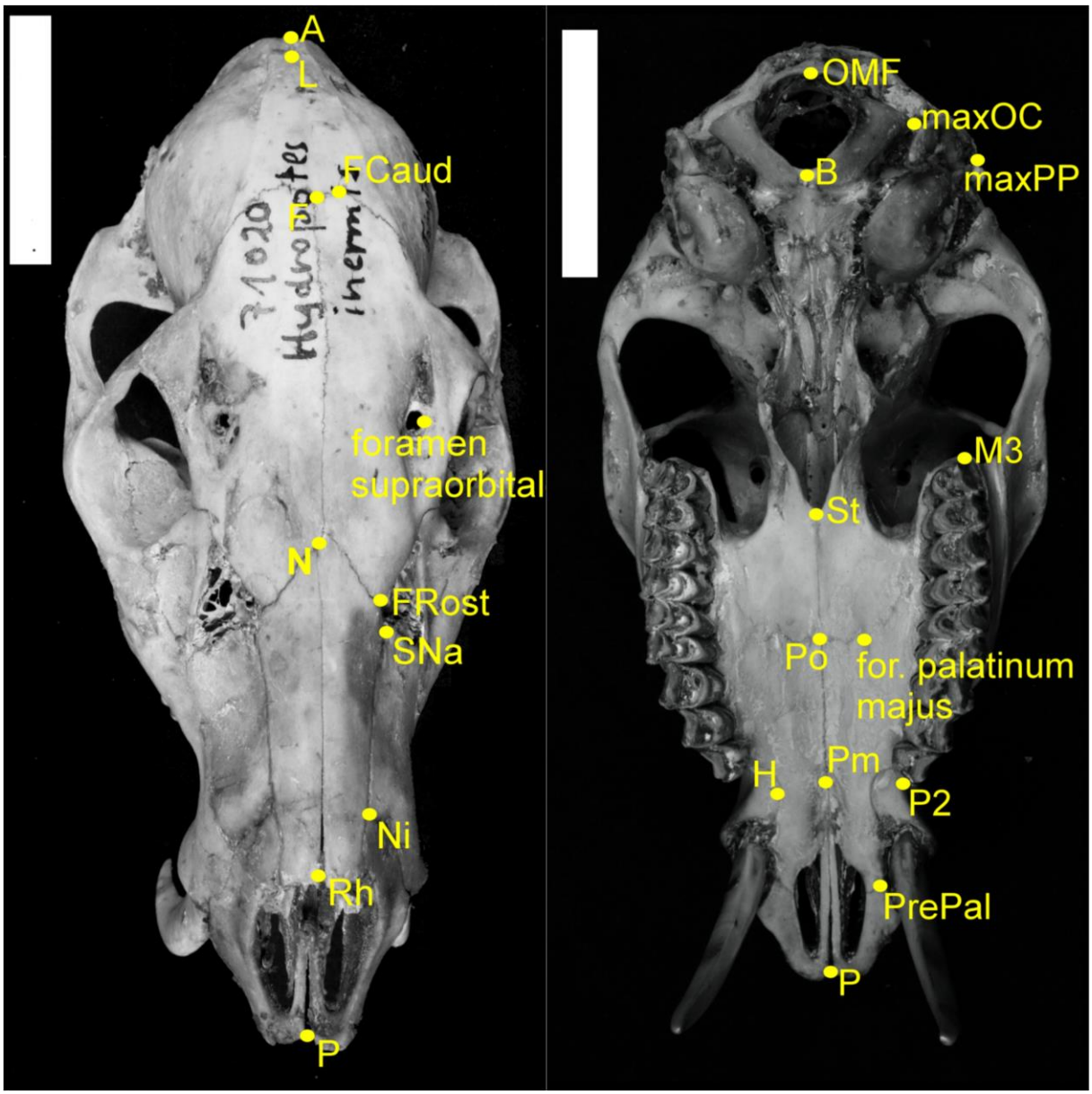

Figure S1. Landmark positions from a dorsal (left) and ventral (right) view in *Hydropotes inermis* (ZMB_Mam_71020). Scale bar: 5 cm. Distances are defined in Appendix 1.

Table S2. Summary statistics for each species. Data are given in log10 (mm). SD: standard deviation; IQR: Interquartile range, 25th, and 75th quartile are given.

	Alces alces	*Capreolus capreolus*	*Cervus elaphus*	*Dama dama*	*Hydropotes inermis*	*Mazama gouazoubira*	*Moschus moschiferus*	*Muntiacus muntjak*	*Pudu pudu*	*Rangifer tarandus*	*Rucervus eldii*	*Tragulus javanicus*
Lacrimal Height												
Minimum	1.54	1.14	1.40	1.34	1.05	1.17	1.18	1.28	0.99	1.31	1.32	1.00
Maximum	1.6	1.3	1.5	1.4	1.1	1.3	1.3	1.4	1.2	1.5	1.5	1.1
Mean (SD)	1.59 (0.03)	1.20 (0.04)	1.44 (0.03)	1.38 (0.04)	1.11 (0.03)	1.23 (0.04)	1.23 (0.04)	1.34 (0.06)	1.09 (0.06)	1.40 (0.05)	1.37 (0.05)	1.07 (0.07)
Median (IQR)	1.58 (1.56, 1.62)	1.20 (1.18, 1.22)	1.43 (1.42, 1.45)	1.36 (1.35, 1.40)	1.11 (1.10, 1.12)	1.23 (1.21, 1.27)	1.24 (1.20, 1.26)	1.35 (1.29, 1.38)	1.10 (1.06, 1.12)	1.41 (1.38, 1.43)	1.36 (1.35, 1.38)	1.08 (1.04, 1.11)
Lacrimojugal Length												
Minimum	1.61	1.07	1.50	1.36	0.89	0.92	0.69	1.31	0.69	1.55	1.47	0.73
Maximum	1.70	1.32	1.68	1.49	1.08	1.20	1.04	1.43	0.90	1.76	1.58	0.85
Mean (SD)	1.66 (0.03)	1.19 (0.05)	1.59 (0.06)	1.42 (0.04)	0.98 (0.06)	1.07 (0.08)	0.89 (0.09)	1.36 (0.04)	0.82 (0.07)	1.63 (0.06)	1.51 (0.04)	0.78 (0.06)
Median (IQR)	1.66 (1.64, 1.68)	1.19 (1.15, 1.22)	1.59 (1.57, 1.60)	1.43 (1.39, 1.44)	0.99 (0.94, 1.03)	1.08 (1.01, 1.13)	0.89 (0.85, 0.93)	1.34 (1.33, 1.39)	0.81 (0.80, 0.87)	1.63 (1.59, 1.68)	1.50 (1.48, 1.54)	0.77 (0.75, 0.81)
Lacrimomaxillar Length												
Minimum	1.18	0.68	1.08	1.26	0.81	0.92	1.12	1.16	0.99	0.98	1.12	0.92
Maximum	1.4	1.1	1.5	1.4	1.1	1.3	1.2	1.5	1.2	1.3	1.4	1.1
Mean (SD)	1.30 (0.08)	0.91 (0.11)	1.33 (0.14)	1.31 (0.04)	0.96 (0.08)	1.13 (0.08)	1.17 (0.03)	1.28 (0.10)	1.07 (0.06)	1.14 (0.10)	1.28 (0.08)	1.00 (0.08)
Median (IQR)	1.31 (1.23, 1.35)	0.93 (0.82, 0.98)	1.36 (1.31, 1.41)	1.31 (1.28, 1.33)	0.97 (0.93, 1.01)	1.13 (1.08, 1.19)	1.16 (1.15, 1.19)	1.25 (1.23, 1.31)	1.07 (1.03, 1.10)	1.15 (1.09, 1.21)	1.30 (1.23, 1.32)	1.02 (0.97, 1.04)

	Alces alces	*Capreolus capreolus*	*Cervus elaphus*	*Dama dama*	*Hydropotes inermis*	*Mazama gouazoubira*	*Moschus moschiferus*	*Muntiacus muntjak*	*Pudu pudu*	*Rangifer tarandus*	*Rucervus eldii*	*Tragulus javanicus*
Lacrimoethmoid Length												
Minimum	1.62	1.10	1.56	1.55	1.20	1.25	0.72	1.13	1.10	1.21	1.59	0.30
Maximum	1.80	1.36	1.72	1.65	1.31	1.46	1.07	1.44	1.30	1.60	1.68	0.68
Mean (SD)	1.69 (0.06)	1.25 (0.05)	1.66 (0.06)	1.61 (0.03)	1.25 (0.04)	1.36 (0.05)	0.91 (0.10)	1.29 (0.08)	1.20 (0.08)	1.49 (0.12)	1.65 (0.03)	0.47 (0.20)
Median (IQR)	1.68 (1.65, 1.74)	1.25 (1.23, 1.28)	1.68 (1.63, 1.71)	1.63 (1.60, 1.63)	1.25 (1.22, 1.28)	1.37 (1.32, 1.38)	0.92 (0.86, 0.97)	1.29 (1.27, 1.31)	1.17 (1.14, 1.26)	1.53 (1.47, 1.56)	1.66 (1.64, 1.66)	0.42 (0.36, 0.55)
Lacrimofrontal Length												
Minimum	1.21	0.80	1.29	1.18	0.77	0.76	0.87	1.22	0.72	1.15	1.27	0.97
Maximum	1.46	1.10	1.39	1.31	0.91	1.16	1.15	1.47	0.88	1.53	1.37	1.10
Mean (SD)	1.30 (0.07)	0.97 (0.06)	1.34 (0.03)	1.24 (0.04)	0.83 (0.05)	0.95 (0.08)	1.02 (0.08)	1.34 (0.09)	0.80 (0.06)	1.36 (0.11)	1.33 (0.04)	1.04 (0.06)
Median (IQR)	1.30 (1.27, 1.32)	0.98 (0.93, 1.02)	1.34 (1.33, 1.34)	1.24 (1.22, 1.27)	0.81 (0.80, 0.87)	0.95 (0.90, 0.99)	1.02 (0.95, 1.07)	1.34 (1.26, 1.40)	0.80 (0.76, 0.85)	1.36 (1.29, 1.42)	1.33 (1.30, 1.35)	1.05 (1.01, 1.08)
Maximal Lacrimal Length												
Minimum	1.8	1.2	1.7	1.7	1.2	1.4	1.2	1.5	1.2	1.7	1.7	1.1
Maximum	1.9	1.5	1.8	1.7	1.4	1.6	1.3	1.6	1.3	1.9	1.8	1.2
Mean (SD)	1.81 (0.03)	1.39 (0.06)	1.78 (0.04)	1.71 (0.03)	1.30 (0.04)	1.45 (0.04)	1.23 (0.03)	1.55 (0.05)	1.26 (0.02)	1.75 (0.05)	1.77 (0.03)	1.13 (0.06)
Median (IQR)	1.81 (1.79, 1.83)	1.38 (1.35, 1.43)	1.79 (1.75, 1.82)	1.73 (1.70, 1.73)	1.31 (1.28, 1.33)	1.45 (1.42, 1.48)	1.23 (1.20, 1.25)	1.54 (1.53, 1.57)	1.27 (1.26, 1.28)	1.74 (1.71, 1.76)	1.77 (1.76, 1.78)	1.14 (1.10, 1.16)

Code for Chapter 2 - Variability, morphometrics, and co-variation of the os lacrimale in Cervidae - code for figures and associated statistics

Ann-Marie Schilling

22 February 2021

This supplement gives the R-code used to generate figures 3-7 and numerical analyses presented in tables 3-6 as well as the text of Chapter 2 of the present dissertation. The data are available as "Chapter2_livingdeer_data.csv". The rational and references for the procedures implemented here are given in the main text of the publication.

Load packages needed

```
library(psych)
library(qwraps2)
library(dplyr)
library(car)
library(ggplot2)
library(egg)
library(rrcov)
library(ggfortify)
library(readxl)
library(smatr)
library(lmodel2)
library(psychometric)
library(stringr) # for string (text) manipulation
library(pcaMethods) # for imputation
library(Matrix)
library(rcompanion)
```

Load data

```
InData <- "Chapter2_livingdeer_data.csv"
mydata <- read.csv(InData, sep = ";", skip = 1, header = T)
```

Helper function for jpeg images

Parameters are optimized for Fig 4, but may be adjusted as desired.

```
save_plot2 <- function(in_plot, file_name, width=8, height=6, ppi = 600)
{
  jpeg(paste(file_name, c("jpeg"), sep="."), width = width, height = height,
       units = "in", res = ppi)
```

```
  plot(in_plot)
  dev.off()
}
```

Log-transform data

```
log_data <- mydata
numeric_cols <- colnames(mydata[10:75])

for (current_column in numeric_cols)
{
  log_data[,current_column] <- log10(log_data[,current_column])
}
```

Code for Figure 3 and associated statistics

Statistics for Figure 3

```
#subset data
sub.data <- mydata[ , c("Family", "Genus", "Sex", "X46_LacFOrb_LacJOrb",
                        "X47_LacJOrb_LJM", "X48_LJM_Letm_caud",
                        "X49_Letm_caudal_Lnetm", "X50__Lfetm_LFOrb",
                        "X54_maxLength_L","X1_AP" )]

columns_for_size = c("X46_LacFOrb_LacJOrb", "X47_LacJOrb_LJM",
                     "X48_LJM_Letm_caud","X49_Letm_caudal_Lnetm",
                     "X50__Lfetm_LFOrb", "X54_maxLength_L", "X1_AP")

# create a new data frame that will store log-transformed data
log_data_3 <- sub.data
for (current_column in columns_for_size) {
  log_data_3[,current_column] <- log10(sub.data[,current_column])
}

# get geomentric mean of lacrimal variables
log_data_3$size_lacbone <- apply(log_data_3[,c(4:9)], 1, mean)

# Calculate and print statistics for allometric line
# Is there interspecific allometry? Is the slope different from one?
regII <- ma(size_lacbone ~ X1_AP, data= log_data_3, log="", slope.test=1)
cat("error message due to removal of rows with no data - may be neglected")
cat("test for slope = 1")
regII

reg2intercept <- lmodel2(size_lacbone ~ X1_AP, data= log_data_3)
cat("confidence intervals for regression coefficients - method MA is the rele
vant one")
reg2intercept
```

```
# extract coefficients for line fitting in plot below
reg2coef <- reg2intercept$regression.results
```

Plot for Figure 3

The warning given upon running the following code is due to the removal of data (specimens) with missing data. That is desired and ok.

The line with slope 1 was plotted such that it intersects with the allometric line at the lower end of the skull size range covered by our data. The basic idea here was that it is not sensible to extrapolate beyond the range actually observed in allometric analyses (see, e.g., Schmidt-Nielsen 1984, p 25).

```
Fig3 <- ggplot(log_data_3, aes(x=X1_AP, y=size_lacbone)) +
  geom_point(aes(shape=Genus, col=Family), size =3.5) +
  labs(x="Skull length (log10(mm))",
       y="Size of the lacrimal facial facet (log10(mm))") +
  scale_shape_manual(values=c(1:12))+
  coord_fixed(ratio=1, xlim = c(1.95, 2.8), ylim=c(0.85, 1.7))+
  geom_abline(slope= reg2coef$Slope[2],color="blue",
              intercept = reg2coef$Intercept[2],
              linetype = "solid",size=1)+
  # since lmodel2 or ma cannot be used as a method here
  geom_abline(slope=1,color="black", intercept = -1.14,
              linetype = "dashed",size=1)+
  # intercept such that the two lines intersect at x = 1.95, i.e.
  # the lower value of the range covered
  theme(axis.title.x=element_text(size=14), # X axis title
  axis.title.y=element_text(size=14),# Y axis title
  axis.text.x = element_text(size=12),
  axis.text.y = element_text(size=12),
  legend.text=element_text(size=12),
  legend.title = element_text(size=14))+
  theme_bw()

save_plot2(Fig3, "Fig_3",width=8, height=8, ppi = 600)
```

Code for Figure 4

Get subset of lacrimal measures and descriptive variables and calculate size of lacrimal (geometric mean of its measures)

```
lacrimal_variables <- c("Family", "Sub_Family", "Genus", "Species",
                        "CollectionID", "Collection", "X46_LacFOrb_LacJOrb",
```

```
                          "X47_LacJOrb_LJM", "X48_LJM_Letm_caud",
                          "X49_Letm_caudal_Lnetm", "X50__Lfetm_LFOrb",
                          "X54_maxLength_L", "Habitat", "Head_Weapons",
                          "Depression_size", "Depression_position",
                          "Sociality", "Qualitative_Body_Size", "Diet",
                          "Coverage")
lac_bone <- droplevels(log_data[,lacrimal_variables])

# add geometric mean as size variable
lac_bone$size <- apply(lac_bone[,c(7:12)], 1, mean)
```

Robust PCA raw data (PCA sensu Jolicoeur (1963))

```
x.cov <- PcaCov(lac_bone[c(7:12)], cov.control = CovControlMMest())
shape <- getPrcomp(x.cov)
```

Plot PCAs dimensions 1 and 2 (dimension 1 = size sensu Jolicoeur (1963))

```
# scaling factor for panels
SFac <- as.numeric(as.factor(levels(as.factor(lac_bone$Genus))))

habitat <- autoplot(shape, data=lac_bone, colour="Habitat",shape="Genus",
 frame=T, x=1, y=2, size = 3) +
 theme_bw(base_size = 14) +
 scale_shape_manual(values= SFac)

sociality <- autoplot(shape, data=lac_bone, colour="Sociality",shape="Genus",
 frame=T, x=1, y=2, size = 3) +
 theme_bw(base_size = 14) +
 scale_shape_manual(values= SFac)

sociality$labels$colour <- "Social behavior" # adjusts legend title
sociality$labels$fill <- "Social behavior"   # both lines are needed!

sub_family <- autoplot(shape, data=lac_bone, colour="Sub_Family", shape = "Ge
nus",
 frame=T, x=1, y=2, size=3) +
 theme_bw(base_size = 14) +
scale_shape_manual(values= SFac)

sub_family$labels$colour <- "(Sub-)Family" # adjusts legend title
sub_family$labels$fill <- "(Sub-)Family"   # both lines are needed!

weapons <- autoplot(shape, data=lac_bone, colour="Head_Weapons", shape = "Gen
us",
 frame=T, x=1, y=2, size=3) +
 theme_bw(base_size = 14)+
```

```
 scale_shape_manual(values= SFac)

weapons$labels$colour <- "Head-Weapons" # adjusts legend title
weapons$labels$fill <- "Head-Weapons"   # both lines are needed!

genus <- autoplot(shape, data=lac_bone, colour="Genus", shape= "Genus",
 frame=T, x=1, y=2, size=3) +
 theme_bw(base_size = 14) +
 scale_shape_manual(values= SFac)

gF <- ggplot_gtable(ggplot_build(genus))
gC <- ggplot_gtable(ggplot_build(sub_family))
gA <- ggplot_gtable(ggplot_build(weapons))
gH <- ggplot_gtable(ggplot_build(habitat))
gS <- ggplot_gtable(ggplot_build(sociality))

# adjust all plots to identical size (gA is the standard)
gC$widths  <- gA$widths; gC$heights <- gA$heights
gF$widths  <- gA$widths; gF$heights <- gA$heights
gH$widths  <- gA$widths; gH$heights <- gA$heights
gS$widths  <- gA$widths; gS$heights <- gA$heights

save_plot2(gF, "4c"); save_plot2(gC, "4e")
save_plot2(gA, "4g"); save_plot2(gH, "4i")
save_plot2(gS, "4k")
```

Plot PCA dimensions 2 and 3 (shape sensu Jolicoeur (1963))

```
habitat.shape <- autoplot(shape, data=lac_bone, colour="Habitat",shape="Genus
",
 frame=T, x=2, y=3, size = 3) +
 theme_bw(base_size = 14) +
 scale_shape_manual(values= SFac)

sub_family.shape <- autoplot(shape, data=lac_bone, colour="Sub_Family", shape
= "Genus",
 frame=T, x=2, y=3, size=3) +
 theme_bw(base_size = 14) +
 theme(legend.position="none") +
 scale_shape_manual(values= SFac)

sub_family.shape$labels$colour <- "(Sub-)Family" # adjusts legend title
sub_family.shape$labels$fill <- "(Sub-)Family"   # both lines are needed!

weapons.shape <- autoplot(shape, data=lac_bone, colour="Head_Weapons", shape
= "Genus",
 frame=T, x=2, y=3, size=3) +
 theme_bw(base_size = 14)+
 theme(legend.position="none") +
 scale_shape_manual(values= SFac)
```

```
weapons.shape$labels$colour <- "Head-Weapons" # adjusts legend title
weapons.shape$labels$fill <- "Head-Weapons"   # bothlines are needed!

genus.shape23 <- autoplot(shape, data=lac_bone, colour="Genus", shape= "Genus
",
 frame=T, x=2, y=3, size=3) +
 theme_bw(base_size = 14) +
 scale_shape_manual(values= SFac)

genus.shape12 <- autoplot(shape, data=lac_bone, colour="Genus", shape= "Genus
",
 frame=T, x=1, y=3, size=3) +
 theme_bw(base_size = 14) +
 theme(legend.position="none") +
 scale_shape_manual(values= SFac)

sociality.shape <- autoplot(shape, data=lac_bone, colour="Sociality",shape="G
enus",
 frame=T, x=2, y=3, size = 3) +
 theme_bw(base_size = 14) +
 scale_shape_manual(values= SFac)

sociality$labels$colour <- "Social behavior" # adjusts legend title
sociality$labels$fill <- "Social behavior"   # both lines are needed!

gX <- ggplot_gtable(ggplot_build(genus.shape12))
gB <- ggplot_gtable(ggplot_build(genus.shape23))
gC <- ggplot_gtable(ggplot_build(sub_family.shape))
gF <- ggplot_gtable(ggplot_build(weapons.shape))
gK <- ggplot_gtable(ggplot_build(habitat.shape))
gL <- ggplot_gtable(ggplot_build(sociality.shape))

# just to adjust all plots to identical size
# gA is taken from above code chunk
gB$widths  <- gA$widths; gB$heights <- gA$heights
gC$widths  <- gA$widths; gC$heights <- gA$heights
gF$widths  <- gA$widths; gF$heights <- gA$heights
gX$widths  <- gA$widths; gX$heights <- gA$heights
gK$widths  <- gA$widths; gK$heights <- gA$heights
gL$widths  <- gA$widths; gL$heights <- gA$heights

save_plot2(gB, "4a"); save_plot2(gX, "4d")
save_plot2(gC, "4f"); save_plot2(gF, "4h")
save_plot2(gK, "4j"); save_plot2(gL, "4l")
```

Shape data as defined by Mosiman & PCA for size-corrected data (shape sensu Mosimann (1970))

The warning displayed upon running the following code is due to numerical precision of computation; may be neglected.

```
#calcualte shape by subtraction
size_corrected_data <- lac_bone
columns_for_size <- c("X46_LacFOrb_LacJOrb","X47_LacJOrb_LJM","X48_LJM_Letm_caud",
                      "X49_Letm_caudal_Lnetm","X50__Lfetm_LFOrb","X54_maxLength_L")
for (i_column in columns_for_size) {
  size_corrected_data[,i_column] <- lac_bone[, i_column] - lac_bone$size
  }

# robust PCA for size-corrected data; shape alla Mosimann 1970

compute.robustPCa.shape <- PcaCov(~., signflip=T, data=size_corrected_data[,7:12])
shape.mosi <- getPrcomp(compute.robustPCa.shape)
# results in a warning - may be neglected, due to computational numerical precision
```

Plot shape sensu Mosimann (1970) - Figure 4b

```
genus.mosi <- autoplot(shape.mosi, data=size_corrected_data, colour="Genus",
 shape="Genus", frame=T, x=1, y=2, size=3) +
 theme_bw(base_size = 14) +
 scale_shape_manual(values=as.numeric(as.factor(levels
                   (as.factor(size_corrected_data$Genus)))))

gB <- ggplot_gtable(ggplot_build(genus.mosi))
gB$widths  <- gA$widths  # gA is taken from above, size plotting
gB$heights <- gA$heights

save_plot2(gB, "4b")
```

For results presented in table 3

Confidence intervals for the loadings originally obtained with the package “FRB”. As of this writing (updating) of this script, the FRB package is available only in archived form and cannot be used with actual versions of R. One way to use it is to download the archived version, extract the function “FRBpcaMM” from it, and apply this using the data in objects “lac_bone[,7:12)]

Alternatively, I implemented a simple bootstrap procedure, based on code given by Gavin Simpson (see: https://stackoverflow.com/questions/31057192/resampling-not-producing-expected-result-of-principal-component-analysis)

Note that this code gives confidence intervals on an absolute scale - so the signs of the intervals need to be adjusted to correspond with the sign of the PC analyzed. This is, however, not an issue as the sign of loadings "is arbitrary and may well be different when you run the code on a different machine, OS, compiler, CPU etc." (Gavin Simpson). What is important, though, is whether all loadings of a PC are of the same sign (cf main text).

Also note that the confidence intervals are obtained by bootstrapping. *That takes some time, so be patient when running the following code chunk*. Also, as this is a bootstrap, it will result in slightly different results each time you run it.

```
# table 3 left side (size-and-shape data)
getLoadings(x.cov)[, 1:3] # for loadings of PC1-PC3
getEigenvalues(x.cov)[1:3] # for eigenvalues
sum (getEigenvalues(x.cov)) # for total variance
summary(x.cov)@importance[,1:3] # for SDs, var explained, & cumulative var

# for confidence intervals of PC1 based on robust pca via rrcov
mydf <- (lac_bone[c(7:12)])
times <- 999
ll <- vector(mode = "list", length = times)
# the following "for"-loop takes quite some time to run. Be patient
for (i in seq_len(times)) {
  tempdf  <- mydf[sample(nrow(mydf), replace = TRUE), ]
  x.cov <- PcaCov(tempdf, cov.control = CovControlMMest())
  shape2 <- getPrcomp(x.cov)
  ll[[i]] <- abs(shape2$rotation) ## NOTE: abs(...)
}

lower <- data.frame(apply(simplify2array(ll), 1:2, quantile, probs = 0.025))[
,1]
upper <- data.frame(apply(simplify2array(ll), 1:2, quantile, probs = 0.975))[
,1]
CiPC1 <- round(data.frame(lower, upper), 2)
rownames(CiPC1) <- colnames(mydf)
CiPC1

# table 3 right side (size-corrected data)
getLoadings(compute.robustPCa.shape)[,1:3] # for loadings of PC1-PC3
getEigenvalues(compute.robustPCa.shape)[1:3] # for eigenvalues
sum(getEigenvalues(compute.robustPCa.shape)) # for total variance
summary(compute.robustPCa.shape)@importance[,1:3] # for SDs, variance
                                  # explained, and cumulative variance
```

For results presented in table 4

Note that since the sign of individual loadings may be inverted based on differences of the actual computing environment (CPU, compiler; cf above), the sign of the correlations calculated below may also vary. But the absolute values of the correlations and their confidence limits are correct.

```
# table 4 "original data" - i.e not size corrected
pcs <- shape$x
plot(pcs[,1], lac_bone$size)
cor(pcs[,1], lac_bone$size)
psychometric::CIr(r = cor(pcs[,1], lac_bone$size), n = length(pcs[,1]), level
= 0.95)
cor(pcs[,2], lac_bone$size)
psychometric::CIr(r = cor(pcs[,2], lac_bone$size), n = length(pcs[,2]), level
= 0.95)
cor(pcs[,3], lac_bone$size)
psychometric::CIr(r = cor(pcs[,3], lac_bone$size), n = length(pcs[,3]), level
= 0.95)

# table 4 "size corrected data"
pcs2 <- shape.mosi$x
cor(pcs2[,1], lac_bone$size)
psychometric::CIr(r = cor(pcs2[,1], lac_bone$size), n = length(pcs2[,1]), lev
el = 0.95)
cor(pcs2[,2], lac_bone$size)
psychometric::CIr(r = cor(pcs2[,2], lac_bone$size), n = length(pcs2[,2]), lev
el = 0.95)
```

For results presented in table 5

```
males.2 <- droplevels(log_data_3[which(log_data_3$Genus %in% c("Capreolus",
           "Hydropotes", "Muntiacus", "Mazama", "Tragulus", "Moschus",
           "Rangifer", "Alces", "Cervus", "Rucervus", "Dama", "Pudu")),])

# lacrimal height vs skull length
cat ("lacrimal height")
regIILM2.height_skull_len <- lmodel2(X46_LacFOrb_LacJOrb ~ X1_AP, data= males
.2)
regIILM2.height_skull_len

# lacriomaxillar length vs skull length
cat("lacrimomaxillar length")
regIILM2.lacmax_skull_len <- lmodel2(X48_LJM_Letm_caud ~ X1_AP, data= males.2
)
regIILM2.lacmax_skull_len
```

```
# lacrimojugal length vs skull length
cat("lacrimojugal length")
regIILM2.lacjug_skull_len <- lmodel2(X47_LacJOrb_LJM ~ X1_AP, data= males.2)
regIILM2.lacjug_skull_len

# lacrimoethmoidal gap length vs skull length
cat("lacrimoethmoi length")
regIILM2.laceth_skull_len <- lmodel2(X49_Letm_caudal_Lnetm ~ X1_AP, data= mal
es.2)
regIILM2.laceth_skull_len

# lacrimofrontal length of the lacrimale vs skull length
cat("lacrimofrontal length")
regIILM2.lacfront_skull_len <- lmodel2(X50__Lfetm_LFOrb ~ X1_AP, data= males.
2)
regIILM2.lacfront_skull_len

# maximal length of the lacrimale vs skull length
cat("Maximal lacrimal length")
regIILM2.lacmaxlaclen_skull_len <- lmodel2(X54_maxLength_L ~ X1_AP, data= mal
es.2)
regIILM2.lacmaxlaclen_skull_len
```

Code for Figure 5

```
# make a new data frame that holds only data needed
forFig5 <- data.frame(lac_bone[, c(3, 7:12, 21)]) # "data.frame" is important
;
# otherwise "forFig5" is a tibble,and subtraction code below will not work

# normalize to size by subtracting size
forFig5_2 <- forFig5 # make acopy in order to keep also original data
forFig5_2[,c(2:8)] <- forFig5_2[,c(2:8)] - forFig5_2[,8]

# extract data and make big dataframe that can be used for plotting
test2 <- aggregate(forFig5_2[,c(2:7)], list(forFig5_2[,1]), mean_ci, simplify
= T)
test3 <- aggregate(forFig5_2[,2], list(forFig5_2[,1]), length, simplify = T)
measures <- data.frame(do.call("rbind", test2[2:7]))
measures$bone <- rep(names(test2[2:7]), each = 12)
measures$species <- rep(test2[[1]], 6)
measures$no <- rep(test3$x, 6)
```

Plot for Figure 5

```
jpeg("Fig_5.jpg", width = 9, height = 7, units = 'in', res = 1000)
```

```
# set parameters etc valid for all plots
head.dist <- 0.5 # distance of header from top of plot, in lines
my.ylim <- c(-0.55, 0.30) # limits for y-axis.
CI.color <- "lightgray" # color for confidence interval
cex.xlab <- 1.2 # font size for x label at bottom (suture names)
my.adj <- c(1.0, -0.0) # for x axisÂ´s labels. must be adjusted to size of ce
x.lab

# set up layout
par(mfrow = c(4,3)) # 3-by-4 grid of plots
par(oma = c(10, 4, 1, 1)) # make room for overall x and y axis titles
par(mar = c(0.5, 2, 2, 1)) # make the plots closer together

# for x-axis labels of last three plots
labels <- c("Lacrimal height", "Lacrimojuagal length",
            "Lacrimomaxillar length", "Lacrimoethmoid length",
            "Lacrimofrontal length", "Maximal lacrimal length")

# function for plotting
plotFig5 <- function (measures, What, x.axis=F, my.lwd=1, my.pch=19, my.cex=1
)
  {
# "measures" is a data table as defined in the previous code chunk
# "What" is the species name, to be written in "", as given i the "species"
# column of measures (measures$species)
# "x.axis": should an x-axis & its labels be printed. Defaults to FALSE
# my.lwd is line width for plot; defaults to 1
# my.pch is symbol for plot. defaults to 19
# my.cex is size of symbol, defaults to 1
pd <- droplevels(subset(measures, measures$species == What))
index <- c(1:6) # needed as a helper to shade confidence interval: DO NOT CHA
NGE
plot(index, pd$lcl, ylim = my.ylim, type="n", las=1, xlab="", ylab ="",  xaxt
="n")
points(pd$ucl, type = "n")
grid()
polygon(c(index, rev(index)), c(pd$lcl,rev(pd$ucl)),col=CI.color, border = NA
)
points(pd$mean, type = "b", lwd = my.lwd, pch = my.pch, cex = my.cex)
description = paste(as.character(pd[1,5]), ", n = ", pd[1,6], sep = "")
title(description, line = head.dist)
if(x.axis){
axis(side=1, at=index, labels = FALSE)
text(x=index, labels = labels, srt = 45, pos = NULL, xpd = NA, par("usr")[3]
- 0.2,
     adj = my.adj, cex = cex.xlab)}
}

plotFig5(measures, "Tragulus", x.axis = F); plotFig5(measures, "Rangifer", x.
axis = F);
```

```
plotFig5(measures, "Capreolus", x.axis = F); plotFig5(measures, "Moschus", x.
axis = F);
plotFig5(measures, "Alces", x.axis = F); plotFig5(measures, "Hydropotes", x.a
xis = F)
plotFig5(measures, "Muntiacus", x.axis = F); plotFig5(measures, "Cervus", x.a
xis = F);
plotFig5(measures, "Mazama", x.axis = F); plotFig5(measures, "Dama", x.axis =
T)
plotFig5(measures, "Rucervus", x.axis = T); plotFig5(measures, "Pudu", x.axis
= T)
mtext("size-normalized suture length (log10); mean and 95% CI", side = 2,
      outer = TRUE, line = 2, cex = 1)
dev.off()
```

Code for Figure 6

Load additional packages needed

```
library(corrplot)
library(ggpubr)
library(ggcorrplot)
```

Select species with nearly complete data, remove colums (measures) with too many missing data

Species selected: Capreolus, Hydropotes, Muntjak. Moschus as outgroup

```
# select species
data.for.correl <- droplevels(mydata[which(mydata$Genus %in%
                   c("Capreolus", "Hydropotes", "Muntiacus", "Moschus")), ])

# remove columns from dataset that do not contain data or are not shared by a
ll species
colsToExclude <- c("Sub_Family", "Collection", "Sex", "Notes",
                   "Spender.Sammler", "X17_maxWidthC", "X19_maxWidth_Calv",
                   "X20_maxLength_Calv", "X21_maxWidth_C", "X22_maxLength_C",
                   "X22a_maxHeight_C", "X22b_height_CM","X22c_IoF_C",
                   "X22d_maxWidthCC_M", "X22e_maxWidth_CC_tip",  "X23_CBL",
                   "X28_p2c", "X28a_p2alv", "X30_minWidth_diastema_d",
                   "X58", "size1", "size2", "size3", "Idx","X44_length_parP",
                   "X55_maxLengthM", "X56_maxWidth_J",
                   "X42_BJ","Habitat_old", "Habitat", "Head_Weapons",
                   "Depression_size", "Depression_position", "Sociality",
                   "Qualitative_Body_Size", "Diet", "Coverage")

#create dataset for imputation, removing the above mentioned columns
data.for.imputation <- data.for.correl[,-which(names(data.for.correl)
                                               %in% colsToExclude)]
```

Now columns are renamed to allow plotting of Figure 6 with de-coded names for measures

```
oDF <-data.frame(data.for.imputation) # copy data.frame

# Lacrimal
colnames(oDF)[colnames(oDF) == "X46_LacFOrb_LacJOrb"] <- "Lacrimal height"
names(oDF)[names(oDF) == "X47_LacJOrb_LJM"] <- "Lacrimojugal length"
names(oDF)[names(oDF) == "X48_LJM_Letm_caud"] <- "Lacrimomaxillar length"
names(oDF)[names(oDF) == "X49_Letm_caudal_Lnetm"] <- "Lacrimoethmoid length"
names(oDF)[names(oDF) == "X50__Lfetm_LFOrb"] <- "Lacrimofrontal length"
names(oDF)[names(oDF) == "X54_maxLength_L"] <- "Maximal lacrimal length"

#nasal for plot
names(oDF)[names(oDF) == "X14_naxWidthN_rostral"] <- "14 "
names(oDF)[names(oDF) == "X15_maxWidthN_caudal"] <- "15 "
names(oDF)[names(oDF) == "X35_maxLength_Prh"] <- "40 "
names(oDF)[names(oDF) == "X36_maxHeigth_Prh"] <- "41 "
names(oDF)[names(oDF) == "X45_Ni_Nlat"] <- "51 "
names(oDF)[names(oDF) == "X5_Nrh"] <- "5 "
names(oDF)[names(oDF) == "X51_NfetmCaud_NfethmRost"] <- "53 "
names(oDF)[names(oDF) == "X52NMethm_Lmethm"] <- "54 "
names(oDF)[names(oDF) == "X18_maxWidth_IoF"] <- "18 "

data.for.imputation <- oDF
#needed in next chunk
numeric.columns <- c(5 : ncol(data.for.imputation))
```

Now impute the data

Each variable contains NAs. We imputed data to eliminate missing values.

Define function for imputation and do species-specific imputations

```
# define two helper functions for imputation
# Impute missing values
# data.in: input data frame
# GenusToUse: String defining for which Genus data should be imputed
# numericColumns: Columns of interest, i.e. columns whose values will be impu
ted

# Subselects species from input data frame and return it
subselectdata <- function(input.df, genus.to.use)
  {
  species.to.use <- droplevels(subset(input.df, input.df$Genus == genus.to.us
e))
  return(species.to.use)
}

impute.missingValues <- function(data.in, GenusToUse, numericColumns)
{
  species.data <- subselectdata(data.in, GenusToUse)
```

```
  # impute data
  pc <- pcaMethods::pca(species.data[, numericColumns],
                        nPcs = 5, method = "bpca", center = T)
  imputed <- completeObs(pc)
  # make new data set for each species with imputed values
  species.data.imp <- cbind(species.data[, -numericColumns], imputed)
  return(species.data.imp)
}

#apply function for imputation
moschus.imp <- impute.missingValues(data.for.imputation,
                                    "Moschus", numeric.columns)
capreolus.imp <- impute.missingValues(data.for.imputation,
                                      "Capreolus", numeric.columns)
hydropotes.imp <- impute.missingValues(data.for.imputation,
                                       "Hydropotes", numeric.columns)
muntiacus.imp <- impute.missingValues(data.for.imputation,
                                      "Muntiacus", numeric.columns)

#create new dataframe containing ALL species
imputed.final <- rbind(capreolus.imp, hydropotes.imp, moschus.imp, muntiacus.
imp)
```

Calculate size and shape for imputed data

```
#size - calculate geometric mean
imputed.final$size <- apply(imputed.final[, numeric.columns], 1, prod)^
                      (1 /length(numeric.columns))

# add size to the numeric columns
shape.columns.imputed <- numeric.columns
size.column.imputed <- ncol(imputed.final)
numeric.columns.imputed <- c(shape.columns.imputed, size.column.imputed)

#shape - divide each value by size and logtransform
imputed.shape <- imputed.final[, shape.columns.imputed] / imputed.final$size
imputed.shape.log <- log10(imputed.shape)

#create dataset with size-corrected data
shape.log <- cbind(imputed.final[, -numeric.columns.imputed], imputed.shape.l
og)
```

Assign variables to the lacrimal or nasal modules

```
lacrimal_bone_idx <- c("Lacrimal height", "Lacrimojugal length",
                       "Lacrimomaxillar length", "Lacrimoethmoid length",
                       "Lacrimofrontal length", "Maximal lacrimal length")

nasal_idx <- c("14 ", "15 ", "40 ", "41 ", "51 ", "5 ", "53 ", "54 ", "18 ")
```

Define function to calculate and tabulate Spearman correlations between nasal and lacrimal variables

Procedure: 1. Compile correlations for each species separately 2. write correlation coefficients in extra data frame 3. assign species names to correlation coefficients 4. check whether correlations per species is significant (1) or not (2), threshold p= 0.05

Note that if classical Pearson's correlation is desired instead of Spearman's, this may be readily implemented by calling the convenience function defined below with the argument "method ="pearson".

```
# define convenience function for Spearman correlation and data handling
# default method is Spearman correlation, but this may be adjusted by
# changing the value of "method". See R help ?cor for details

compute.lac.cor <- function(input.df, genus.to.use, module.idx,
                            p_value_threshold=0.05, method = "spearman")
{
  species.to.use <- subselectdata(input.df, genus.to.use)
  cols.of.interest <- c(lacrimal_bone_idx, module.idx)
  data.to.use <- species.to.use[, cols.of.interest]

  # compute correlations
  correlated.data <- cor(data.to.use, method = method)
    # get confidence interval and p value using the cor.mtest command
  correlated.additional.data <- cor.mtest(data.to.use, method = method)

  # set to 0 if over p_threshold, otherwise 1
  significant_correlation <- as.matrix(apply(correlated.additional.data$p,
                           1:2, function(x) {ifelse(any(x >= p_value_threshold
), 0,1)}))

  # set row and col names
  rownames(correlated.additional.data$p) <- cols.of.interest
  colnames(correlated.additional.data$p) <- cols.of.interest
  rownames(significant_correlation) <- cols.of.interest
  colnames(significant_correlation) <- cols.of.interest

  # pack all in a named list
  output_data <- list(correlation=correlated.data[lacrimal_bone_idx,
              module.idx],
              p_value=correlated.additional.data$p[lacrimal_bone_idx,
              module.idx],
              significant_correlation=significant_correlation[lacrimal_bone_i
dx,
              module.idx])
  return (output_data)
}
```

Calculate correlations between nasal and lacrimal variables using above function

```
#nasal
capreolus.cor.nasal <- compute.lac.cor(shape.log, "Capreolus", nasal_idx )
hydropotes.cor.nasal <- compute.lac.cor(shape.log, "Hydropotes", nasal_idx )
moschus.cor.nasal <- compute.lac.cor(shape.log, "Moschus", nasal_idx )
muntiacus.cor.nasal <- compute.lac.cor(shape.log, "Muntiacus", nasal_idx )
```

Plot these correlations (Figure 6 in published research article)

```
# add a small ',' on a column to force ggplot to treat labels as strings.
# !! This is important, otherwise ggcorrplot will not work.
# The '.' will be removed again before final printing
y_labels <- c("14", "15", "40", "41", "51", "5,",  "53", "54", "18")
colnames(capreolus.cor.nasal$correlation) <- y_labels
colnames(hydropotes.cor.nasal$correlation) <- y_labels
colnames(muntiacus.cor.nasal$correlation) <- y_labels
colnames(moschus.cor.nasal$correlation) <- y_labels

# reorder columns
new.col.order <- c("5,", "14", "15", "18", "40", "41", "51", "53", "54")

X1 <- ggcorrplot(capreolus.cor.nasal$correlation[, new.col.order],
                 ggtheme=theme_bw(base_size = 18),
                 title = "Capreolus capreolus",
                 legend.title ="Correlation", lab=T, pch.col = "grey",
                 pch=1, pch.cex = 12, show.legend=FALSE, tl.srt=90)

X2 <- ggcorrplot(hydropotes.cor.nasal$correlation[, new.col.order],
                 ggtheme=theme_bw(base_size = 18),
                 title = "Hydropotes inermis",
                 legend.title ="Correlation", lab=T, pch.col = "grey",
                 pch=1, pch.cex = 12, show.legend=FALSE, tl.srt=90)

X3 <- ggcorrplot(muntiacus.cor.nasal$correlation[, new.col.order],
                 ggtheme=theme_bw(base_size = 18),
                 title = "Muntiacus muntjak",
                 legend.title ="Correlation", lab=T, pch.col = "grey",
                 pch=1, pch.cex = 12, show.legend=FALSE,  tl.srt=90)

X4 <- ggcorrplot(moschus.cor.nasal$correlation[, new.col.order],
                 ggtheme=theme_bw(base_size = 18),
                 title = "Moschus moschiferus",
                 legend.title ="Correlation", lab=T, pch.col = "grey",
                 pch=1, pch.cex = 12, show.legend=FALSE, tl.srt=90)

# correct printing of y labels (i.e., replace "5," by "5")
a <- as.factor(rep(c(5, 14, 15, 18, 40, 41, 51, 53, 54), each = 6))
X1$data$Var2 <- a; X2$data$Var2 <- a; X3$data$Var2 <- a; X4$data$Var2 <- a
```

```
save_plot2(X1, "Fig_6_capreolus", width=4, height=8)
save_plot2(X2, "Fig_6_hydropotes", width=4, height=8)
save_plot2(X3, "Fig_6_muntiacus", width=4, height=8)
save_plot2(X4, "Fig_6_moschus", width=4, height=8)
```

Code for Figure 7

```
for_depression <- log_data_3
for_depression$Depression_size <- as.factor(log_data$Depression_size)
for_depression$Depression_position <- as.factor(log_data$Depression_position)

# for Fig 7 A
p1 <- ggplot(for_depression, aes(x=Depression_size, y=size_lacbone)) +
      theme_light(base_size = 12) +
      theme(panel.grid.minor = element_blank()) +
      scale_x_discrete(limits=c("Absent", "Small", "Medium", "Large")) +
      labs(x="Depression size",
      y="Size of the lacrimal facial facet (log10(mm))")
jit <- position_jitter(seed = 123, width = 0.2)
Fig_7A <- p1 + geom_jitter(aes(shape = Genus), size = 3, position = jit) +
      scale_shape_manual(values = c(1:12))

gFig7A <- ggplot_gtable(ggplot_build(Fig_7A))
save_plot2(gFig7A, "Fig_7_A", width=6, height=8, ppi = 600)

# For Fig 7 B
p2 <- ggplot(for_depression, aes(x=Depression_position, y=size_lacbone)) +
      theme_light(base_size = 12) +
      theme(panel.grid.minor = element_blank()) +
      scale_x_discrete(limits=c("Absent", "Ventral", "Central", "Dorsal")) +
      labs(x="Depression size",
      y="Size of the lacrimal facial facet (log10(mm))") +
      geom_boxplot(outlier.shape = NA)
jit <- position_jitter(seed = 123, width = 0.2)
Fig_7B <- p2 + geom_jitter(aes(shape = Genus), size = 3, position = jit) +
     scale_shape_manual(values = c(1:12))

gFig7B <- ggplot_gtable(ggplot_build(Fig_7B))
save_plot2(gFig7B, "Fig_7_B", width=6, height=8, ppi = 600)
```

Code for correlations, cf p 1081 & 1082 and Table 6

The following code implements the calculation of correlations of lacrimal measures with other skull measures. It also allows to select the strongest (both positive and negative) correlations (cf function “reduced_output” defined below). Lastly, correlations among selected species and per nasal measure are compared. In the published research article (Chapter 2 of this dissertation), the results may be found in table 6 and its associated text.

Define convenience function needed to select strong correlations

This function requires, as input, a matrix of correlations and a number between 1 and 100 that gives the percentage of correlations to be considered. Note that fractional (not integer) results of this % selection are rounded to the next integer.

```
reduced_output <- function(Data, Percent){
  # function to generate an output where only a selected percentage of
  # all data is shown - the X Percent largest and smallest ones.
  # Data is a matrix (of correlation values)
  # Percent gives the percentage of these that should be considered "strong".
  # Will be rounded to integer numbers
he <- sort(abs(Data)) # convert to abs values, make vector & sort
DatAbs <- abs(Data) # a copy with absolute Data values
DatSign <- sign(Data) # copy holding the sign (+ or -) of the data
X <- round(length(he) * (100 - Percent)/100) # The position in vector "he"
                        # of value corresponding to the percentage chosen is
defined
DatAbs[DatAbs < he[X]] <- 0 # in the Copy w abs values, those smaller than
                            # the value of he[X] are replaced by zero.
Data <- DatAbs * DatSign # Finally, remaining values are multiplied with the
                         # sign of the orig. data to restore pos/neg values
return(Data)
}
```

Select species to be analyzed, preprocess data

```
sub.data1 <- droplevels(mydata[which(mydata$Genus %in% c("Capreolus",
             "Hydropotes", "Muntiacus", "Tragulus", "Moschus")), ])
sub.data2 <- sub.data1[, -c(4,74,79:88)] # do not contain data used here
```

Log 10 transfrom raw measurements and assign measurements to cranial modules

```
sub.data2[,9:76] <- log10(sub.data2[,9:76])

module <- c('na', 'na', 'na', 'na', 'na', 'na', 'na', 'na', 'none', 'none',
            'none', 'vault', 'nasal', 'vault', 'vault', 'vault', 'vault',
            'vault', 'none', 'vault', 'vault', 'nasal', 'nasal', 'oral',
            'dental', 'facial', 'dental', 'dental','dental', 'dental',
            'dental', 'dental', 'dental', 'dental', 'dental', 'none', 'none',
            'oral', 'oral', 'dental','oral', 'oral', 'oral', 'oral', 'oral',
            'oral', 'base','base', 'nasal', 'nasal', 'oral',  'vault',
            'vault', 'none', 'none', 'vault', 'base', 'base', 'base',
            'nasal', 'lacrimal', 'lacrimal', 'lacrimal', 'lacrimal',
            'lacrimal', 'nasal','vault', 'nasal', 'lacrimal', 'nasal',
            'jugal', 'jugal', 'vault',  'na', 'na', 'na')

# modify column labels (names of measurements) such that they also include
# the module name (or a abbreviation of this name)
```

```
measures <- colnames(sub.data2)
mo_meas <- str_c (module, measures, sep = "_")
# rename columns with new names of the form "module_measure"
colnames(sub.data2) <- mo_meas
```

Impute missing data and then calculate correlations

For each species, missing data are imputed separately. See p 1081 of the publication for details and the basic logic of the imputation. The output gives summary information about imputed data.

Capreolus

```
capreolus <- droplevels(subset(sub.data2, sub.data2$na_Genus == "Capreolus"))
# remove X_17, X19 to X22e, X28, X28a and X_30 since there are only a
# few observations for these measures in capreolus

capreolus22 <- as.data.frame(capreolus[, -c(25, 27:35, 41,42,44)])
#str(capreolus22)
checkData(capreolus22[, 9:ncol(capreolus22)], verbose=TRUE)
# impute data
pc <- pcaMethods::pca(capreolus22[, 9:ncol(capreolus22)],
                      nPcs=5, method="bpca", center = T)

# % missing
a <- pc@missing
table(a)["TRUE"]/(table(a)["FALSE"] + table(a)["TRUE"]) * 100
imputed <- pcaMethods::completeObs(pc)
capreolus2 <- cbind(capreolus22[,1:8], imputed)

cap.all.4 <- cor(capreolus2[, 9:ncol(capreolus2)], use = "na.or.complete")
```

Muntiacus

```
munt <- droplevels(subset(sub.data2, sub.data2$na_Genus == "Muntiacus"))
munt22 <- munt # no need to drop data, since mostly complete;
               # just to have same name structure as for other species

# impute data
pc <- pcaMethods::pca(munt22[, 9:ncol(munt22)], nPcs=5, method="bpca", center
= T)

# % missing
a <- pc@missing
table(a)["TRUE"]/(table(a)["FALSE"] + table(a)["TRUE"]) * 100
imputed <- pcaMethods::completeObs(pc)
munt2 <- cbind(munt22[,1:8], imputed)

munt.all.4 <- cor(munt2[, 9:ncol(munt2)], use = "na.or.complete")
```

Moschus

```
moschus <- droplevels(subset(sub.data2, sub.data2$na_Genus == "Moschus"))

# remove X_30 and size1, size2, size3, since there are only 4 complete
# observations with these values
moschus22 <- moschus[, -c(44, 74, 75, 76)]
moschus22[1:4, 33] <- NA # replace "Inf" and "NaN" introduced when "log10" wa
s applied

# impute data
pc <- pcaMethods::pca(moschus22[, 9:ncol(moschus22)], nPcs=5, method="bpca",
center = T)

# % missing
a <- pc@missing
table(a)["TRUE"]/(table(a)["FALSE"] + table(a)["TRUE"]) * 100
imputed <- pcaMethods::completeObs(pc)
moschus2 <- cbind(moschus22[,1:8], imputed)

moschus.all.4 <- cor(moschus2[, 9:ncol(moschus2)], use = "na.or.complete")
```

Hydropotes

```
hydro <- droplevels(subset(sub.data2, sub.data2$na_Genus == "Hydropotes"))

# remove X_30 and size1, size2, size3, since there are only 4 complete
# observations with these values

hydro22 <- hydro[, -c(44, 74, 75, 76)]

# impute data
pc <- pcaMethods::pca(hydro22[, 9:ncol(hydro22)], nPcs=5, method="bpca", cent
er = T)

# % missing
a <- pc@missing
table(a)["TRUE"]/(table(a)["FALSE"] + table(a)["TRUE"]) * 100
imputed <- pcaMethods::completeObs(pc)
hydro2 <- cbind(hydro22[,1:8], imputed)

hyd.all.4 <- cor(hydro2[, 9:ncol(hydro2)], use = "na.or.complete")
```

Calculate correlations based on size and select variables present in all species

```
capreolus.lac <- cap.all.4[ , grepl( "lacrimal" , colnames(cap.all.4) ) ]
hydropotes.lac <- hyd.all.4[ , grepl( "lacrimal" , colnames(hyd.all.4) ) ]
muntiacus.lac <- munt.all.4[ , grepl( "lacrimal" , colnames(munt.all.4) ) ]
moschus.lac <- moschus.all.4[ , grepl( "lacrimal" , colnames(moschus.all.4) )
```

```
]

ca.rownames <- rownames(capreolus.lac)
hy.rownames <- rownames(hydropotes.lac)
mun.rownames <- rownames(muntiacus.lac)
mo.rownames <- rownames(moschus.lac)

common.rownames <- Reduce(intersect, list(ca.rownames, hy.rownames,
                                          mun.rownames, mo.rownames))

capreolus.lac2 <- capreolus.lac[common.rownames, ]
hydropotes.lac2 <- hydropotes.lac[common.rownames, ]
muntiacus.lac2 <- muntiacus.lac[common.rownames, ]
moschus.lac2 <- moschus.lac[common.rownames, ]
```

Remove some measures:

This was done to remove correlations between lacrimal variables, and also to remove some measures which could not unambiguously be assigned to a specific module.

```
capreolus.reduced <- capreolus.lac2[-c(18, 36, 38, 40:44, 48:50), ]
hydropotes.reduced <- hydropotes.lac2[-c(18, 36, 38, 40:44, 48:50), ]
muntiacus.reduced <- muntiacus.lac2[-c(18, 36, 38, 40:44, 48:50), ]
moschus.reduced<- moschus.lac2[-c(18, 36, 38, 40:44, 48:50), ]
```

select the 10 % strongest (positive or negative) correlations

```
capreolus7 <-reduced_output(capreolus.reduced, 10)
hydropotes7 <- reduced_output(hydropotes.reduced, 10)
muntiacus7 <- reduced_output(muntiacus.reduced, 10)
moschus7 <- reduced_output(moschus.reduced, 10)
```

Count strong (i.e., the percentage selected) correlations per module

```
# define modules of data present in data to be counted
mo2 <- c('none', 'none', 'none', 'vault', 'nasal', 'vault', 'vault', 'vault',
         'vault', 'vault', 'none', 'vault', 'vault', 'nasal', 'nasal',
         'oral', 'facial', 'none', 'oral', 'oral', 'dental','oral', 'oral',
         'oral', 'base','base', 'nasal', 'nasal', 'oral', 'vault', 'vault',
         'none', 'none', 'vault', 'base', 'nasal', "nasal", 'vault',
         'nasal', 'jugal', 'vault')

# strong correlations in capreolus; numbers are strong corr. in modules
#  base, dental & oral, vault, nasal & facial, jugal, none (in this order)
Num <- as.vector(by(as.data.frame(capreolus7), mo2, Matrix::nnzero))
cap <- c(Num[1], Num[2] + Num[7], Num[8], Num[5] + Num[3], Num[4], Num[6])

# strong correlations in hydropotes; numbers are strong corr. in modules
#  base, dental & oral, vault, nasal & facial, jugal, none (in this order)
Num <- as.vector(by(as.data.frame(hydropotes7), mo2, Matrix::nnzero))
hyd <- c(Num[1], Num[2] + Num[7], Num[8], Num[5] + Num[3], Num[4], Num[6])
```

```
# strong correlations in muntiak; numbers are strong corr. in modules
#  base, dental & oral, vault, nasal & facial, jugal, none (in this order)
Num <- as.vector(by(as.data.frame(muntiacus7), mo2, Matrix::nnzero))
mun <- c(Num[1], Num[2] + Num[7], Num[8], Num[5] + Num[3], Num[4], Num[6])

# strong correlations in moschus; numbers are strong corr. in modules
#  base, dental & oral, vault, nasal & facial, jugal, none (in this order)
Num <- as.vector(by(as.data.frame(moschus7), mo2, Matrix::nnzero))
mos <- c(Num[1], Num[2] + Num[7], Num[8], Num[5] + Num[3], Num[4], Num[6])
```

In the following code chunk, p-values are calculated as given in Table 6, left column. Note that values may vary slightly for different runs due to the (minor) influence of imputing (above). The key point is, however, that none of the p vales gets anywhere near 0.05.

```
# compare species with each other
four.species.highest <-t(data.frame(cap, hyd,mun, mos))
four.species.highest
PT <- pairwiseNominalIndependence(four.species.highest, fisher = T,
                                  gtest  = F,
                                  chisq  = F, method = "fdr", digits =2)
PT[, c(1,3)]
```

Test whether correlations are clustered in any one module

If the correlations are not clustered, i.e. if they are randomly distributed, we expect large values for p (i.e., > 0.05). *Note that p-values are obtained by bootstrapping - so they are predicted to vary somewhat for each instance that this code is run*.

"p" gives the expected relative frequencies of all possible correlations per module. These are numbers of possible correlations divided by their largest common divisor (6). This approach is chosen to get as close as possible to the number of correlations actually analyzed (26). Otherwise, estimates of p would get erroneously low. This is for the results shown on p 1082, left column.

```
p <- c(3,8,13,9,1,8) # expected relative frequencies
                     # (possible correlations per module)

cap2 <- matrix(c(cap, p), nrow = 2, byrow = T)
#colnames(cap2) <- c("base", "oral", "vault", "nasal", "jugal", "none")
cat ("Capreolus")
fisher.test(cap2, simulate.p.value = T, B = 2000)

hyd2 <- matrix(c(hyd, p), nrow = 2, byrow = T)
cat ("Hydropotes")
fisher.test(hyd2, simulate.p.value = T, B = 2000)

mun2 <- matrix(c(mun, p), nrow = 2, byrow = T)
cat("Muntiak")
```

```
fisher.test(mun2, simulate.p.value = T, B = 2000)

mos2 <- matrix(c(mos, p), nrow = 2, byrow = T)
cat("Moschus")
fisher.test(mos2, simulate.p.value = T , B = 2000)
```

Count strong correlations per lacrimal measure per species

```
cap.lac <- as.vector(colSums(capreolus7 != 0)) # for capreolus
hyd.lac <- as.vector(colSums(hydropotes7 != 0)) # for hydropotes
mun.lac <- as.vector(colSums(muntiacus7 != 0)) # for muntiak
mos.lac <- as.vector(colSums(moschus7 != 0)) # for moschus
```

Inter-species comparison.

Note that the column "p.adj.Fisher" is the one giving the p values adjusted for the multiple comparisons that are done. This is for the data results shown in table 6, right hand column.

```
# compare species with each other
four.species.highest.lac <-t(data.frame(cap.lac, hyd.lac,mun.lac, mos.lac))
four.species.highest.lac

PTlac <- pairwiseNominalIndependence(four.species.highest.lac, fisher=T,
                                     gtest=F,
                                     chisq=F, digits = 2)
PTlac
```

Test whether pattern in species deviates from expectation

This is for the p values presented on p 1082, right-hand column.

"p.lac" gives the expected relative frequencies of all possible correlations per lacrimal measure if each measure had the same probability to be involved in a strong correlation. The actual number chosen (4) results from the desire to get a sum as close as possible to the actual number of correlations tested (26). This is for results shown in the text on p 1082, right hand column. Again, we deal with bootstrap p values that may vary slightly from run to run.

```
p.lac <- c(4,4,4,4,4,4) # almost 26; this distribution is expected if all
                        # lacrimal measures equally participate in strong
                        # correlations

cat("Are strong correlations distributed randomly across lacrimal varialbles?
")
cap2.lac <- matrix(c(cap.lac, p.lac), nrow = 2, byrow = T)
cat("capreolus")
fisher.test(cap2.lac, simulate.p.value = T, B = 2000)

hyd2.lac <- matrix(c(hyd.lac, p.lac), nrow = 2, byrow = T)
cat("hydropotes")
```

```
fisher.test(hyd2.lac, simulate.p.value = T, B = 2000)

mun2.lac <- matrix(c(mun.lac, p.lac), nrow = 2, byrow = T)
cat("muntiak")
fisher.test(mun2.lac, simulate.p.value = T, B = 2000)

mos2.lac <- matrix(c(mos.lac, p.lac), nrow = 2, byrow = T)
cat("moschus")
fisher.test(mos2.lac, simulate.p.value = T , B = 2000)
```

References

JOLICOEUR, P. (1963) 193. Note: The Multivariate Generalization of the Allometry Equation. *Biometrics* **19**, 497. JSTOR.

MOSIMANN, J.E. (1970) Size allometry: size and shape variables with characterizations of the lognormal and generalized gamma distributions. *J. Am. Stat. Assoc.* **65**, 930–945. Taylor & Francis Group.

SCHMIDT-NIELSEN, K. (1984) Scaling. Why is animal size so important? Cambridge, Cambridge University Press.

7.2 Supplementary data and code for Chapter 3

7.2.1 Chapter 3, Supplement 1: Raw data for fossil and recent deer

File: Chapter3_fossildeer_data.csv

7.2.2 Chapter 3, Supplement 2: Code for Chapter 3

File: Chapter3_Rcode.Rmd

7.2.3 Chapter 3, Supplement 3: Skull, antler and height data from literature (Ceacero 2016; Haber 2016; Clutton-Brock, Albon, and Harvey 1980)

File: Chapter3_supplement3.xlsx

The data and code are available online.

Code for Chapter 3 - The size and shape of the lacrimal facial facet in Candiacervus and Megaloceros, two cervids from the Pleistocene

Ann-Marie Schilling

15 January 2021

This supplement gives the R-code used to generate the figures and numerical analyses presented in Chapter 3 of the present thesis. The data are available as Supplement 1 to Chapter 3 ("Chapter3_fossildeer_data.csv").

Load libraries

```
library(colorspace)
library(RColorBrewer)
library(ggplot2)
library(GGally)
library(smatr)
library(lmodel2)
```

R code preparation

Define details for plots (background etc)

```
# see
# http://www.noamross.net/blog/2013/11/20/formatting-plots-for-pubs.html
science_theme = theme_minimal() + theme(panel.grid.major = element_line(size
= 0.5,
    color = "grey"), axis.line = element_line(size = 0.7, color = "black"),
    legend.position = c(0.85, 0.7), text = element_text(size = 14))
```

A little helper function to subset data

```
subselectdata <- function(input.df, genus.to.use) {
    species.to.use <- droplevels(subset(input.df, input.df$Genus == genus.to.
use))
    return(species.to.use)
}
```

Data preparation

Read in original data

```
mydata <- read.csv("Chapter3_fossildeer_data.csv", sep = ";", skip = 1,
    na.strings = c("NA", "na", "?", ""))
```

Select lacrimal and skull length data

For Figure 2, we are interested only in the lacrimal bone variables and cranial length. Therefore, we subset data, selecting species and variables of interest. The tragulids Hyemoschus and Moschiola were excluded, as too few specimens per group are available, i.e., 2 males and 4 females respectively:

```
sub.data <- droplevels(mydata[which(mydata$Genus %in% c("Capreolus", "Hydropo
tes",
    "Muntiacus", "Mazama", "Tragulus", "Moschus", "Rangifer", "Alces",
    "Cervus", "Rucervus", "Dama", "Pudu", "Megaloceros", "Candiacervus")),
    ])

# eliminate row 124, as data for the lacrimal facial facet could not be
# taken
sub.data <- sub.data[-124, c("Family", "Genus", "Sex", "X46_LacFOrb_LacJOrb",
    "X47_LacJOrb_LJM", "X48_LJM_Letm_caud", "X49_Letm_caudal_Lnetm", "X50__Lf
etm_LFOrb",
    "X54_maxLength_L", "X1_AP", "X24_BP"), ]
```

Log10-transform data

A rationale for log-transformation may be found in Whitlock & Schluter (2015, p. 378).

```
columns_for_size = c("X46_LacFOrb_LacJOrb", "X47_LacJOrb_LJM", "X48_LJM_Letm_
caud",
    "X49_Letm_caudal_Lnetm", "X50__Lfetm_LFOrb", "X54_maxLength_L", "X1_AP",
    "X24_BP")

num.cols <- length(columns_for_size)

# create a new data frame that will store log-transformed data
log_data <- sub.data
for (current_column in columns_for_size) {
    log_data[, current_column] <- log10(sub.data[, current_column])
}
```

Data analyses

Estimate bone and skull size

We use the geometric mean of the lacrimal bone variables, a common approach to estimate size. We use the skull length as proxy for skull size. Using a single variable is very approximate, but a valuable tool for size estimation (Klingenberg, 2016).

```
log_data$size_lacbone <- apply(log_data[, c(4:9)], 1, mean)

# check data distribution: my_plot <- ggplot(log_data, aes(x=Genus,
# y=size_lacbone)) + geom_boxplot() + science_theme + theme(axis.text.x
# = element_text(angle = 45, hjust = 1)) + labs(x='', y='Bone size')

# my_plot
```

For each genus, data are approximately normally distributed, though sample size is small. Alces, Rangifer and Muntiacus have the largest bone and Tragulus has the smallest bones. Moschus, Capreolus and Hydropotes are inbetween. Except Muntiacus, this reflects a body size signal.

```
log_data$size_skull <- log_data$X1_AP

# check data distribution: my_plot <- ggplot(log_data, aes(x=Genus,
# y=size_skull)) + geom_boxplot() + science_theme + theme(axis.text.x =
# element_text(angle = 45, hjust = 1)) + labs(x='Genus',
# y='Size_skull') my_plot
```

Data distribution more irregular (“bumpy”), but still proximate to normal. The boxplots reflect the pattern seen in the boxplots for bone size. Muntiacus is somewhat closer to medium-sized species.

Code for Figure 3

This piece of code replots Figure 2 from Chapter 2, into which the current fossil data are then integrated.

```
# living species
log_data_live <- droplevels(log_data[which(log_data$Genus %in% c("Capreolus",
    "Hydropotes", "Muntiacus", "Mazama", "Tragulus", "Moschus", "Rangifer",
    "Alces", "Cervus", "Rucervus", "Dama", "Pudu")), ])

# only choose males log_data.m <-
# droplevels(log_data[which(log_data$Sex=='m'),])
log_data_live.m <- droplevels(log_data_live[which(log_data_live$Sex ==
    "m"), ])

# subset for fossil data only
log_data_fossil <- droplevels(log_data[which(log_data$Genus %in% c("Megalocer
```

```
os",
    "Candiacervus")), ])
```

In the following we want to integrate the de Vos Vos (1984) data of skull length in our plot. As de Vos only reports the basilar skull length (X24_BP) which we used only for a subset of the recent species, we estimate the full skull length of Candiacervus (X1_AP) for the de Vos specimens. The ratio of X24_BP and X1_AP for our one complete specimen is 0.8804. This factor is used to estimate the AP for the de Vos specimens.

```
# candiacervus data only
log_data_candi <- droplevels(log_data[which(log_data$Genus %in% c("Candiacerv
us")),
    ])
X24_BP_deVos <- c(192, 196.7)  # range de Vos 1984, Table 7 female male, Gera
ni 4 only
X1_AP_deVos <- X24_BP_deVos/0.8804  # estimates of X1_AP in de Vos
# based on X24/X1 ratio of the one complete specimen in my sample
X1_AP_deVoslog <- log10(X1_AP_deVos)
```

Add fossil data to Figure 3.2

```
# Is there allometry? Is the slope different from one? (to compare with Chapt
er 2)
regII <- ma(size_lacbone ~ X1_AP, data= log_data_live.m, log="", slope.test=1
)
summary(regII)

reg2intercept <- lmodel2(size_lacbone ~ X1_AP, data= log_data_live.m)
cat("confidence intervals ror regression coefficients - method MA is the rele
vant one")
reg2intercept
# extract coefficients for line fitting in plot below
reg2coef <- reg2intercept$regression.results

mycol_candi <- c("red", "blue","grey", "red", "blue", "red", "blue", "grey")
mycol_mega <- c("red", "red", "blue","blue", "blue", "blue", "red",
                "red","blue","blue", "blue", "blue", "red","blue", "grey", "r
ed",
                "blue", "red", "blue", "grey")

allo.grey <- ggplot(log_data_live.m, aes(x=X1_AP, y=size_lacbone)) +
  geom_point(aes(shape=Genus), color= "grey50", size =2.5) +
  labs(x="Skull length (log10 mm)", y="Size of the lacrimal facial facet (log
10)") +
  geom_abline(slope= reg2coef$Slope[2],color="black",
              intercept = reg2coef$Intercept[2], linetype = "solid",size=1)+
   # geom_smooth(method = lm, col="black") +
  scale_shape_manual(values=c(1:14)) +
  #scale_color_grey () +
  geom_point(data= log_data_fossil, aes(x=X1_AP, y=size_lacbone, shape= Genus
),
             size= 2.5, colour= mycol_mega)+
```

```
  # the next two lines to be commented out if filled triangle is not wanted
  geom_point(data= log_data_fossil, aes(x=X1_AP[16], y=size_lacbone[16]), sha
pe= 17,
             size= 2.5, colour= "red")+
  geom_hline (data= log_data_candi, aes(yintercept=size_lacbone), colour=myco
l_candi) +
  geom_vline(xintercept = X1_AP_deVoslog)+
  geom_vline(xintercept = 2.265, col= "black", lty=5) # lower limit of the sk
ull size based on the size of the lacrimal facial facet for Candiacervus

#adaptations for publication
science_theme = theme(panel.grid.major = element_line(size = 0.5, color = "gr
ay"),
                      panel.background = element_rect(fill = "white", colour
= "gray50"),
                      axis.line = element_line(size = 0.7, color = "black"),
                      #legend.position = c(0.85, 0.7),
                      text = element_text(size = 14))

fig2.grey <- allo.grey + science_theme
print(fig2.grey)
#export plot
ggsave("Fig_3_3.jpg", width = 8, height = 5, dpi = 600)
```

Code for Figure 3.4

```
# select rows
sub.data <- droplevels(mydata[which(mydata$Genus %in% c("Capreolus", "Hydropo
tes",
    "Muntiacus", "Mazama", "Tragulus", "Moschus", "Rangifer", "Alces",
    "Cervus", "Rucervus", "Dama", "Pudu", "Megaloceros", "Candiacervus")),
    ])

# select variables eliminate row 124, as no data available
sub.data <- sub.data[-124, c("Family", "Genus", "Sex", "X46_LacFOrb_LacJOrb",
    "X47_LacJOrb_LJM", "X48_LJM_Letm_caud", "X49_Letm_caudal_Lnetm", "X50__Lf
etm_LFOrb",
    "X54_maxLength_L", "X1_AP", "X24_BP"), ]

# eliminate genera for which no data on females are available
sub.data <- droplevels(mydata[which(mydata$Genus %in% c("Capreolus", "Hydropo
tes",
    "Muntiacus", "Mazama", "Tragulus", "Rangifer", "Alces", "Megaloceros",
    "Candiacervus")), ])
```

Log transform data and size-correct the data

```
# select columns of interest
columns_for_log <- c("X46_LacFOrb_LacJOrb", "X47_LacJOrb_LJM", "X48_LJM_Letm_
caud",
```

```
    "X49_Letm_caudal_Lnetm", "X50__Lfetm_LFOrb", "X54_maxLength_L", "X11_maxW
idth",
    "X1_AP")

# create a new data frame that will store log-transformed data
log_data <- sub.data
for (current_column in columns_for_log) {
    log_data[, current_column] <- log10(sub.data[, current_column])
}

# select colums for size correction lacrimal bone, only numeric columns
columns_for_size = c("X46_LacFOrb_LacJOrb", "X47_LacJOrb_LJM", "X48_LJM_Letm_
caud",
    "X49_Letm_caudal_Lnetm", "X50__Lfetm_LFOrb", "X54_maxLength_L")

# create dataframe used for size-corrected data
shape <- log_data
columns_to_use <- c("Genus", "Sex", "X46_LacFOrb_LacJOrb", "X47_LacJOrb_LJM",
    "X48_LJM_Letm_caud", "X49_Letm_caudal_Lnetm", "X50__Lfetm_LFOrb", "X54_ma
xLength_L")
genus_to_use = c("Alces", "Capreolus", "Hydropotes", "Mazama", "Muntiacus",
    "Rangifer", "Tragulus", "Megaloceros", "Candiacervus")
data_subset = shape[shape$Genus %in% genus_to_use, ]
data_subset = data_subset[, columns_to_use]
male_row_index = data_subset$Sex == "m"
female_row_index = data_subset$Sex == "f"

# split data by sex
male_data = data_subset[male_row_index, ]
female_data = data_subset[female_row_index, ]
male_data = male_data[!is.na(male_data$Sex), ]
female_data = female_data[!is.na(female_data$Sex), ]
```

Summary of male and female data

```
# get rid of empty rows which will bug analysis
male_data <- droplevels(male_data)
summary(male_data)

female_data <- droplevels(female_data)
summary(female_data)
```

Size correction based on the geometric mean - shape data

We obtain the size-corrected data by subtracting the geometric mean of the lacrimal facial facet from the raw data, that were used to calculate the geometric mean (see Falsetti, Jungers, & Cole, 1993, Mosimann (1970))

```
# calculate geometric mean for males and females
columns_for_size <- 3:ncol(male_data)
male_data$size <- apply(male_data[, columns_for_size], 1, mean)
```

```
columns_for_size <- 3:ncol(female_data)
female_data$size <- apply(female_data[, columns_for_size], 1, mean)

# create data frame with size-corrected data
shape.males <- male_data
for (i_column in columns_for_size) {
    shape.males[, i_column] <- male_data[, i_column] - male_data$size
}

shape.females <- female_data
for (i_column in columns_for_size) {
    shape.females[, i_column] <- female_data[, i_column] - female_data$size
}
```

Code for Figures 3.4C and 3.4D

```
# data to use
axes_columns = c("X46_LacFOrb_LacJOrb", "X47_LacJOrb_LJM", "X48_LJM_Letm_caud
",
    "X49_Letm_caudal_Lnetm", "X50__Lfetm_LFOrb", "X54_maxLength_L")

# rename datacolumns in plot
mylabels <- c("Lacrimal height", "Lacrimojugal length", "Lacrimomaxillary len
gth",
    "Lacrimoethmoid length", "Lacrimofrontal length", "maximal lacrimal lengt
h")

# add correct names of variables and exlude GM from plotting
current_plot_males = ggparcoord(shape.males, columns = 3:8, showPoints = T,
    groupColumn = "Genus", scale = "globalminmax", title = "males") +
    theme(axis.text.x = element_text(angle = 45, hjust = 1),
        legend.position = "none") + facet_wrap(~Genus) + labs(x = "",
    y = "size-normalized suture length (log10)") + scale_shape_manual(values
= c(1:14)) +
    scale_x_discrete(labels = mylabels) + coord_cartesian(ylim = c(-0.7,
    0.4))

print(current_plot_males)

# export plot
ggsave("Fig_3_4C.jpg", width = 8, height = 5, dpi = 600)
# the height/width ratio defines the aspect of the plot
current_plot_females = ggparcoord(shape.females, columns = 3:8,
    showPoints = T, groupColumn = "Genus", scale = "globalminmax",
    title = "females") + theme(axis.text.x = element_text(angle = 45,
    hjust = 1), legend.position = "none") + facet_wrap(~Genus) +
    labs(x = "", y = "size-normalized suture length (log10)") +
    scale_shape_manual(values = c(1:14)) + scale_x_discrete(labels = mylabels
) +
    coord_cartesian(ylim = c(-0.7, 0.4))
```

```
print(current_plot_females)

# export plot
ggsave("Fig_3_4D.jpg", width = 8, height = 5, dpi = 600)
```

Note for FEMALE fossil data: in each of the Megaloceros and the Candiacervus panel, there is one female that differs from the other Megaloceros and Candiacervus females/its conspecifics, i.e., there are two "outliers", one Candiacervus and one Megaloceros. If these two outliers are compared to each other though, they have the same patterning of the shape of the lacrimal bone.

Code for Figures 3.4A and 3.4B

```
data_fossils = data_subset[data_subset$Genus %in% c("Megaloceros",
    "Candiacervus"), ]
columns_for_size_fossils <- 3:ncol(data_fossils)
data_fossils$size <- apply(data_fossils[, columns_for_size_fossils],
    1, mean)

# create dataframe with size-corrected data
shape.fossils <- data_fossils
for (i_column in columns_for_size_fossils) {
    shape.fossils[, i_column] <- data_fossils[, i_column] - data_fossils$size
}

shape.megaloceros = shape.fossils[shape.fossils$Genus == "Megaloceros",
    ]
shape.candiacervus = shape.fossils[shape.fossils$Genus == "Candiacervus",
    ]

current_plot_mega = ggparcoord(shape.megaloceros, columns = 3:8,
    showPoints = T, title = "Megaloceros", groupColumn = "Sex",
    scale = "globalminmax") + theme(axis.text.x = element_text(angle = 45,
    hjust = 1), legend.position = "none") + labs(x = "", y = "") +
    scale_shape_manual(values = c(1:14)) + scale_x_discrete(labels = mylabels
) +
    scale_colour_manual(values = c("red", "blue"))

print(current_plot_mega)
ggsave("Fig_3_4A.jpg", width = 4, height = 3, dpi = 600)

current_plot_candia = ggparcoord(shape.candiacervus, columns = 3:8,
    showPoints = T, title = "Candiacervus", groupColumn = "Sex",
    scale = "globalminmax") + theme(axis.text.x = element_text(angle = 45,
    hjust = 1), legend.position = "none") + labs(x = "", y = "") +
    scale_shape_manual(values = c(1:14)) + scale_x_discrete(labels = mylabels
) +
    scale_colour_manual(values = c("red", "blue", "grey"))

print(current_plot_candia)
ggsave("Fig_3_4B.jpg", width = 4, height = 3, dpi = 600)
```

References

FALSETTI, A.B., JUNGERS, W.L. & COLE, T.M. (1993) Morphometrics of the Callitrichid Forelimb - A Case Study in Size and Shape. *Int. J. Primatol.* **14**, 551–572.

KLINGENBERG, C.P. (2016) Size, shape, and form: concepts of allometry in geometric morphometrics. *Dev. Genes Evol.* **226**, 113–137.

MOSIMANN, J.E. (1970) Size allometry: size and shape variables with characterizations of the lognormal and generalized gamma distributions. *J. Am. Stat. Assoc.* **65**, 930–945. Taylor & Francis Group.

VOS, J. DE (1984) The endemic Pleistocene deer of Crete. *Verh. der K. Ned. Akad. van Wet.* **31**, 1–100.

WHITLOCK, M. & SCHLUTER, D. (2015) *The Analysis of Biological Data*. In p. 818, 2nd editions. Roberts; Company Publishers, Greenwood Village, Colorado.